



---

All Theses and Dissertations

---

2008-12-01

# Theoretical Determination of Subcritical Sequent Depths for Complete and Incomplete Hydraulic Jumps in Closed Conduits of Any Shape

Nathan John Lowe

*Brigham Young University - Provo*

Follow this and additional works at: <https://scholarsarchive.byu.edu/etd>



Part of the [Civil and Environmental Engineering Commons](#)

---

## BYU ScholarsArchive Citation

Lowe, Nathan John, "Theoretical Determination of Subcritical Sequent Depths for Complete and Incomplete Hydraulic Jumps in Closed Conduits of Any Shape" (2008). *All Theses and Dissertations*. 1619.

<https://scholarsarchive.byu.edu/etd/1619>

This Thesis is brought to you for free and open access by BYU ScholarsArchive. It has been accepted for inclusion in All Theses and Dissertations by an authorized administrator of BYU ScholarsArchive. For more information, please contact [scholarsarchive@byu.edu](mailto:scholarsarchive@byu.edu), [ellen\\_amatangelo@byu.edu](mailto:ellen_amatangelo@byu.edu).

THEORETICAL DETERMINATION OF SUBCRITICAL SEQUENT  
DEPTHS FOR COMPLETE AND INCOMPLETE HYDRAULIC  
JUMPS IN CLOSED CONDUITS OF ANY SHAPE

by

Nathan J. Lowe

A thesis submitted to the faculty of

Brigham Young University

in partial fulfillment of the requirements for the degree of

Master of Science

Department of Civil and Environmental Engineering

Brigham Young University

December 2008



BRIGHAM YOUNG UNIVERSITY

GRADUATE COMMITTEE APPROVAL

of a thesis submitted by

Nathan J. Lowe

This thesis has been read by each member of the following graduate committee and by majority vote has been found to be satisfactory.

\_\_\_\_\_

Date

\_\_\_\_\_

Rollin H. Hotchkiss, Chair

\_\_\_\_\_

Date

\_\_\_\_\_

E. James Nelson

\_\_\_\_\_

Date

\_\_\_\_\_

A. Woodruff Miller



BRIGHAM YOUNG UNIVERSITY

As chair of the candidate's graduate committee, I have read the thesis of Nathan J. Lowe in its final form and have found that (1) its format, citations, and bibliographical style are consistent and acceptable and fulfill university and department style requirements; (2) its illustrative materials including figures, tables, and charts are in place; and (3) the final manuscript is satisfactory to the graduate committee and is ready for submission to the university library.

---

Date

---

Rollin H. Hotchkiss  
Chair, Graduate Committee

Accepted for the Department

---

E. James Nelson  
Graduate Coordinator

Accepted for the College

---

Alan R. Parkinson  
Dean, Ira A. Fulton College of Engineering  
and Technology



## ABSTRACT

### THEORETICAL DETERMINATION OF SUBCRITICAL SEQUENT DEPTHS FOR COMPLETE AND INCOMPLETE HYDRAULIC JUMPS IN CLOSED CONDUITS OF ANY SHAPE

Nathan J. Lowe

Department of Civil and Environmental Engineering

Master of Science

In order to predict hydraulic jump characteristics for channel design, the jump height may be determined by calculating the subcritical sequent depth from momentum theory. In closed conduits, however, outlet submergence may fill the conduit entirely before the expected sequent depth is reached. This is called an incomplete or pressure jump (as opposed to a complete or free-surface jump), because pressure flow conditions prevail downstream.

Since the momentum equation involves terms for the top width, area, and centroid of flow, the subcritical sequent depth is a function of the conduit shape in addition to the upstream depth and Froude number. This paper reviews momentum theory as applicable to closed-conduit hydraulic jumps and presents general solutions to the sequent depth





problem for four commonly-shaped conduits: rectangular, circular, elliptical, and pipe arch. It also provides a numerical solution for conduits of any shape, as defined by the user. The solutions conservatively assume that the conduits are prismatic, horizontal, and frictionless within the jump length; that the pressure is hydrostatic and the velocity is uniform at each end of the jump; and that the effects of air entrainment and viscosity are negligible. The implications of these assumptions are briefly discussed.

It was found that these solutions may be applied successfully to determine the subcritical sequent depth for hydraulic jumps in closed conduits of any shape or size. In practice, this may be used to quantify jump size, location, and energy dissipation.



## ACKNOWLEDGMENTS

I would first and foremost like to thank my mentor and friend, Dr. Rollin H. Hotchkiss, for his patient guidance which he freely gave from the very inception of this project. As I have approached him with concerns and ideas, he has challenged and inspired me to push myself beyond my limits, for which I will forever be grateful. I would also like to thank Dr. E. James Nelson and Dr. A. Woodruff Miller for serving on my graduate committee and providing guidance when I needed it.

I also owe thanks to Chris Smemoe and especially to Eric Jones from Aquaveo, LLC, for patiently answering my tireless questions about elliptical, pipe arch, and user-defined conduits as defined in HY-8. I appreciate Dr. Sergio Montes for his practical approach to the sequent depth solution, and for his kindness in answering my questions regarding his charts. I also greatly appreciate the Federal Highway Administration for indirectly funding my research, and I hope that they will consider allowing Aquaveo to implement it into HY-8 for them.

Finally, I would like to thank my family and friends, whose prayers and moral (and edible) support kept me going at times when I didn't want to. They may not have understood much of this, but they certainly helped me learn how to explain it.



## TABLE OF CONTENTS

<b>1</b>	<b>Introduction.....</b>	<b>1</b>
<b>2</b>	<b>Hydraulic Jump Theory .....</b>	<b>3</b>
2.1	The Hydraulic Jump.....	3
2.2	History and Applications .....	4
2.3	Parameters of Interest .....	5
2.4	The Momentum Equation .....	5
2.5	Closed Conduit Jumps .....	10
<b>3</b>	<b>Methodology .....</b>	<b>13</b>
3.1	Comparison of Methods.....	13
3.2	Dimensionless Parameters .....	15
3.3	Complete Jumps.....	16
3.4	Incomplete Jumps .....	16
3.5	Transitional Jumps.....	17
3.6	Conduit Shapes .....	18
<b>4</b>	<b>Solutions.....</b>	<b>23</b>
<b>5</b>	<b>Discussion and Analysis.....</b>	<b>31</b>
5.1	General Observations.....	31
5.2	Rectangular Conduits.....	32
5.3	Circular Conduits.....	32
5.4	Elliptical Conduits .....	33
5.5	Pipe Arch Culverts.....	35

5.6	User-Defined Conduits .....	36
<b>6</b>	<b>Summary and Application .....</b>	<b>37</b>
	<b>References .....</b>	<b>39</b>
	<b>Appendix A. Literature Review .....</b>	<b>45</b>
A.1	The Hydraulic Jump.....	45
A.2	Jump Height.....	47
A.3	Jump Length .....	52
A.4	Hydraulic Jumps in Open Channels.....	54
A.5	Hydraulic Jumps in Closed Conduits .....	60
A.6	Hydraulic Jump Classification.....	64
A.7	Elliptical Culvert Geometry.....	72
A.8	Pipe Arch Culvert Geometry .....	78
A.9	Summary of Referenced Studies.....	90
	<b>Appendix B. Sequent Depth Derivations .....</b>	<b>107</b>
B.1	General Solution .....	107
B.2	Rectangular Conduits.....	118
B.3	Circular Conduits.....	123
B.4	Elliptical Culverts .....	126
B.5	Pipe Arch Culverts.....	132
B.6	User-Defined Conduits .....	145
	<b>Appendix C. Example Problems .....</b>	<b>161</b>
C.1	Example 1: Box Culvert .....	161
C.2	Example 2: Circular Culvert .....	162
C.3	Example 3: Elliptical Culvert .....	165
C.4	Example 4: Pipe Arch Culvert.....	168

C.5 Example 5: User-Defined Culvert .....	176
<b>Appendix D. Computer Implementation .....</b>	<b>187</b>
D.1 General Logic .....	187
D.2 Rectangular Conduits.....	192
D.3 Circular Conduits.....	193
D.4 Elliptical Conduits (Simple) .....	195
D.5 Elliptical Conduits (Complex).....	198
D.6 Pipe Arch Conduits .....	205
D.7 User-Defined Conduits .....	211





## LIST OF TABLES

Table A-1 Classical Hydraulic Jump Classification .....	65
Table A-2 Sloped Channel Jump Classification .....	66
Table A-3 Positive Step Jump Classification.....	68
Table A-4 Negative Step Jump Classification .....	68
Table A-5 Submerged Sill Jump Classification.....	69
Table A-6 Weir Jump Classification.....	70
Table A-7 Abruptly Expanded Channel Jump Classification.....	71
Table A-8 Steel or Aluminum Elliptical Culvert Sizes .....	75
Table A-9 Concrete Elliptical Culvert Sizes.....	77
Table A-10 Steel or Aluminum Pipe Arch Culvert Sizes - Variable Corner Radii - 2-2/3 x 1/2 in Corrugation.....	81
Table A-11 Steel or Aluminum Pipe Arch Culvert Sizes - 18 in or greater Corner Radii - 3 x 1 in Corrugation .....	81
Table A-12 Steel or Aluminum Pipe Arch Culvert Sizes - Variable Corner Radii - 3 x 1 or 5 x 1 in Corrugation.....	82
Table A-13 Steel or Aluminum Pipe Arch Culvert Sizes (Historic) - Variable Corner Radii - 2-2/3 x 1/2 in Corrugation.....	82
Table A-14 Steel or Aluminum Pipe Arch Culvert Sizes (Historic) - 18 in or less Corner Radii - 3 x 1 in Corrugation.....	83
Table A-15 Steel Structural Plate Pipe Arch Culvert Sizes - 18 in corner radius.....	83
Table A-16 Steel Structural Plate Pipe Arch Culvert Sizes - 31 in corner radius.....	84
Table A-17 Steel Structural Plate Pipe Arch Culvert Sizes – 47 in corner radius.....	85

Table A-18 Aluminum Structural Plate Pipe Arch Culvert Sizes.....	86
Table A-19 Aluminum Structural Plate Pipe Arch Culvert Sizes (Historic).....	87
Table A-20 Concrete Pipe Arch Culvert Sizes .....	89
Table A-21 Summary of Referenced Studies .....	90
Table B-1 Example Pipe Arch Parameters .....	133
Table B-2 Example User-Defined Coordinates .....	146
Table C-1 Dimensionless Coordinates for Example 5.....	179
Table C-2 Upstream Condition Calculations for Example 5.....	181
Table C-3 Full Condition Calculations for Example 5.....	182

## LIST OF FIGURES

Figure 2-1 Typical forces acting on a hydraulic jump .....	7
Figure 2-2 Forces acting on complete and incomplete hydraulic jumps in closed conduits.....	12
Figure 3-1 Cross section for rectangular conduits .....	19
Figure 3-2 Cross section for circular conduits .....	20
Figure 3-3 Cross section for elliptical conduits .....	20
Figure 3-4 Example cross section for a pipe arch culvert.....	21
Figure 3-5 Example cross section for a user-defined conduit.....	21
Figure 4-1 Solution for rectangular conduits .....	24
Figure 4-2 Solution for circular conduits.....	25
Figure 4-3 Solution for elliptical conduits .....	26
Figure 4-4 Solution for pipe arch culverts .....	27
Figure 4-5 Solution for user-defined culverts.....	29
Figure 5-1 Error distribution of ellipse assumption for metal elliptical culverts.....	34
Figure 5-2 Error distribution of ellipse assumption for concrete elliptical culverts.....	35
Figure A-1 Parameters to be used in this study for elliptical culverts .....	73
Figure A-2 Parameters to be used in this study for pipe arch culverts .....	79
Figure B-1 Forces acting on complete and incomplete hydraulic jumps in closed conduits.....	108
Figure B-2 Cross section for rectangular conduits .....	118
Figure B-3 Sequent depth ratio chart for rectangular conduits.....	122

Figure B-4 Cross section for circular conduits .....	123
Figure B-5 Sequent depth ratio chart for circular conduits.....	125
Figure B-6 Cross section for elliptical culverts .....	126
Figure B-7 Sequent depth ratio chart for elliptical conduits.....	129
Figure B-8 Error distribution of ellipse assumption for metal and concrete elliptical culverts.....	131
Figure B-9 Cross section for pipe arch culverts.....	133
Figure B-10 Bottom, middle and top pipe arch sections .....	134
Figure B-11 Parameters used for the bottom section of a pipe arch.....	137
Figure B-12 Parameters used for the first middle section of a pipe arch culvert .....	138
Figure B-13 Parameters used for the second middle section of a pipe arch culvert .....	140
Figure B-14 Parameters used for the top section of a pipe arch culvert.....	141
Figure B-15 Sequent depth ratio chart for the pipe arch culvert associated with the parameters listed Table B-1 .....	144
Figure B-16 Example cross section for user-defined coordinates in Table B-2.....	145
Figure B-17 Example cross section for a user-defined conduit.....	147
Figure B-18 Definition of terms used for incremental vertical sections.....	149
Figure B-19 Parameters for triangular, rectangular, and trapezoidal cross sections.....	150
Figure B-20 Cases to consider for the analysis of each incremental vertical section of a user-defined conduit .....	153
Figure B-21 Sequent depth ratio chart for the user-defined culvert associated with the coordinates listed Table B-2.....	159
Figure C-1 Graphical solution to Example 1 .....	163
Figure C-2 Graphical solution to Example 2 .....	166
Figure C-3 Graphical solution to Example 3 .....	169

Figure C-4 Graphical solution to Example 4 .....	177
Figure C-5 Graphical solution to Example 5 .....	186
Figure D-1 General logic for sequent depth calculation .....	188
Figure D-2 General logic for complete jumps .....	189
Figure D-3 General logic for incomplete jumps .....	191
Figure D-4 General logic for no jump .....	191



## LIST OF SYMBOLS

<u>Symbol</u>	<u>Description</u>
A	Cross-sectional area (ft <sup>2</sup> , m <sup>2</sup> )
A'	Dimensionless area = A/BD
B	Span of conduit (ft, m)
B'	Dimensionless span (pipe arch only) = B/D
D	Rise of conduit (ft, m)
dA	Incremental area at x (ft <sup>2</sup> , m <sup>2</sup> )
dV	Incremental volume at x (ft <sup>3</sup> , m <sup>3</sup> )
dW	Incremental weight of fluid at x (lbs, N)
dx	Incremental longitudinal distance at x (ft, m)
dλ	Incremental distance around P <sub>w</sub> at x (ft, m)
F	Force (i.e. frictional forcer, F <sub>f</sub> ) (lbs, N)
Fr	Froude number
g	Acceleration due to gravity (ft/s <sup>2</sup> , m/s <sup>2</sup> )
H	Pressure head above conduit (ft, m)
H'	Dimensionless pressure head above conduit = H/D
h	Height from bottom of conduit (pipe arch and user-defined only) (ft, m)
h'	Dimensionless height from bottom of conduit (pipe arch only) = h/D
L	Length (i.e. jump length) (ft, m)
M	Momentum flux (lbs, N)
P	Pressure force (lbs, N); Perimeter (i.e. wetted perimeter, P <sub>w</sub> ) (ft, m)
Q	Flow rate through channel or conduit (cfs, cms)



<u>Symbol</u>	<u>Description</u>
R	Radius (pipe arch only) (ft, m)
R'	Dimensionless radius (pipe arch only) = R/D
T	Top width of flow (ft, m)
T'	Dimensionless top width = T/B
V	Flow velocity (ft/s, m/s)
W	Weight of fluid within control volume (lbs, N)
x	Distance, parallel to channel or conduit axis, measured from upstream control surface downstream (ft, m)
	Horizontal distance, perpendicular to the conduit axis, measured from left side of conduit (user-defined only) (ft, m)
y	Flow depth (ft, m)
y'	Dimensionless depth = y/D
$\bar{z}$	Distance from the water surface to the centroid of A (ft, m)
$(\bar{z}A)$	Centroid-area = $\bar{z} * A$ (ft <sup>3</sup> , m <sup>3</sup> )
$(\bar{z}A)'$	Dimensionless centroid-area = $(\bar{z}A)/BD^2$
$\beta$	Coefficient (i.e. velocity distribution coefficients, $\beta_1$ & $\beta_2$ )
	Dimensionless ratio (i.e. air entrainment ratio, $\beta_a$ )
$\Gamma$	Dimensionless top width function
$\theta$	Internal flow angle (radians)
$\lambda$	Distance around $P_w$ , measured from one side to a point along $P_w$ at x (ft, m)
$\rho$	Fluid density (slugs/ft <sup>3</sup> , kg/m <sup>3</sup> )
$\tau$	Shear stress (psf, Pa)
$\phi$	Bed slope angle from the horizontal (radians)
$\Psi$	Dimensionless centroid-area function
$\Omega$	Dimensionless area function

<u>Subscript</u>	<u>Description</u>
0	Boundary layer (i.e. shear stress at boundary layer, $\tau_0$ )
1	Upstream cross-section First (i.e. $h_1$ for trapezoidal shape) (user-defined only)
2	Downstream cross-section Second (i.e. $h_2$ for trapezoidal shape) (user-defined only)
A	Lowest value (i.e. incremental height, $(h_A)_i$ ) (user defined only)
a	Air entrainment (i.e. air entrainment ratio, $\beta_a$ )
B	Second lowest value (i.e. incremental height, $(h_B)_i$ ) (user defined only)
b	Bottom section (pipe arch only) Bottom coordinate (user-defined only)
C	Second highest value (i.e. incremental height, $(h_C)_i$ ) (user defined only)
D	Highest value (i.e. incremental height, $(h_D)_i$ ) (user defined only)
f	Friction (i.e. frictional force, $F_f$ ) Full conduit (i.e. $y_f$ )
i	Place-holder (i.e. for subscripts 1, 2, or f) Incremental (user-defined only)
j	Jump (i.e. jump length, $L_j$ )
m	Middle section (pipe arch only)
m1	Middle section 1 (pipe arch only)
m2	Middle section 2 (pipe arch only)
max	Maximum value (user-defined only)
min	Minimum value (user-defined only)
rect	Rectangular shape (user-defined only)
s	Streamwise direction (i.e. force in the streamwise direction, $F_s$ )

<u>Subscript</u>	<u>Description</u>
t	Transition from complete to incomplete jumps (i.e. transitional Froude number, $(Fr_1)_t$ )
	Top section (pipe arch only)
	Top coordinate (user-defined only)
trap	Trapezoidal shape (user-defined only)
tri	Triangular shape (user-defined only)
w	Wetted (i.e. wetted perimeter, $P_w$ )
	Water (i.e. density of water, $\rho_w$ )

# 1 Introduction

A common phenomenon that occurs in hydraulic behavior is an abrupt rise in water surface elevation, caused by deeper, slower-moving water downstream. This is known as a hydraulic jump, and has been the focus of interest for hydraulics engineers for almost two centuries, mostly because of its potential for energy dissipation (Chow 1959). Hydraulic jumps can also be highly erosive to the channels that contain them. In order to determine the required channel protection, practicing engineers must be able to predict the height, length, and location of a potential jump, which may be a difficult task depending on the channel shape.

The length of a hydraulic jump is typically obtained from empirical functions of the jump height, based solely upon experimentation (Sturm 2001), and the location depends on both the length and height of the jump, as well as the upstream and downstream water surface profiles (Chow 1959). The jump height, however, may be predicted quite accurately using momentum theory alone (Hotchkiss et al. 2003). Typically, the discharge and upstream depth are already known, and what remains to be determined is the downstream “sequent depth” (Chadwick et al. 2004). This holds true for hydraulic jumps in closed conduits, although in this case a jump in water surface can potentially fill the conduit completely, producing pressure flow conditions downstream and preventing the surface from reaching the expected sequent depth (Hager 1999).

The purpose of this study, therefore, is to develop general solutions to the sequent depth problem for prismatic conduits of any shape, to help determine the size and location of a potential hydraulic jump. The theory and methodology behind the development of these solutions are first reviewed, followed by a presentation of the solutions themselves, which includes a series of equations for each shape (and in some cases a dimensionless sequent depth chart), and a general procedure for applying them. Four common shapes are analyzed based on geometry: rectangular, circular, elliptical, and pipe arch conduits. A numerical algorithm is also developed for conduits of any shape, which are referred to in this paper as “user-defined” conduits.

For this study the momentum equation is reduced to its simplest form, such that the effects of slope, friction, air entrainment, and other external factors are neglected for simplicity. For the most part these assumptions are conservative, but their rationalization and implications are discussed briefly for completeness.

## **2 Hydraulic Jump Theory**

In order to understand the context and application of this study, a basic review of hydraulic jump theory is necessary. This chapter therefore presents a concise overview of hydraulic jumps in closed conduits, and how the momentum equation may be used to predict the subcritical sequent depth of a conduit of any shape. A more detailed review of hydraulic jump theory and assumptions may be found in Appendix A.

### **2.1 The Hydraulic Jump**

The hydraulic jump is an example of rapidly varied flow in which supercritical flow abruptly becomes subcritical, typically due to high tailwater (Chow 1959; Rajaratnam 1967). In this process, the water surface “jumps” through critical depth as kinetic energy is converted to potential energy (Franzini and Finnemore 1997; Thompson and Kilgore 2006). The transition is always accompanied by an energy loss as kinetic energy is converted into turbulence and then into sound and heat (Haindl 1957; Sturm 2001).

Most jumps vary in appearance between two extremes. The first has a fully-developed surface roller, which is characterized by a relatively smooth and continuous water surface as flow continues along channel bottom downstream. At some point, bubbles rise intensively to a stagnation point, where flow either proceeds downstream or

“rolls” back towards the toe, or beginning, of the jump. The second extreme is a standing wave, in which flow is immediately deflected to the surface at the toe. The toe moves downstream while the end of the jump moves upstream, creating a shorter jump characterized by heavy surface waves and eruptions (Hager et al. 1990).

## **2.2 History and Applications**

The hydraulic jump has many useful applications in hydraulic design, typically as an energy dissipater (Chow 1959). As mentioned above, the hydraulic jump naturally dissipates energy through turbulence, which can be highly erosive if proper channel protection is not installed (Hager 1992). It is therefore preferable, when a hydraulic jump is expected, to control the size and location of the jump in order to localize energy dissipation and erosion (Stahl and Hager 1999).

Because of this, hydraulic jumps have been the focus of interest among engineers for almost 200 years, starting with Giorgio Bidone, an Italian, in 1818 (Chow 1959), and then the French hydraulician Jean-Baptiste Bélanger, who developed his famous equation in 1838 relating the supercritical and subcritical depths to the upstream Froude number (Hager 1999). Comprehensive histories of the study of hydraulic jumps may be found in several hydraulics texts, including Chow (1959), Rajaratnam (1967), Hager (1992), and Montes (1998); therefore the history is not repeated here. It should be noted that the main focus of these studies has been to predict the size and location of hydraulic jumps under various channel conditions so that the hydraulic structures containing them may be designed accordingly.

### **2.3 Parameters of Interest**

Typically the flow rate and depth entering a hydraulic jump is already known, and the tailwater depth may be determined from water surface profile calculations (Chadwick et al. 2004). Therefore the two main parameters of interest when predicting hydraulic jump behavior are (1) the subcritical sequent depth, and (2) the length of the jump (Thompson and Kilgore 2006). Not only do these parameters describe the size of the jump, but if the subcritical sequent depth is compared to the tailwater profile, the location may be determined as well (Chow 1959). Furthermore, once both sequent depths are known, flow areas (and therefore velocities by continuity) may be calculated, from which the energy loss may be determined by the energy equation (Thompson and Kilgore 2006). The jump length is typically expressed as an empirical function of the sequent depths or the upstream Froude number (Hotchkiss et al. 2003); therefore this study focuses entirely on determining the subcritical sequent depth.

### **2.4 The Momentum Equation**

Because of energy losses, the size and location of a hydraulic jump cannot be predicted using the energy equation. However, because momentum is conserved across hydraulic jumps under the assumptions of this study, momentum theory may be applied to determine the jump size and location (Hotchkiss et al. 2003). The general momentum equation, which may be derived from the Reynolds Transport Theorem, states that “the vector sum of forces acting on the control volume is equal to the time rate of change of linear momentum inside the control volume plus the net momentum flux out of the control volume through the control surface.” In simpler terms, the momentum equation states that “the change in momentum of the entering and exiting stream is balanced by the

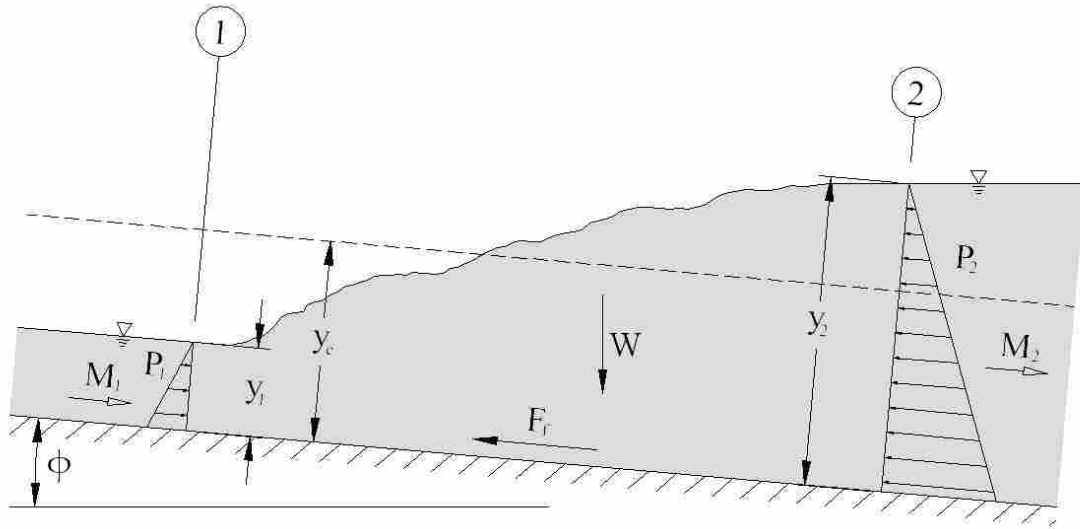


resultant of the forces acting on the control volume” (Thompson and Kilgore 2006). In essence this is Newton’s second law applied to a fluid within a control volume. Assuming steady, one-dimensional flow, where the entering and exiting velocities are uniform and perpendicular to the control surface, the momentum equation may be written as:

$$\sum \bar{F}_s = \sum (\bar{M}_s)_{out} - \sum (\bar{M}_s)_{in} \quad (2-1)$$

where  $F_s$  represents the external forces (lbs, N) acting on the water within the control volume, and  $M_s$  represents the momentum flux (lbs, N) through the control volume, both in the streamwise direction (Sturm 2001).

The hydraulic jump is an ideal candidate for the application of momentum theory, because a "precise mathematical description of the internal flow pattern is not possible" due to its complexity (Sturm 2001), and the stability of a jump depends entirely upon the equilibrium between the momentum flux across the jump, and the external forces acting upon it (Chadwick et al. 2004). Figure 1 on the next page depicts the forces typically considered when applying momentum theory to a hydraulic jump.



**Figure 2-1 Typical forces acting on a hydraulic jump ( $y_1, y_2$  = flow depth;  $y_c$  = critical depth;  $M_1, M_2$  = momentum forces;  $P_1, P_2$  = pressure forces;  $W$  = weight;  $F_f$  = friction force;  $\phi$  = bed slope angle)**

According to this figure, Equation 2-1 may be expanded as:

$$P_1 - P_2 + W \sin \phi - F_f = M_2 - M_1 \quad (2-2)$$

where  $P_1$  and  $P_2$  are the pressure forces (lbs, N) at sections (1) and (2), respectively;  $W$  is the weight (lbs, N) of the fluid within the control volume;  $\phi$  is the bed slope angle from the horizontal;  $F_f$  is the friction force (lbs, N) caused by the channel or conduit; and  $M_1$  and  $M_2$  are the momentum fluxes (lbs, N) at sections (1) and (2), respectively.

To simplify the problem several assumptions are commonly made. First, for this study the channel is assumed to be straight and prismatic. This precludes any corrections needed for longitudinal anomalies, such as abrupt expansions or steps. Second, the slope is assumed to be horizontal. This assumption eliminates the weight term, and is

justifiable for slopes up to 5% (Hager 1999). Third, the channel is assumed to be relatively smooth, such that the effects of friction within the control volume may be considered negligible when compared to the other forces involved. The length of the jump is typically short enough for this to be a valid assumption (Montes 1998). Fourth, the pressure distributions at sections (1) and (2) are assumed to be hydrostatic, such that the pressure forces may be expressed in terms of the cross-sectional area of flow ( $\text{ft}^2$ ,  $\text{m}^2$ ),  $A$ , and the distance (ft, m) from the water surface to the centroid of the cross-sectional area,  $\bar{z}$ . This assumption may be unrealistic, but correcting for it appears to make little difference (Hughes and Flack 1984). Fifth, the velocity distributions at sections (1) and (2) are assumed to be uniform, which allows for the use of average velocity. This is also hardly accurate, but it produces acceptable results nonetheless, since the effects of turbulence flux appear to counteract the effects of velocity distribution (Harleman 1959). Sixth, air entrainment is assumed in this study to be negligible, such that section (2) may still be considered one-phase flow. The effects of air entrainment increase exponentially with the upstream Froude number (Kalinske and Robertson 1943; Haindl and Sotornik 1957), but in relatively flat conduits such as those considered in this study, Froude numbers are typically small enough (i.e. less than 5) to have little effect on the solution. And seventh, the effects of viscosity are assumed to be negligible, typically justified by the large Reynolds numbers involved (Rajaratnam 1968b).

Given these assumptions, Equation 2-2 may be rewritten as:

$$\rho g(\bar{z}A)_1 - \rho g(\bar{z}A)_2 = \rho Q(V_2 - V_1) \quad (2-3)$$

where  $\rho$  is the water density (slugs/ft<sup>3</sup>, kg/m<sup>3</sup>);  $g$  is the acceleration (ft/s<sup>2</sup>, m/s<sup>2</sup>) due to gravity;  $(\bar{z}A)_1$  and  $(\bar{z}A)_2$  are the centroid-areas of flow (ft<sup>3</sup>, m<sup>3</sup>) at sections (1) and (2), respectively;  $Q$  is the flow rate (cfs, cms) through the channel or conduit; and  $V_1$  and  $V_2$  are the streamwise flow velocities (ft/s, m/s) at sections (1) and (2), respectively.

The height of a hydraulic jump is typically defined in terms of the depths (ft, m) of flow upstream ( $y_1$ ) and downstream ( $y_2$ ) of the jump. These are called sequent depths, because they share the same specific force (Chow 1959; Straub 1978). Because the area and centroid of flow are both functions of the channel shape and flow depth, it follows that for a given channel shape and flow rate, there exists a specific combination of  $y_1$  and  $y_2$  such that Equation 2-3 is satisfied.

In the case of wide, rectangular, horizontal, frictionless channels, the momentum equation may be rewritten explicitly in terms of the subcritical sequent depth, as discovered by Bélanger in 1838 (Hager 1992). Unfortunately, no such equation exists for other channel or conduit shapes; rather, these have implicit solutions that require iteration (French 1985; Jeppson 1970). Although due to modern technology this is not as tedious as it once was, most practicing engineers still prefer a quick solution that does not require iteration.

## 2.5 Closed Conduit Jumps

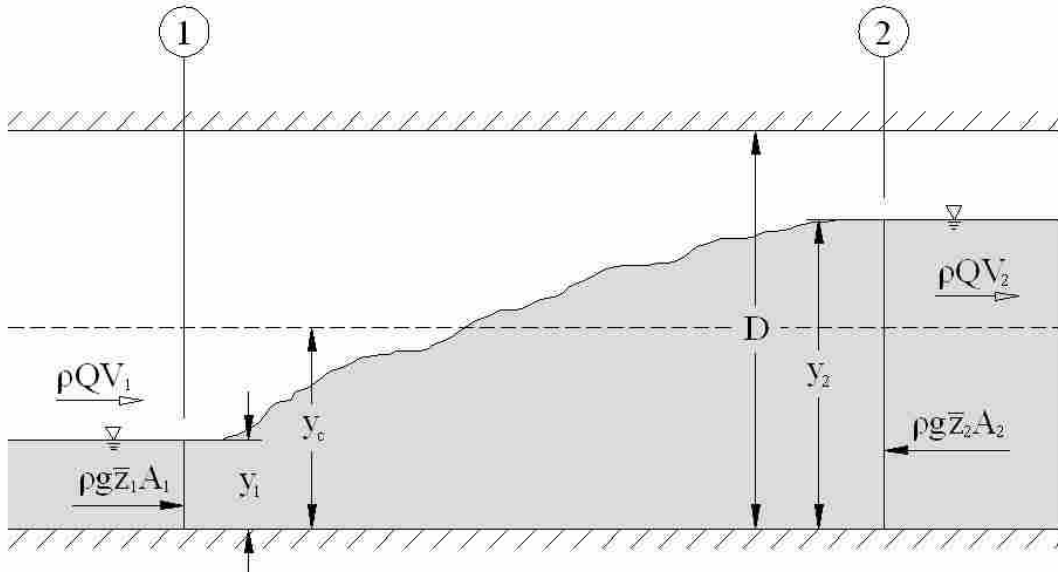
Most research on hydraulic jumps has dealt with open channel rather than closed conduit flow (Montes 1998), although researchers have been studying the latter since 1938, beginning with Lane and Kinsvatar (1938). Since the focus of this study is on hydraulic jumps in closed conduits, open-channel jumps are not discussed here.

Hydraulic jumps in closed conduits behave similarly to open-channel jumps, as long as a free surface remains and sufficient air is supplied above the flow. What makes closed-conduit jumps different is that they potentially can, due to downstream submergence, fill the conduit completely, resulting in pressure flow conditions within the barrel (Caric 1977; Hager 1999). This phenomenon is known as an incomplete or pressure jump, as opposed to a complete or free-surface jump (Hotchkiss et al. 2003; Montes 1998), and because of the inherent dissimilarities between the two, each must be approached differently.

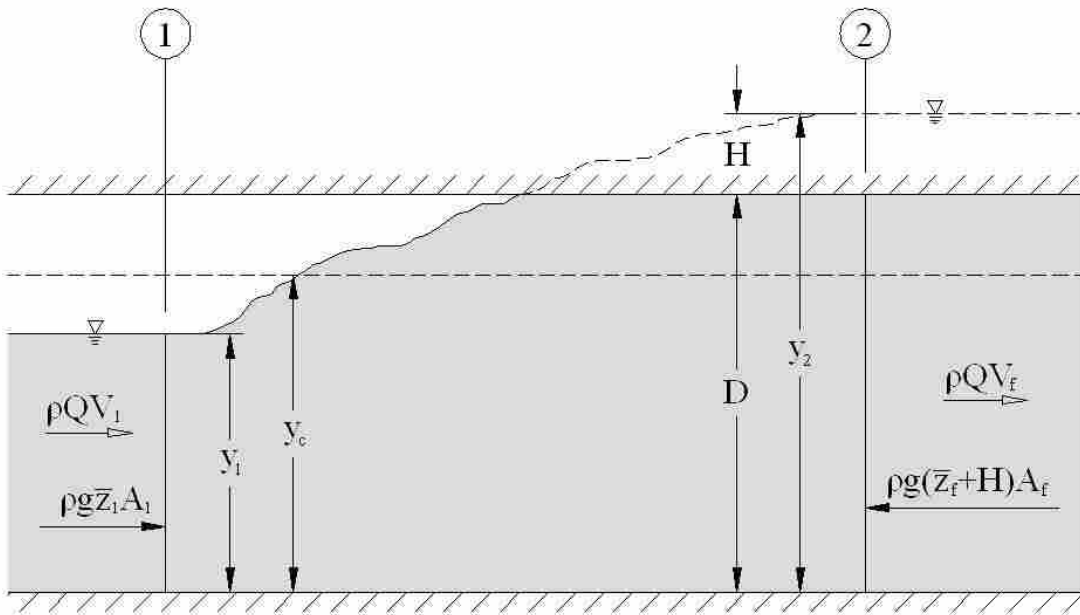
One example of closed-conduit jump behavior occurs within culvert barrels. Under inlet control conditions, in which flow through a culvert becomes supercritical, high flow velocities at the outlet can potentially scour the streambed and undercut the culvert barrel. Oftentimes to prevent this from happening, culvert designers will install energy dissipaters at the outlet or within the culvert itself, but these devices can be costly. A significantly less-expensive alternative is to force a hydraulic jump to occur within the culvert barrel by controlling the tailwater. The culvert itself protects the channel against erosion, while the hydraulic jump dissipates energy, thereby reducing the need for further dissipaters downstream (Hotchkiss et al. 2005). If the outlet of the culvert is not submerged, a complete hydraulic jump can form within the culvert barrel; otherwise the jump must be incomplete.

Figure 2 on the next page depicts typical profiles for complete and incomplete closed-conduit jumps. In the case of complete jumps, the subcritical sequent depth is less than the rise (ft, m) of the conduit (i.e.  $y_2 < D$ ), whereas in the case of incomplete jumps, it is greater (i.e.  $y_2 > D$ ). Since the flow depth in incomplete jumps cannot reach the expected sequent depth, the deficit is supplemented by the hydrostatic pressure head (ft, m) against the top of the conduit, symbolized in this figure as  $H$  (Montes 1998). It should be noted that the pressure head at section (2) depends only upon the pressure head at the outlet, the slope of the conduit, and the hydraulic grade line, not on the jump itself;  $H$  is merely used to solve for  $y_2$  when the jump is at equilibrium (Haindl 1957).

Hypothetically, a point should exist at which the conduit becomes “just full” at section (2), or at which the subcritical flow depth exactly meets the crown of the conduit (i.e.  $y_2 = D$ ). This situation marks the transition between complete and incomplete jumps, and is therefore named here as a “transitional” jump. In practice, this condition is rare if not impossible, because as  $y$  approaches  $D$ , “choking” occurs, in which the flow abruptly and spontaneously fills the conduit and becomes pressurized (Hager 1999). In theory, however, it is important to determine the conditions under which this transition will occur, so that the appropriate method (i.e. complete or incomplete) may be used to calculate the subcritical sequent depth.



(a)



(b)

**Figure 2-2 Forces acting on (a) complete and (b) incomplete hydraulic jumps in closed conduits ( $\rho$  = water density;  $g$  = acceleration of gravity;  $Q$  = flow rate;  $V_1$ ,  $V_2$ ,  $V_f$  = average flow velocity;  $\bar{z}_1$ ,  $\bar{z}_2$ ,  $\bar{z}_f$  = distance to centroid of flow;  $A_1$ ,  $A_2$ ,  $A_f$  = area of flow;  $H$  = pressure head against top of conduit)**

### **3 Methodology**

This chapter presents the method and procedure used in this study to calculate the subcritical sequent depth for complete and incomplete hydraulic jumps in closed conduits. It first compares methods used by others, and then explains the approach chosen for this study, introducing the dimensionless parameters to be used. A more comprehensive summary of this material is given in Appendix B.

#### **3.1 Comparison of Methods**

In order to solve the momentum equation for closed-conduit hydraulic jumps and generalize the solution visually, several approaches exist that vary in complexity and versatility. Open channel jumps lend themselves easily to solutions similar to those provided by the Bélanger equation – that is, expressing the ratio between sequent depths as a function of the upstream Froude number (Bradley and Peterka 1957; Chow 1959; Rajaratnam 1965; 1967). Others (Smith and Chen 1989; Husain et al. 1994) have attempted to extend this method to closed-conduit jumps for consistency, but the resultant sequent depth chart can be difficult to interpret. Multiple curves corresponding to various values of  $y_1/D$  overlap, and the transition between complete and incomplete jumps is marked separately on each curve.



Another common approach, used by Rajaratnam (1965; 1967), Thiruvengadam (1961), Hjelmfeldt (1967), Hsu et al. (1980), Hager (1990; 1992; 1999), and Sturm (2001), results in a much more readable chart, which could easily have been extended to incomplete jumps (although most researchers have not done so). The downside to this method is that it requires the use of an otherwise meaningless dimensionless ratio in place of the upstream Froude number involving the flow rate and conduit dimensions.

As an alternative, some researchers (Frank 1942; Caric 1977) have found  $y_2/D$  as a function of  $y_0/D$  and  $y_1/D$ , while others (Mavis 1946) have resorted to nomographs for graphical solutions. These approaches are effective, but do not use quantities commonly calculated when dealing with hydraulic jumps, and therefore provide little insight into the meaning behind the solution.

Montes (1998) instead decided to find  $y_2/D$  as a function of  $y_1/D$  for given values of  $Fr_1$ , which poses several advantages over the alternatives mentioned above. First, like the first method it uses the Froude number, which is directly applicable to hydraulic jump size and behavior. Second, it clearly shows the delineation between complete and incomplete jumps. And third, it unmistakably demonstrates what Smith and Chen (1989) observed, which is that the jump height increases as  $y_1$  approaches approximately two-thirds the conduit rise, but decreases dramatically for all  $Fr_1$  as  $y_1$  approaches full conditions, such that no jump occurs at all when a conduit is flowing full. The methodology used in this study, therefore, is modeled after Montes' approach due to its relative simplicity and versatility.

### 3.2 Dimensionless Parameters

When creating sequent depth charts, it is generally convenient to use dimensionless ratios in order to provide a solution that is applicable independent of scale or units. In this study, such ratios are denoted (except for the Froude number) by the prime symbol, as listed below:

$$Fr_1 \equiv \frac{V_1}{\sqrt{g A_1 / T_1}} = \frac{Q}{\sqrt{g A_1^3 / T_1}} = \frac{Q}{\sqrt{g B^2 D^3 A_1' / T_1}} \quad (3-1)$$

$$y'_i \equiv \frac{y_i}{D} \quad (3-2)$$

$$T'_i \equiv \frac{T_i}{B} = \Gamma(\text{shape}, y'_i) \quad (3-3)$$

$$A'_i \equiv \frac{A_i}{BD} = \Omega(\text{shape}, y'_i) \quad (3-4)$$

$$(\bar{z}A)'_i \equiv \frac{(\bar{z}A)_i}{BD^2} = \Psi(\text{shape}, y'_i) \quad (3-5)$$

where  $Fr_1$  is the upstream Froude number;  $y_i$  is the depth of flow (ft, m) at section (i);  $B$  and  $D$  are the span (width) and rise (height) of the conduit (ft, m), respectively;  $T_i$  is the top width of flow (ft, m) at section (i);  $A_i$  is the cross-sectional area of flow (ft<sup>2</sup>, m<sup>2</sup>) at

section (i); and  $(\bar{z}A)_i$  is the centroid-area of flow ( $\text{ft}^3, \text{m}^3$ ) at section (i). The functions  $\Gamma$ ,  $\Omega$ , and  $\Psi$  are derived in the next chapter for each of the conduit shapes in this study.

### 3.3 Complete Jumps

As defined earlier, a complete hydraulic jump is one in which the free surface continues past the end of the jump, (i.e.  $y_2 < D$ ; see Figure 2a). For this situation, Equation 2-3 may be simply rearranged and rewritten as follows:

$$\text{Fr}_1^2 = \frac{T_1 A'_2 [(\bar{z}A)'_2 - (\bar{z}A)'_1]}{A_1'^2 (A'_2 - A'_1)} \quad (3-6)$$

This equation may be used for any conduit shape to generate the complete or normal jump portion of a sequent depth chart similar to those found in Montes (1998). Unfortunately, in most cases it cannot be solved for  $y'_2$  explicitly. In this study, the interval halving method (Sturm 2001) was used to iteratively find solutions.

### 3.4 Incomplete Jumps

Incomplete hydraulic jumps were defined previously as jumps in which the downstream subcritical flow becomes pressurized due to outlet submergence (i.e.  $y_2 > D$ ; see Figure 2b). Therefore Equation 2-3 must be rewritten as follows:

$$\text{Fr}_1^2 = \frac{T_1 A'_f [(\bar{z}A)'_f + H' A'_f - (\bar{z}A)'_1]}{A_1'^2 (A'_f - A'_1)} \quad (3-7)$$

where  $H' \equiv H/D$  is the dimensionless pressure head above the conduit, and the subscript 'f' is used to denote full conditions. Since only  $H'$  is a function of  $y'_2$ , Equation 3-7 may be rewritten instead as an explicit solution:

$$y'_2 = 1 + \frac{1}{T_1 A'_f{}^2} \left\{ Fr_1^2 A'_1{}^2 (A'_f - A'_1) - T_1 A'_f [(\bar{z}A)'_f - (\bar{z}A)'_1] \right\} \quad (3-8)$$

This equation may be used for any conduit shape to generate the incomplete jump portion of a sequent depth chart similar to those found in Montes (1998).

### 3.5 Transitional Jumps

Transitional hydraulic jumps were previously defined as jumps in which the conduit at section (2) is barely full without being pressurized (i.e.  $y_2 = D$ ). Under these conditions, the transitional upstream Froude number,  $(Fr_1)_t$ , may be found explicitly by:

$$(Fr_1)_t^2 = \frac{T_1 A'_f [(\bar{z}A)'_f - (\bar{z}A)'_1]}{A'_1{}^2 (A'_f - A'_1)} \quad (3-9)$$

This equation may be used for any conduit shape to find the upstream Froude number associated with the transition between complete and incomplete jumps. If the actual  $Fr_1$  is less than  $(Fr_1)_t$ , then a complete jump may form, and  $y'_2$  should be calculated using Equation 3-6; otherwise, the jump will be incomplete, and  $y'_2$  should instead be calculated using Equation 3-8.

### 3.6 Conduit Shapes

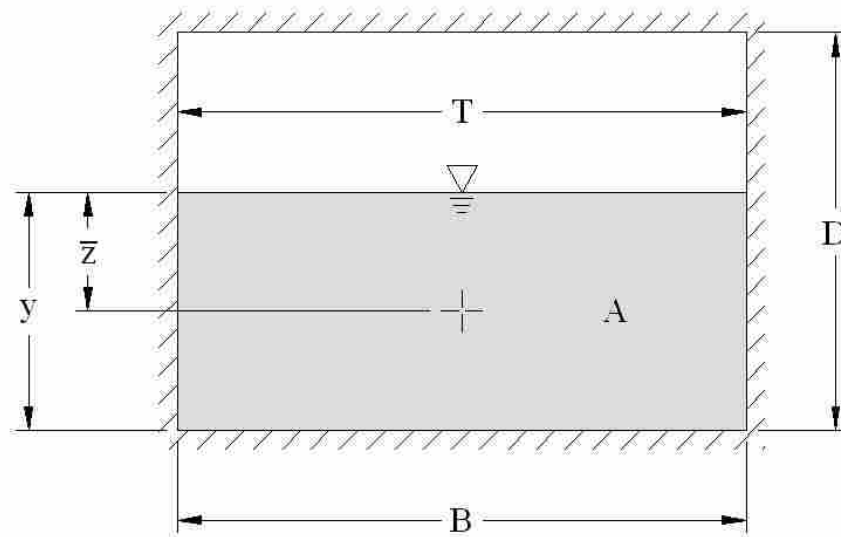
In his study, Montes (1998) provided formulas similar to Equations 3-6 and 3-8 for closed conduits, as well as general solutions for finding the dimensionless area and centroid-area by integration. This requires, however, that a conduit shape be defined by an analytic mathematical expression, which is not always possible. Furthermore, Montes did not provide a general equation for top width, and he only provided graphical solutions for circular, horseshoe-, and egg-shaped conduits, without posting the specific equations he used to derive them.

This study therefore adds to Montes' analysis the solutions for rectangular, elliptical, and pipe-arch culverts. It also recreates the solutions for circular and inverted egg-shaped conduits for comparison, although the inverted egg shape is defined here by a series of coordinates rather than by its geometry, to demonstrate the application of an algorithm for finding the sequent depth of flow within conduits of any shape.

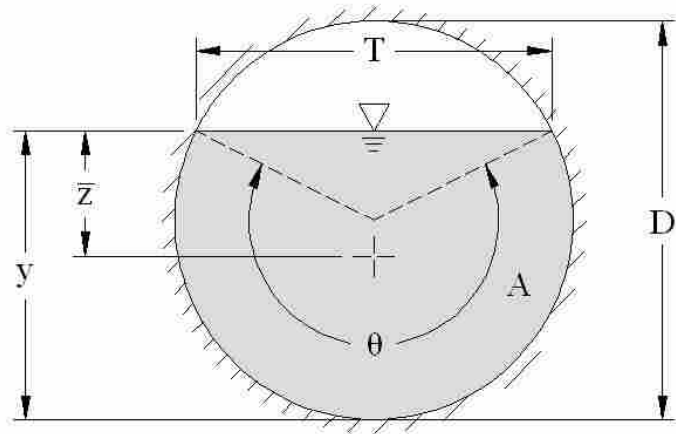
This general case is referred to in this study as "user-defined". The main concept behind the user-defined conduit analysis is that the inner walls of any conduit shape may be defined by a series of coordinates, such that for every horizontal distance,  $x_i$ , away from the left-most point perpendicular to the conduit axis, two vertical ordinates exist relative to the lowest point in the conduit representing the location of the bottom and top inner edges of the barrel at that point, denoted by  $(y_b)_i$  and  $(y_t)_i$ , respectively. Defining the coordinates in this manner rather than listing two  $x$  values for every  $y$  value provides two major advantages for this analysis. First, it significantly simplifies the calculation of the centroid-area, and second, it allows for the addition of multiple top widths and areas, which may occur when sediment deposits and splits the flow into two or more streams.

The conduit can therefore be analyzed by dividing it into multiple vertical sections, each with a thickness  $\Delta x = x_{i+1} - x_i$ .

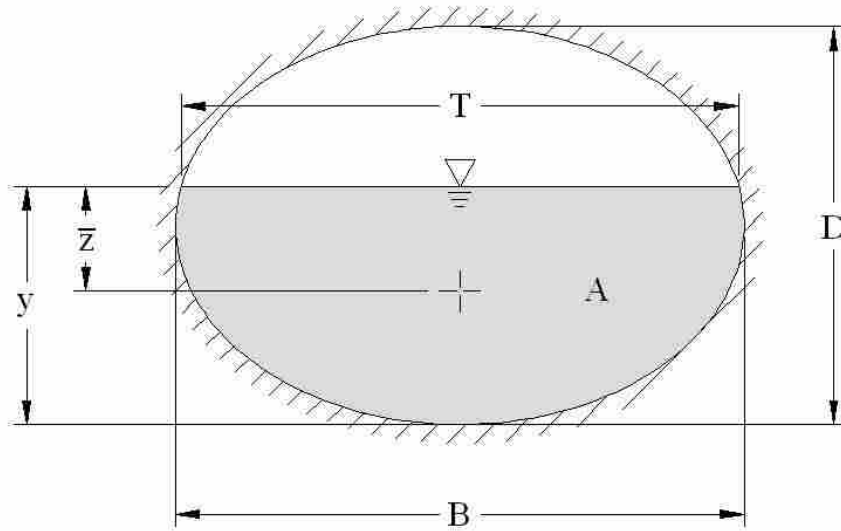
Figures 3 through 7 below depict the cross section for each of the conduit shapes analyzed in this study. Figure 7 is an example of how a set of coordinates might be defined for the inverted-egg-shaped conduit.



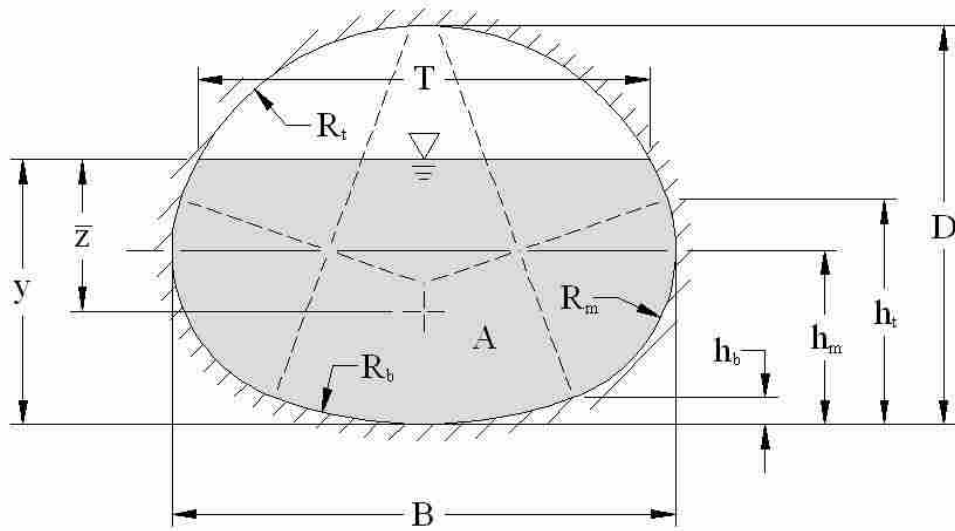
**Figure 3-1 Cross section for rectangular conduits ( $B$  = span;  $D$  = rise;  $T$  = top width)**



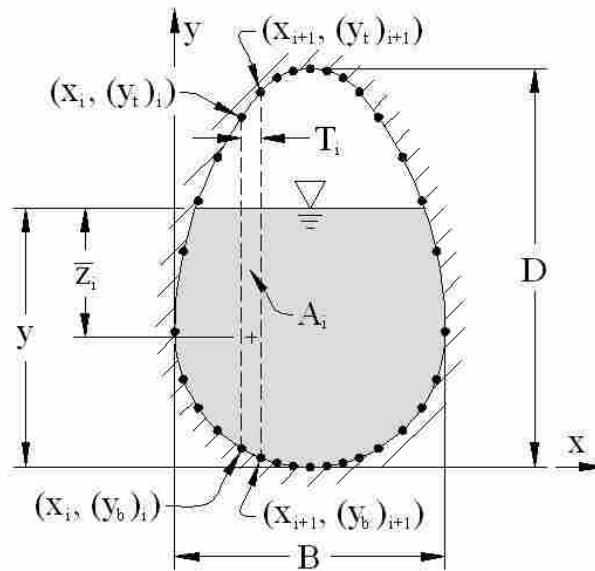
**Figure 3-2 Cross section for circular conduits ( $\theta$  = internal flow angle)**



**Figure 3-3 Cross section for elliptical conduits**



**Figure 3-4 Example cross section for a pipe arch culvert ( $R_b$  = bottom radius;  $R_m$  = middle radius;  $R_t$  = top radius;  $h_b$  = bottom transition height;  $h_m$  = neutral axis height;  $h_t$  = top transition height)**



**Figure 3-5 Example cross section for a user-defined conduit**





## 4 Solutions

The solutions to Equations 3-6, 3-8, and 3-9 for the subcritical sequent depth ratio are presented in this chapter for rectangular, circular, elliptical, pipe arch, and user-defined conduits, as Figures 4-1 through 4-5. Full derivations of these solutions are included in Appendix B for reference. Solutions steps are as follows: (1) calculate all dimensionless parameters such as  $T'$ ,  $A'$ , and  $(\bar{z}A)'$  for upstream and full conditions; (2) calculate  $Fr_1$  to determine whether the flow is supercritical and therefore whether a jump is possible; (3) calculate  $(Fr_1)_t$  and compare it to  $Fr_1$  to determine whether the jump is complete or incomplete; and (4) calculate  $y'_2$ , and then  $y_2$ , based on the appropriate equation.

Alternatively,  $y'_2$  may be found from the sequent depth charts using the values for  $y'_1$  and  $Fr_1$  calculated in Steps 1 and 2, respectively. A sequent depth chart is not presented here for pipe arch culverts, because there are too many differences in relative shape among manufactured sizes to warrant a unique solution (see Appendix A.8). Likewise, a chart is not presented here for user-defined conduits, for obvious reasons. However, for this study an example set of parameters was chosen for both of these shapes, from which charts were derived to demonstrate the application of the solutions. An example problem for each conduit shape is presented in Appendix C for reference, and the Visual Basic code used to generate the solutions is presented in Appendix D.

	Complete:
	$y'_2 = \frac{y'_1}{2} \left( \sqrt{1 + 8\text{Fr}_1^2} - 1 \right)$
	Incomplete:
	$y'_2 = \frac{1}{2} + \left( \text{Fr}_1^2 + \frac{1}{2} \right) y_1'^2 - \text{Fr}_1^2 y_1'^3$
	Transitional Froude number:
	$(\text{Fr}_1)_t = \sqrt{\frac{1 + y_1'}{2y_1'^2}}$

$\text{Fr}_1 = \frac{Q}{\sqrt{gB^2 y_1^3}}$	$y' \equiv \frac{y}{D}$	
---	-------------------------	--

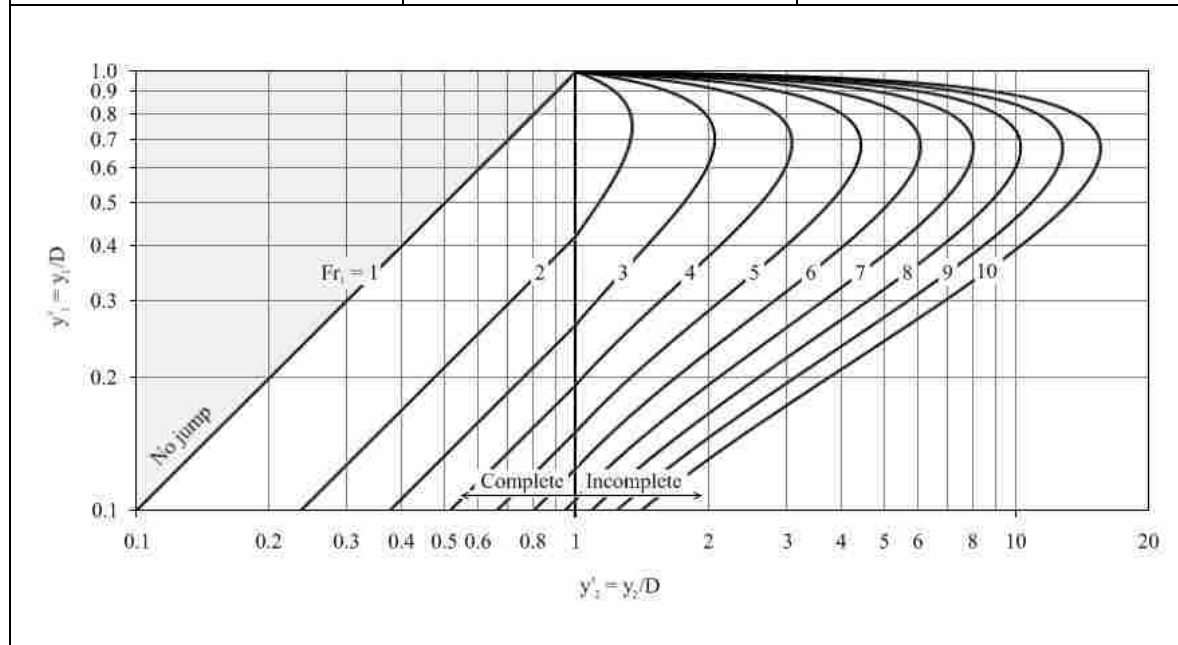
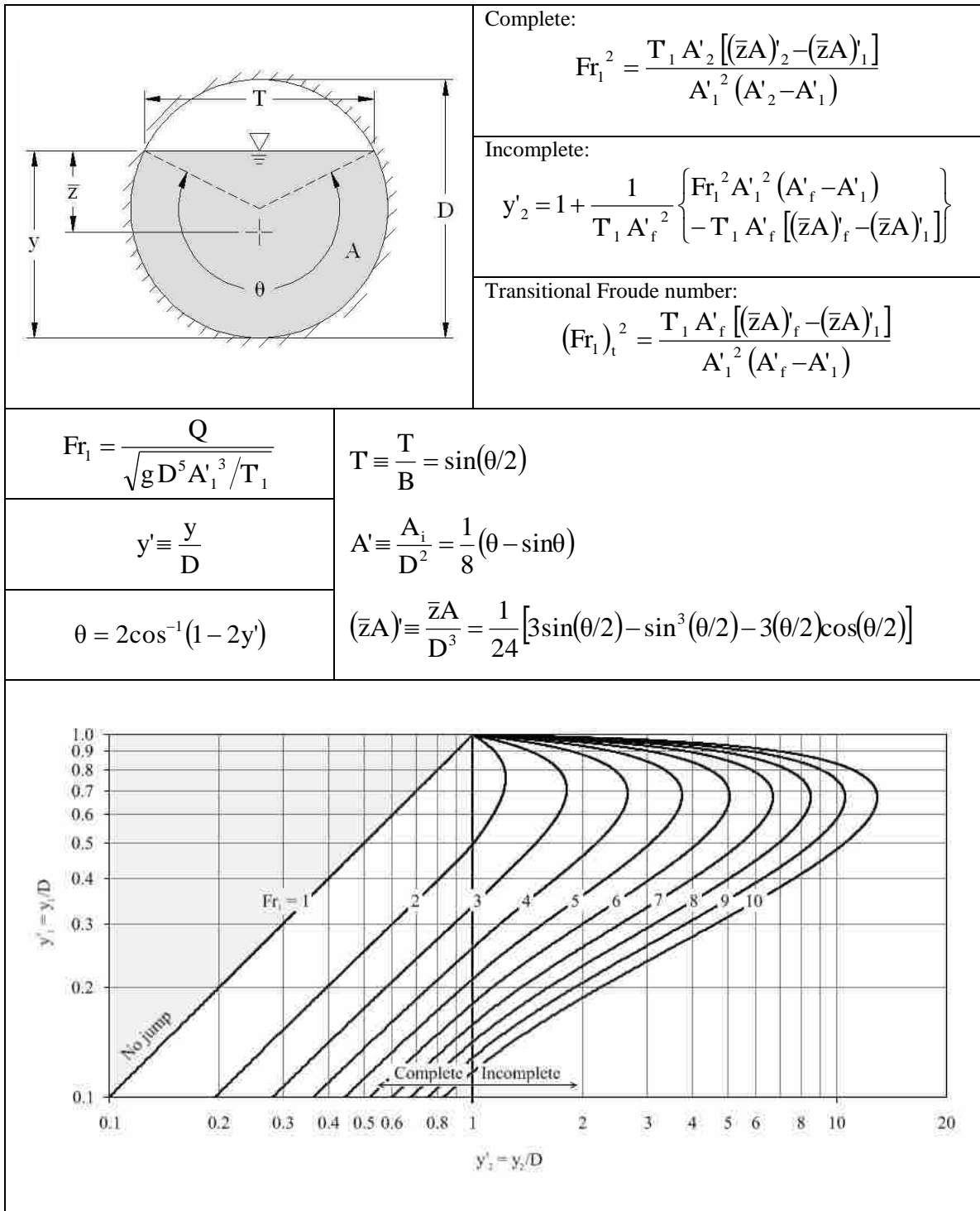
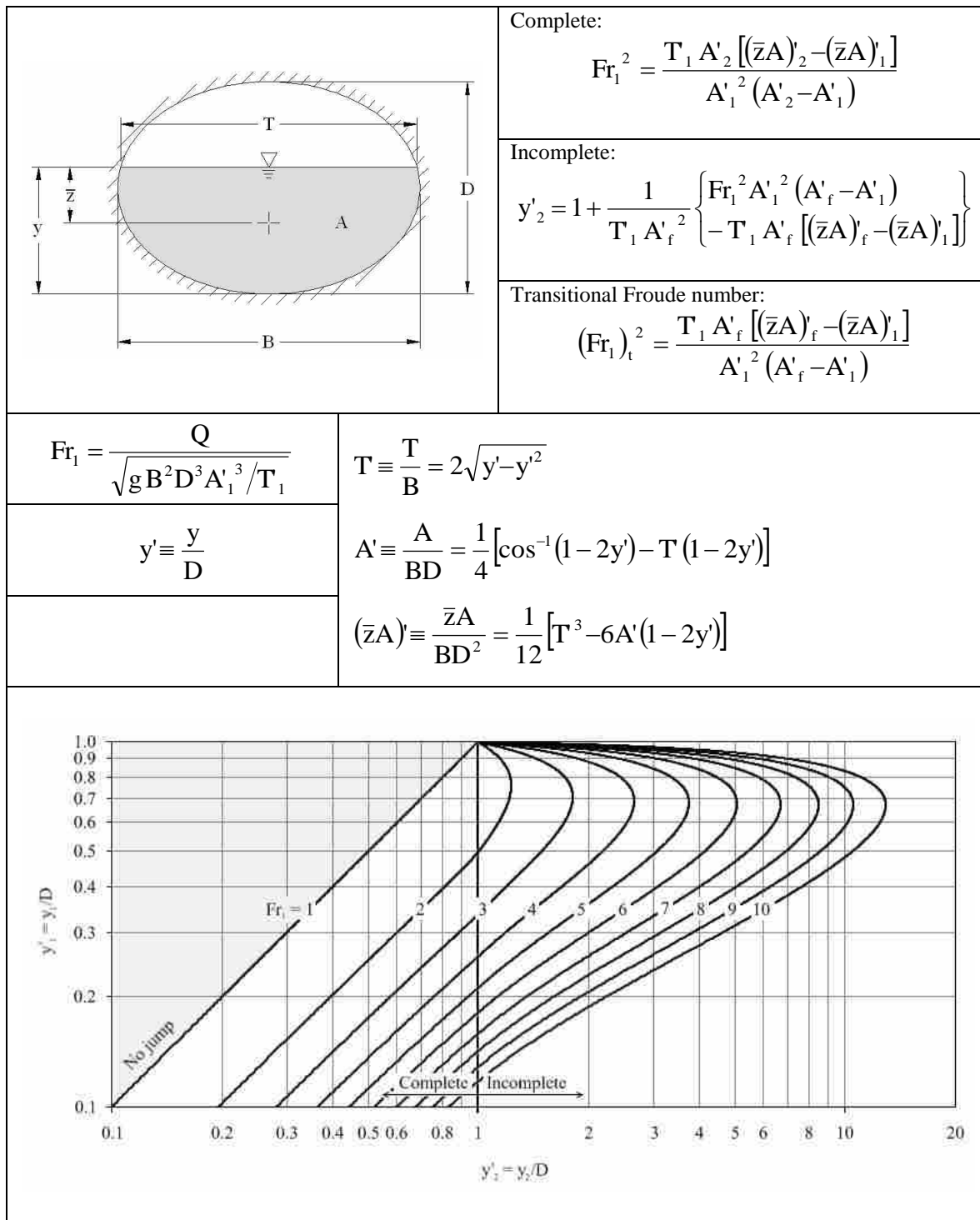


Figure 4-1 Solution for rectangular conduits



**Figure 4-2 Solution for circular conduits**



**Figure 4-3 Solution for elliptical conduits**

	<p>Complete:</p> $Fr_1^2 = \frac{T_1 A'_2 [(\bar{z}A)'_2 - (\bar{z}A)'_1]}{A'_1{}^2 (A'_2 - A'_1)}$
	<p>Incomplete:</p> $y'_2 = 1 + \frac{1}{T_1 A'_f{}^2} \left\{ Fr_1^2 A'_1{}^2 (A'_f - A'_1) - T_1 A'_f [(\bar{z}A)'_f - (\bar{z}A)'_1] \right\}$
	<p>Transitional Froude number:</p> $(Fr_1)_t^2 = \frac{T_1 A'_f [(\bar{z}A)'_f - (\bar{z}A)'_1]}{A'_1{}^2 (A'_f - A'_1)}$
$Fr_1 = \frac{Q}{\sqrt{g B^2 D^3 A'_1{}^3 / T_1}}$	
$T = \sum T_i = \begin{cases} \Gamma_b  ^{y'} & \text{for } 0 < y' \leq h'_b \\ \Gamma_{m1}  ^{y'} + \Gamma_{m2}  ^{y'} & \text{for } h'_b < y' \leq h'_t \\ \Gamma_t  ^{y'} & \text{for } h'_t < y' \leq 1 \end{cases}$	
$A' = \sum A'_i = \begin{cases} \Omega_b  ^{y'} & \text{for } 0 < y' \leq h'_b \\ \Omega_b  ^{h'_b} + \Omega_{m1}  _{h'_b}^{y'} + \Omega_{m2}  _{h'_b}^{y'} & \text{for } h'_b < y' \leq h'_t \\ \Omega_b  ^{h'_b} + \Omega_{m1}  _{h'_b}^{h'_t} + \Omega_{m2}  _{h'_b}^{h'_t} + \Omega_t  _{h'_t}^{y'} & \text{for } h'_t < y' \leq 1 \end{cases}$	
$(\bar{z}A)' = \sum (\bar{z}A)'_i = \begin{cases} \Psi_b  ^{y'} & \text{for } 0 < y' \leq h'_b \\ \Psi_b  ^{h'_b} + (y' - h'_b) \Omega_b  ^{h'_b} + \Psi_{m1}  _{h'_b}^{y'} - (y' - h'_b) \Omega_{m1}  _{h'_b}^{y'} + \Psi_{m2}  _{h'_b}^{y'} - (y' - h'_b) \Omega_{m2}  _{h'_b}^{y'} & \text{for } h'_b < y' \leq h'_t \\ \Psi_b  ^{h'_b} + (y' - h'_b) \Omega_b  ^{h'_b} + \Psi_{m1}  _{h'_b}^{h'_t} + (y' - h'_t) \Omega_{m1}  ^{h'_t} - (y' - h'_b) \Omega_{m1}  ^{h'_b} + \Psi_{m2}  _{h'_b}^{h'_t} + (y' - h'_t) \Omega_{m2}  ^{h'_t} - (y' - h'_b) \Omega_{m2}  ^{h'_b} + \Psi_t  _{h'_t}^{y'} - (y' - h'_t) \Omega_t  ^{h'_t} & \text{for } h'_t < y' \leq 1 \end{cases}$	

Figure 4-4 Solution for pipe arch culverts

$\Gamma_b(y') = 2\left(\frac{R'_b}{B'}\right)\sin(\theta_b/2)$ $\Omega_b(y') = \frac{R'_b{}^2}{2B'}(\theta_b - \sin\theta_b)$ $\Psi_b(y') = \frac{R'_b{}^3}{3B'}\left[3\sin(\theta_b/2) - \sin^3(\theta_b/2)\right]$ $\theta_b = 2\cos^{-1}\left(1 - \frac{y'}{R'_b}\right)$	$\Gamma_{m2}(y') = 2\left(\frac{R'_m}{B'}\right)\sin(\theta_m/2)$ $\Omega_{m2}(y') = \frac{R'_m{}^2}{2B'}(\theta_m - \sin\theta_m)$ $\Psi_{m2}(y') = \frac{R'_m{}^3}{3B'}\left[3\sin(\theta_m/2) - \sin^3(\theta_m/2)\right]$ $\theta_m = 2\cos^{-1}\left(1 - \frac{1}{R'_m}(y' - h'_m + R'_m)\right)$
$\Gamma_{m1}(y') = \frac{1}{B'}(B' - 2R'_m)$ $\Omega_{m1}(y') = \frac{1}{B'}(B' - 2R'_m)(y' - h'_m + R'_m)$ $\Psi_{m1}(y') = \frac{1}{2B'}(B' - 2R'_m)(y' - h'_m + R'_m)^2$	$\Gamma_t(y') = 2\left(\frac{R'_t}{B'}\right)\sin(\theta_t/2)$ $\Omega_t(y') = \frac{R'_t{}^2}{2B'}(\theta_t - \sin\theta_t)$ $\Psi_t(y') = \frac{R'_t{}^3}{3B'}\left[3\sin(\theta_t/2) - \sin^3(\theta_t/2)\right]$ $\theta_t = 2\cos^{-1}\left(\frac{1 - y'}{R'_t} - 1\right)$
$y' \equiv \frac{y}{D}$	$R'_t \equiv \frac{R_t}{D} = \frac{B(4R_m - B) - 4(D - h_m)^2}{8(R_m - D + h_m)}$
$B' \equiv \frac{B}{D}$	$h'_b \equiv \frac{h_b}{D} = R_b \left(\frac{h_m - R_m}{R_b - R_m}\right)$
$R'_b \equiv \frac{R_b}{D}$	$h'_m \equiv \frac{h_m}{D} = R_b - \sqrt{(R_b - R_m)^2 - (B/2 - R_m)^2}$
$R'_m \equiv \frac{R_m}{D}$	$h'_t \equiv \frac{h_t}{D} = D - R_t \left(1 - \frac{\sqrt{(R_t - R_m)^2 - (B/2 - R_m)^2}}{(R_t - R_m)}\right)$

Figure 4-4 (cont.) Solution for pipe arch culverts

	<p>Complete:</p> $Fr_1^2 = \frac{T_1 A'_2 [(\bar{z}A)'_2 - (\bar{z}A)'_1]}{A'_1{}^2 (A'_2 - A'_1)}$	
	<p>Incomplete:</p> $y'_2 = 1 + \frac{1}{T_1 A'_f{}^2} \left\{ Fr_1^2 A'_1{}^2 (A'_f - A'_1) - T_1 A'_f [(\bar{z}A)'_f - (\bar{z}A)'_1] \right\}$	
	<p>Transitional Froude number:</p> $(Fr_1)_t^2 = \frac{T_1 A'_f [(\bar{z}A)'_f - (\bar{z}A)'_1]}{A'_1{}^2 (A'_f - A'_1)}$	
$Fr_1 = \frac{Q}{\sqrt{g B^2 D^3 A'_1{}^3 / T_1}}$	$\left. \begin{aligned} T &\equiv \frac{T}{B} = \sum_{i=1}^{n-1} T_i \\ A' &\equiv \frac{A}{BD} = \sum_{i=1}^{n-1} A'_i \\ (\bar{z}A)' &\equiv \frac{\bar{z}A}{BD^2} = \sum_{i=1}^{n-1} (\bar{z}A)'_i \end{aligned} \right\} \text{(see next page)}$	
$B = x_{i=n}$		
$D = ((y_t)_i)_{\max}$		
$y' \equiv \frac{y}{D}$	$x'_i \equiv \frac{x_i}{B}$	
$(h'_A)_i \equiv \frac{(h_A)_i}{D} = \frac{1}{D} \min((y_b)_i, (y_b)_{i+1})$	$(h'_C)_i \equiv \frac{(h_C)_i}{D} = \frac{1}{D} \min((y_t)_i, (y_t)_{i+1})$	
$(h'_B)_i \equiv \frac{(h_B)_i}{D} = \frac{1}{D} \max((y_b)_i, (y_b)_{i+1})$	$(h'_D)_i \equiv \frac{(h_D)_i}{D} = \frac{1}{D} \max((y_t)_i, (y_t)_{i+1})$	

**Figure 4-5 Solution for user-defined culverts**



$\mathbf{T}'_i = \begin{cases} 0 & \text{for } (0 < y' \leq (h'_A)_i) \\ (x'_{i+1} - x'_i) \left( \frac{y' - (h'_A)_i}{(h'_B)_i - (h'_A)_i} \right) & \text{for } ((h'_A)_i < y' \leq (h'_B)_i) \\ x'_{i+1} - x'_i & \text{for } ((h'_B)_i < y' \leq (h'_C)_i) \\ (x'_{i+1} - x'_i) \left( \frac{(h'_D)_i - y'}{(h'_D)_i - (h'_C)_i} \right) & \text{for } ((h'_C)_i < y' \leq (h'_D)_i) \\ 0 & \text{for } ((h'_D)_i < y') \end{cases}$	
$\mathbf{A}'_i = \begin{cases} 0 & \text{for } (0 < y' \leq (h'_A)_i) \\ \frac{1}{2} \mathbf{T}'_i (y' - (h'_A)_i) & \text{for } ((h'_A)_i < y' \leq (h'_B)_i) \\ \frac{1}{2} \mathbf{T}'_i [(y' - (h'_A)_i) + (y' - (h'_B)_i)] & \text{for } ((h'_B)_i < y' \leq (h'_C)_i) \\ \frac{1}{2} \left\{ (x'_{i+1} - x'_i) [(y' - (h'_A)_i) + (y' - (h'_B)_i)] \right. \\ \left. - (x'_{i+1} - x'_i - \mathbf{T}'_i)(y' - (h'_C)_i) \right\} & \text{for } ((h'_C)_i < y' \leq (h'_D)_i) \\ \frac{1}{2} (x'_{i+1} - x'_i) [(h'_D)_i + (h'_C)_i - (h'_B)_i - (h'_A)_i] & \text{for } ((h'_D)_i < y') \end{cases}$	
$(\bar{\mathbf{Z}}\mathbf{A})'_i = \begin{cases} 0 & \text{for } (0 < y' \leq (h'_A)_i) \\ \frac{1}{6} \mathbf{T}'_i (y' - (h'_A)_i)^2 & \text{for } ((h'_A)_i < y' \leq (h'_B)_i) \\ \frac{1}{6} \mathbf{T}'_i [(y' - (h'_A)_i)^2 + (y' - (h'_A)_i)(y' - (h'_B)_i) + (y' - (h'_B)_i)^2] & \text{for } ((h'_B)_i < y' \leq (h'_C)_i) \\ \frac{1}{6} \left\{ (x'_{i+1} - x'_i) \left[ \begin{aligned} &(y' - (h'_A)_i)^2 + (y' - (h'_B)_i)^2 \\ &+ (y' - (h'_A)_i)(y' - (h'_B)_i) \end{aligned} \right] \right. \\ \left. - (x'_{i+1} - x'_i - \mathbf{T}'_i)(y' - (h'_C)_i)^2 \right\} & \text{for } ((h'_C)_i < y' \leq (h'_D)_i) \\ \frac{1}{6} (x'_{i+1} - x'_i) \left[ \begin{aligned} &3y'((h'_D)_i + (h'_C)_i - (h'_B)_i - (h'_A)_i) \\ &+ ((h'_A)_i)^2 + (h'_A)_i(h'_B)_i + (h'_B)_i^2 \\ &- ((h'_C)_i)^2 + (h'_C)_i(h'_D)_i + (h'_D)_i^2 \end{aligned} \right] & \text{for } ((h'_D)_i < y') \end{cases}$	

**Figure 4-5 (cont.) Solution for user-defined culverts**

## 5 Discussion and Analysis

This chapter discusses both generally and individually the solutions presented in the previous chapter. It also presents the results of an error analysis performed on the simplification of the elliptical conduit solution. Further discussion and analysis is included in Appendix B.

### 5.1 General Observations

As noted previously, the solutions presented in this study resemble those developed by Montes (1998), where  $y'_2$  is on the x-axis,  $y'_1$  is on the y-axis, and the relationship between the two is given for different values of  $Fr_1$ . One reason for this particular formatting convention is to reiterate that although  $y_2$  is treated as the unknown in all cases, it is not the dependant variable. Rather, all three variables are independent of each other, and specific combinations of the three define the occurrence, size, and location of a hydraulic jump. Like Montes' charts, these display solutions for upstream Froude numbers as high as 10; however in practice Froude numbers are typically much smaller for flow within relatively flat conduits.

The left side of the charts (i.e.  $y'_2 < 1$ ) indicates free-surface flow conditions. Note that for all conduit shapes, critical flow (i.e.  $Fr_1 = 1$ ) produces a straight line corresponding to  $y'_1 = y'_2$ . To the top-left of this line, flow is subcritical and jumps

cannot exist, and to the bottom-right of this line, any jump will be a complete jump. The right side of the charts (i.e.  $y'_2 > 1$ ) indicates pressure flow conditions, and any jump in this region will be an incomplete jump. Note that for all conduit shapes and all values of  $Fr_1$ ,  $y'_2$  increases as  $y'_1$  approaches approximately  $2/3$ , but decreases dramatically as  $y'_1$  approaches 1, converging to a single point at  $y'_1 = y'_2 = 1$ . This indicates that no jump occurs at all when a conduit is flowing full, as observed by Smith and Chen (1989).

## 5.2 Rectangular Conduits

By comparison between sequent depth charts, it is evident that rectangular conduits produce higher values of  $y'_2$  than other conduit shapes, given similar values of  $y'_1$  and  $Fr_1$ . This means that among all possible conduit shapes passing flow at identical depths and Froude numbers, the rectangular conduit will require the highest tailwater to induce a hydraulic jump. Producing a sustained high tailwater can be challenging, so nonrectangular conduits may be preferable to rectangular ones whenever an alternative is possible.

## 5.3 Circular Conduits

The only noteworthy observation of the solution for circular conduits is that it matches the analysis given by Montes, with the exception that it is given in terms of the conduit diameter instead of the radius for continuity; they differ exactly by a factor of two. The circular analysis unitizes the commonly-used intermediate variable  $\theta$ , which is defined as the internal angle of flow (radians).

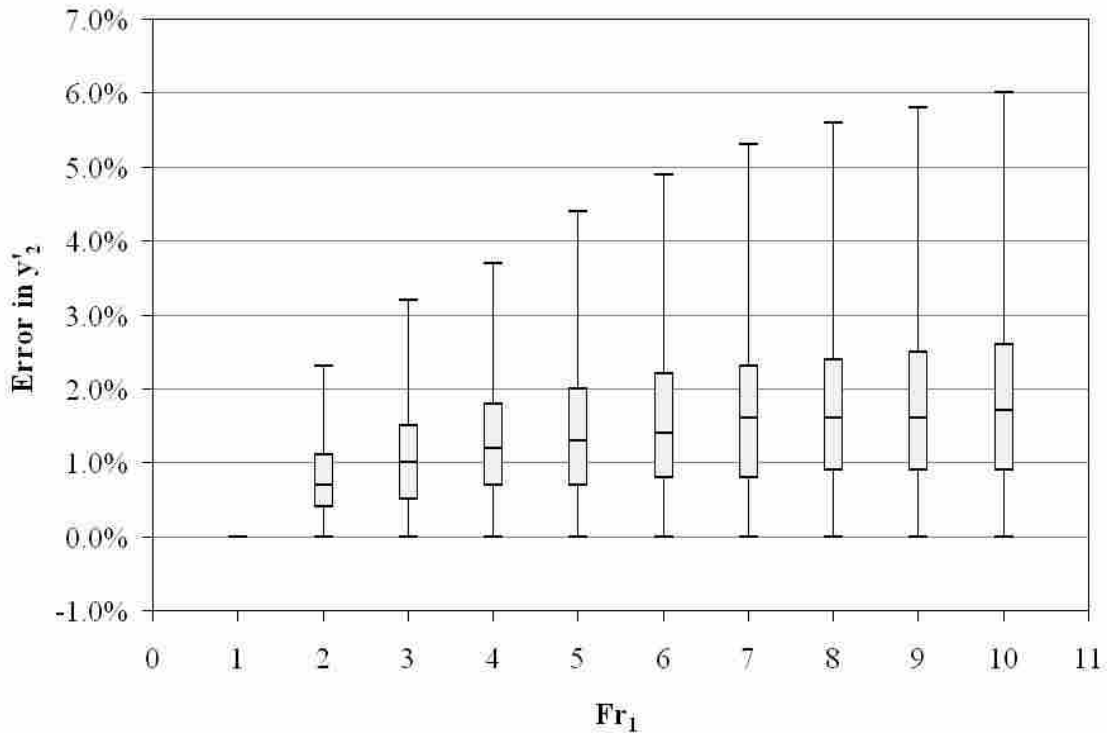
## 5.4 Elliptical Conduits

The solution for elliptical conduits results in a sequent depth chart that is identical to the one developed for circular conduits, even though the two are derived completely differently. This is to be expected, since the elliptical functions for  $T'$ ,  $A'$ , and  $(\bar{z}A)'$  are an alternative method used for circular conduits (Hjelmfeldt 1967; Hager 1999), where the span and rise are both equal to the diameter. Since both sets of functions are dimensionless, it does not matter whether the span and rise or the diameter is used, so circular conduits can simply be considered a unique type of elliptical conduit.

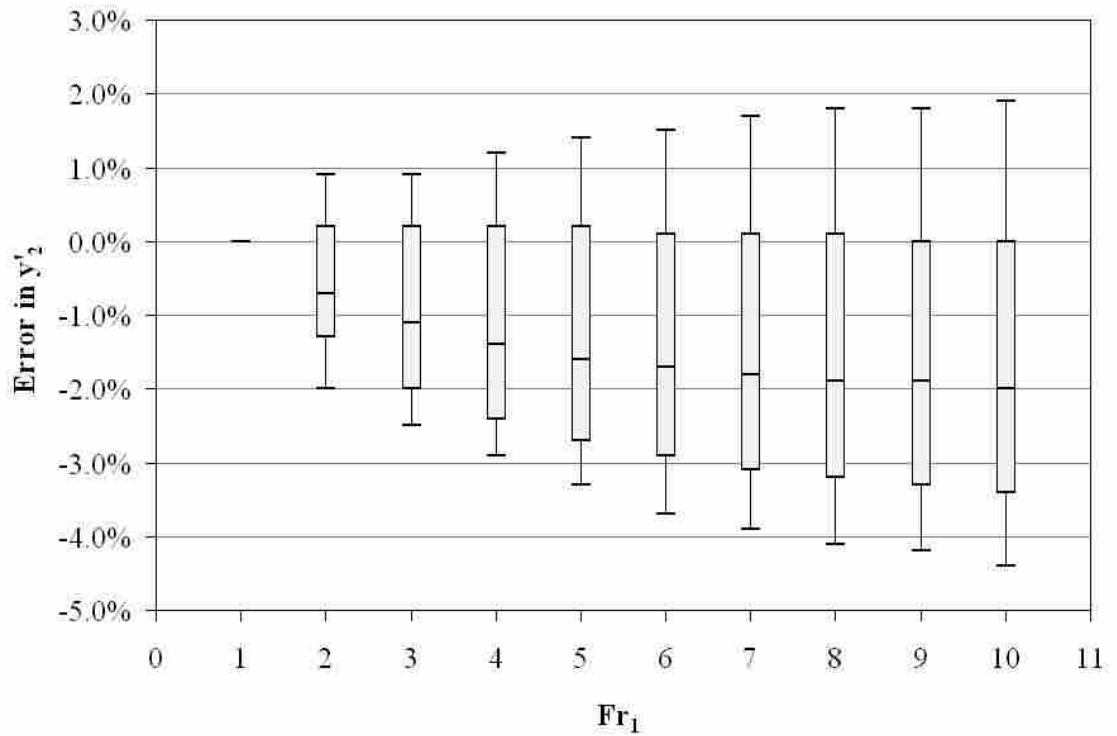
It should be noted here that elliptical culverts are not truly mathematically elliptical; rather, they are typically defined by a span, rise, and two radii (ASTM C507 2007). Elliptical culverts may be treated in a similar fashion to pipe arches (see Appendix A.7), but this would require a unique, complex solution for each culvert shape. By assuming elliptical culverts to be mathematically elliptical, only one solution is required and the computation for that solution is reduced considerably. The solution for elliptical conduits presented in the previous chapter is based upon this simplification.

However, like any assumption this simplified solution introduces error, which may be undesirable to potential users depending on the accuracy required. To quantify this error, an analysis was therefore performed, in which 1,000 solutions were generated for each of 102 unique culvert sizes (79 metal and 23 concrete), and for each integer Froude number between 1 and 10, using the complex logic typically reserved for pipe arches. The relative error between each of these solutions and the corresponding simplified solutions was then calculated. Finally, the number of solutions that fell within specified error ranges, each with a bin size of 0.1%, was cumulatively tabulated for all

culvert sizes. The results of this analysis, in the form of box and whisker plots, are displayed by culvert material and Froude number in Figures 13 and 14 below. As the figures indicate, if an elliptical culvert is assumed to be mathematically elliptical, the error in  $y'_2$  generally increases with the upstream Froude number, as might be expected. It is also evident from these plots that the simplifying assumption generally overestimates  $y'_2$  for the metal elliptical culvert shapes, but underestimates it for the concrete ones. For Froude numbers less than 5, the error is expected to fall between 0.0 and 4.4% in the case of metal elliptical culverts, and between -3.3 and 1.4% in the case of concrete ones.



**Figure 5-1 Error distribution of ellipse assumption for metal elliptical culverts**



**Figure 5-2 Error distribution of ellipse assumption for concrete elliptical culverts**

## 5.5 Pipe Arch Culverts

The solution for pipe arch culverts is obviously far more involved than any of the previous shapes, due to its geometric complexity. Because so many unique shapes of pipe arches are currently in use, it would be impossible to accurately generalize them with one sequent depth chart. At the same time it is impractical to generate a unique solution for each one. As previously mentioned, an example chart was generated to demonstrate the possibility of generating such a chart, but it would be far simpler to use the formulas provided to obtain a single solution than to derive a complete chart from many. Another alternative would be to treat the pipe arch as a user-defined conduit, but

this would require the additional effort of defining the set of coordinates, without significantly simplifying the computation required. In short, pipe arches are complicated to analyze.

## 5.6 User-Defined Conduits

The solution for user-defined conduits in some ways is just as complex as that for pipe arch culverts. Note that  $B$  and  $D$  must be derived from the coordinates, and that the values for  $T'_i$ ,  $A'_i$ , and  $(\bar{z}A)'_i$  depend on the location of  $y'$  relative to the intermediate variables  $h'_A$ ,  $h'_B$ ,  $h'_C$ , and  $h'_D$ . However, the advantage of this solution is that it may be applied to any conduit shape, as long as the coordinates are defined properly. As previously noted, an example set of coordinates were used to test this solution, defining an inverted egg shape. The chart generated from this set of coordinates matched the one developed by Montes exactly, demonstrating the validity of a numerical approximation.

Obviously, the more coordinates used, the closer this approximation will be to the actual shape and the more accurate the solution will be. However, more iterations will also be required to find the solution. A user must therefore decide how many coordinates are necessary to define a particular shape in order to predict the subcritical sequent depth with sufficient accuracy in a given situation.

## **6 Summary and Application**

The purpose of this study was to develop general solutions for finding the subcritical sequent depth of complete and incomplete hydraulic jumps within prismatic conduits of any shape. A review of the theory and methodology behind these solutions was presented, and solutions were derived for rectangular, circular, elliptical, pipe arch, and user-defined conduits, based on the methodology of Montes (1998). A procedure for applying these solutions was given, and the significance and implications of the solutions were also discussed. The results are valid for small slopes, and conservatively neglect the effects of friction and air entrainment, as these factors lie beyond the scope of this study.

The solutions presented herein are intended to be used primarily by culvert designers. By forcing a jump to occur within the culvert barrel, an engineer may considerably reduce the cost of downstream energy dissipation. In order to choose an efficient and cost-effective design, however, it is necessary to determine the size and location of a potential hydraulic jump for a given flow rate, regardless of whether or not the outlet is submerged. These solutions may therefore be used to determine the theoretical subcritical sequent depth of supercritical flow through culverts, from which the length and location of the jump may be subsequently calculated.





## References

- Advani, R. M. (1962). "A New Method for Hydraulic Jump in Circular Channels." *Water Power*, 14(9), 349-350.
- American Iron & Steel Institute. (1999). *Modern Sewer Design, 4th Ed.* American Iron & Steel Institute, Washington, D. C.
- American Society for Testing and Materials (ASTM) C506. (2007). "Standard Specification for Reinforced Concrete Arch Culvert, Storm Drain, and Sewer Pipe." *ASTM International*, 02.02 358-364.
- American Society for Testing and Materials (ASTM) C507. (2007). "Standard Specification for Reinforced Concrete Elliptical Culvert, Storm Drain, and Sewer Pipe." *ASTM International*, 02.02 372-380.
- Aryopoulos, P. A. (1962). "General Solution of the Hydraulic Jump in Sloping Channels." *Journal of the Hydraulics Division*, 88(HY4), 61-75.
- Ayoub, S. A. I. (1959). *Characteristics of the Hydraulic Jump In Sloping Circular Conduits*. PhD thesis, Colorado State University, Fort Collins, CO.
- Beirami, M. K., and Chamani, M. R. (2006). "Hydraulic Jumps in Sloping Channels: Sequent Depth Ratio." *Journal of Hydraulic Engineering*, 132(10), 1061-1068.
- Bradley, J. N., and Peterka, A. J. (1957). "The Hydraulic Design of Stilling Basins: Hydraulic Jumps on a Horizontal Apron." *Journal of the Hydraulics Division*, 83(HY5), 12-24.
- Bremen, R., and Hager, W. H. (1993). "T-Jump in Abruptly Expanding Channel." *Journal of Hydraulic Research*, 31(1), 61-78.
- Bushra, A., and Noor, A. (2006). "Hydraulic Jump in Circular and U-Shaped Channels." *Journal of Hydraulic Research*, 44(4), 567-576.
- Caric, D. M. (1977). "Flow in Circular Conduits." *Water Power and Dam Construction*, 29(11), 29-33.

- Carollo, F. G., Ferro, V., and Pampalone, V. (2007). "Hydraulic Jumps on Rough Beds." *Journal of Hydraulic Engineering*, 133(9), 989-999.
- Chadwick, A., Morfett, J., and Borthwick, M. (2004). *Hydraulics in Civil and Environmental Engineering, 4th Ed.* Spon Press, London.
- Chow, V. T. (1959). *Open Channel Hydraulics*. McGraw-Hill, New York.
- CONTECH. (2007). *Structural Plate Design Guidelines*. CONTECH Bridge Solutions, Inc., West Chester, OH.
- Ead, S. A., and Rajaratnam, N. (2002). "Hydraulic Jumps on Corrugated Bends." *Journal of Hydraulic Engineering*, 138(7), 656-663.
- Federal Highway Administration (FHWA), and Aquaveo, L. (2007). "HY-8." 7.1.
- Frank, J. (1942). "Schiessen und Strömen im Kreisquerschnitt." *Wasserkraft Und Wasserwirtschaft*, 37(2), 25-29.
- Franzini, J. B., and Finnemore, E. J. (1997). *Fluid Mechanics with Engineering Applications, 9th Ed.* McGraw-Hill, Boston.
- French, R. H. (1985). *Open Channel Hydraulics*. McGraw-Hill, New York.
- Gill, M. A. (1980). "Effect of Boundary Roughness on Hydraulic Jump." *Water Power and Dam Construction*, 32(1), 22-24.
- Gunal, M., and Narayanan, R. (1996). "Hydraulic Jump in Sloping Channels." *Journal of Hydraulic Engineering*, 132(8), 436-442.
- Hager, W. H. (1999). *Wastewater Hydraulics*. Springer-Verlag, Berlin.
- Hager, W. H. (1992). *Energy Dissipators and Hydraulic Jump*. Kluwer Academic Publishers, Dordrecht, The Netherlands.
- Hager, W. H. (1990). "Basiswerte der Kanisations-Hydraulik (Basic Values of Hydraulic Sewers)." *Gas-Wasser Abwasser*, 70(11), 785-787.
- Hager, W. H., and Bremen, R. (1989). "Classical Hydraulic Jump: Sequent Depths." *Journal of Hydraulic Research*, 27(5), 565-585.
- Hager, W. H., Bremen, R., and Kawagoshi, N. (1990). "Classical Hydraulic Jump: Length of Roller." *Journal of Hydraulic Research*, 28(5), 591-608.
- Haindl, K. (1957). "Hydraulic Jumps in Closed Conduits." *Proceedings of the International Association for Hydraulic Research*, Delft, Holland, D32-1 to D32-12.
- Haindl, K., and Sotornik, V. (1957). "Quantity of air drawn into a conduit by the hydraulic jump and its measurement by gamma-radiation." *Proceedings of the*

- International Association for Hydraulics Research*, Vol. 2, Lisbon, Spain, D31.1-D31.7.
- Harleman, D. R. F. (1959). "Discussion to Rouse, et al." *Transactions of the American Society of Civil Engineers*, 124 959-962.
- Hibbeler, R. C. (2001). *Engineering Mechanics: Statics, 9th Ed.* Prentice-Hall, Inc., Upper Saddle River, NJ.
- Hjelmfeldt, A. T. (1967). "Flow in Elliptical Channels." *Water Power*, 19(10), 429-431.
- Hotchkiss, R. H., Flanagan, P. J., and Donahoo, K. (2003). "Hydraulic Jumps in Broken-Back Culverts." *Transportation Research Record*, 1851 35-44.
- Hotchkiss, R. H., Larson, E. A., and Admiraal, D. A. (2005). "Energy Dissipation in Culverts by Forced Hydraulic Jump Within a Barrel." *Transportation Research Record*, 1904 124-132.
- Hsu, S. T., Wang, J. S., and Elder, R. A. (1980). "Hydraulic Designs of Open-Channel Flows in Circular Conduits." *International Conference on Water Resources Development*, Taipei, Taiwan, 1019-1031.
- Hughes, W. C., and Flack, J. E. (1984). "Hydraulic Jump Properties Over a Rough Bed." *Journal of Hydraulic Engineering*, 110(12), 1755-1771.
- Husain, D., Alhamid, A. A., and Negm, A. M. (1994). "Length and Depth of Hydraulic Jump in Sloping Channels." *Journal of Hydraulic Research*, 32(6), 899-910.
- Jeppson, R. W. (1970). "Graphical Solution to Hydraulic Jump." *Journal of the Hydraulics Division*, 96(HY1), 103-108.
- Kalinske, A. A., and Robertson, J. M. (1943). "Closed Conduit Flow." *Transactions of the American Society of Civil Engineers*, 108 1435-1447.
- Kinsvatar, C. E. (1944). "The Hydraulic Jump in Sloping Channels." *Transactions of the American Society of Civil Engineers*, 109 1107-1154.
- Lane, E. W., and Kinsvatar, C. E. (1938). "Hydraulic Jump in Enclosed Conduits." *Engineering News-Record*, Dec. 29 815-817.
- Leutheusser, H. J., and Birk, W. M. (1991). "Drownproofing of Low Outflow Structures." *Journal of Hydraulic Engineering*, 117(2), 205-213.
- Matsushita, F. (1989). "On the Hydraulic Jump in a Downward Sloping Closed Conduit." *Transactions of the Japanese Society of Irrigation Drainage and Reclamation Engineering*, 144 33-42.

- Mavis, F. T. (1946). "Critical Flow in Circular Conduits Analyzed by Nomagraph." *Engineering News-Record*, 136(3), 361-362.
- Mehrotra, S. C. (1976). "Length of Hydraulic Jump." *Journal of the Hydraulics Division*, 102(7), 1027-1033.
- Montes, S. (1998). *Hydraulics of Open-Channel Flow*. ASCE Press, Reston, VA.
- Moore, W. L., and Morgan, C. W. (1957). "The Hydraulic Jump at an Abrupt Drop." *Journal of the Hydraulics Division*, 83(HY6), 1-21.
- Negm, A. M. (2000). "Generalization of Belanger Equation." [http://kfki.baw.de/fileadmin/conferences/ICHE/2000-Seoul/pdf/1/PAP\\_015.pdf](http://kfki.baw.de/fileadmin/conferences/ICHE/2000-Seoul/pdf/1/PAP_015.pdf) (6/22, 2007).
- Normann, J. M., Houghtalen, R. J., and Johnson, W. J. (1985). *Hydraulic Design Series No. 5, 2nd Ed. - Hydraulic Design of Highway Culverts*. Federal Highway Administration, Washington, D. C.
- Ohtsu, I., and Yasuda, Y. (1991b). "Transition from Supercritical to Subcritical Flow at an Abrupt Drop." *Journal of Hydraulic Research*, 29(3), 309-338.
- Ohtsu, I., and Yasuda, Y. (1991a). "Hydraulic Jump on Sloping Channels." *Journal of Hydraulic Engineering*, 117(7), 905-921.
- Ohtsu, I., Yasuda, Y., and Gotoh, H. (2001). "Hydraulic Condition for Undular-Jump Formations." *Journal of Hydraulic Research*, 39(2), 203-209.
- Ohtsu, I., Yasuda, Y., and Ishikawa, M. (1999). "Submerged Hydraulic Jumps Just Below Abrupt Expansions." *Journal of Hydraulic Engineering*, 135(5), 492-499.
- Rajaratnam, N. (1968a). "Hydraulic Jumps Below Abrupt Symmetrical Expansions." *Journal of the Hydraulics Division*, 94(HY2), 481-503.
- Rajaratnam, N. (1968b). "Hydraulic Jumps on Rough Beds." *Transactions of the Engineering Institute of Canada*, 11(A-2), 1-8.
- Rajaratnam, N. (1967). "Hydraulic Jumps." *Advances in Hydrosience*, Vol. 4, V. T. Chow, ed., Academic Press, New York, 197-280.
- Rajaratnam, N. (1965). "Hydraulic Jump in Horizontal Conduits." *Water Power and Dam Construction*, 17(2), 80-83.
- Rajaratnam, N. (1964). "The Forced Hydraulic Jump." *Water Power*, 16(2), 14-19 and 61-65.
- Serre, M. (1950). "Transition from Free Surface Flow Under Pressure in Pipes." *La Houille Blanche*, 5(2), 65-67.

- Silvester, R. (1964). "Hydraulic Jump in All Shapes of Horizontal Channels." *Journal of the Hydraulics Division*, 90(HY1), 23-55.
- Smith, C. D. (1989). "The Submerged Hydraulic Jump in an Abrupt Lateral Expansion." *Journal of Hydraulic Research*, 27(2), 257-266-28(3), 387-391.
- Smith, C. D., and Chen, W. (1989). "The Hydraulic Jump in a Steeply Sloping Square Conduit." *Journal of Hydraulic Research*, 27(3), 385-399.
- Stahl, H., and Hager, W. H. (1999). "Hydraulic Jump in Circular Pipes." *Canadian Journal of Civil Engineering*, 26 368-373.
- Stevens, J. C. (1933). "The Hydraulic Jump in Standard Conduits: General Formula for Rectangular Channels Extended to Trapezoidal and Curvilinear Sections." *Civil Engineering*, 3(10), 565-567.
- Straub, W. O. (1978). "A Quick and Easy Way to Calculate Critical and Conjugate Depths in Circular Open Channels." *Civil Engineering*, 1978(Dec), 70-71.
- Sturm, T. W. (2001). *Open Channel Hydraulics*. McGraw-Hill, New York.
- Thiruvengadam, A. (1961). "Hydraulic Jump in Circular Channels." *Water Power*, Dec 1961 496-497.
- Thompson, P. L., and Kilgore, R. T. (2006). "Hydraulic Jump." *Hydraulic Engineering Series No. 14, 3rd. Ed. - Hydraulic Design of Energy Dissipators for Culverts and Channels*, Federal Highway Administration, Washington, D. C., 6-1 to 6-14.
- Young, D. F., Munson, B. R., and Okiishi, T. H. (2004). *A Brief Introduction to Fluid Mechanics, 3rd Ed.* John Wiley & Sons, Inc., York, PA.



## **Appendix A. Literature Review**

### **A.1 The Hydraulic Jump**

#### **A.1.1 Description**

The hydraulic jump is an example of rapidly varied flow in which supercritical flow abruptly becomes subcritical, typically due to high tailwater (Chow 1959; Rajaratnam 1967). In this process, the water surface passes upwards through critical depth as kinetic energy is converted to potential energy (Franzini and Finnemore 1997; Thompson and Kilgore 2006). The transition is always accompanied by an energy loss, however, as kinetic energy is converted into turbulence and then into sound and heat (Haindl 1957; Sturm 2001).

Most jumps vary in appearance between two extremes. The first is a fully-developed surface roller, which is characterized by a relatively smooth and continuous water surface, as flow continues along channel bottom and diverges downstream. At this point, bubbles rise intensively to a stagnation point, where flow either proceeds downstream or “rolls” back towards the toe, or beginning, of the jump. The second extreme is a standing wave, in which flow is immediately deflected to the surface at the toe. The toe moves downstream while the end of the jump moves upstream, creating a shorter jump, characterized by heavy surface waves and eruptions (Hager et al. 1990).



### **A.1.2 History and Applications**

The hydraulic jump has many useful applications in hydraulic design. Among these are: (1) to dissipate energy in water flowing over dams, weirs, and other hydraulic structures and thus prevent scouring downstream from the structures; (2) to recover head or raise the water level on the downstream side of a measuring flume and thus maintain high water level in the channel for irrigation or other water-distribution purposes; (3) to increase weight on an apron and thus reduce uplift pressure under a masonry structure by raising the water depth on the apron; (4) to increase the discharge of a sluice by holding back tailwater, since the effective head will be reduced if tailwater is allowed to drown the jump; (5) to indicate special flow conditions, such as the existence of supercritical flow or the presence of a control section so that a gauging station may be located; (6) to mix chemicals used for water purification, and so forth; (7) to aerate water for city water supplies; and (8) to remove air pockets from water-supply lines and thus prevent air locking (Chow 1959).

The turbulence in a hydraulic jump can be highly erosive if proper channel protection is not installed (Hager 1992). In the case of steep culverts, high velocities can induce a hydraulic jump at the outlet, which can scour and erode the natural channel and undercut the culvert (Hotchkiss et al. 2005). It is therefore preferable, when a hydraulic jump is expected, to control the size and location of the jump in order to localize energy dissipation and erosion (Stahl and Hager 1999).

Because of these applications and concerns, hydraulic jumps have been the focus of interest among engineers for almost 200 years, starting with Giorgio Bidone, an Italian, in 1818 (Chow 1959), and then the French hydraulician Jean-Baptiste Bélanger, who developed his famous equation in 1838 relating the supercritical and subcritical

depths to the upstream Froude number (Hager 1999). Comprehensive histories of the study of hydraulic jumps may be found in several hydraulics texts, including Chow (1959), Rajaratnam (1967), Hager (1992), and Montes (1998). For this reason the history is not repeated here, but it should be noted that the main focus of these studies has been to predict the size and location of hydraulic jumps under various channel conditions, so that the hydraulic structures containing them may be designed accordingly.

### **A.1.3 Parameters of Interest**

Typically the flow rate entering a hydraulic jump is already known, as well as the upstream and tailwater depths, which may be determined from water surface profile calculations (Chadwick et al. 2004). Therefore the two main parameters of interest when predicting hydraulic jump behavior are (1) the subcritical sequent depth, and (2) the length of the jump (Thompson and Kilgore 2006). Not only do these parameters describe the size of the jump, but if the subcritical sequent depth is compared to the tailwater profile, the location may be found as well (Chow 1959). Furthermore, once both sequent depths are known, flow areas (and therefore velocities by continuity) may be calculated, from which the energy loss may be determined by Bernoulli's equation (Thompson and Kilgore 2006).

## **A.2 Jump Height**

### **A.2.1 Sequent Depths**

The height of a hydraulic jump is defined by the depths of flow upstream and downstream of the jump. These depths are called "sequent" or "conjugate" depths, not to be confused with "alternate" depths, which have the same specific energy (French 1985;

Franzini and Finnemore 1997; Chow 1959). As noted previously, the upstream sequent depth is supercritical, while the downstream sequent depth is subcritical. This may seem counterintuitive, since the upstream depth is smaller than the downstream depth, but the terms “supercritical” and “subcritical” refer to the Froude number of the flow, which in essence is the ratio of flow velocity to the surface wave celerity, as given by the following equation (Hager 1992; 1999):

$$Fr = \frac{V}{c} = \frac{V}{\sqrt{gd}} = \frac{V}{\sqrt{gA/T}} = \frac{V}{\sqrt{gA/(dA/dy)}} \quad (A-1)$$

where  $V$  is the flow velocity (ft/s, m/s),  $c$  is the wave celerity (ft/s, m/s),  $g$  is the acceleration due to gravity (ft/s<sup>2</sup>),  $d$  is the hydraulic depth (ft, m),  $A$  is the flow area (ft<sup>2</sup>, m<sup>2</sup>),  $T$  is the top width of flow (ft, m), and  $y$  is the maximum depth of flow (ft, m).

If the Froude number is less than 1, then the flow is said to be “subcritical”; the velocity is less than the celerity, and waves can propagate upstream. If the ratio equals 1, then the flow is said to be “critical”; the velocity and celerity are equal, and waves can no longer move upstream. If the ratio is greater than 1, then the flow is said to be “supercritical”; the velocity is greater than the celerity, and all waves move downstream (Hager 1999). With hydraulic jumps, the upstream Froude number largely determines the size and shape of the jump. As the Froude number increases, or as the upstream flow becomes more supercritical, the jump height and energy loss across the jump also increase (Chadwick et al. 2004). Thus the Froude number becomes important to consider when analyzing a hydraulic jump.

### A.2.2 The Momentum Equation

Because of energy losses, the size and location of a hydraulic jump cannot be predicted using the energy equation. However, because momentum is conserved across hydraulic jumps, momentum theory may instead be applied in determining the size and location (Hotchkiss et al. 2003). The general momentum equation, which may be derived from the Reynolds Transport Theorem, states that “the vector sum of forces acting on the control volume is equal to the time rate of change of linear momentum inside the control volume plus the net momentum flux out of the control volume through the control surface.” (Thompson and Kilgore 2006) Mathematically, this may be written as:

$$\sum \vec{F} = \frac{d}{dt} \int_{cv} \vec{V} \rho dV + \int_{cs} \vec{V} \rho (\vec{V} \cdot \vec{n}) dA \quad (A-2)$$

In essence, this is Newton’s second law applied to a fluid within a control volume. If the flow is assumed to be steady (i.e.  $\frac{d}{dt} \int_{cv} \vec{V} \rho dV = 0$ ), and if the flow velocity entering and exiting the control volume is assumed to be perpendicular to the control surface (i.e.  $\vec{V} \parallel \vec{n}$ ), and if the streamwise direction of flow is considered exclusively, then taking into account continuity (i.e.  $Q = VA$ ), the momentum equation may be rewritten as:

$$\sum F_s = \sum (\beta \rho Q V_s)_{out} - \sum (\beta \rho Q V_s)_{in} \quad (A-3)$$

where  $F_s$  represents the external forces (lbs, N) acting on the body of fluid with a control volume in the streamwise direction,  $\beta$  is the Boussinesq velocity distribution coefficient

to account for nonuniform velocity distribution,  $\rho$  is the density (slugs/ft<sup>3</sup>, kg/m<sup>3</sup>) of the fluid,  $Q$  is the flow rate (cfs, cms), and  $V_s$  is the flow velocity (ft/s, m/s) in the streamwise direction (Sturm 2001). In simpler terms, the momentum equation states that "the change in momentum of the entering and exiting stream is balanced by the resultant of the forces acting on the control volume" (Thompson and Kilgore 2006).

In the absence of other forces, the left side of Equation A-3 includes only hydrostatic pressure forces acting on the control surface on the upstream and downstream sides of the control volume. This allows the momentum equation to be rewritten in terms of "specific force", which is the sum of the pressure force and the momentum flux at one of the control surfaces. If the subscripts '1' and '2' are used to denote the upstream and downstream sides, respectively, then:

$$\bar{z}_1 A_1 + \frac{Q^2}{gA_1} = \bar{z}_2 A_2 + \frac{Q^2}{gA_2} \quad (\text{A-4})$$

where  $A$  is the cross-sectional area (ft<sup>2</sup>, m<sup>2</sup>), and  $\bar{z}$  is the distance (ft, m) from the water surface to the centroid of the cross-sectional area (Sturm 2001); both are functions of the channel shape and flow depth. This means that when the assumptions stated above apply, the specific force remains constant across a control volume (Hager 1999). If the specific force is plotted against depth for a given flow rate, a plot similar to the specific energy diagram may be obtained, showing that specific force, like specific energy, reaches a minimum at critical depth (Sturm 2001).

The hydraulic jump is an ideal candidate for the application of momentum theory, because a "precise mathematical description of the internal flow pattern is not possible"

due to its complexity (Sturm 2001). The stability of a jump depends entirely upon the equilibrium between the momentum flux across the jump, and the external forces acting upon it, that is, if  $y_1$ ,  $y_2$ , and  $Q$  conform to the relationship given in Equation A-4 (Chadwick et al. 2004). If the tailwater increases, the hydrostatic pressure downstream will increase, causing a net force in the upstream direction, which will push the jump upstream. Conversely, if the tailwater decreases, the jump will move downstream. Likewise, if the upstream velocity increases, the momentum flux upstream will increase, causing a net force in the downstream direction, which will increase the size of the jump and push it downstream. Conversely, if the upstream velocity decreases, the jump will decrease in size and move upstream. Therefore, in the absence of channel friction, the size and location of the hydraulic jump is highly sensitive to fluctuations in depth and velocity (Montes 1998).

### **A.2.3 General Solution**

Solving the momentum equation to find the subcritical sequent depth can be tedious, especially for non-rectangular channels. Therefore several studies have attempted to generalize the hydraulic jump problem and present it visually, so as to provide a quick solution to practicing engineers without supplementary work. One option is to simply use the specific force diagram. If the specific force curve is plotted for a given flow rate, then “for any depth  $y_1$  other than  $y_c$ , there exists another depth  $y_2$  such that the specific force is numerically the same” (Straub 1978). This method would require, however, that a unique specific force diagram be created for each possible flow rate, and for each possible channel, which would be impractical.

Perhaps a better approach is to generalize the chart by using dimensionless ratios in place of depths and flow rates. Several variations on this idea have been attempted, the most common of which being to plot the ratio between the upstream and downstream sequent depths on the y-axis, versus the upstream Froude number on the x-axis. It would be convenient indeed if all channel conditions (i.e. closed vs. open channels, shape, slope, etc.) could be described effectively by this same format, so that a user could make comparisons between them. It turns out, however, that some methods appear to be effective for some situations, but become cumbersome and confusing for others.

### **A.3 Jump Length**

#### **A.3.1 Definition**

The process of determining the jump length turns out to be much different than that of finding the depth, partially because of a lack of a sound definition. Most agree that the jump begins at the “toe”, where the water surface first begins to rise. But definitions of the end of the jump vary widely, partially because of the surface waves and residual turbulence that occur at this point (Carollo et al. 2007; Mehrotra 1976). Rajaratnam (1967) defined the end of a jump as the section beyond which the water surface is essentially level. From a practical standpoint, the end of the jump represents the point at which no further bed protection is necessary, or in other words, when surface turbulence is extinguished, large bubbles are removed, gradually varied flow resumes, and bottom erosion decreases due to lower shear stress (Bradley and Peterka 1957; Hager 1999; Carollo et al. 2007).

However, because these definitions are difficult to measure (Rajaratnam 1967), some instead prefer to use the length of the roller, which is defined as the distance from

the toe to the point at which the high-velocity jet leaves the channel floor, or to a point immediately downstream of the surface roller, where flow stagnates and separates between forward and backward flow (Chow 1959; Hager 1999; Montes 1998). This point is obviously not fixed either, which requires that measurements be averaged over time (Hager 1992), but measurements of the roller length are typically more reliable than jump length measurements (Bradley and Peterka 1957). Unfortunately, though, the roller length underestimates the length required by a hydraulic jump to reach its subcritical sequent depth and to dissipate its energy, especially at lower Froude numbers. Roller length is therefore not the best indicator of jump length (Rajaratnam 1967; Hager et al. 1990).

### **A.3.2 General Solution**

Unlike the jump height, the length of a hydraulic jump cannot be determined theoretically, not even from momentum analysis. It can only be obtained experimentally (Sturm 2001), and results vary depending on flow and channel conditions. Hotchkiss et al. (2003) provided a comprehensive list of references for finding jump length under various conditions, including also the limits of application for each study. It is apparent from these references that depending on the channel conditions, the jump length may be expressed in terms of  $Fr_1$ ,  $y_1$ , or  $y_2$ . In most cases, the jump length is between four and six times the subcritical sequent depth,  $y_2$  (Franzini and Finnemore 1997).



## **A.4 Hydraulic Jumps in Open Channels**

### **A.4.1 Description**

The hydraulic jump is most often considered as an open-channel phenomenon, and may be found using the momentum equation analysis in almost any open channel hydraulics text. Among others, French (1985), Harleman (1959), Montes (1998), Negm (2000), Bradley and Peterka (1957), and Silvester (1964) present decent general analyses of jump height and length. They also take into account such variables as the channel shape, slope, friction, fluid viscosity, and correction terms for velocity, turbulence-flux, and pressure distribution. However, such solutions still require some experimental input and/or verification to be practical. Conservative assumptions are often made, therefore, to simplify the problem by reducing the number of independent variables, so that the hydraulic jump may be analyzed more easily.

### **A.4.2 Common Assumptions**

The most common assumptions made for open-channel jumps are listed below, in general order of importance. Not every study mentions all of them explicitly, but they are at least implied in every study. Many studies focus on the effects of a particular assumption or assumptions on the accuracy of a solution. In almost all cases, however, the assumptions have been found to be conservative, meaning that they overestimate the jump height and/or length. Therefore, in the absence of sufficient information it is advisable to use these assumptions when they can be justified.

#### **A.4.2.1 Straight, Prismatic Channel**

One assumption that is commonly made is of a straight, prismatic channel. The main advantage of this is that no pressure corrections for longitudinal channel shape are needed in the momentum equation. Obviously this could not apply to jumps in abrupt expansions, contractions, or bends, or over steps, sills, or baffle blocks; the straight, prismatic channel represents the simplest plan and profile possible for a hydraulic jump, and is therefore used where applicable.

If this assumption does not apply, then various studies may be consulted to account for anomalies in the channel profile. For positive steps, use Hager (1992), Husain et al. (1994), and Montes (1998). For negative steps, use Moore and Morgan (1957), Rajaratnam (1967), Ohtsu and Yasuda (1991b), Hager (1992), Husain et al. (1994), and Montes (1998). For sills, use Rajaratnam (1964), Rajaratnam (1967), Hager (1992), Montes (1998), and Hotchkiss et al. (2005). And for abrupt expansions, use Rajaratnam (1967), Rajaratnam (1968a), Smith (1989), Hager (1992), Bremen and Hager (1993), and Ohtsu et al. (1999)

#### **A.4.2.2 Horizontal Slope**

Another common assumption is that the channel slope is horizontal. The main advantage of this assumption is that it eliminates the need to consider the weight of the fluid within the hydraulic jump itself, which is difficult to estimate accurately anyway (Chow 1959). One reason for this is that the jump spans a relatively short distance anyway (Caric 1977), but also, since the streamwise component of the weight is a function of the sine of the slope angle, the weight of the jump is negligible for small angles compared to the hydrostatic pressure at each end. Thompson and Kilgore (2006)

state that a channel may be assumed to be horizontal for slopes up to 18% (or a 10-degree angle from the horizontal) without introducing serious error, while Hager (1999) reduces this number to only 5%. It would obviously not be justifiable for steep channels or spillways, but for most situations, when a channel is relatively flat, this assumption is a valid one (Aryropoulos 1962; Smith and Chen 1989).

If the slope is to be considered, the following studies provide analyses of jumps on sloped channels, complete with figures, momentum equations, and methods for finding the weight term, the sequent depths and the jump location: Kinsvatar (1944), Rajaratnam (1967), French (1985), Ohtsu and Yasuda (Ohtsu and Yasuda 1991a), Hager (1992), Husain et al. (1994), Montes (1998), Beirami and Chamani (2006), and Thompson and Kilgore (2006).

#### **A.4.2.3 Frictionless Channel**

It is also common to assume that the channel is frictionless, or at least that the boundary resistance is relatively small compared to the other forces at play (Gill 1980). The area over which the shear force acts within the control volume is typically not large enough to make much of a difference (Montes 1998; Thompson and Kilgore 2006). This is indeed a significant assumption, as it is extremely difficult to accurately measure the shear stress along the boundary, especially because velocities are so unpredictable within the jump itself.

However, for straight, prismatic, horizontal channels, the integrated bed shear stress is perhaps the most important additional term to be considered, since it has by far the largest effect on jump behavior of any of the variables listed hereafter (Harleman 1959). Neglecting bed shear tends to over-predict the height and length of hydraulic

jumps, especially for shallow flows, narrow channels, high flow velocities, and large relative roughness values (Hager 1999; Hager and Bremen 1989; Montes 1998; Rajaratnam 1968b). Therefore, if friction is not neglected, and the so-called “rough jump” (Hager 1992) is to be considered, then the following studies may be consulted: Harleman (1959), Rajaratnam (1967), Rajaratnam (1968b), Gill (1980), Hughes and Flack (1984), Hager and Bremen (1989), Smith and Chen (1989), Hager (1992), Montes (1998), Hager (1999), Negm (2000), Ead and Rajaratnam (2002), and Carollo et al. (2007). It should be noted, however, that although many studies have been conducted on this problem, current information regarding boundary roughness remains incomplete (Carollo et al. 2007).

#### **A.4.2.4 Hydrostatic Pressure Distribution**

Another common assumption is that the pressure before and after the jump is hydrostatic, which requires that the flow is parallel to the channel before and after the jump. This makes estimating the pressure distribution easier, which facilitates the use of the momentum equation (Montes 1998). This may not be a realistic assumption “because of the intense mixing, flow curvatures, and air entrainment within the jump” which increases with  $Fr_1$  (Rajaratnam 1967), but the few studies that have been performed on this topic have found that the correction factors for streamwise pressure distribution do not make a significant difference (Hughes and Flack 1984).

#### **A.4.2.5 Uniform Velocity Distribution**

It is also common to assume that the velocity distributions at the upstream and downstream ends of the jump are uniform throughout the cross-section. This is never a

realistic assumption in hydraulics, especially in cases of highly turbulent flow, such as is the case with hydraulic jumps (Stevens 1933; Rajaratnam 1967), but the few studies conducted on this have shown that the effects of velocity distribution and turbulence flux tend to cancel each other (Harleman 1959). The velocity distribution factors into the momentum equation as the Boussinesq velocity distribution coefficient,  $\beta$  (also called the momentum-flux correction factor) which is typically some value slightly greater than 1 (Hager 1999; Harleman 1959). When this assumption is in place, however,  $\beta$  is assumed to equal 1, which bypasses the effort required to determine its true value (Montes 1998).

#### **A.4.2.6 Other Assumptions**

Some of the less-commonly mentioned assumptions made deal with the effects of air entrainment, turbulence and viscosity. Air entrainment is treated with closed conduits in Appendix A.5, and the other two factors contribute so little in comparison to the other forces at play that they are almost always disregarded. Turbulence, as noted previously, is counteracted by the effects of velocity distribution (Harleman 1959), and the Reynolds number is typically high enough in hydraulic jumps to disregard the effects of fluid viscosity (Rajaratnam 1968b).

#### **A.4.3 Example: The Classical Hydraulic Jump**

The simplest example of a jump on a smooth, horizontal, prismatic channel as described above is aptly named the “classical hydraulic jump.” Rajaratnam (1967) defined it as "a jump formed in a smooth, wide, and horizontal rectangular channel... [in which the] water surface starts rising abruptly at the beginning, or toe of the jump, which oscillates about a mean position, and it continues to rise up to a section beyond which it is

essentially level... [which] denotes the end of the jump." This final assumption, that the channel is wide and rectangular, proves to be highly unique and significant as shown hereafter.

#### **A.4.3.1 Jump Height**

The solution to the momentum equation – and therefore the jump height – for classical hydraulic jumps was first solved by Bélanger in 1838, and has been widely used ever since (Hager 1992; 1999). Most hydraulics texts, such as Hager (1999), Young et al. (2004), or Chadwick et al. (2004), include a full derivation of this equation, so it is not repeated here, but what is significant about this solution is that it explicitly expresses the ratio between the two sequent depths solely as a function of the upstream Froude number:

$$\frac{y_2}{y_1} = \frac{1}{2} \left( \sqrt{1 + 8Fr_1^2} - 1 \right) \quad (\text{A-5})$$

This solution is easily plotted on a  $y_2/y_1$  vs.  $Fr_1$  chart as a near-straight line (Chow 1959; Silvester 1964; Thompson and Kilgore 2006), with which experimentation agrees quite well (Chow 1959; Bradley and Peterka 1957; Montes 1998). Unfortunately, no equation analogous to this one can be derived for any channel shape other than rectangular (French 1985); other shapes have implicit solutions that require iteration (Jeppson 1970). Thus, the classical hydraulic jump is the simplest example of a hydraulic jump available.

#### **A.4.3.2 Jump Length**

Of all studies made on determining the length of hydraulic jumps, the most by far have been conducted on classical jumps. Several empirical relationships have been developed, as listed and compared by Silvester (1964), but perhaps the most accurate and therefore the most commonly used equation today was developed by Bradley and Peterka (1957), as shown below:

$$\frac{L_j}{y_2} = 220 \tanh\left(\frac{Fr_1 - 1}{22}\right) \quad (A-6)$$

or simply  $L_j/y_2 = 6$  for  $4 < Fr_1 < 12$  (Hager 1992). Hager and Bremen (1990) determined, however, that for  $Fr_1 > 8$ , the jump length is also a function of the upstream Reynolds number and channel aspect ratio.

### **A.5 Hydraulic Jumps in Closed Conduits**

#### **A.5.1 Description**

Compared to open channels, hydraulic jumps in closed conduits have received relatively little attention (Montes 1998), although they appear to have been first studied as early as 1938 by Lane and Kinsvatar. Closed conduits behave similarly to open channels, as long as a free surface remains and sufficient air is supplied above the flow. What makes hydraulic jumps in closed conduits different, however, is that due to downstream submergence, a jump can potentially fill the conduit completely, resulting in pressure flow conditions downstream (Caric 1977; Hager 1999). This is called an “incomplete” or pressure jump, as opposed to a “complete” or free-surface jump

(Hotchkiss et al. 2003; Montes 1998), and because of the interesting problems it poses for design, it has received relatively much more attention than complete jumps in closed conduits (Stahl and Hager 1999).

In the case of incomplete jumps, the subcritical sequent depth is greater than the height of the conduit, but since the flow cannot reach this depth, the deficit is made up by hydrostatic pressure against the top of the conduit (Montes 1998). Decent diagrams depicting this situation may be found in Smith and Chen (1989), Rajaratnam (1965), Hsu et al. (1980), and Haindl (1957). The energy loss in incomplete jumps has been found to be smaller than that for corresponding open channels with identical upstream Froude numbers, due to the fact that the flow is confined by the conduit and therefore has less room for energy dissipation (Haindl 1957; Hsu et al. 1980).

The point at which the conduit becomes “just full”, or when the subcritical flow depth exactly meets the crown of the conduit, marks the transition between complete and incomplete jumps. In practice, however, when a conduit is flowing near full, the flow abruptly and unpredictably fills or “chokes” the conduit and becomes pressurized (Normann et al. 1985; Stahl and Hager 1999; Hager 1999). Careful experimentation has failed to produce the full-flow condition corresponding to free pipe-full flow without pressure surcharge (Hager 1999). Therefore in reality the “just-full” condition does not exist.

#### **A.5.2 Air Entrainment**

The fact that hydraulic jumps entrain air introduces the problem of two-phase flow into the momentum equation. Not only does this reduce the volume (and therefore weight) of the water within the jump itself, but it reduces the downstream flow area as



well. Although this effects both open-channel and closed-conduit flow (Rajaratnam 1967), it is mostly a problem for incomplete jumps in closed conduits, because in the absence of an upstream air supply, a vacuum can form upstream of the jump as air is sucked into the roller, which moves the jump upstream to rebalance the pressure (Lane and Kinsvatar 1938; Haindl and Sotornik 1957). Meanwhile, if the flow velocity isn't sufficient to sweep entrained air downstream, an air bubble forms at the top of the conduit just below the jump, which can periodically burst back through the jump to equalize the pressure and supply more air. This is termed "blowback" and is responsible for pressure surges, vibrations, and even cavitation within pipelines (Lane and Kinsvatar 1938; Haindl and Sotornik 1957; Hsu et al. 1980; Matsushita 1989; Smith 1989; Hager 1999).

Sometimes the air bubble can extend completely to the end of the conduit, which causes the water level to return to normal depth under higher pressure, parallel to the conduit (Kalinske and Robertson 1943; Ayoub, S. A. I. 1959; Montes 1998). This increases the flow velocity to supercritical, making it possible in steeper slopes for multiple jumps to form in series, each pumping the same amount of air, and increasing the pressure in the conduit incrementally (Kalinske and Robertson 1943).

The amount of air entrained into a hydraulic jump is expressed as the air entrainment ratio,  $\beta_a$ , given by the following equation (Kalinske and Robertson 1943):

$$\beta_a \equiv \frac{Q_a}{Q_w} = 0.0066(Fr_1 - 1)^{1.4} \quad (A-7)$$

This was based on circular conduits, but Haindl and Sotornik (1957) found that this relationship applied also to rectangular conduits, regardless of slope and sequent depth ratio, suggesting that it is generally applicable in any situation (Rajaratnam 1965). Therefore if air entrainment is to be considered, as recommended by Rajaratnam, then the momentum equation should include this air entrainment term.

### **A.5.3 General Solution**

#### **A.5.3.1 Jump Height**

Just as with open-channel hydraulic jumps, the height of the jump can be obtained by finding the sequent depths from the momentum equation (Lane and Kinsvatar 1938). Examples of this may be found in Montes (1998), Kalinske and Robertson (1943), Hager (1999), and Smith and Chen (1989). The pressure head on the conduit at the subcritical end of the jump is treated differently by different authors, but it should be noted that it depends only upon the pressure head at the outlet, the slope of the conduit, and the pressure head line, not on the jump itself (Haindl 1957). By analyzing the momentum equation for incomplete jumps, it was observed by Smith and Chen (1989) that the jump height increases as  $y_1$  approaches two-thirds the conduit rise, but decreases dramatically for all flow rates as  $y_1$  approaches full conditions, such that no jump occurs at all when a conduit is flowing full.

#### **A.5.3.2 Jump Length**

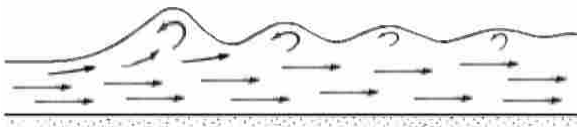


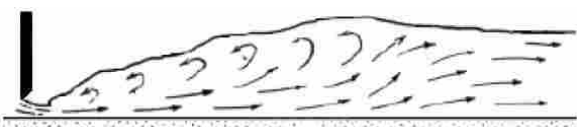
Studies of the length of incomplete hydraulic jumps in closed conduits are few and far between, but it should be noted that it is defined differently than for open channels; Hager (1999) defines incomplete jump length as the "distance between the toe

of the jump and the point where the profile meets the conduit soffit". Given this definition, the jump length becomes shorter as the upstream depth-to-rise ratio increases (Smith and Chen 1989). This does not, however, define the distance needed for the pressure head to reach the subcritical sequent depth, nor does it define the full distance needed for energy dissipation, although some authors assume that it does. Further research is needed, therefore, to adequately predict the length of incomplete jumps in closed conduits.


## **A.6 Hydraulic Jump Classification**

Throughout the history of hydraulic jump research, observations of jump behavior in response to flow conditions and channel shape have led to various systems of classification that differentiate between those conditions and provide a universal language among hydraulicians to communicate such behavior more easily. This section is an attempt to consolidate each of these classification systems into a single list for easy reference. It is not assumed to be comprehensive, although from this extensive literature review it may be considered sufficient. It includes classifications for classical hydraulic jumps, sloped channel jumps, positive and negative step jumps, sill jumps, and expanded channel jumps, each summarized in a table below. References for the classifications as well as any studies pertaining to the classifications are cited within each table, and listed at the end of the appendix.

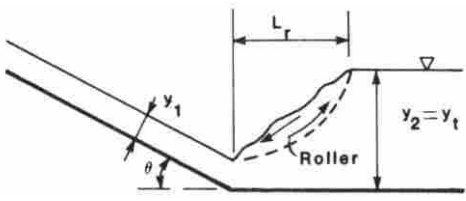
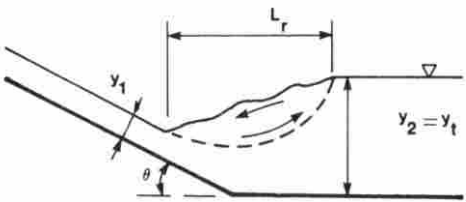
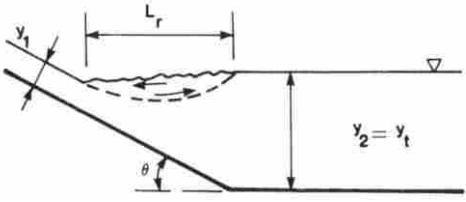
**Table A-1 Classical Hydraulic Jump Classification**

<b>Fr<sub>1</sub></b>	<b>Profile</b>	<b>Comments</b>
1 to 1.7		<p>Undular Jump Slight difference between <math>y_1</math> and <math>y_2</math>, separated by a long transition of standing waves &lt;5% energy dissipation</p>
1.7 to 2.5		<p>A – “Weak Jump” or “Prejump Stage” Smooth surface, fairly uniform velocities throughout, with a series of small surface rollers 5 to 15% energy dissipation</p>
2.5 to 4.5		<p>B – “Oscillating Jump” or “Transition Stage” Entering jet oscillates from bottom to surface with no regular period, causing undesirable and erosive surface waves that can travel far downstream 15 to 45% energy dissipation</p>
4.5 to 9.0		<p>C – “Steady” or “Well-Balanced” Jump Stable jump, in which the jet consistently leaves the bottom near end of the surface roller, and the downstream water surface is relatively smooth 45 to 70% energy dissipation</p>

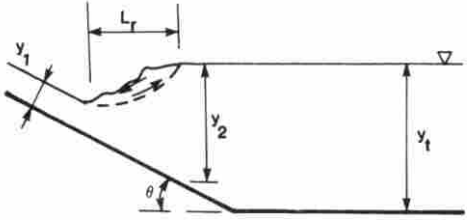
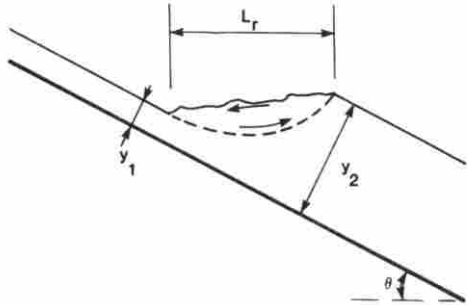
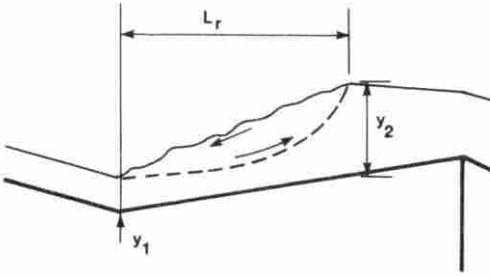
**Table A-1 (cont.) Classical Hydraulic Jump Classification**

Fr <sub>1</sub>	Profile	Comments
<p>&gt; 9</p>		<p>D – “Strong” or “Rough” Jump Sensitive and unpredictable jump, in which "slugs of water rolling down the front face of the jump intermittently fall into the high-velocity jet generating additional waves downstream, and a rough surface can prevail" 70 to 85% energy dissipation</p>
<p>References: Bradley and Peterka (1957); Chow (1959); Hager (1992); Franzini and Finnemore (1997); Montes (1998); Ohtsu et al. (2001); Sturm (2001); Thompson and Kilgore (2006)</p>		

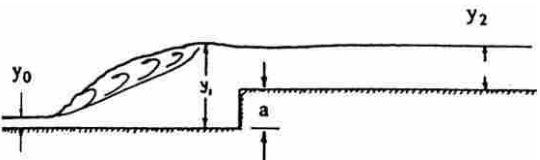
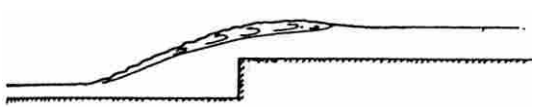
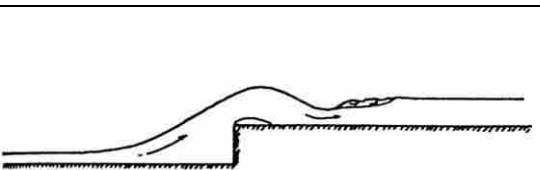
**Table A-2 Sloped Channel Jump Classification**

Type	Profile	Comments
<p>A</p>		<p>Forms entirely on horizontal section Common form for horizontal channels Tends to move downstream</p>
<p>B</p>		<p>Begins on steep positive slope and ends on horizontal section</p>
<p>C</p>		<p>Begins on steep positive slope and ends at the transition between steep and horizontal sections</p>

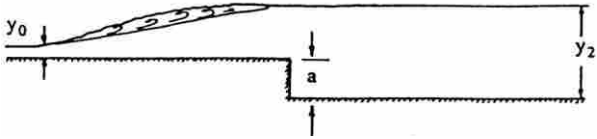
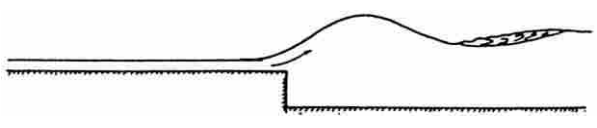
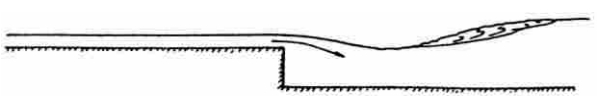
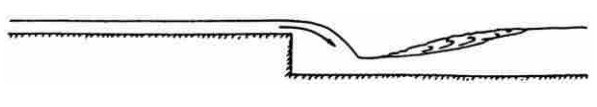
**Table A-2 (cont.) Sloped Channel Jump Classification**

Type	Profile	Comments
D		<p>Located entirely on steep positive slope Most common form used for jumps in sloping channels</p>
E		<p>Located entirely on mild positive slope Uncommon, since supercritical flows do not naturally form on mild slopes</p>
F		<p>Forms on adverse (negative) slopes Uncommon Unstable and almost impossible to control Tends to move downstream</p>
<p>References: Kinsvatar (1944); Rajaratnam (1967); French (1985); Hager (1992); Montes (1998); Beirami and Chamani (2006); Thompson and Kilgore (2006)</p>		

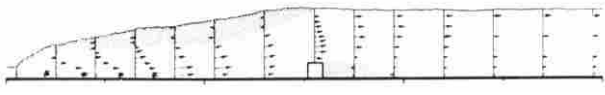
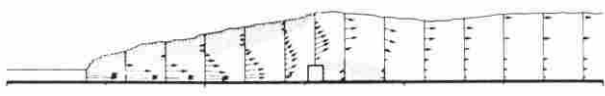

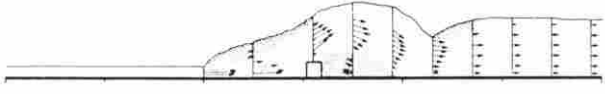

**Table A-3 Positive Step Jump Classification**

Type	Profile	Comments
A		Begins upstream of the step, and ends at the step Highest tailwater before jumps moves upstream
B		Begins upstream of the step and ends downstream Lower tailwater than A-jumps, but higher than W-jumps
W		Forms a standing wave that passes over the step May or may not be aerated Entirely supercritical flow, and poor energy dissipation Lower tailwater than B-jumps
References: Hager (1992); Husain et al.(1994); Montes (1998)		

**Table A-4 Negative Step Jump Classification**

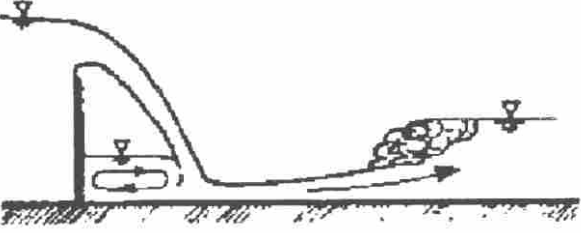
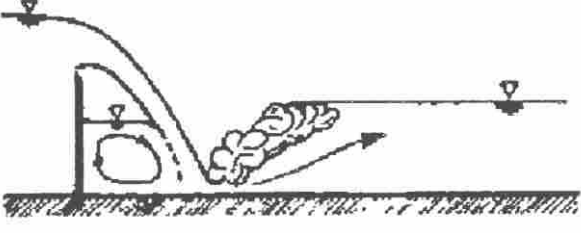
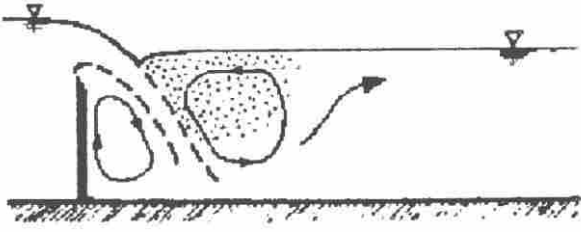
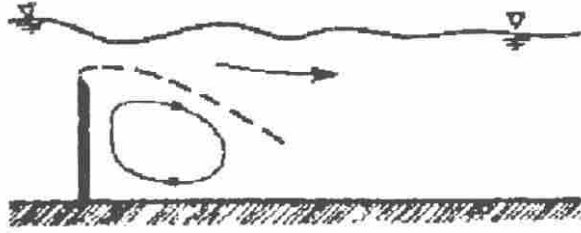
Type	Profile	Comments
A		Begins upstream of the step, and ends at the step Highest tailwater before jump moves upstream
W		Forms a standing wave that begins at the step Lower tailwater than A-jumps, but higher than B-jumps
B		Begins at the step and ends downstream Lower tailwater than W-jumps
Min B		Begins downstream of step Lowest tailwater before jump moves downstream
References: Moore and Morgan (1957); Rajaratnam (1967); Ohtsu and Yasuda (1991b); Hager (1992); Husain et al. (1994); Montes (1998)		

**Table A-5 Submerged Sill Jump Classification**

Type	Profile	Comments
A or I		Begins upstream of the sill, and ends at the sill Highest tailwater before jump moves upstream
B or I/III		Lower tailwater than A- jumps, but higher than C- jumps Shorter and less stable than A- jumps Surface boil appears at sill
Min B or II*		Lowest tailwater before main flow begins striking channel bottom Plunging after the sill, followed by a second surface roller
C or IV		Lower tailwater than B-jumps, but higher than W-jumps Heavy plunging and striking of main flow on channel bottom, causing erosion in unprotected channels
W or VI		Forms a standing wave that passes over the sill Lower tailwater than C-jumps Entirely supercritical flow, and poor energy dissipation
References: Rajaratnam (1964); Rajaratnam (1967); Hager (1992); Montes (1998); Hotchkiss et al. (2005)		

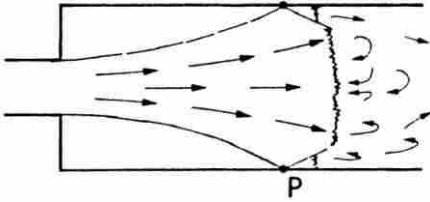
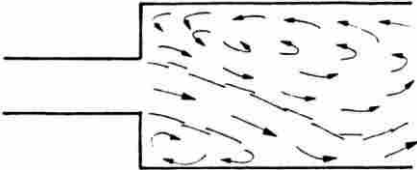
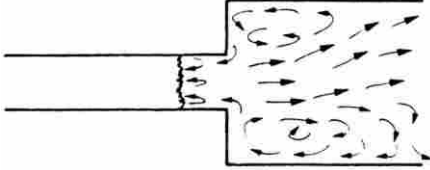


**Table A-6 Weir Jump Classification**

Case	Profile	Comments
A		<p>Swept-out jump                      Lower tailwater than B-jumps                      Similar to classical jumps</p>
B		<p>Optimum jump                      Higher tailwater than A-jumps, but lower than C-jumps                      Jump toe is ideally located immediately downstream of the point of nappe impact, to minimize channel protection</p>
C		<p>Plunging nappe                      Higher tailwater than B-jumps, but lower than D-jumps                      Jump is pushed against the weir and the nappe plunges, submerging the jump and creating an aerated "hydraulic"</p>
D		<p>Surface nappe                      Higher tailwater than C-jumps                      Weir is immersed completely, the nappe stays at the surface, and no jump occurs</p>

References: Leutheusser and Birk (1991)

**Table A-7 Abruptly Expanded Channel Jump Classification**

Type	Plan View	Comments
R		<p>“Repelled” Jump                      Supercritical flow is swept out into expanded channel, where toe forms at point ‘P’                      Limiting condition, where jump cannot move further upstream without collapsing into an S-Jump</p>
S		<p>“Spatial” Jump                      Oscillatory asymmetric extension of supercritical flow into expanded channel, where long fronts between forward and backward flow replace the toe                      Undesirable because of unpredictability, length, and efficiency, since it is closer to a jet than a jump                      May shift to an R-Jump periodically</p>
T		<p>“Transitional” Jump                      A well-developed toe forms perpendicular to the flow upstream of the expansion, while the jump extends past the expansion                      May be symmetric or asymmetric, depending on the jump position relative to the expansion</p>
<p>References: Rajaratnam (1967); Rajaratnam (1968a); Smith (1989); Hager (1992); Bremen and Hager (1993); Ohtsu et al. (1999)</p>		

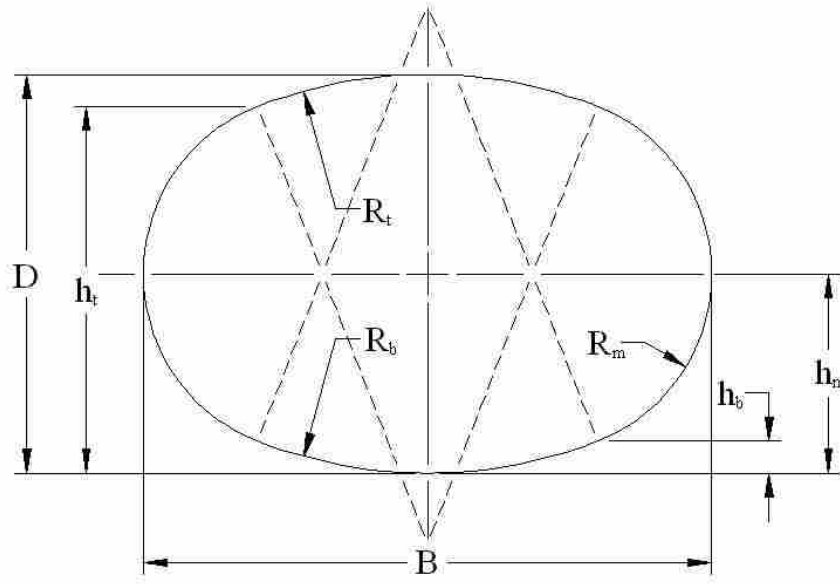
## **A.7 Elliptical Culvert Geometry**

### **A.7.1 Introduction**

Elliptical culverts are a common alternative to circular culverts due to the fact that they allow more height or width clearance for the same flow area. They may be installed horizontally or vertically (ASTM C507 2007), and they may be constructed of either corrugated metal or concrete (FHWA 2007). This appendix defines the geometry of elliptical culverts for use in this study on hydraulic jumps. Although the analysis of elliptical conduits in Appendix B assumes a mathematical ellipse for simplification, the parameters presented here allow an elliptical culvert to be treated as a pipe arch culvert (see Appendix A.8), since the two shapes share common parameters, thereby eliminating the error due to simplification.

### **A.7.2 Definitions**

The geometry of an elliptical culvert is defined in ASTM C507 (2007) by a span, rise, and two radii. For purposes of continuity within this study, however, the same eight parameters used for pipe arch culverts are applied to elliptical culverts. Figure A-1 on the next page depicts the geometry of an elliptical culvert according to these parameters.



**Figure A-1 Parameters to be used in this study for elliptical culverts**

### A.7.3 Calculating Missing Parameters

Obviously not all of the parameters in Figure A-1 are necessary for defining the shape of an elliptical culvert, especially since only  $B$ ,  $D$ ,  $R_b$ , and  $R_m$  are typically given. In fact, it may be shown that only  $B$ ,  $D$ , and  $R_b$  are actually needed; all other parameters may be derived from these. Due to measurement and rounding errors, mathematical discontinuities can occur when using too many independent variables to define the shape. It is therefore recommended that if a pipe arch analysis is to be used instead of the simplified elliptical analysis in Appendix B, then all other parameters except for these three should be derived, using the equations listed on the next page. ASTM C507 (2007) specifies that the span and rise must be within 2% of given values, but no other restriction is given that would preclude using the derived values rather than the given ones.

$$R_t = R_b \quad (\text{A-8})$$

$$h_m = \frac{D}{2} \quad (\text{A-9})$$

$$R_m = \frac{1}{2} \left[ R_b + \frac{B}{2} - \frac{(R_b - D/2)^2}{(R_b - B/2)} \right] \quad (\text{A-10})$$

$$h_b = R_b \left( \frac{h_m - R_m}{R_b - R_m} \right) \quad (\text{A-11})$$

$$h_t = D - h_b \quad (\text{A-12})$$

#### A.7.4 Historic and Current Sizes

The following tables list the dimensions of elliptical culverts currently or historically manufactured. Note that  $R_m$ ,  $R_t$ ,  $h_b$ ,  $h_m$ , and  $h_t$  (all values in grey) are derived from the other parameters to avoid discontinuities. Note also that all standard sizes listed are horizontal elliptical (i.e.  $B > D$ ).

**Table A-8 Steel or Aluminum Elliptical Culvert Sizes (CONTECH 2007)**

<b>B (in)</b>	<b>D (in)</b>	<b>R<sub>b</sub> (in)</b>	<b>R<sub>m</sub> (in)</b>	<b>R<sub>t</sub> (in)</b>	<b>h<sub>b</sub> (in)</b>	<b>h<sub>m</sub> (in)</b>	<b>h<sub>t</sub> (in)</b>
232.000	153.000	150.000	53.555	150.000	35.686	76.500	117.314
241.000	156.000	157.000	53.257	157.000	37.445	78.000	118.555
242.000	143.000	164.000	43.009	164.000	38.619	71.500	104.381
250.000	146.000	171.000	43.609	171.000	39.453	73.000	106.547
252.000	182.000	157.000	71.242	157.000	36.172	91.000	145.828
263.000	157.000	178.000	48.296	178.000	41.451	78.500	115.549
270.000	188.000	171.000	70.653	171.000	39.786	94.000	148.214
276.000	169.000	185.000	54.051	185.000	43.018	84.500	125.982
279.000	191.000	178.000	70.357	178.000	41.577	95.500	149.423
292.000	203.000	185.000	76.112	185.000	43.134	101.500	159.866
294.000	176.000	198.000	53.873	198.000	46.884	88.000	129.116
302.000	179.000	205.000	54.479	205.000	47.696	89.500	131.304
305.000	201.000	198.000	70.786	198.000	46.248	100.500	154.752
313.000	218.000	198.000	81.816	198.000	46.326	109.000	171.674
315.000	190.000	212.000	59.163	212.000	49.710	95.000	140.290
324.000	194.000	219.000	59.939	219.000	51.027	97.000	142.973
326.000	229.000	205.000	86.497	205.000	48.443	114.500	180.557
335.000	233.000	212.000	87.275	212.000	49.675	116.500	183.325
337.000	205.000	226.000	64.622	226.000	53.046	102.500	151.954
346.000	209.000	233.000	65.398	233.000	54.360	104.500	154.640
353.000	239.000	226.000	86.682	226.000	53.237	119.500	185.763
361.000	242.000	233.000	87.283	233.000	53.913	121.000	188.087
363.000	215.000	247.000	65.698	247.000	56.949	107.500	158.051
374.000	254.000	240.000	93.038	240.000	55.463	127.000	198.537
376.000	227.000	253.000	70.806	253.000	59.286	113.500	167.714
385.000	230.000	260.000	70.509	260.000	61.046	115.000	168.954
387.000	266.000	247.000	98.792	247.000	57.010	133.000	208.990
396.000	269.000	253.000	97.843	253.000	59.773	134.500	209.227
398.000	241.000	267.000	75.189	267.000	63.072	120.500	177.928
409.000	280.000	260.000	102.520	260.000	61.879	140.000	218.121
415.000	248.000	281.000	76.570	281.000	65.195	124.000	182.805
419.000	256.000	281.000	81.551	281.000	65.441	128.000	190.559
421.000	292.000	267.000	109.184	267.000	62.287	146.000	229.713
432.000	268.000	288.000	87.306	288.000	67.007	134.000	200.993
446.000	266.000	302.000	81.734	302.000	70.289	133.000	195.711
110.000	80.000	68.000	31.346	68.000	16.055	40.000	63.945
119.000	84.000	75.000	32.121	75.000	17.279	42.000	66.721

**Table A-8 (cont.) Steel or Aluminum Elliptical Culvert Sizes (CONTECH 2007)**

<b>B (in)</b>	<b>D (in)</b>	<b>R<sub>b</sub> (in)</b>	<b>R<sub>m</sub> (in)</b>	<b>R<sub>t</sub> (in)</b>	<b>h<sub>b</sub> (in)</b>	<b>h<sub>m</sub> (in)</b>	<b>h<sub>t</sub> (in)</b>
127.000	87.000	81.000	32.071	81.000	18.920	43.500	68.080
131.000	95.000	81.000	37.048	81.000	19.262	47.500	75.738
136.000	90.000	88.000	31.775	88.000	20.699	45.000	69.301
140.000	99.000	88.000	37.826	88.000	20.474	49.500	78.526
144.000	107.000	88.000	42.805	88.000	20.825	53.500	86.175
145.000	93.000	95.000	31.478	95.000	22.466	46.500	70.534
149.000	102.000	95.000	37.530	95.000	22.266	51.000	79.734
153.000	110.000	95.000	42.507	95.000	22.610	55.000	87.390
154.000	97.000	102.000	32.255	102.000	23.758	48.500	73.242
158.000	105.000	102.000	37.234	102.000	24.043	52.500	80.957
162.000	114.000	102.000	43.286	102.000	23.825	57.000	90.175
163.000	100.000	109.000	31.959	109.000	25.525	50.000	74.475
167.000	108.000	109.000	36.936	109.000	25.810	54.000	82.190
171.000	117.000	109.000	42.989	109.000	25.612	58.500	91.388
175.000	125.000	109.000	47.965	109.000	25.957	62.500	99.043
179.000	134.000	109.000	54.019	109.000	25.735	67.000	108.265
88.000	66.000	54.000	26.950	54.000	12.078	33.000	53.922
97.000	69.000	61.000	26.660	61.000	13.927	34.500	55.073
106.000	72.000	68.000	26.367	68.000	15.734	36.000	56.266
110.000	81.000	68.000	32.413	68.000	15.452	40.500	65.548
115.000	76.000	75.000	27.136	75.000	17.024	38.000	58.976
119.000	84.000	75.000	32.121	75.000	17.279	42.000	66.721
124.000	79.000	82.000	26.844	82.000	18.816	39.500	60.184
128.000	87.000	82.000	31.826	82.000	19.078	43.500	67.922
132.000	96.000	82.000	37.875	82.000	18.816	48.000	77.184
133.000	82.000	88.000	25.878	88.000	21.421	41.000	60.579
136.000	90.000	88.000	31.775	88.000	20.699	45.000	69.301
140.000	99.000	88.000	37.826	88.000	20.474	49.500	78.526
144.000	107.000	88.000	42.805	88.000	20.825	53.500	86.175
141.000	85.000	95.000	26.500	95.000	22.190	42.500	62.810
145.000	94.000	95.000	32.550	95.000	21.982	47.000	72.018
149.000	102.000	95.000	37.530	95.000	22.266	51.000	79.734
153.000	110.000	95.000	42.507	95.000	22.610	55.000	87.390
150.000	88.000	102.000	26.204	102.000	23.949	44.000	64.051
154.000	97.000	102.000	32.255	102.000	23.758	48.500	73.242
158.000	105.000	102.000	37.234	102.000	24.043	52.500	80.957
162.000	114.000	102.000	43.286	102.000	23.825	57.000	90.175

**Table A-8 (cont.) Steel or Aluminum Elliptical Culvert Sizes (CONTECH 2007)**

<b>B (in)</b>	<b>D (in)</b>	<b>R<sub>b</sub> (in)</b>	<b>R<sub>m</sub> (in)</b>	<b>R<sub>t</sub> (in)</b>	<b>h<sub>b</sub> (in)</b>	<b>h<sub>m</sub> (in)</b>	<b>h<sub>t</sub> (in)</b>
163.000	100.000	109.000	31.959	109.000	25.525	50.000	74.475
167.000	108.000	109.000	36.936	109.000	25.810	54.000	82.190
171.000	117.000	109.000	42.989	109.000	25.612	58.500	91.388
175.000	125.000	109.000	47.965	109.000	25.957	62.500	99.043
179.000	134.000	109.000	54.019	109.000	25.735	67.000	108.265

**Table A-9 Concrete Elliptical Culvert Sizes (ASTM C507 2007)**

<b>B (in)</b>	<b>D (in)</b>	<b>R<sub>b</sub> (in)</b>	<b>R<sub>m</sub> (in)</b>	<b>R<sub>t</sub> (in)</b>	<b>h<sub>b</sub> (in)</b>	<b>h<sub>m</sub> (in)</b>	<b>h<sub>t</sub> (in)</b>
22.750	14.250	20.000	6.078	20.000	1.504	7.125	12.746
30.250	19.250	26.250	8.265	26.250	1.984	9.625	17.266
34.000	21.500	29.250	9.156	29.250	2.321	10.750	19.179
37.750	24.000	32.750	10.297	32.750	2.484	12.000	21.516
42.000	26.750	36.250	11.469	36.250	2.788	13.375	23.962
45.500	28.750	39.250	12.250	39.250	3.090	14.375	25.660
49.500	31.500	42.750	13.500	42.750	3.288	15.750	28.212
53.250	34.000	46.000	14.609	46.000	3.503	17.000	30.497
60.000	38.250	51.500	16.375	51.500	4.033	19.125	34.217
68.000	43.500	58.500	18.688	58.500	4.500	21.750	39.000
75.500	48.250	65.000	20.719	65.000	5.000	24.125	43.250
83.000	53.000	71.500	22.750	71.500	5.500	26.500	47.500
90.500	57.750	78.000	24.781	78.000	6.000	28.875	51.750
98.000	62.750	84.500	27.000	84.500	6.430	31.375	56.320
105.500	67.500	90.750	29.000	90.750	6.981	33.750	60.519
113.000	72.500	97.250	31.219	97.250	7.410	36.250	65.090
120.500	77.250	103.750	33.250	103.750	7.910	38.625	69.340
128.000	82.000	110.000	35.250	110.000	8.462	41.000	73.538
135.500	87.000	116.250	37.438	116.250	8.942	43.500	78.058
143.000	91.750	122.750	39.469	122.750	9.442	45.875	82.308
150.750	96.340	129.250	41.301	129.250	10.094	48.170	86.246
165.500	106.500	142.000	45.906	142.000	10.852	53.250	95.648
180.750	116.000	154.750	49.859	154.750	12.011	58.000	103.989



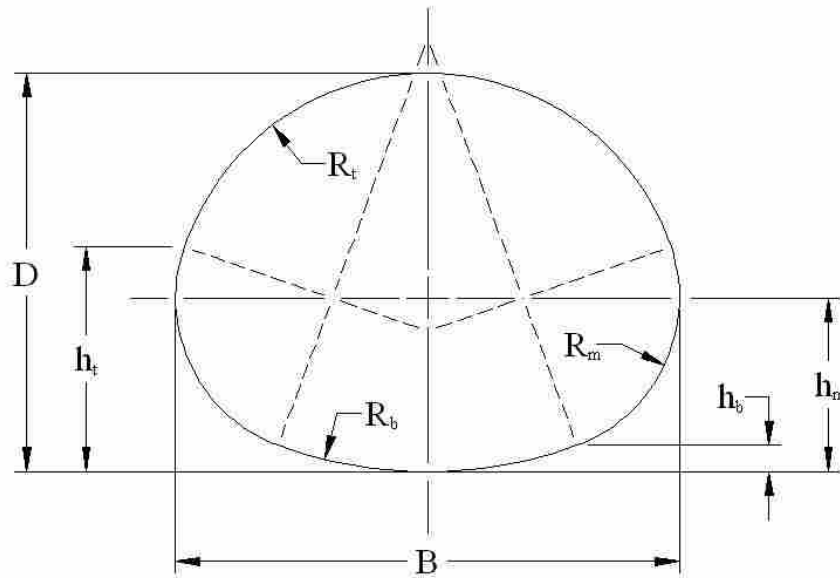
## **A.8 Pipe Arch Culvert Geometry**

### **A.8.1 Introduction**

Pipe arch culverts (also called "arch" (ASTM C506 2007) or "horseshoe" (Hager 1999) culverts) are often used in place of circular culverts because they allow more height clearance than their circular counterparts due to their compact shape (Hager 1999). They are manufactured either by concrete or by corrugated steel or aluminum, and in the case of corrugated metal, they may either be reshaped from a single tube or pieced together using structural plates (CONTECH 2007). This appendix defines the geometry of pipe arch culverts for use in this study on hydraulic jumps.

### **A.8.2 Definitions**

The geometry of an elliptical culvert is defined in ASTM C506 (2007) by a span, rise, three lengths, and two radii, although different parameters are used by different manufacturers. For this study, the following eight parameters are used to define the pipe arch shape: span ( $B$ ), rise ( $D$ ), bottom radius ( $R_b$ ), middle radius ( $R_m$ ), top radius ( $R_t$ ), bottom transition height ( $h_b$ ), neutral axis height ( $h_m$ ), and top transition height ( $h_t$ ). Figure A-2 on the next page depicts the geometry of a pipe arch culvert according to these parameters.



**Figure A-2 Parameters to be used in this study for pipe arch culverts**

### **A.8.3 Calculating Missing Parameters**

Obviously not all of the parameters in Figure A-2 are necessary for defining the shape of a pipe arch culvert, especially since only  $B$ ,  $D$ ,  $R_b$ ,  $R_m$ ,  $R_t$ , and  $h_m$  are typically given. In fact, it may be shown that only  $B$ ,  $D$ ,  $R_b$ , and  $R_m$  are actually needed; all other parameters may be derived from these. Due to measurement and rounding errors, mathematical discontinuities can occur when using too many independent variables to define the shape. It is therefore recommended for the analysis presented in this study that all other parameters except for these four should be derived using the equations listed on the next page. ASTM C506 (2007) specifies that the span and rise must be within 2% of given values, but no other restriction is given that would preclude using the derived values rather than the given ones.

$$h_m = R_b - \sqrt{(R_b - R_m)^2 - (B/2 - R_m)^2} \quad (\text{A-13})$$

$$R_t = \frac{B(4R_m - B) - 4(D - h_m)^2}{8(R_m - D + h_m)} \quad (\text{A-14})$$

$$h_b = R_b \left( \frac{h_m - R_m}{R_b - R_m} \right) \quad (\text{A-15})$$

$$h_t = D - R_t \left( 1 - \frac{\sqrt{(R_t - R_m)^2 - (B/2 - R_m)^2}}{(R_t - R_m)} \right) \quad (\text{A-16})$$

#### A.8.4 Historic and Current Sizes

The following tables list the dimensions of pipe arch culverts currently or historically manufactured. Note that  $R_t$ ,  $h_b$ ,  $h_m$ , and  $h_t$  (all values in grey) are derived from the other parameters to avoid discontinuities.

**Table A-10 Steel or Aluminum Pipe Arch Culvert Sizes – Variable  
Corner Radii - 2-2/3 x 1/2 in Corrugation (AISI 1999)**

<b>B (in)</b>	<b>D (in)</b>	<b>R<sub>b</sub> (in)</b>	<b>R<sub>m</sub> (in)</b>	<b>R<sub>t</sub> (in)</b>	<b>h<sub>b</sub> (in)</b>	<b>h<sub>m</sub> (in)</b>	<b>h<sub>t</sub> (in)</b>
17.000	13.000	25.625	3.500	8.517	0.663	4.072	5.181
21.000	15.000	33.125	4.125	10.509	0.810	4.834	5.056
24.000	18.000	34.625	4.875	12.005	1.008	5.741	6.424
28.000	20.000	42.250	5.500	14.015	1.146	6.497	6.827
35.000	24.000	55.125	6.875	17.634	1.353	8.059	9.142
42.000	29.000	66.125	8.250	21.126	1.625	9.672	10.824
49.000	33.000	77.250	9.625	24.820	1.892	11.281	13.246
57.000	38.000	88.250	11.000	28.940	2.294	13.008	15.429
64.000	43.000	99.250	12.375	32.410	2.566	14.621	17.110
71.000	47.000	110.250	13.750	36.158	2.837	16.233	19.541
77.000	52.000	121.250	15.125	38.968	2.978	17.731	20.712
83.000	57.000	132.250	16.500	41.827	3.121	19.232	21.877

**Table A-11 Steel or Aluminum Pipe Arch Culvert Sizes - 18 in or greater  
Corner Radii - 3 x 1 in Corrugation (FHWA 2007)**

<b>B (in)</b>	<b>D (in)</b>	<b>R<sub>b</sub> (in)</b>	<b>R<sub>m</sub> (in)</b>	<b>R<sub>t</sub> (in)</b>	<b>h<sub>b</sub> (in)</b>	<b>h<sub>m</sub> (in)</b>	<b>h<sub>t</sub> (in)</b>
60.000	46.000	51.125	18.750	31.753	3.186	20.767	30.170
66.000	51.000	56.250	20.750	34.661	3.455	22.931	32.762
73.000	55.000	63.750	22.875	39.759	3.646	25.213	38.723
81.000	59.000	82.625	20.875	41.607	4.284	24.077	30.806
87.000	63.000	92.250	22.625	44.876	4.244	25.828	33.662
95.000	67.000	100.250	24.375	49.959	4.770	27.985	38.411
103.000	71.000	111.625	26.125	55.184	5.029	29.977	42.709
112.000	75.000	120.250	27.750	61.750	5.745	32.169	47.611
117.000	79.000	131.750	29.500	64.012	5.410	33.699	49.692
128.000	83.000	139.750	31.250	73.704	6.518	36.311	56.196
137.000	87.000	149.500	33.000	81.490	7.110	38.541	61.019
142.000	91.000	162.375	34.750	83.320	6.688	40.006	63.135

**Table A-12 Steel or Aluminum Pipe Arch Culvert Sizes – Variable  
Corner Radii - 3 x 1 or 5 x 1 in Corrugation (AISI 1999)**

<b>B (in)</b>	<b>D (in)</b>	<b>R<sub>b</sub> (in)</b>	<b>R<sub>m</sub> (in)</b>	<b>R<sub>t</sub> (in)</b>	<b>h<sub>b</sub> (in)</b>	<b>h<sub>m</sub> (in)</b>	<b>h<sub>t</sub> (in)</b>
53.000	41.000	73.438	10.188	26.628	2.484	12.327	17.685
58.500	48.500	51.125	18.750	29.334	2.764	20.500	22.864
65.000	54.000	56.250	20.750	32.575	3.170	22.751	25.077
72.500	58.250	63.750	22.875	36.726	3.509	25.125	31.073
79.000	62.500	82.625	20.875	39.516	3.848	23.751	24.609
86.500	67.250	92.250	22.625	43.331	4.140	25.750	27.751
93.500	71.750	100.250	24.375	46.943	4.458	27.749	30.926
101.500	76.000	111.625	26.125	51.253	4.730	29.748	34.947
108.500	80.500	120.250	27.750	54.934	5.040	31.627	37.815
116.500	84.750	131.750	29.500	59.424	5.315	33.625	41.806
123.500	89.250	139.750	31.250	63.225	5.635	35.625	45.008
131.000	93.750	149.500	33.000	67.400	5.935	37.625	48.442
138.500	98.000	162.375	34.750	71.684	6.045	39.502	51.907
146.000	102.000	172.000	36.000	75.958	6.488	41.130	54.723
153.000	107.000	180.000	38.000	79.699	6.742	43.319	57.916
159.000	113.000	184.000	40.000	82.131	7.058	45.523	59.437
165.000	118.500	190.000	41.000	84.440	7.518	46.896	59.011

**Table A-13 Steel or Aluminum Pipe Arch Culvert Sizes (Historic) -  
Variable Corner Radii - 2-2/3 x 1/2 in Corrugation (FHWA 2007)**

<b>B (in)</b>	<b>D (in)</b>	<b>R<sub>b</sub> (in)</b>	<b>R<sub>m</sub> (in)</b>	<b>R<sub>t</sub> (in)</b>	<b>h<sub>b</sub> (in)</b>	<b>h<sub>m</sub> (in)</b>	<b>h<sub>t</sub> (in)</b>
18.100	11.000	19.120	3.500	10.157	1.248	4.519	6.452
21.700	13.300	37.060	4.000	11.411	0.804	4.717	6.244
25.300	15.500	33.500	4.000	13.133	1.472	5.297	6.580
28.900	17.800	55.000	4.500	14.743	1.078	5.490	6.559
36.100	22.200	73.250	5.000	18.253	1.352	6.259	7.132
43.300	26.600	91.560	5.500	21.804	1.627	7.029	7.782
50.600	31.700	97.250	6.000	25.379	2.200	8.064	8.604
57.800	35.500	115.690	7.000	29.079	2.373	9.229	10.120
65.000	40.000	129.310	8.000	32.709	2.665	10.500	11.539
72.200	44.400	142.940	9.000	36.355	2.956	11.770	12.996
79.400	48.700	145.550	10.000	40.063	3.537	13.294	14.843
85.000	54.000	154.500	11.000	42.658	3.768	14.500	15.597

**Table A-14 Steel or Aluminum Pipe Arch Culvert Sizes (Historic) -  
18 in or less Corner Radii - 3 x 1 in Corrugation (FHWA 2007)**

<b>B (in)</b>	<b>D (in)</b>	<b>R<sub>b</sub> (in)</b>	<b>R<sub>m</sub> (in)</b>	<b>R<sub>t</sub> (in)</b>	<b>h<sub>b</sub> (in)</b>	<b>h<sub>m</sub> (in)</b>	<b>h<sub>t</sub> (in)</b>
43.000	27.000	54.750	7.750	22.482	2.395	9.806	12.588
50.000	31.000	67.000	9.000	26.282	2.600	11.251	14.653
58.000	36.000	82.000	10.500	30.402	2.792	12.935	16.805
65.000	40.000	91.250	12.000	34.447	3.106	14.697	19.586
72.000	44.000	98.500	13.250	38.415	3.572	16.342	22.005
73.000	55.000	76.250	18.000	36.698	3.948	21.016	23.628
81.000	59.000	92.750	18.000	40.725	4.301	21.467	23.995
87.000	63.000	100.500	18.000	43.640	4.921	22.040	23.921
95.000	67.000	116.000	18.000	47.675	5.380	22.545	24.499
103.000	71.000	132.250	18.000	51.707	5.813	23.022	25.013
112.000	75.000	151.750	18.000	56.304	6.253	23.512	25.775
117.000	79.000	160.500	18.000	58.654	6.619	23.876	25.439
128.000	83.000	185.000	18.000	64.368	7.157	24.460	26.723
137.000	87.000	201.000	18.000	68.997	7.805	25.106	27.613
142.000	91.000	210.000	18.000	71.314	8.159	25.460	27.409

**Table A-15 Steel Structural Plate Pipe Arch Culvert Sizes -  
18 in corner radius (AISI 1999)**

<b>B (in)</b>	<b>D (in)</b>	<b>R<sub>b</sub> (in)</b>	<b>R<sub>m</sub> (in)</b>	<b>R<sub>t</sub> (in)</b>	<b>h<sub>b</sub> (in)</b>	<b>h<sub>m</sub> (in)</b>	<b>h<sub>t</sub> (in)</b>
73.000	55.000	76.320	18.000	36.697	3.942	21.012	23.620
76.000	57.000	98.640	18.000	38.062	3.082	20.520	21.939
81.000	59.000	83.520	18.000	40.819	5.079	21.984	24.985
84.000	61.000	104.160	18.000	42.135	4.123	21.410	23.308
87.000	63.000	136.200	18.000	43.534	3.207	20.783	21.712
92.000	65.000	109.800	18.000	46.231	5.232	22.374	24.673
95.000	67.000	137.880	18.000	47.588	4.240	21.686	23.070
98.000	69.000	182.880	18.000	49.015	3.261	20.940	21.495
103.000	71.000	141.000	18.000	51.663	5.330	22.650	24.422
106.000	73.000	178.680	18.000	53.052	4.290	21.858	22.839
112.000	75.000	144.600	18.000	56.353	6.668	23.838	26.274
114.000	77.000	177.480	18.000	57.112	5.389	22.842	24.202
117.000	79.000	227.760	18.000	58.527	4.286	21.947	22.602
123.000	81.000	178.320	18.000	61.761	6.690	24.014	25.979
128.000	83.000	153.240	18.000	64.641	9.137	26.064	29.037
131.000	85.000	180.360	18.000	65.875	7.891	25.104	27.351
137.000	87.000	157.920	18.000	69.459	10.644	27.431	30.891
139.000	89.000	183.240	18.000	70.006	9.127	26.230	28.735

**Table A-15 (cont.) Steel Structural Plate Pipe Arch Culvert Sizes -  
18 in corner radius (AISI 1999)**

<b>B (in)</b>	<b>D (in)</b>	<b>R<sub>b</sub> (in)</b>	<b>R<sub>m</sub> (in)</b>	<b>R<sub>t</sub> (in)</b>	<b>h<sub>b</sub> (in)</b>	<b>h<sub>m</sub> (in)</b>	<b>h<sub>t</sub> (in)</b>
142.000	91.000	216.360	18.000	71.284	7.866	25.212	27.068
148.000	93.000	186.480	18.000	74.776	10.602	27.579	30.545
150.000	95.000	216.840	18.000	75.397	9.100	26.345	28.459
152.000	97.000	257.400	18.000	76.158	7.668	25.132	26.460
154.000	100.000	314.760	18.000	77.007	6.283	23.924	24.208
161.000	101.000	254.760	18.000	80.807	9.037	26.398	28.177
167.000	103.000	220.680	18.000	84.283	11.841	28.876	31.634
169.000	105.000	254.160	18.000	84.919	10.285	27.556	29.567
171.000	107.000	297.600	18.000	85.681	8.803	26.270	27.587
178.000	109.000	254.280	18.000	89.641	11.752	28.920	31.322
184.000	111.000	226.800	18.000	93.282	14.721	31.553	34.861
186.000	113.000	255.720	18.000	93.793	13.061	30.141	32.738
188.000	115.000	291.480	18.000	94.443	11.481	28.772	30.707
190.000	118.000	338.160	18.000	95.133	9.926	27.397	28.455
197.000	119.000	290.880	18.000	99.156	12.945	30.144	32.429
199.000	121.000	332.760	18.000	99.852	11.348	28.734	30.403

**Table A-16 Steel Structural Plate Pipe Arch Culvert Sizes -  
31 in corner radius (AISI 1999)**

<b>B (in)</b>	<b>D (in)</b>	<b>R<sub>b</sub> (in)</b>	<b>R<sub>m</sub> (in)</b>	<b>R<sub>t</sub> (in)</b>	<b>h<sub>b</sub> (in)</b>	<b>h<sub>m</sub> (in)</b>	<b>h<sub>t</sub> (in)</b>
159.000	112.000	192.600	31.000	79.916	8.879	38.450	42.484
162.000	114.000	219.960	31.000	81.248	7.840	37.735	40.809
168.000	116.000	197.880	31.000	84.643	10.245	39.640	44.427
170.000	118.000	222.600	31.000	85.345	9.024	38.767	42.253
173.000	120.000	256.560	31.000	86.693	7.888	37.935	40.510
179.000	122.000	227.760	31.000	90.035	10.300	39.898	44.063
184.000	124.000	208.560	31.000	92.939	12.694	41.807	47.185
187.000	126.000	232.080	31.000	94.162	11.495	40.960	45.437
190.000	128.000	260.640	31.000	95.443	10.327	40.099	43.726
195.000	130.000	236.040	31.000	98.307	12.759	42.083	46.869
198.000	132.000	263.160	31.000	99.560	11.542	41.182	45.134
204.000	134.000	240.960	31.000	103.084	14.195	43.369	48.724
206.000	136.000	266.760	31.000	103.684	12.744	42.263	46.506
209.000	138.000	297.960	31.000	104.965	11.516	41.317	44.789
215.000	140.000	270.600	31.000	108.431	14.163	43.541	48.334
217.000	142.000	299.760	31.000	109.080	12.733	42.416	46.187
223.000	144.000	274.560	31.000	112.587	15.430	44.688	49.732
225.000	146.000	302.280	31.000	113.204	13.964	43.532	47.581
231.000	148.000	278.640	31.000	116.755	16.723	45.863	51.147

**Table A-16 (cont.) Steel Structural Plate Pipe Arch Culvert Sizes -  
31 in corner radius (AISI 1999)**

<b>B (in)</b>	<b>D (in)</b>	<b>R<sub>b</sub> (in)</b>	<b>R<sub>m</sub> (in)</b>	<b>R<sub>t</sub> (in)</b>	<b>h<sub>b</sub> (in)</b>	<b>h<sub>m</sub> (in)</b>	<b>h<sub>t</sub> (in)</b>
234.000	150.000	305.160	31.000	117.945	15.402	44.838	49.395
236.000	152.000	336.480	31.000	118.602	13.934	43.651	47.279
239.000	154.000	374.280	31.000	119.908	12.652	42.604	45.572
245.000	156.000	338.160	31.000	123.318	15.352	44.945	49.063
247.000	158.000	373.560	31.000	124.011	13.877	43.725	46.970

**Table A-17 Steel Structural Plate Pipe Arch Culvert Sizes – 47 in corner radius  
(FHWA 2007)**

<b>B (in)</b>	<b>D (in)</b>	<b>R<sub>b</sub> (in)</b>	<b>R<sub>m</sub> (in)</b>	<b>R<sub>t</sub> (in)</b>	<b>h<sub>b</sub> (in)</b>	<b>h<sub>m</sub> (in)</b>	<b>h<sub>t</sub> (in)</b>
240.000	167.000	223.600	47.000	122.180	19.997	62.794	74.031
246.000	171.000	255.700	47.000	124.418	17.557	61.330	70.283
257.000	174.000	236.700	47.000	131.714	22.958	65.400	78.223
263.000	179.000	268.100	47.000	133.444	20.352	63.784	73.695
269.000	183.000	307.100	47.000	135.763	17.899	62.160	70.061
280.000	187.000	280.200	47.000	142.541	23.246	66.347	77.114
290.000	191.000	262.100	47.000	149.131	28.783	70.622	83.853
296.000	194.000	292.200	47.000	151.313	25.940	68.768	80.519
302.000	199.000	328.600	47.000	153.101	23.231	66.908	76.215
307.000	203.000	373.300	47.000	154.796	20.443	64.869	72.136
319.000	207.000	339.400	47.000	162.176	26.126	69.508	79.581
330.000	210.000	315.800	47.000	169.834	32.056	74.285	87.340
336.000	214.000	350.200	47.000	171.618	29.095	72.191	83.433
341.000	219.000	392.300	47.000	172.729	25.950	69.841	78.652
352.000	222.000	361.100	47.000	180.110	31.859	74.712	86.302
364.000	226.000	339.100	47.000	188.575	38.389	80.068	94.225



**Table A-18 Aluminum Structural Plate Pipe Arch Culvert Sizes (CONTECH 2007)**

<b>B (in)</b>	<b>D (in)</b>	<b>R<sub>b</sub> (in)</b>	<b>R<sub>m</sub> (in)</b>	<b>R<sub>t</sub> (in)</b>	<b>h<sub>b</sub> (in)</b>	<b>h<sub>m</sub> (in)</b>	<b>h<sub>t</sub> (in)</b>
79.000	68.000	69.900	31.750	41.709	1.458	32.545	52.485
83.000	69.000	102.900	31.750	44.008	0.971	32.421	51.664
87.000	71.000	188.300	31.750	45.059	0.531	32.192	47.103
93.000	72.000	83.800	31.750	52.020	3.435	33.884	55.662
97.000	73.000	108.100	31.750	53.931	2.633	33.610	54.424
101.000	75.000	150.100	31.750	54.321	1.896	33.245	50.921
106.000	76.000	93.000	31.750	62.063	5.776	35.554	58.196
111.000	77.000	112.600	31.750	65.110	4.968	35.317	57.613
115.000	78.000	141.600	31.750	66.451	3.945	34.811	56.094
119.000	80.000	188.700	31.750	66.212	2.973	34.223	53.049
123.000	81.000	278.800	31.750	67.784	2.029	33.548	51.462
129.000	82.000	139.600	31.750	78.453	6.592	36.843	59.478
133.000	84.000	172.000	31.750	77.253	5.363	36.123	56.621
137.000	85.000	222.000	31.750	78.398	4.181	35.333	54.889
141.000	86.000	309.500	31.750	79.591	3.027	34.466	53.087
147.000	87.000	165.200	31.750	92.024	8.293	38.449	61.349
151.000	89.000	200.000	31.750	90.156	6.880	37.538	58.572
155.000	90.000	251.700	31.750	90.846	5.505	36.561	56.658
157.000	98.000	143.600	31.750	88.923	13.145	41.989	60.266
157.000	100.000	300.800	31.750	81.674	4.576	35.843	46.983
167.000	101.000	132.000	31.750	101.246	18.947	46.140	67.331
168.000	103.000	215.700	31.750	90.471	8.884	39.327	53.816
167.000	113.000	159.300	31.750	85.768	13.700	42.720	51.823
171.000	115.000	176.300	31.750	87.434	12.642	42.115	50.411
176.000	116.000	166.200	31.750	91.219	15.245	44.082	54.387
179.000	118.000	183.000	31.750	92.013	13.865	43.209	52.283
184.000	120.000	173.000	31.750	95.457	16.528	45.244	55.562
187.000	122.000	189.600	31.750	96.228	15.110	44.329	53.467
193.000	124.000	179.700	31.750	100.532	18.123	46.671	57.382
196.000	126.000	196.100	31.750	101.224	16.638	45.694	55.254
201.000	128.000	186.500	31.750	104.783	19.415	47.860	58.574
204.000	130.000	202.500	31.750	105.465	17.932	46.871	56.491
207.000	132.000	221.700	31.750	106.257	16.425	45.822	54.379
213.000	134.000	208.900	31.750	110.506	19.508	48.293	58.291
216.000	136.000	227.300	31.750	111.242	17.992	47.229	56.204
221.000	138.000	215.300	31.750	114.765	20.822	49.502	59.548
224.000	140.000	233.700	31.750	115.468	19.244	48.379	57.424
230.000	141.000	221.500	31.750	120.358	22.456	50.988	61.861
233.000	143.000	239.700	31.750	120.919	20.810	49.804	59.675
238.000	145.000	227.700	31.750	124.646	23.818	52.247	63.147
241.000	147.000	245.300	31.750	125.201	22.187	51.066	61.009

**Table A-18 (cont.) Aluminum Structural Plate Pipe Arch Culvert Sizes  
(CONTECH 2007)**

<b>B (in)</b>	<b>D (in)</b>	<b>R<sub>b</sub> (in)</b>	<b>R<sub>m</sub> (in)</b>	<b>R<sub>t</sub> (in)</b>	<b>h<sub>b</sub> (in)</b>	<b>h<sub>m</sub> (in)</b>	<b>h<sub>t</sub> (in)</b>
241.000	150.000	310.800	31.750	122.446	16.138	46.239	52.780
250.000	151.000	251.200	31.750	130.283	23.807	52.548	62.804
253.000	153.000	270.900	31.750	130.905	22.169	51.320	60.679
258.000	155.000	257.300	31.750	134.560	25.146	53.793	64.093
241.000	167.000	225.400	47.000	122.837	20.019	62.844	74.422
247.000	171.000	257.600	47.000	125.040	17.596	61.386	70.676
257.000	175.000	238.600	47.000	131.283	22.662	65.198	77.177
263.000	179.000	270.000	47.000	133.403	20.134	63.630	73.438

**Table A-19 Aluminum Structural Plate Pipe Arch Culvert Sizes (Historic)  
(FHWA 2007)**

<b>B (in)</b>	<b>D (in)</b>	<b>R<sub>b</sub> (in)</b>	<b>R<sub>m</sub> (in)</b>	<b>R<sub>t</sub> (in)</b>	<b>h<sub>b</sub> (in)</b>	<b>h<sub>m</sub> (in)</b>	<b>h<sub>t</sub> (in)</b>
71.000	65.000	104.400	31.800	37.695	0.136	31.894	56.652
74.000	68.000	68.700	31.800	37.169	0.686	32.168	40.090
78.000	69.000	121.500	31.800	39.427	0.392	32.089	42.582
82.000	71.000	91.300	31.800	41.473	1.098	32.516	42.341
87.000	72.000	82.100	31.800	45.060	2.252	33.180	48.143
91.000	74.000	78.000	31.800	47.238	3.508	33.878	48.536
95.000	76.000	96.700	31.800	48.805	2.872	33.728	45.944
98.000	77.000	303.400	31.800	49.734	0.609	32.345	41.352
103.000	79.000	177.200	31.800	52.632	1.634	33.141	43.479
106.000	81.000	291.600	31.800	53.659	0.972	32.666	40.413
111.000	82.000	189.500	31.800	57.014	2.152	33.591	44.444
116.000	84.000	152.800	31.800	60.144	3.625	34.671	46.804
121.000	85.000	134.300	31.800	64.256	5.372	35.900	50.750
125.000	87.000	164.600	31.800	65.498	4.459	35.397	48.510
128.000	89.000	210.800	31.800	66.101	3.439	34.720	45.679
132.000	91.000	289.000	31.800	67.643	2.566	34.084	43.601
138.000	92.000	155.900	31.800	73.637	7.169	37.507	52.058
140.000	94.000	292.200	31.800	72.043	3.161	34.617	44.621
145.000	95.000	229.500	31.800	75.872	4.916	36.035	48.234
149.000	97.000	296.200	31.800	77.225	3.888	35.271	46.118
154.000	99.000	238.300	31.800	80.607	5.779	36.808	48.806
157.000	100.000	300.800	31.800	81.702	4.568	35.885	47.092
163.000	102.000	246.800	31.800	86.000	6.685	37.623	50.310
168.000	103.000	215.100	31.800	90.535	8.907	39.390	53.967
167.000	113.000	159.300	31.800	85.784	13.684	42.752	51.904

**Table A-19 (cont.) Aluminum Structural Plate Pipe Arch Culvert Sizes (Historic)  
(FHWA 2007)**

<b>B (in)</b>	<b>D (in)</b>	<b>R<sub>b</sub> (in)</b>	<b>R<sub>m</sub> (in)</b>	<b>R<sub>t</sub> (in)</b>	<b>h<sub>b</sub> (in)</b>	<b>h<sub>m</sub> (in)</b>	<b>h<sub>t</sub> (in)</b>
171.000	115.000	176.200	31.800	87.451	12.637	42.156	50.504
176.000	116.000	166.200	31.800	91.239	15.228	44.114	54.468
179.000	118.000	183.000	31.800	92.030	13.849	43.243	52.362
184.000	120.000	173.000	31.800	95.477	16.511	45.276	55.640
187.000	122.000	189.600	31.800	96.245	15.094	44.362	53.544
193.000	124.000	179.700	31.800	100.552	18.107	46.703	57.459
196.000	126.000	196.100	31.800	101.241	16.623	45.727	55.329
201.000	128.000	186.300	31.800	104.815	19.431	47.914	58.685
204.000	130.000	202.500	31.800	105.483	17.916	46.903	56.564
207.000	132.000	221.300	31.800	106.283	16.452	45.888	54.500
213.000	134.000	208.900	31.800	110.525	19.492	48.325	58.363
216.000	136.000	227.300	31.800	111.258	17.977	47.262	56.274
221.000	138.000	215.200	31.800	114.789	20.821	49.544	59.634
224.000	140.000	233.300	31.800	115.499	19.275	48.448	57.546
230.000	141.000	221.500	31.800	120.379	22.440	51.019	61.932
233.000	143.000	239.300	31.800	120.954	20.844	49.874	59.800
238.000	145.000	227.700	31.800	124.667	23.802	52.278	63.216
241.000	147.000	245.300	31.800	125.219	22.172	51.098	61.077
241.000	150.000	310.800	31.800	122.456	16.125	46.275	52.846
250.000	151.000	251.200	31.800	130.302	23.791	52.579	62.872
253.000	153.000	270.900	31.800	130.922	22.154	51.353	60.745
258.000	155.000	257.200	31.800	134.585	25.144	53.835	64.175

**Table A-20 Concrete Pipe Arch Culvert Sizes (ASTM C506 2007)**

<b>B (in)</b>	<b>D (in)</b>	<b>R<sub>b</sub> (in)</b>	<b>R<sub>m</sub> (in)</b>	<b>R<sub>t</sub> (in)</b>	<b>h<sub>b</sub> (in)</b>	<b>h<sub>m</sub> (in)</b>	<b>h<sub>t</sub> (in)</b>
18.000	11.000	22.875	4.031	10.603	0.810	4.698	7.337
22.000	13.500	27.500	5.250	13.738	0.934	6.006	9.868
26.000	15.500	35.500	5.250	14.771	1.185	6.260	9.309
28.500	18.000	40.688	4.594	14.561	1.483	5.909	7.048
36.250	22.500	51.000	6.031	18.750	1.879	7.688	9.555
43.750	26.625	62.000	6.375	22.503	2.456	8.578	10.340
51.125	31.313	73.000	7.563	26.251	2.816	10.087	12.120
58.500	36.000	84.000	8.750	30.000	3.177	11.596	13.901
65.000	40.000	92.500	9.813	33.375	3.550	12.986	15.635
73.000	45.000	105.000	11.219	37.504	3.887	14.691	17.761
88.000	54.000	126.000	12.563	45.004	4.935	17.006	20.108
102.000	62.000	162.500	13.969	51.999	5.131	18.659	21.839
115.000	72.000	183.000	19.281	58.997	5.056	23.805	29.049
122.000	77.250	218.000	20.063	61.997	4.713	24.342	28.691
138.000	87.125	269.000	22.375	69.997	4.851	26.822	31.377
154.000	96.875	301.375	24.000	77.974	5.553	29.111	33.651
168.750	106.500	329.000	26.875	85.492	6.013	32.397	37.619

## A.9 Summary of Referenced Studies

The following table lists in chronological order the studies that have been conducted on hydraulic jumps. Note that it does not provide a summary or abstract of each reference, but rather it summarizes only the information pertinent to this study, sorted by topic.

**Table A-21 Summary of Referenced Studies**

<b>Author</b>	<b>Topic</b>	<b>Notes</b>
Stevens (1933)	Circular Conduits	Derivation of sequent depth formulas for circular conduits using similar logic as elliptical culverts
Lane and Kinsvater (1938)	Circular Conduits	Variable flow in a blocked 6-in transparent pipe Theory and experimentation matched well, although the momentum lessened somewhat, possibly due to boundary friction, non-uniform velocity distribution below the jump, and lower densities due to entrained air bubbles downstream When pipe fills, air supply is cut off, but air continues to become entrained in water within jump, and bubbles travel downstream, causing a vacuum upstream, which moves the jump upstream to rebalance pressure, thus submerging the jump and possibly causing vibrations and cavitation
	Closed Conduits	Momentum equation still applies to closed conduits, for the most part, and therefore may be applied to any type of open channel or closed conduit
Frank (1942)	Circular Conduits	$y_2/D$ on $x$ axis, vs. $y_1/D$ and $y_c/D$ , for complete and incomplete jumps
Kalinske and Robertson (1943)	Circular Conduits	Original source for air entrainment equation Equation for weight of aerated water in jump is validated Tested at slopes of 0, 5, 10, 20, 30% Weight term for steep slopes was found to be up to 75% of $F_1+M_1$ Tested in 6" diameter transparent Lucite

**Table A-21 (cont.) Summary of Referenced Studies**

Author	Topic	Notes
Kalinske and Robertson (1943) (cont.)	Air Entrainment	<p>Original source for air entrainment equation</p> <p>Expanded on work by Lane and Kinsvatar (1938) by considering sloped closed conduits and finding expression for air-pumping capacity</p> <p>Tested on hydraulic jump in sloping circular pipe, and flow high enough that entrained air was carried out of pipe line</p> <p>Air pocket geometry depends on <math>Fr_1</math>, pocket under constant pressure</p> <p>Flow below jump becomes open channel flow, such that hydraulic grade line ran almost parallel to invert of pipe</p> <p>Rate of air entrainment depends on relative intensity of turbulence, which depends on <math>Fr_1</math>. Slope had little effect.</p> <p>Developed air-pumping capacity of closed conduit jumps with slopes up to 30% as function of <math>Fr_1</math></p> <p>If slope of conduit is less than the hydraulic gradient, then bubbles forced through the jump will pass easily downstream; otherwise they build a pocket just downstream of the jump which extends to the outlet; bubble such that water flows at normal depth for slope and flow; air in bubble is under higher pressure, since the jump is incomplete</p> <p>Equation for air pumping capacity, used to find downstream density</p> <p>The pressure in the bubble remains constant, such that the pressure line is parallel to the water surface, as shown by figure</p> <p>At steeper slopes, several identical jumps form in series, each jump forming an air pocket with higher pressure</p>
	Closed Conduits	Full momentum equation taking slope and air entrainment into account
Kinsvatar (1944)	Slope	<p>Original jump classification based on location relative to the sloping channel, A through D</p> <p>First solution for sequent depth in rectangular channels</p> <p>Original classification of sloped channel jumps, using a 1:6 slope</p>
Mavis (1946)	Circular Conduits	Nomograph for circular conduits
Serre (1950)	Closed Conduits	Use of H to denote pressure head above crown of conduit

**Table A-21 (cont.) Summary of Referenced Studies**

Author	Topic	Notes
Haindl (1957)	Rectangular Conduits	Focus of study Air pumping capacity from Stahl and Hager (1999) found to apply also to box conduits Friction neglected, $\alpha_1 = 1$ Closed rectangular (box) cross section $L_r/y_1$ vs. $Fr_1$ is similar to open channel flow, whereas results of $L_r/(D+H)$ and $L_r/(D+H-y_1)$ vs. $Fr_1$ were "greatly dispersed" Equation for energy loss in rectangular conduits Used length of roller instead
	Slope	Approximate weight of jump based on assumptions of linear limitation and linear change in gamma
	Air Entrainment	$\rho = 1/(1+\beta_a)$ , where $\beta_a$ is the air entrainment ratio "Energy loss in the hydraulic jump in a conduit is always... smaller or at the most equal to the energy loss in the hydraulic jump with free surface at identical Froude number in front of the jump" "The air sucked into the region of the roller in the upper part of the jump is driven into the lower zone of the jump in the form of air bubbles" "Near the ceiling the bubbles form air pockets moving along the ceiling, which cause pressure surges in the pipe in the course of flow"
	Closed Conduits	Good diagram for closed conduit flow, including location within conduit "Energy loss in the hydraulic jump in a conduit is always... smaller or at the most equal to the energy loss in the hydraulic jump with free surface at identical Froude number in front of the jump" Use of H to denote pressure head above ceiling of conduit H only depends on pressure head at pipe outlet, and the slopes of the pipe and pressure head line, not on the jump itself

**Table A-21 (cont.) Summary of Referenced Studies**

<b>Author</b>	<b>Topic</b>	<b>Notes</b>
Haindl and Sotornik (1957)	Air Entrainment	Air pumping capacity from Kalinske and Robertson (1943) found to apply also to box conduits Air entrainment isn't dependant on slope or depth ratio Similar study to Kalinske and Robertson (1943) for rectangular conduits, by supposedly more accurate means (gamma radiation), produced similar results, resulting in the same equation produced in Kalinske and Robertson (1943). The "usual law of similarity is not valid for problems of aerated water" These results "point to a wider range of application"
Ayoub (1959)	Circular Conduits	Equation for weight of aerated water in jump is validated
	Slope	For any slope the length $L_j$ increases as the discharge increases, and that for any discharge it decreases as the slope increases
	Air Entrainment	In a sloping conduit the piezometric head on the invert increases up to a certain section, beyond which it will remain constant... the hydraulic grade line will be parallel to the invert, when all entrained air bubbles join together to form a long air pocket.
Chow (1959)	Belanger Equation	A hydraulic jump will form in the channel if $Fr_1$ , $y_1$ , and $y_2$ satisfy the Belanger equation Verified with many experimental data
Harleman (1959)	Friction	"Bed shear is by far the most important corrective term."
	Velocity Distribution	"It can be shown that the momentum-flux corrections and the turbulence-flux corrections tend to cancel each other."
Thiruvengadam (1961)	Circular Conduits	$Z^2$ vs. $y_1/y_2$ equation and chart
	Other Conduits	Similar solutions can also be obtained for other geometrical shapes by this method if $z$ and $A$ can be expressed as mathematical functions
Advani (1962)	Circular Conduits	"A new method based on the use of specific energy and force equations expressed in terms of suitable non-dimensional parameters"
Aryropoulos (1962)	Slope	Formulas for weight term
	Shape	The length and general development of a hydraulic jump is affected by conduit shape



**Table A-21 (cont.) Summary of Referenced Studies**

Author	Topic	Notes
Silvester (1964)	Circular Conduits	<p><math>y_2/y_1</math> vs. <math>y_1/D</math> and <math>Fr_1</math> for closed circular conduits</p> <p>Narrow band of solutions for <math>y_2 &lt; D</math>, curves diverge for <math>y_2 &gt; D</math> depending on <math>y_1/D</math></p> <p>In nonrectangular channels, where jet enters the jump over a smaller width than the downstream surface, more recirculation occurs which probably is the reason for higher energy dissipation</p> <p>Formula for <math>L_j</math> in circular channels</p>
Rajaratnam (1965)	Rectangular Conduits	<p>Momentum equations for box conduits, accounting for air entrainment, for complete and incomplete jumps in horizontal frictionless conduits</p> <p><math>y_2/y_1</math> vs. <math>Fr_1</math> and <math>D/y_1</math> for closed rectangular conduits - difficult to read</p> <p>Study assumes horizontal conduit</p> <p>Direct solution of sequent depth ratio for complete and incomplete jumps, taking into account air entrainment</p>
	Circular Conduits	<p>Air entrainment was only tested for <math>y_1/D</math> up to 0.6, so no analysis was extrapolated for values outside this range</p> <p><math>y_2/y_1</math> vs. <math>Z^2</math> and <math>y_1/D</math> for complete jumps only, <math>Z^2</math> can be easily calculated from <math>Q</math> and <math>D</math>, dotted lines shown for <math>y_1/D</math> over 0.8, "since the nature of flow in that region is not well understood"</p> <p><math>y_2/y_1</math> vs. <math>Fr_1</math> and <math>y_1/D</math> for closed conduits - difficult to read, and transition is marked as a cross line on each line separately; all lines overlap up to <math>Fr_1 = 3</math> and then diverge; this format is used for easy comparison with other charts of other shapes, and <math>Fr_1</math> is applicable since <math>Fr_1 = 1</math> marks critical flow; variation is reversed and curves start crossing each other for <math>y_1/D &gt; 0.5</math>; for <math>y_1/D = 0.7</math> or <math>0.8</math>, <math>y_2/y_1</math> decreases fast with <math>Fr_1</math></p> <p>Chart in Thiruvengadam (1961) should not be used for incomplete jumps</p> <p>Study assumes horizontal conduit</p> <p>Direct solution of sequent depth ratio for complete and incomplete jumps</p> <p>Momentum equations for circular conduits, accounting for air entrainment, for complete and incomplete jumps in horizontal frictionless conduits</p>

**Table A-21 (cont.) Summary of Referenced Studies**

<b>Author</b>	<b>Topic</b>	<b>Notes</b>
Rajaratnam (1965) (cont.)	Closed Conduits	Figure depicting incomplete jump
	Air Entrainment	Air entrainment equation developed by Kalinske and Robertson (1943) may be reasonably applied to all shapes The effect of air entrainment is appreciable Use of air entrainment correction is recommended
Hjelmfeldt (1967)	Elliptical Conduits	Use of $Z^2$ -like format, taking into account complete and incomplete jumps, which gives the same solution as for circular conduits as found by Thiruvengadam (1961) $h_2/D$ vs. $Q^2/gy_1^5*(D/B)^2$ and $y_1/D$ - also applicable for circular conduits
Rajaratnam (1967)	Circular Conduits	Equation for complete jumps plotted in a convenient form, $y_2/y_1$ vs. $Z^2$ and $y_1/D$ Less-convenient form $y_2/y_1$ vs. $Fr_1$ and $y_1/D$ up to 0.6, with "cross-cuts" to indicate transition between complete and incomplete jumps Simple equation for weight of fluid in sloping circular conduit, taking into account air entrainment Equation given for complete jumps and incomplete jumps
	Closed Conduits	"In the case of jumps formed in nonrectangular channels the flow expands in the horizontal direction in addition to the vertical direction, and the front of the jump is in the form of two oblique wings, which may either meet at the center of the channel or be bridged by a partial normal front." Non-rectangular channels are more efficient than rectangular channels "Jumps in horizontal conduits appear to have first studied by Lane and Kinsvatar in 1938"
	Friction	Shear stress for unit channel width given as function of $Fr_1$ only Expression for shear stress ( $\tau_0 = F_f/A_s$ ) as a function of the skin friction coefficient ( $c'_f$ , which is a function of location along the jump only), density of the fluid, and mean velocity "It was found that the boundary shear stress decreases continuously with the distance from the toe of the jump and becomes essentially constant towards the end of the jump"

**Table A-21 (cont.) Summary of Referenced Studies**

Author	Topic	Notes
Rajaratnam (1967) (cont.)	Friction (cont.)	<p><math>Fr_1</math> vs. <math>y_2/y_1</math> for corrected Belanger equation for friction</p> <p>In-depth investigation</p> <p>"The difference in <math>y_2/y_1</math> predicted by [the Belanger equation and the corrected momentum equation] increases with <math>Fr_1</math> and reaches about 4% for <math>Fr_1</math> of 10."</p> <p>Corrected equation for bed shear stress, and experimentation agrees</p>
	Velocity Distribution	<p>Supercritical velocities found not to be uniform, but to resemble a wall jet velocity distribution, which</p> <p>"increases from zero at the boundary to a maximal velocity of <math>u_m</math> and then decreases as <math>y</math> increases further to zero."</p>
	Pressure Distribution	<p>"It is often assumed that the pressure distribution in the entire jump is hydrostatic. At the same time it is difficult to accept this assumption, because of the intense mixing, flow curvatures, and air entrainment inherent in the jump. ...there are appreciable departures from the generally assumed hydrostatic pressure distribution. ...the departure... increases with increasing <math>Fr_1</math>... In all cases, however, there appears to be a narrow region (~2.5% of depth), close to the bed, where the pressure distribution is essentially hydrostatic."</p>
	Air Entrainment	<p>Turbulence and air entrainment in classical jumps</p>
Rajaratnam (1968b)	Friction	<p>As relative roughness increases, tailwater depth decreases asymptotically, such that <math>y_t/y_2 = 0.783</math> for <math>k_e/y_1 = 0.50</math></p> <p>Relative roughness on bed to supercritical depth ranged from 0.02 to 0.43</p> <p>First symmetric study on "rough jumps."</p> <p><math>y_2/y_1</math> vs. <math>Fr_1</math> and <math>k_e/y_1</math> (testing range <math>Fr_1</math> 3 to 10)</p> <p>(No correction to the velocity observations was made for the effects of entrained air, turbulence, and pitot-displacement)</p> <p>"For <math>k_e/y_1</math> greater than about 0.05, the length of the roller for the rough jump is reduced to roughly one half when compared with that of the smooth bed jump" (testing range <math>Fr_1</math> 3 to 10)</p>

**Table A-21 (cont.) Summary of Referenced Studies**

Author	Topic	Notes
Rajaratnam (1968b) (cont.)	Friction (cont.)	<p>"The length of the surface roller as well as the length of the jump are roughly about half of the corresponding smooth bed jump for the relative roughness greater than about 0.10 (testing range <math>Fr_1</math> 3 to 10)</p> <p>"In a certain range <math>Fr_1</math>, the energy dissipation in the rough jump is appreciably larger than that of the corresponding classical jump, when the relative roughness is not too small, which one might expect"</p> <p>"For large values of the relative roughness, the reduction in the tailwater depth required is appreciable and the length of the jump gets reduced considerably"</p> <p>"Because the rough bed jump needs a smaller tailwater depth and is much shorter when compared with the corresponding smooth bed jump, it could advantageously be used for energy dissipation purposes"</p>
	Rectangular Channels	Nomographs for rectangular channels
	Circular Conduits	<p><math>y_2/D</math> on x axis, versus <math>y_1/D</math> and <math>y_c/D</math> for complete and incomplete jumps, with good figures, and pretty easy to read, complete and incomplete jumps are clearly separated, and equations used are identified in caption</p> <p>Equation for specific force for complete (iterative) and incomplete (explicit) jumps</p>
	Closed Conduits	"The change of flow from a low stage to a high stage, resulting in a hydraulic jump, may occur in a close conduit under part-full flow or pressure-flow conditions downstream of the jump."
Rajaratnam (1968b)	Circular Conduits	<p>Equations are complex, so explicit solutions are "probably impossible to calculate"</p> <p>Iteration is required</p> <p>Approximation of Froude number and <math>y_2</math> using <math>y_1</math> and approximation of <math>y_c</math> for <math>y_c &lt; 0.85D</math></p> <p>"Virtually impossible to maintain critical flow near the top of a circular conduit" (<math>y_c/D &gt; 0.85</math>)</p> <p>Use of undular, steady, strong, and so forth for circular channels</p> <p>For open channel flow: <math>Fr_1</math> up to 1.7 – undular; above 1.7 – steady to strong</p>

**Table A-21 (cont.) Summary of Referenced Studies**

Author	Topic	Notes
Gill (1980)	Friction	Rectangular, horizontal channel considered Bed shear is by far the most important corrective term for the momentum equation The Belanger equation was found to only slightly over-predict the sequent depth ratio by neglecting friction
Hsu et al. (1980)	Circular Conduits	$y_1/y_2$ vs. $Z^2$ and $y_1/D$ , multiple charts corresponding to different slopes (0, 5, 10, 30, 60%) for complete and incomplete jumps "Conduit capacity and flow velocity reach their maximum when the depth is about 90-95% of the conduit diameter. In practice, these maximum conditions seldom occur because any flow disturbance... tends to seal the conduit Fr is relatively insensitive to y for $y/D = 0.1$ to $0.7$ ; Max Fr occurs at about $y/D = 0.4$ Length = $f(\text{Fr}_1, y_1, \text{slope})$ , for complete and incomplete jumps
	Slope	Weight term considered for circular pipes, taking into account $y_1$ , $\text{Fr}_1$ , full area, gamma, and air entrainment ratio
	Air Entrainment	"In general, except for high water discharges, a jump pumps air into the flow at a higher rate than the flow beyond the jump can handle and periodic blowback occurs. The air blowback will cause the jump to temporarily move downstream."
	Closed Conduits	Good definition sketch of incomplete jump, accounting for slope "The energy loss of a hydraulic jump in a closed conduit is smaller than the similar condition in open channel with identical $\text{Fr}_1$ , because the flow is confined by the conduit and cannot expand to the full sequent depth."
Hughes and Flack (1984)	Friction	"Observations showed that boundary roughness reduces both the sequent depth and the length of a hydraulic jump, and that the observed reductions were related to both Froude number and the degree of roughness. The observed hydraulic jump characteristics are consistent with theory, and a proposed approximation for a theoretical hydraulic jump equation compares favorably with the observed characteristics." Rectangular flume used to test this
	Pressure Distribution	Correction factors for streamwise pressure distribution found not to make a significant difference

**Table A-21 (cont.) Summary of Referenced Studies**

Author	Topic	Notes
French (1985)	Circular Conduits	Empirical equations for finding sequent depth in circular conduits
Normann et al. (1985)	Closed Conduits	"Just-full flow" = full pipe without pressure, like open channel flow
Hager and Bremen (1989)	Friction	<p>Time-averaged 2D velocity Distributions along classical jumps, with jump shape equations</p> <p>Study limited to <math>2 &lt; Fr_1 &lt; 12</math></p> <p>Additional term in momentum equation for friction derived for classical jumps</p> <p>Function of <math>Fr_1</math>, aspect ratio, and <math>Re_1</math></p> <p>Explicit approximation for sequent depth ratio based on these</p> <p>Observations normally found to deviate from equations by only 2%</p> <p>Series of charts for rectangular hydraulic jump for sequent depth ratio as function of <math>Fr_1</math>, <math>Re_1</math>, and aspect ratio</p> <p>Belanger equation always overestimates actual observed SD ratio, especially with small <math>y_1</math>, because of frictional forces</p>
Matsushita (1989)	Air Entrainment	<p>Tentative classification: (1) single jump - normal incomplete jump; (2) transition jump - jump pushed upstream by accumulation of bubble downstream; eventually the bubble blows out through the jump and the jump returns to a single jump, to restart the process; (3) multi-jump - many stable jumps occur in series, separated by air pockets; all types are affected by tailwater, hydraulic properties of discharge, pipe diameter and slope, and the existence of exhaust vents or pipes; diagrams of each type</p>
Smith and Chen (1989)	Rectangular Conduits	<p>Equation from Kalinske and Robertson (1943) modified slightly for square and rectangular conduits</p> <p><math>\beta_1, \beta_2, \beta_a, \beta_j</math> (to account for air recirculation), <math>K</math>, slope used</p> <p>"Theoretical curves of <math>H_j/D</math> versus <math>Fr_1</math> could not be determined analytically for a sloping conduit"</p> <p><math>H_j/D</math> vs. <math>Fr_1</math> and <math>y_1/D</math>, separate chart for <math>S = 0, 0.10, 0.20, 0.30, 0.4</math>, composite chart - very confusing, transition from complete to incomplete jumps denoted by a dotted line</p> <p>Empirical equations given, interpolation needed</p> <p>Jump height must be determined experimentally</p>

**Table A-21 (cont.) Summary of Referenced Studies**

Author	Topic	Notes
Smith and Chen (1989) (cont.)	Rectangular Conduits (cont.)	For a constant $y_1/D$ , an explicit expression can be written relating jump height to $Fr_1$ Experiments agreed with theory, but jump height was in reality slightly smaller than predicted, and the difference became more pronounced as $Fr_1$ increased, due to the omission of post-jump air-water ratio and friction terms Equation for transition given explicitly, and equations for complete and incomplete jumps provided
	Closed Conduits	Good diagram of incomplete jump Jump height increases for $y_1/D$ up to about 2/3, then decreases As $y_1/D$ approaches 1, the jump height approaches 0, so no jump occurs at all when the pipe flows full Jump height is function of $Fr_1$ , $y_1/D$ , slope, $\beta_a$ , $\beta_j$ , $L_j/D$ , $K$ , and friction - too many to solve analytically, even if friction is ignored, and velocity coefficients are assume to be 1; must be determined experimentally "For the special case of a horizontal closed conduit, and with some simplifying assumptions, a theoretical solution can be obtained" Jump length becomes shorter in closed conduits as $y_1/D$ becomes larger
	Friction	Omission of friction overestimates jump height; departure increases with $Fr_1$
	Slope	$H_j/D$ vs. $Fr_1$ and $y_1/D$ , separate chart for $S = 0, 0.10, 0.20, 0.30, 0.4$ , composite chart - very confusing, transition from complete to incomplete jumps denoted by a dotted line Empirical equations given, interpolation needed
	Air Entrainment	Omission of air entrainment overestimates jump height Blowback explained
Hager (1990)	Circular Conduits	$h_2/D$ vs. $Z^2$ and $y_1/D$ for complete jumps only
Ohtsu and Yasuda (1991a)	Slope	If slope is larger than 23 degrees, no clearly identifiable surface roller forms, but a high-velocity jet continues along the channel bed far downstream Practical equations for $L_j$ on sloped channels for $B, D$ jumps

**Table A-21 (cont.) Summary of Referenced Studies**

<b>Author</b>	<b>Topic</b>	<b>Notes</b>
Hager (1992)	Circular Conduits	<p>Circular chart: <math>Z</math> vs. <math>y_2/D</math>, with simplified equation (for complete jumps only)</p> <p>Circular channel jumps may or may not have a surface roller</p> <p>"Few experimental studies are available [for circular channels]... The conventional momentum approach is again in agreement with observations".</p> <p><math>L_j = 5</math> to <math>7</math> times <math>y_2</math></p> <p>"The conventional momentum approach is again in agreement with observations, as for... non-rectangular channels."</p>
	Friction	<p><math>\kappa = k_e/y_1</math>, <math>k_e</math> = equivalent roughness height, <math>y_2/y_1 = Fr_1 + 0.41(Fr_1 - 1)\exp(-6\kappa)</math>, <math>y_2</math> and jump length reduced considerably compared to classical jump</p>
Bremen and Hager (1993)	Belanger Equation	Linear approximation for Belanger equation
Husain et al. (1994)	Slope	<p><math>K</math> is defined as correction coefficient for shape, function of <math>Fr_1</math> and slope</p> <p><math>Fr_1</math> corrected for slope terms</p> <p><math>y_2/y_1</math> vs. <math>Fr_1</math> for multiple slopes (applicable for rectangular channels, <math>4 &lt; Fr_1 &lt; 12</math>, <math>1 &lt; S &lt; 10</math>)</p> <p>Explicit linear solution for <math>L_j/d_1</math>, <math>L_j/d_2</math>, or <math>L_j/(d_2 - d_1)</math> as function of slope and <math>Fr_1</math></p> <p>Explicit linear solution for sequent depth ratio as function of slope and <math>Fr_1</math></p>
Gunal and Narayanan (1996)	Slope	<p>Tested for <math>S = 0</math> to <math>10\%</math></p> <p>Rectangular channel</p> <p>"The estimate of the roller length by visual observations can be as much as <math>1.6</math> times that obtained from the mean velocity profiles. For a particular Froude number it is likely to be affected by such factors as the Reynolds number, the upstream velocity profiles, and the depth to width ratio of the channel."</p>
Montes (1998)	Circular Conduits	<p>Use of <math>Fr_1</math> instead of <math>Z^2</math> vs. <math>y_2/y_1</math> - all lines converge to a point at <math>Fr_1 = 1</math>. (This cannot be used for incomplete jumps)</p> <p>Charts for complete and incomplete jumps in circular conduits using <math>y'_1</math> vs. <math>y'_2</math> with <math>Fr_1</math> on lines</p>
	Other Conduits	Use iterative method to find $y_2$ or solve for $Fr_1$ directly and create chart
	Friction	Narrower channels tend to produce shorter jumps (because of friction)



**Table A-21 (cont.) Summary of Referenced Studies**

Author	Topic	Notes
Montes (1998) (cont.)	Air Entrainment	Because incomplete jumps limit the supply of air entrainment, unless sufficient air is supplied by vents, etc., the jump will create a vacuum which will pull the jump upstream. Also, the air is released downstream at the crown of the culvert, creating a bubble that restricts flow and thus increases velocities
	Closed Conduits	<p>Experimental verification for jumps in closed conduits is relatively weak compared with open channels</p> <p>"If the conjugate depth <math>y_2</math> is greater than the height of the section, the conduit runs full, and an incomplete jump develops. However, the deficit in the depth, which cannot itself exceed the maximum height of the conduit, is made up by the hydrostatic pressure against the crown."</p> <p>Momentum equation for incomplete jumps</p> <p>Momentum equation rearranged to produce general equation based on <math>Fr_1</math> instead of <math>Z^2</math></p> <p>Experimental verification for jumps in closed conduits is relatively weak compared with open channels</p>
Hager (1999)	Rectangular Conduits	$L_r/y_1 = 5.75(Fr_1 - 2)$ for $Fr_1 < 10$ Ventilation length $L_a = 10Q/b$ (metric) $L_j/h_1 = f(Fr_1, S_0)$
	Circular Conduits	<p>For <math>Fr_1 \leq 1.5</math>, jump is undular; <math>1.5 &lt; Fr_1 &lt; 2</math> undulations begin to break; <math>Fr_1 &gt; 2</math> direct hydraulic jump; For <math>y_1/D &lt; 1/3</math> lateral wings and surface jet form with two asymmetric separation zones and bottom recirculation, because of a large increase in surface width from downstream to upstream; for <math>y_1/D &gt; 1/3</math> a classical-looking jump forms, with a straight front, surface roller, and bottom forward flow; Figure</p> <p>Energy dissipation is significantly smaller, and jump stability is lower than for equivalent rectangular jumps</p> <p><math>y_2/D</math> vs. <math>Z</math> and <math>y_1/D</math> for complete jumps, dotted line to indicate <math>Fr_1 = 1</math>, good diagram of jump within chart, only up to <math>y_1/D = 0.8</math>, easy to read</p> <p><math>y_2/D</math> vs. <math>Z</math> (<math>qD</math>) and <math>y_1/D</math> for <math>S_0 = 0, 10, 20, \text{ and } 30\%</math> (separate charts) for complete and incomplete jumps, transition marked by a dotted line, explanation and commentary provided</p> <p><math>zA</math> and <math>A</math> given in terms of <math>\theta</math></p>

**Table A-21 (cont.) Summary of Referenced Studies**

Author	Topic	Notes
Hager (1999) (cont.)	Circular Conduits (cont.)	Dimensionless specific force equation given as $Z^2 = f(zA', A')$ Approximate solutions that can be solved explicitly Full momentum equation for closed conduit flow in circular conduits including weight term as function of $L_j$ and $S_0$ , and air entrainment term Approximate expression for choking discharge
	Elliptical Conduits	$zA$ and $A$ given in terms of $B, D, y_1$ Reduces to circular equation for $B=D$ Same as circular, except for definition of $Z$ No experimental study up-to-date on elliptical or pipe arches
	Pipe arch Conduits	Approximated by ellipse for $B:D = 2:1.5$ , which is same as circular, except for definition of $Z$ No experimental study up-to-date on elliptical or pipe arches
	Closed Conduits	Causes of transition to pressurized flow: "downstream submergence, large discharge, or conduit damage,... insufficient ventilation of the flow, wave formation due to flow disturbances... especially in supercritical flows, or the formation of... hydraulic jumps caused by downstream submergence" $L_j$ for closed conduits defined as the "distance between the toe of the jump and the point where the profile meets the conduit soffit" "The hydraulic jump can, for example, occur... for a supercritical flow in a closed channel impinging suddenly on a pool of standing water downstream." Transition may be termed "surcharge" or "choking", and is abrupt "Careful experiments have failed to produce the so-called full flow condition, corresponding to free pipe full flow without surcharge" Full momentum equation for closed conduit flow in circular conduits including weight term as function of $L_j$ and $S_0$ , and air entrainment term
	Slope	As of 1999, no studies of effects of bottom slope on hydraulic jumps in circular conduits
	Friction	"Values of $y_2$ calculated after taking into account the influence of friction are always slightly smaller than the corresponding values obtained experimentally. The sequent flow depths obtained [analytically] may be considered as the upper bound, therefore."

**Table A-21 (cont.) Summary of Referenced Studies**

<b>Author</b>	<b>Topic</b>	<b>Notes</b>
Hager (1999) (cont.)	Air Entrainment	In all cases "air bubbles are either transported along with the flow or the bubbles return upstream due to buoyancy" Possible disadvantages: "pulsating slug flow, reduction of discharge due to two-phase flow, and uncontrolled air outblow"
Stahl and Hager (1999)	Circular Conduits	Simplified hydraulic computation compared with experimentation to determine sequent depth ratio in circular conduits, based on $Fr_1$ Choking criteria for circular conduits based on $Fr_1$ (compare to transition equation?) Two types of jumps found in circular conduits, depending on upstream depth ratio: $y'_1 < 1/3 \rightarrow$ lateral recirculation, $y'_1 > 1/3 \rightarrow$ direct (classical) jump Height and $L_j$ Tested for $1.5 < Fr_1 < 6.5$ , $0.2 < y'_1 < 0.7$
	Closed Conduits	Complete jumps in closed conduits have received little attention relative to incomplete jumps (sources cited) Term "choking" used to describe transition between complete and incomplete jumps
Negm (2000)	Friction	Roughness taken into account
	Slope	Slope taken into account
Sturm (2001)	Circular Conduits	Circular momentum function Chart with $Z^2$ vs $y_2/y_1$
	Rectangular Channels	Rectangular momentum function
Ead and Rajaratnam (2002)	Friction	Sequent depth ratio for corrugated or rough beds in rectangular channels "It was found that the tailwater depth required to form a jump was appreciably smaller than that for the corresponding jumps on smooth beds. Further, the length of the jumps was about half of those on smooth beds. The integrated bed shear stress on the corrugated bed was about 10 times that on smooth beds."
Hotchkiss et al. (2003)	Circular Conduits	References for computing sequent depth References for computing $L_j$ Experimentation on circular culverts seem to limit $y'_1$ to 0.7 or 0.85
	Closed Conduits	Complete vs. incomplete defined

**Table A-21 (cont.) Summary of Referenced Studies**

Author	Topic	Notes
Beirami and Chamani (2006)	Slope	<p>Sequent depth ratio equation for sloped rectangular channels given                      Applicable for <math>4.5 &lt; Fr_1 &lt; 12</math>                      “Observations showed that in those cases where the gravity force component in the jump was opposite to the flow direction, the water surface of the surface roller became undular and unstable. The hydraulic jump on an entirely adverse slope was almost impossible to control. The analysis of experimental data showed that the negative slope of the basin reduces the sequent depth ratio, while a positive slope increases the sequent depth ratio.”                      (Friction ignored in study, which explains slight deviation between theory and experimentation; difference becomes more notable with higher values of friction and <math>Fr_1</math>)</p>
Bushra and Noor (2006)	Circular Conduits	<p>Use of dimensionless parameters (like <math>y/D</math>, <math>A/D^2</math>, <math>hcA/D^3</math>, <math>Q^2/gD^5</math>), conversion from <math>Z^2</math> to <math>Fr_1^2</math>                      Approximate solutions for dimensionless area and area*centroid with max error 20% for <math>y_1/D = 0.2</math> to 0.9  <math>L_j/h_2</math> is independent of <math>Fr_1</math> for large <math>Fr_1</math></p>
Thompson and Kilgore (2006)	Circular Conduits	<p><math>Fr_1</math> vs <math>y_2/y_1</math>                      For incomplete jumps in circular pipes, use <math>L_j = 7(y_2 - y_1)</math></p>
Carollo et al. (2007)	Friction	<p>Tests performed in a rectangular flume to find new solution to sequent depth and <math>L_j</math> taking roughness into account                      Use of beta to alter Belanger equation                      Sequent depth ratio and <math>L_j</math> decrease as roughness increases, and the reduction increases with <math>Fr_1</math>                      Error of 5% in estimate of sequent depth ratio</p>



## Appendix B. Sequent Depth Derivations

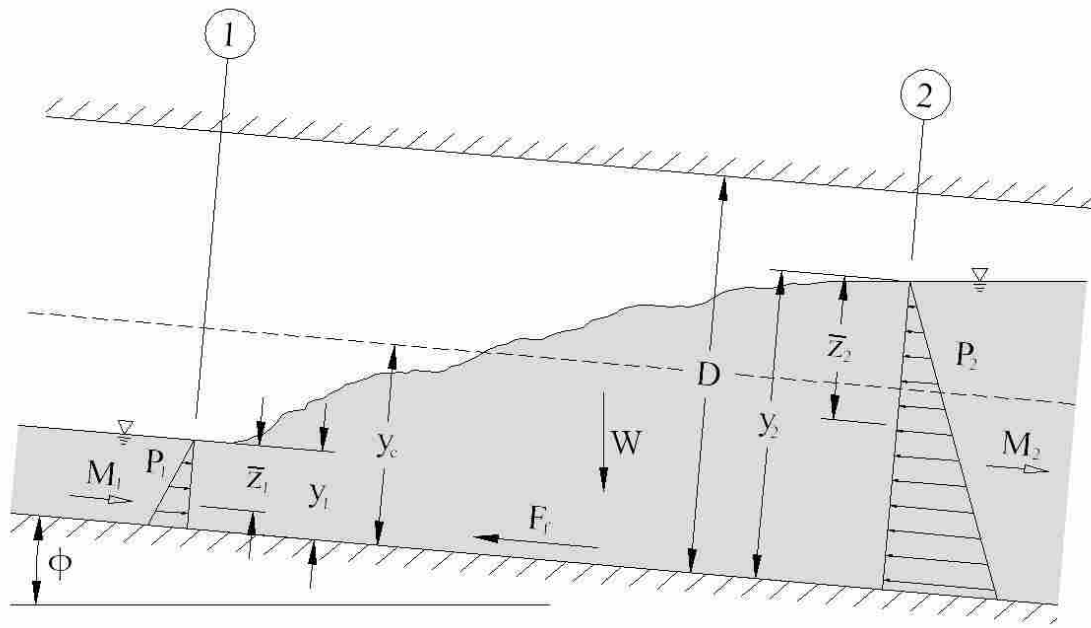
### B.1 General Solution

#### B.1.1 Momentum Equation

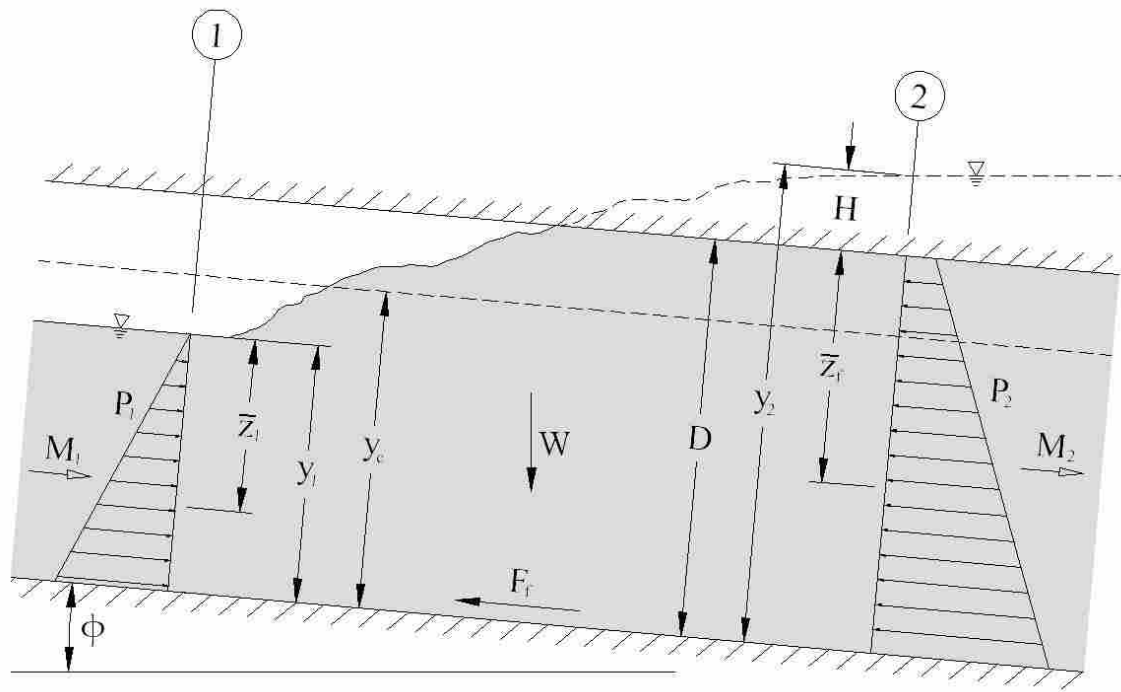
Momentum theory states that the sum of the external forces acting upon a system equals the change in momentum across that system (Thompson and Kilgore 2006). This principle can successfully be applied to complete or incomplete hydraulic jumps such as those shown in Figure B-1 on the next page. According to this figure, and using an axis parallel to the channel or conduit bed, a one-dimensional form of the momentum equation may be written:

$$P_1 - P_2 + W\sin\phi - F_f = M_2 - M_1 \quad (\text{B-1})$$

where  $P_1$  and  $P_2$  are the pressure forces (lbs, N) at sections (1) and (2), respectively;  $W$  is the weight (lbs, N) of the fluid within the control volume;  $\phi$  is the bed slope angle (degrees) from the horizontal;  $F_f$  is the force of friction (lbs, N) caused by the channel or conduit; and  $M_1$  and  $M_2$  are the momentum fluxes (lbs, N) at sections (1) and (2), respectively.



(a)



(b)

**Figure B-1 Forces acting on (a) complete and (b) incomplete hydraulic jumps in closed conduits**

On the left side of the equation, assuming hydrostatic pressure distribution, the pressure force at section (1) is given by:

$$P_1 = \rho_1 g \bar{z}_1 A_1 \cos\phi \quad (\text{B-2})$$

where  $\rho_1 = \rho_w$  is the density of water (slugs/ft<sup>3</sup>, kg/m<sup>3</sup>) at section (1);  $g$  is the acceleration (ft/s<sup>2</sup>, m/s<sup>2</sup>) due to gravity;  $\bar{z}_1$  is the distance (ft, m) from the water surface to the centroid of the cross-sectional area at section (1), perpendicular to the channel; and  $A_1$  is the cross-sectional area (ft<sup>2</sup>, m<sup>2</sup>) at section (1).

Again assuming hydrostatic pressure distribution, the pressure force at section (2) is given by:

$$P_2 = \rho_2 g \bar{z}_2 A_2 \cos\phi \quad (\text{B-3})$$

where  $\rho_2$  is the average density of the water (slugs/ft<sup>3</sup>, kg/m<sup>3</sup>) at section (2);  $\bar{z}_2$  is the distance (ft, m) from the water surface to the centroid of the cross-sectional area at section (2), perpendicular to the channel; and  $A_2$  is the cross-sectional area (ft<sup>2</sup>, m<sup>2</sup>) at section (2). Due to air entrainment within the jump, the density of the water leaving the control volume is on average less than that entering it, such that  $\rho_2$  is given approximately by:

$$\rho_2 \approx \frac{\rho_w}{1 + \beta_a} \quad (\text{B-4})$$



where  $\beta_a$  is the ratio of air to water after the jump. Kalinske and Robertson (1943) and Haindl and Sotornik (1957) found this to be a function of the upstream Froude number only, regardless of channel shape or slope (see Appendix A.4).

It is appropriate at this point to note that the area  $A$  and centroid  $\bar{z}$  are functions of both the shape of the conduit and the depth of flow through the conduit. These functions are quite simple for some shapes (i.e. rectangular), but in the case of more complex shapes which must be treated in parts (i.e. pipe arches), the area and centroid must be computed by (Hibbeler 2001):

$$A = \sum A_i \quad (\text{B-5})$$

$$\bar{z} = \frac{\sum \bar{z}_i A_i}{\sum A_i} \quad (\text{B-6})$$

In the case of the centroid, taking the weighted average can be cumbersome, so instead the product of the centroid and area is used, given by:

$$\bar{z}A = \sum \bar{z}_i A_i \quad (\text{B-7})$$

Since the centroid is never computed alone in this study,  $\bar{z}_1$  is hereafter combined with  $A_1$  and written instead as  $(\bar{z}A)_1$ , as is  $\bar{z}_2$  with  $A_2$ .

Returning to the momentum equation, the weight of the fluid within the control volume may be expressed in a variety of different ways. Conceptually, if the distance (ft,

m) parallel to the channel or conduit axis is measured from section (1) downstream, denoted by  $x$ , then the weight may be approximated mathematically as the integral of the incremental weight of the water summed over the entire control volume, given by:

$$W = \int dW = \int \rho g dV = \int_0^{L_j} \rho g A dx \quad (\text{B-8})$$

The frictional force may also be expressed in a variety of ways, but conceptually it is the cumulative shear stress (psf, Pa),  $\tau_0$ , over the wetted surface between sections (1) and (2). If the distance (ft, m) around the wetted perimeter ( $P_w$ ) from one side to a point along the wetted perimeter at any point ( $x$ ) along the jump is measured, denoted by  $\lambda$ , then the frictional force may be approximated mathematically as the integral of the shear stress over the cumulative wetted area, given by:

$$F_f = \int \tau_0 dA = \int_0^{L_j} \left( \int_0^{P_w} \tau_0 d\lambda \right) dx \quad (\text{B-9})$$

On the right side of the momentum equation, the momentums at sections (1) and (2) are given by:

$$M_1 = \beta_1 \rho_1 Q V_1 \quad (\text{B-10})$$

$$M_2 = \beta_2 \rho_2 Q V_2 \quad (\text{B-11})$$

where  $\beta_1$  and  $\beta_2$  are the Boussinesq velocity distribution coefficients at sections (1) and (2), respectively,  $V_1$  and  $V_2$  are the velocities (ft/s, m/s) at sections (1) and (2), respectively, and  $Q$  is the flow rate (cfs, cms) through the channel or conduit. By continuity,  $V_1 = Q/A_1$  and  $V_2 = Q/A_2$ .

Combining these equations, the momentum equation in its full form may be written as:

$$\rho_w g(\bar{z}A)_1 \cos\phi - \left( \frac{\rho_w}{1 + \beta_a} \right) g(\bar{z}A)_2 \cos\phi + \left( \int_0^{L_j} \rho g A dx \right) \sin\phi - \int_0^{L_j} \left( \int_0^{P_w} \tau_0 d\lambda \right) dx = \frac{\beta_2 \rho_w Q^2}{A_2(1 + \beta_a)} - \frac{\beta_1 \rho_w Q^2}{A_1} \quad (\text{B-12})$$

Dividing through by  $\rho_w$ , and assuming a horizontal bed slope (i.e.  $\phi = 0^\circ$ ), no air entrainment (i.e.  $\beta_a = 0$ ), no friction (i.e.  $\tau_0 = 0$ ), and uniform velocity distributions at sections (1) and (2) (i.e.  $\beta_1 = \beta_2 = 1$ ), the momentum equation may be reduced to its simplest form:

$$g(\bar{z}A)_1 - g(\bar{z}A)_2 = \frac{Q^2}{A_2} - \frac{Q^2}{A_1} \quad (\text{B-13})$$

This simplified form of the momentum equation is the one used for the remainder of this study.

### B.1.2 Dimensionless Parameters

When creating sequent depth charts, it is often convenient to use ratios such as the Froude number to generalize the solution and eliminate the need for units. In this study, such ratios are expressed as dimensionless parameters, denoted by the ‘prime’ superscript (except for the Froude number), as defined below:

$$Fr_1 \equiv \frac{V_1}{\sqrt{g A_1 / T_1}} = \frac{Q}{\sqrt{g A_1^3 / T_1}} = \frac{Q}{\sqrt{g B^2 D^3 A_1' / T_1}} \quad (\text{B-14})$$

$$y'_i \equiv \frac{y_i}{D} \quad (\text{B-15})$$

$$T_i \equiv \frac{T_i}{B} = \Gamma(\text{shape}, y'_i) \quad (\text{B-16})$$

$$A'_i \equiv \frac{A_i}{BD} = \Omega(\text{shape}, y'_i) \quad (\text{B-17})$$

$$(\bar{z}A)'_i \equiv \frac{(\bar{z}A)_i}{BD^2} = \Psi(\text{shape}, y'_i) \quad (\text{B-18})$$

where  $Fr_1$  is the upstream Froude number;  $y_i$  is the depth of flow (ft, m) at section (i);  $D$  is the rise (or maximum height) of the conduit (ft, m);  $T_i$  is the top width of flow (ft, m) at section (i);  $B$  is the span (or maximum width) of the conduit (ft, m);  $A_i$  is the cross-sectional area of flow (ft<sup>2</sup>, m<sup>2</sup>) at section (i); and  $(\bar{z}A)_i$  is the product of the cross-

sectional area of flow at section (i), and the distance from the water surface to the centroid of that area (ft<sup>3</sup>, m<sup>3</sup>). The functions  $\Gamma$ ,  $\Omega$ , and  $\Psi$  are derived hereafter for each of the five conduit shapes in this study.

### B.1.3 Complete Jumps

Complete hydraulic jumps are defined here as closed conduit jumps in which the downstream subcritical flow remains open channel or gravity flow, i.e.  $y_2 < D$  (see Figure B-1a). If  $T_1$  is defined as the top width of flow (ft, m) at section (1), then by rearranging Equation B-13 and multiplying both sides of by  $T_1/A_1^3$ , the following relationship may be found (Montes 1998):

$$\frac{Q^2 T_1}{g A_1^3} = \frac{T_1 A_2 [(\bar{z}A)_2 - (\bar{z}A)_1]}{A_1^2 (A_2 - A_1)} \quad (\text{B-19})$$

The left side of this equation is equivalent to the square of the upstream Froude number ( $Fr_1$ ), and the top width  $T$ , area  $A$ , and centroid-area  $\bar{z}A$  are functions of both the shape of the conduit and the depth of flow through the conduit at sections (1) and (2).

By dividing the numerator and denominator of the right side of Equation B-19 by  $B^3 D^3$ , the equation may be rewritten in its dimensionless form:

$$Fr_1^2 = \frac{T_1 A'_2 [(\bar{z}A)'_2 - (\bar{z}A)'_1]}{A_1'^2 (A'_2 - A'_1)} \quad (\text{B-20})$$

where  $Fr_1$ ,  $T_1$ ,  $A'_{1,2}$ , and  $(\bar{z}A)'_{1,2}$  are defined by Equations B-14 through B-18. This equation may be used for any conduit shape to generate the complete or normal jump portion of a sequent depth chart similar to those found in Montes (1998). Unfortunately, in most cases it cannot be solved for  $y'_2$  explicitly. In this study, the interval halving method (Sturm 2001) was used to iteratively find the solutions.

#### **B.1.4 Incomplete Jumps**

Incomplete hydraulic jumps are defined here as closed conduit jumps in which the downstream subcritical flow becomes pressurized, i.e.  $y_2 \geq D$  (see Figure B-1b). In this the sequent depth  $y_2$  does not exist except in theory, because the water surface meets the top of the conduit within the control volume before such a depth can be reached. The depth  $y_2$  may instead be considered as the pressure head (ft, m) at section (2), measured from the conduit bottom, or the sum of the rise of the conduit,  $D$ , and the pressure head (ft, m),  $H$ , above the conduit (Montes 1998). In its dimensionless form,  $y'_2$  is therefore expressed as:

$$y'_2 = 1 + H' \tag{B-21}$$

where  $H' \equiv H/D$  is the dimensionless pressure head above the conduit.

The flow area  $A_2$  cannot exceed the cross sectional area of the conduit itself, so for pressure flow the subscript '2' is replaced by 'f' to denote full conditions (i.e.  $y'_f = 1$ ). The centroid  $\bar{z}_2$  may also be considered as the sum of the centroid at full conditions,  $\bar{z}_f$ ,

and the pressure head above the top of the conduit,  $H$ . With this notation, Equation B-19 may be rewritten in a dimensionless form for incomplete jumps:

$$Fr_1^2 = \frac{T_1 A'_f [(\bar{z}A)'_f + H' A'_f - (\bar{z}A)'_1]}{A_1'^2 (A'_f - A'_1)} \quad (B-22)$$

In this case only  $H'$  is a function of  $y'_2$ , such that it may be solved for explicitly:

$$H' = \frac{1}{T_1 A_1'^2} \left\{ Fr_1^2 A_1'^2 (A'_f - A'_1) - T_1 A'_f [(\bar{z}A)'_f - (\bar{z}A)'_1] \right\} \quad (B-23)$$

Combining Equations B-21 and B-23 results in the following explicit solution for  $y'_2$ :

$$y_2' = 1 + \frac{1}{T_1 A_1'^2} \left\{ Fr_1^2 A_1'^2 (A'_f - A'_1) - T_1 A'_f [(\bar{z}A)'_f - (\bar{z}A)'_1] \right\} \quad (B-24)$$

where  $Fr_1$ ,  $T_1$ ,  $A'_{1,f}$ , and  $(\bar{z}A)'_{1,f}$  are defined by Equations B-14 through B-18. This equation may be used for any conduit shape to generate the incomplete jump portion of a sequent depth chart similar to those found in Montes (1998).

### B.1.5 Transitional Jumps

Transitional hydraulic jumps are defined here as closed conduit jumps in which the conduit at section (2) is barely full without being pressurized, i.e.  $y_2 = D$ . In practice, this condition is rare if not impossible, because as  $y$  approaches  $D$ , “choking” occurs, in

which the flow abruptly and spontaneously fills the conduit and becomes pressurized (Hager 1999). In theory, however, it is important to determine at what value of the upstream Froude number to expect the transition between a complete and incomplete jump, so that the appropriate equation may be used to calculate the sequent depth. The transitional upstream Froude number,  $(Fr_1)_t$ , may be found either by substituting the subscript 'f' for '2' in Equation B-20, or by setting  $y'_2 = 1$  within Equation B-24; both methods produce the same result:

$$(Fr_1)_t^2 = \frac{T_1 A'_f [(\bar{z}A)'_f - (\bar{z}A)'_1]}{A'_1{}^2 (A'_f - A'_1)} \quad (B-25)$$

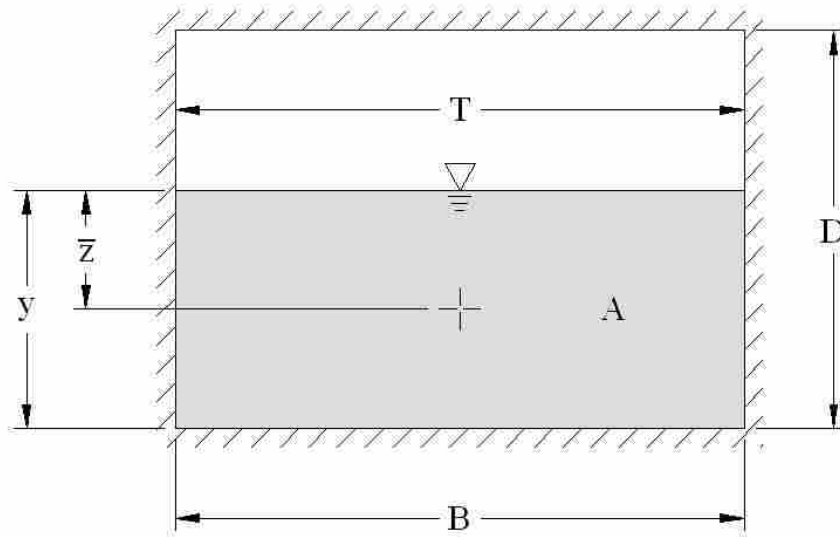
where  $T_1$ ,  $A'_{1,f}$ , and  $(\bar{z}A)'_{1,f}$  are defined by Equations B-15 through B-18. This equation may be used for any conduit shape to find the upstream Froude number associated with the transition between complete and incomplete jumps. If the actual  $Fr_1$  is less than  $(Fr_1)_t$ , then a complete jump may form and  $y'_2$  should be calculated using Equation B-20; otherwise, the jump will be incomplete and  $y'_2$  should instead be calculated using Equation B-24.



## B.2 Rectangular Conduits

### B.2.1 Definitions

Figure B-2 below depicts the parameters used for rectangular conduits.



**Figure B-2 Cross section for rectangular conduits**

The top width ( $\Gamma$ ), area ( $\Omega$ ), and centroid-area ( $\Psi$ ) functions for rectangular conduits are given by the following equations (Sturm 2001):

$$\Gamma(\text{rect}, y') = T = \frac{T}{B} = \frac{B}{B} = 1 \quad (\text{B-26a})$$

$$\Omega(\text{rect}, y') = A' = \frac{A}{BD} = \frac{By}{BD} = \frac{y}{D} = y' \quad (\text{B-26b})$$

$$\Psi(\text{rect}, y') = (\bar{z}A)' = \frac{\bar{z}A}{BD^2} = \frac{By^2}{2BD^2} = \frac{1}{2} \left( \frac{y}{D} \right)^2 = \frac{1}{2} (y')^2 \quad (\text{B-26c})$$

## B.2.2 Solution

### B.2.2.1 Complete Jumps

Inserting Equations B-26a through B-26c into Equation B-20 using Equations B-15 through B-18 yields the following equation for complete jumps:

$$\text{Fr}_1^2 = \frac{(1)(y'_2) \left[ \left( \frac{1}{2} y'_2{}^2 \right) - \left( \frac{1}{2} y'_1{}^2 \right) \right]}{(y'_1)^2 [(y'_2) - (y'_1)]} = \frac{1}{2} \left( \frac{y'_2}{y'_1} \right)^2 + \frac{1}{2} \left( \frac{y'_2}{y'_1} \right) \quad (\text{B-27})$$

This may be further reduced to a dimensionless form of the well-known Belanger equation, as follows:

$$\frac{1}{2} \left( \frac{y'_2}{y'_1} \right)^2 + \frac{1}{2} \left( \frac{y'_2}{y'_1} \right) - \text{Fr}_1^2 = 0 \quad (\text{B-28})$$

$$\frac{y'_2}{y'_1} = \frac{-\left(\frac{1}{2}\right) \pm \sqrt{\left(\frac{1}{2}\right)^2 - 4\left(\frac{1}{2}\right)(-\text{Fr}_1^2)}}{2\left(\frac{1}{2}\right)} = \frac{1}{2} \left( \sqrt{1 + 8\text{Fr}_1^2} - 1 \right) \quad (\text{B-29})$$

$$y'_2 = \frac{y'_1}{2} \left( \sqrt{1 + 8\text{Fr}_1^2} - 1 \right) \quad (\text{B-30})$$

### B.2.2.2 Incomplete Jumps

Inserting Equations B-26a through B-26c into Equation B-24 using Equations B-15 through B-18 yields the following equation:

$$y'_2 = 1 + \frac{1}{(1)(y'_f)^2} \left\{ Fr_1^2 (y'_1)^2 [(y'_f) - (y'_1)] - (1)(y'_f) \left[ \left( \frac{1}{2} y'_f{}^2 \right) - \left( \frac{1}{2} y'_1{}^2 \right) \right] \right\} \quad (B-31)$$

By combining like terms and rearranging, and noting that  $y'_f$  by definition equals 1, the following equation is obtained for incomplete jumps:

$$y'_2 = \frac{1}{2} + \left( Fr_1^2 + \frac{1}{2} \right) y'_1{}^2 - Fr_1^2 y'_1{}^3 \quad (B-32)$$

### B.2.2.3 Transitional Jumps

Inserting Equations B-26a through B-26c into Equation B-25 using Equations B-15 through B-18 yields the following equation for the transition between complete and incomplete jumps:

$$(Fr_1)_t^2 = \frac{(1)(y'_f) \left[ \left( \frac{1}{2} y'_f{}^2 \right) - \left( \frac{1}{2} y'_1{}^2 \right) \right]}{(y'_1)^2 [(y'_f) - (y'_1)]} \quad (B-33)$$

which reduces to:

$$(Fr_1)_t = \sqrt{\frac{1 + y'_1}{2y'_1{}^2}} \quad (B-34)$$

### B.2.3 Sequent Depth Chart

A visual representation of Equations B-30, B-32, and B-34 is shown Figure B-3 on the next page. This is modeled after the format used by Montes (1998), and provides a simple and effective shortcut for finding the sequent depth for any upstream depth and Froude number in rectangular conduits.

Several observations should be made at this point about graphically determining the sequent depth using this type of chart. Note that although the sequent depth is often treated as the dependant variable as in this derivation,  $y'_2$  in Figure B-3 is placed on the abscissa to suggest that hydraulic jumps are induced by downstream conditions, not upstream, although supercritical flow is also a prerequisite for the formation of a hydraulic jump. Note also that for all  $Fr_1$ , as  $y'_1$  increases and approaches about 0.67,  $y'_2$  reaches a maximum, and as  $y'_1$  approaches 1,  $y'_2$  also approaches 1, consistent with the observations of Smith and Chen (1989). This suggests that for conduits flowing less than  $2/3$  full, the downstream depth increases with the upstream depth and Froude number; for conduits flowing more than  $2/3$  full, the downstream depth still increases with the upstream Froude number, but decreases with the upstream depth; for conduits flowing full, no jump will occur for any upstream Froude number. As the following sections demonstrate, these observations apply to all closed conduit shapes.

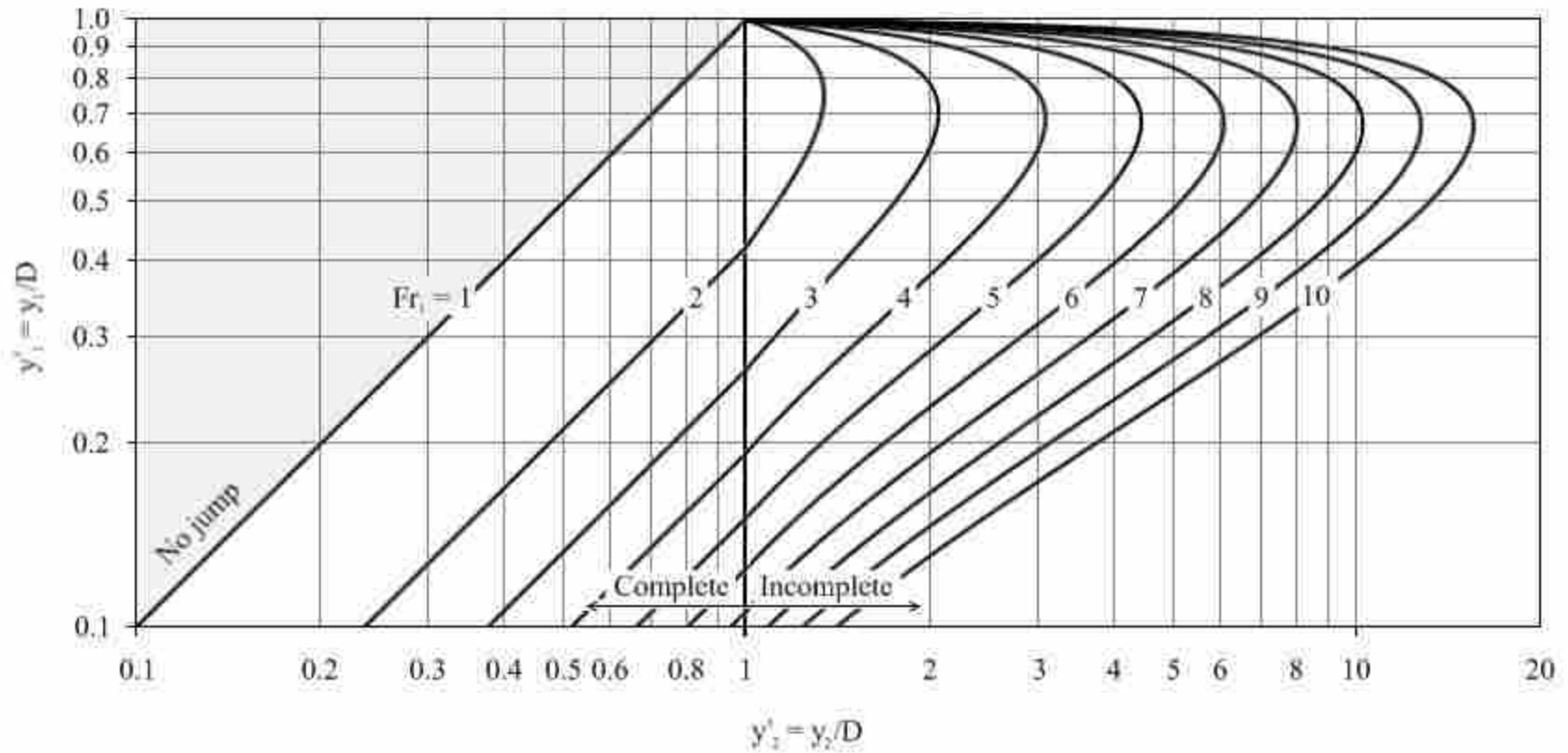
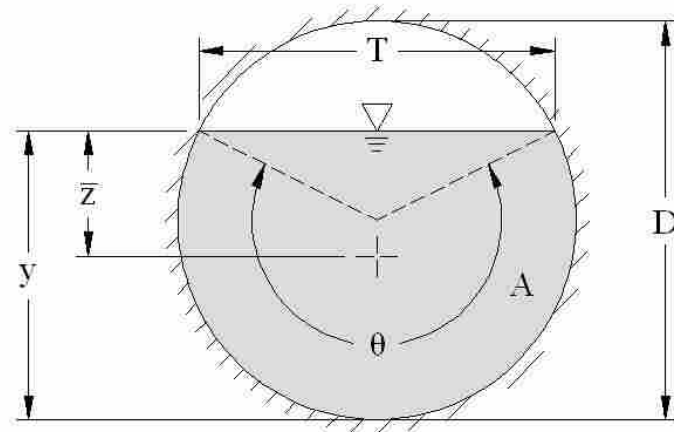


Figure B-3 Sequent depth ratio chart for rectangular conduits

### B.3 Circular Conduits

#### B.3.1 Definitions

Figure B-4 below depicts the parameters used for circular conduits.



**Figure B-4 Cross section for circular conduits**

In order to simplify the equations, the internal flow angle  $\theta$  is typically used as an intermediate variable. The top width ( $\Gamma$ ), area ( $\Omega$ ), and centroid-area ( $\Psi$ ) functions for circular conduits are given by the following equations (Sturm 2001):

$$\Gamma(\text{cir}, y') = T = \frac{T}{B} = \frac{D \sin(\theta/2)}{D} = \sin(\theta/2) \quad (\text{B-35a})$$

$$\Omega(\text{cir}, y') = A' = \frac{A}{BD} = \frac{1}{D^2} \left( \frac{D^2}{8} (\theta - \sin\theta) \right) = \frac{1}{8} (\theta - \sin\theta) \quad (\text{B-35b})$$

$$\begin{aligned}
\Psi(\text{cir}, y') &= (\bar{z}A)' = \frac{\bar{z}A}{BD^2} \\
&= \frac{1}{D^3} \left[ \frac{D^3}{24} \left[ 3\sin(\theta/2) - \sin^3(\theta/2) - 3(\theta/2)\cos(\theta/2) \right] \right] \\
&= \frac{1}{24} \left[ 3\sin(\theta/2) - \sin^3(\theta/2) - 3(\theta/2)\cos(\theta/2) \right] \tag{B-35c}
\end{aligned}$$

$$\theta = 2\cos^{-1} \left[ 1 - 2 \left( \frac{y}{D} \right) \right] = 2\cos^{-1}(1 - 2y') \tag{B-35d}$$

### B.3.2 Solution

The sequent depth equation for complete jumps in circular conduits may be derived from Equation B-20. In this case  $y'_2$  cannot be obtained explicitly in terms of  $y'_1$  and  $Fr_1^2$ , so the sequent depth must be obtained iteratively. Likewise, the sequent depth equation for incomplete jumps may be derived from Equation B-24, and the transitional upstream Froude number may be derived from Equation B-25. In each of these cases, Equations B-35a through B-35d are used to evaluate Equations B-16 through B-18.

### B.3.3 Sequent Depth Chart

A visual representation of this solution is shown in Figure B-5 on the next page. This is modeled after the format used by Montes (Montes 1998), and provides a simple and effective shortcut for finding the sequent depth for any upstream depth and Froude number in circular conduits.

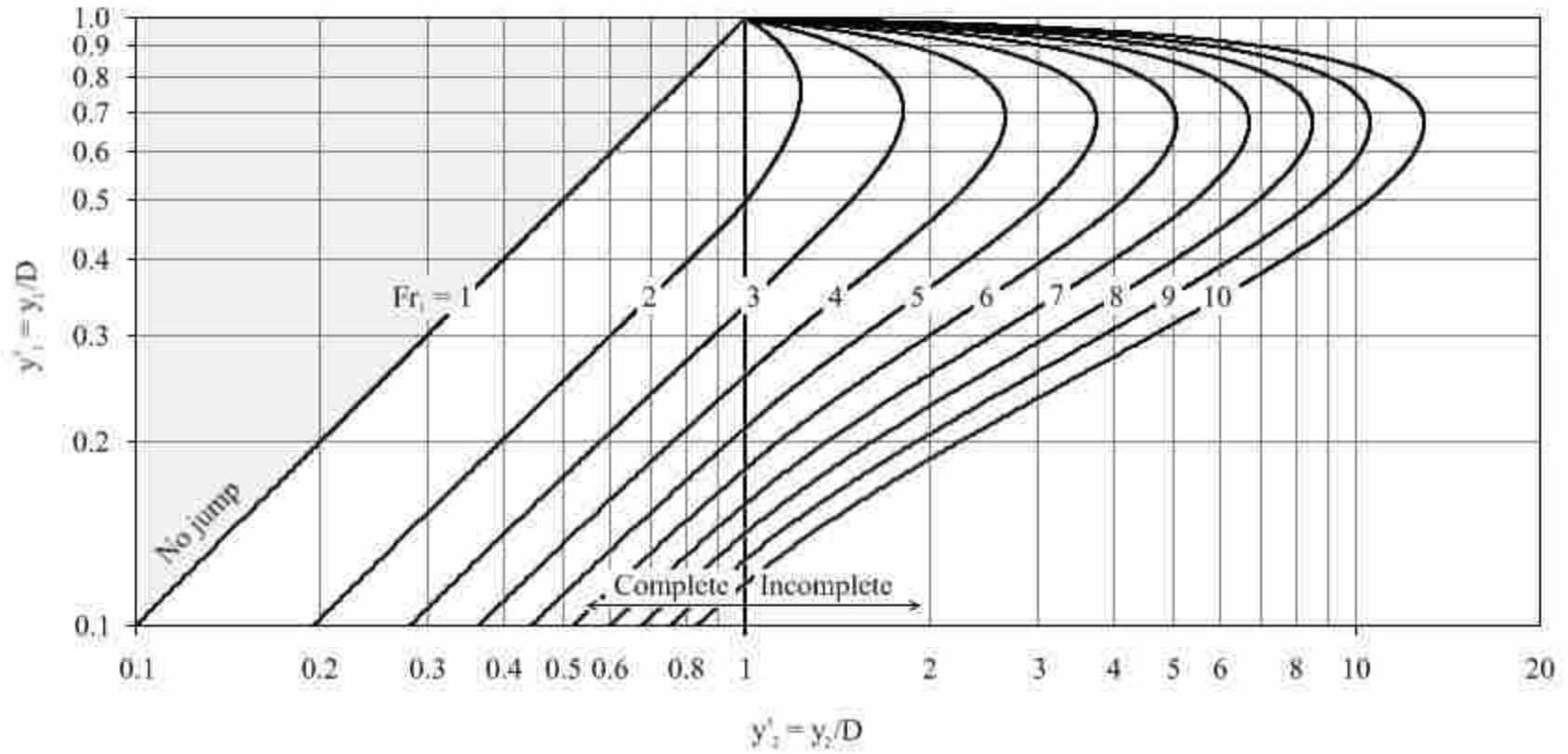


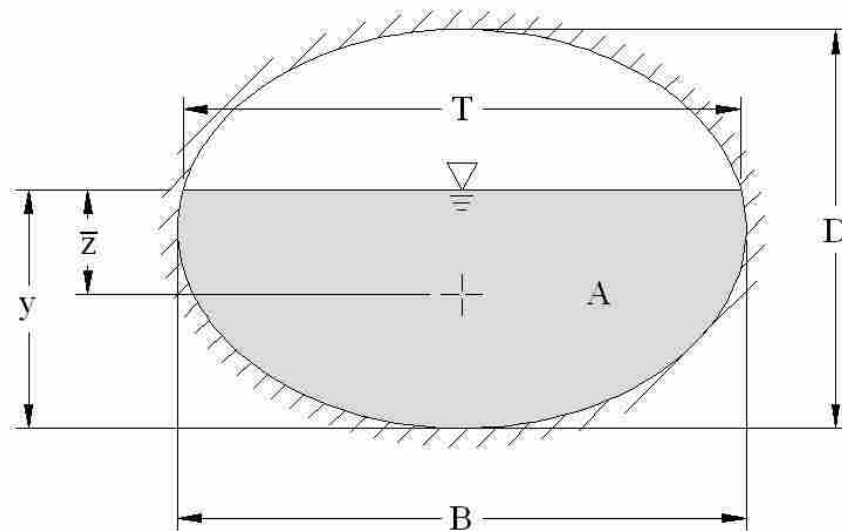
Figure B-5 Sequent depth ratio chart for circular conduits



## B.4 Elliptical Culverts

### B.4.1 Definitions

Elliptical culverts are often manufactured such that they are defined by a span, rise, bottom radius, and middle radius (see Appendix A.7). For simplicity in this study, however, they are assumed to be mathematically elliptical, defined only in terms of the span ( $B$ ) and rise ( $D$ ) of the culvert barrel. The error associated with this assumption is addressed later on in this section. Figure B-6 below depicts the simplified parameters used for elliptical conduits.



**Figure B-6 Cross section for elliptical culverts**

The top width ( $\Gamma$ ), area ( $\Omega$ ), and centroid-area ( $\Psi$ ) functions for elliptical culverts are given by the following equations (Hjelmfeldt 1967):

$$\Gamma(\text{ell}, y') = \mathbf{T} = \frac{\mathbf{T}}{\mathbf{B}} = \frac{1}{\mathbf{B}} \left( 2\mathbf{B} \sqrt{\left(\frac{y}{\mathbf{D}}\right)^2 - \left(\frac{y'}{\mathbf{D}}\right)^2} \right) = 2\sqrt{y'-y'^2} \quad (\text{B-36a})$$

$$\begin{aligned} \Omega(\text{ell}, y') &= A' = \frac{A}{\mathbf{BD}} = \frac{\int dA}{\mathbf{BD}} = \frac{\int_0^y \mathbf{T} dy}{\mathbf{BD}} = \int_0^{y'} \mathbf{T} dy' = \int_0^{y'} 2\sqrt{y'-y'^2} dy' \\ &= \frac{1}{4} \cos^{-1}(1-2y') - \frac{1}{2} (1-2y') \sqrt{y'-y'^2} \\ &= \frac{1}{4} [\cos^{-1}(1-2y') - \Gamma(\text{ell}, y')(1-2y')] \end{aligned} \quad (\text{B-36b})$$

$$\begin{aligned} \Psi(\text{ell}, y') &= (\bar{z}A)' = \frac{\bar{z}A}{\mathbf{BD}^2} = \frac{1}{\mathbf{BD}^2} \left( y - \frac{\int y dA}{\int dA} \right) \int dA = \frac{1}{\mathbf{BD}^2} (yA - \int y dA) \\ &= \frac{1}{\mathbf{BD}^2} \left( yA - \int_0^y y \mathbf{T} dy \right) = y' \Omega(\text{ell}, y') - \int_0^{y'} y' \mathbf{T} dy' \\ &= y' \Omega(\text{ell}, y') - \int_0^{y'} 2y' \sqrt{y'-y'^2} dy' \\ &= y' \Omega(\text{ell}, y') - \left[ \frac{1}{8} \cos^{-1}(1-2y') - \frac{1}{4} (1-2y') \sqrt{y'-y'^2} - \frac{2}{3} (y'-y'^2)^{3/2} \right] \\ &= y' \Omega(\text{ell}, y') - \frac{1}{8} \left[ \cos^{-1}(1-2y') - (1-2y') \Gamma(\text{ell}, y') - \frac{2}{3} \Gamma^3(\text{ell}, y') \right] \\ &= y' \Omega(\text{ell}, y') - \frac{1}{8} \left[ 4\Omega(\text{ell}, y') - \frac{2}{3} \Gamma^3(\text{ell}, y') \right] \\ &= \frac{1}{12} [\Gamma^3(\text{ell}, y') - 6\Omega(\text{ell}, y')(1-2y')] \end{aligned} \quad (\text{B-36c})$$

#### **B.4.2 Solution**

The sequent depth equation for complete jumps in elliptical culverts may be derived from Equation B-20. In this case  $y_2$  cannot be obtained explicitly in terms of  $y_1$  and  $Fr_1^2$ , so the sequent depth must be obtained iteratively. Likewise, the sequent depth equation for incomplete jumps may be derived from Equation B-24, and the transitional upstream Froude number may be derived from Equation B-25. In each of these cases, Equations B-36a through B-36c are used to evaluate Equations B-16 through B-18.

#### **B.4.3 Sequent Depth Chart**

A visual representation of this solution is shown in Figure B-7 on the next page. This is modeled after the format used by Montes (1998), and provides a simple and effective shortcut for finding the sequent depth for any upstream depth and Froude number in elliptical conduits. Note that this chart is identical to the one presented for circular conduits, which is expected since a circle is simply a special case of an ellipse in which  $B = D$ , causing the dimensionless parameters of the two shapes to be equivalent (Hjelmfeldt 1967).

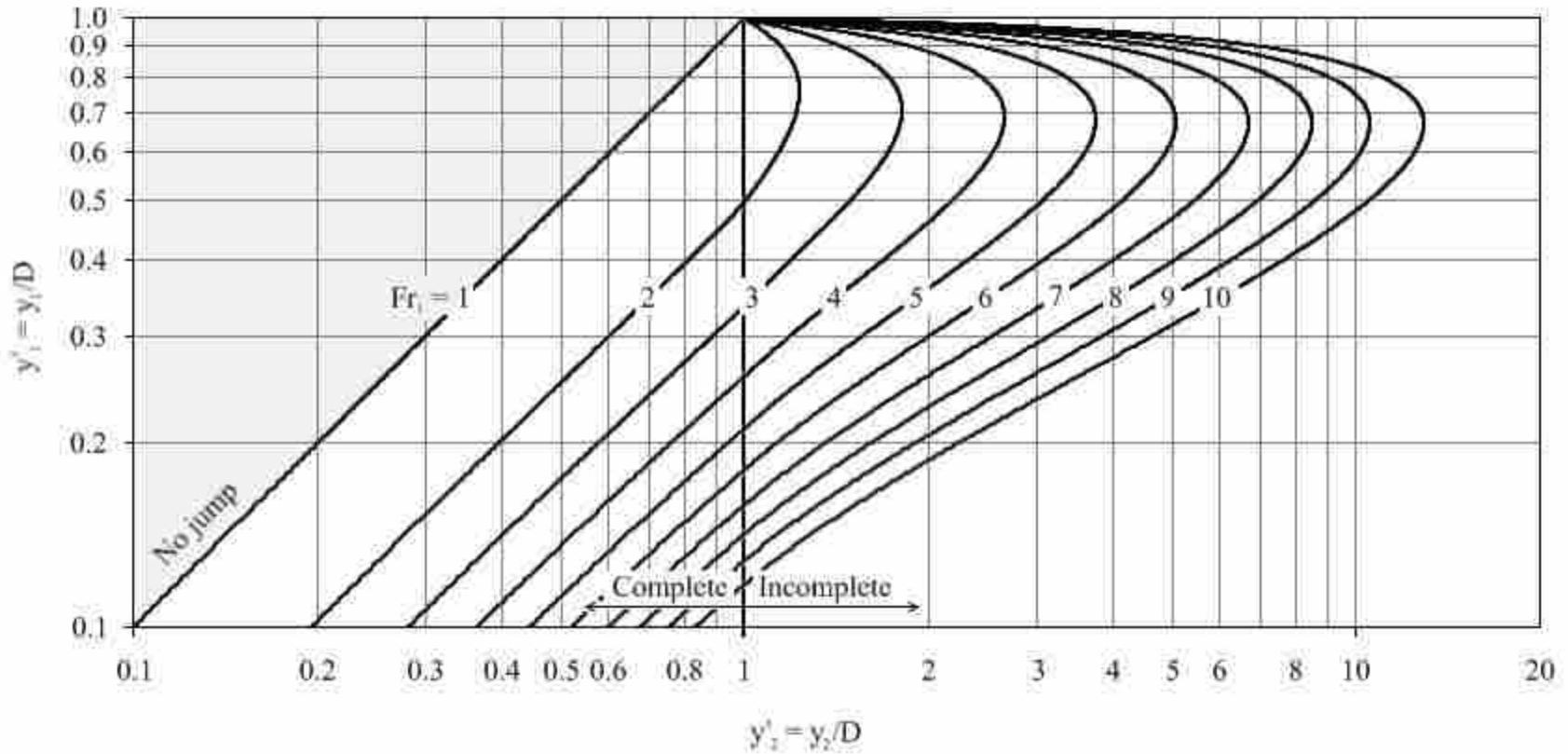
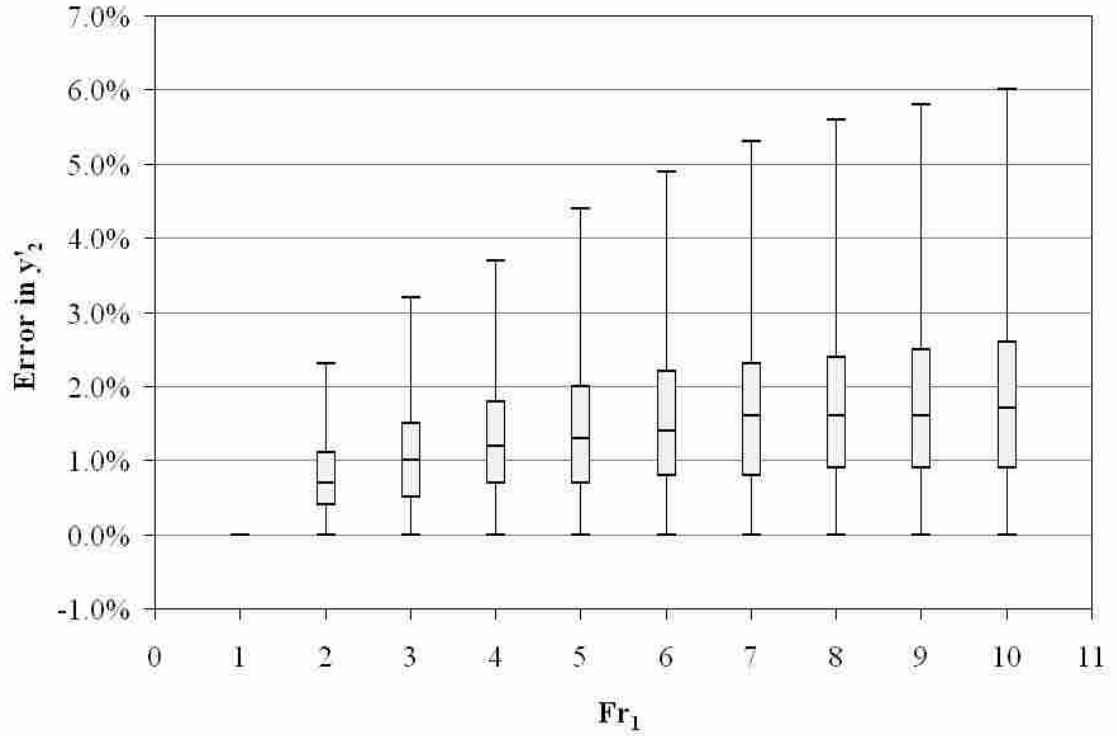


Figure B-7 Sequent depth ratio chart for elliptical conduits

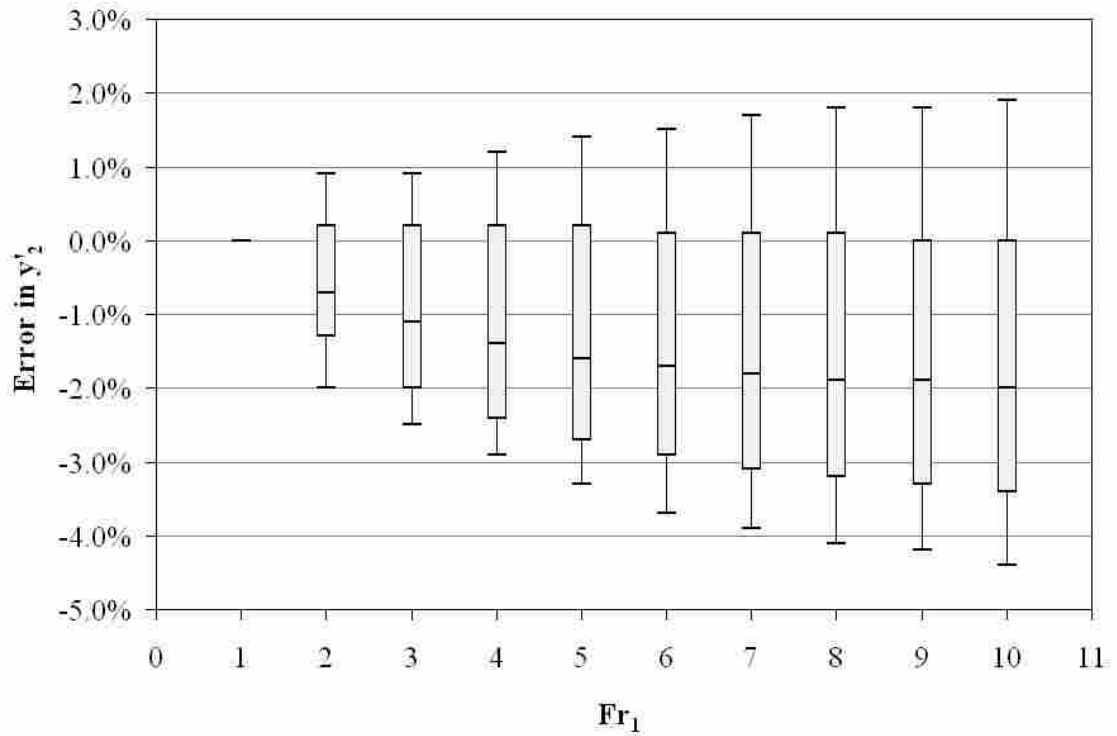
#### B.4.4 Error Analysis

By assuming elliptical culverts to be mathematically elliptical, the sequent depth problem is greatly simplified, but a certain amount of error is introduced in the process since an ellipse does not precisely define the shape of an elliptical culvert as previously explained. In an attempt to quantify this error, a similar chart to Figure B-7 was generated for each elliptical culvert in Appendix A.7, using the same eight parameters as for pipe arch culverts (see Section A.5). Then the relative difference in values obtained for  $y'_2$  between the elliptical and pipe arch analyses was calculated for each combination of  $y'_1$  from 0 to 1 and  $Fr_1$  from 1 to 10, and the number of solutions that fell within specific error margins, each with a bin size of 0.1%, was tabulated cumulatively for all culvert shapes. Finally, the first, second, third, and fourth quartile ranges were determined from the distribution data, and then the error distribution was plotted against  $Fr_1$  in the form of box and whisker plots to observe the trends in the data. It was observed that  $y'_2$  was typically overestimated for metal elliptical culverts, but underestimated for concrete ones

Figure B-8 on the next page shows the results of this analysis. It is evident from this graph that the margin of error from the elliptical equations increases with  $Fr_1$ , such that at  $Fr_1=5$ , the error in  $y'_2$  will fall between 0.0 and 4.4% for metal culverts, and between -3.3 and 1.4% for concrete culverts. This error may be higher than desired, in which case a user may prefer to apply the same logic for pipe arch culverts to an elliptical culvert, despite the added complexity. This would eliminate the error caused by simplification and provide a more accurate estimate of  $y'_2$ .



(a)



(b)

**Figure B-8 Error distribution of ellipse assumption for (a) metal and (b) concrete elliptical culverts**

## **B.5 Pipe Arch Culverts**

### **B.5.1 Definitions**

#### **B.5.1.1 Shape Definitions**

Pipe arch culverts (also called "arch" (ASTM C506) culverts) are often used in place of circular culverts because they allow more height clearance than their circular counterparts due to their compact shape (Hager 1999). They are defined by up to eight shape parameters (see Appendix A.8), which makes finding the area and centroid of flow far more complex than it is for the other shapes previously discussed. These parameters include the span ( $B$ ), rise ( $D$ ), bottom radius ( $R_b$ ), middle radius ( $R_m$ ), top radius ( $R_t$ ), bottom transition height ( $h_b$ ), neutral axis height ( $h_m$ ), and top transition height ( $h_t$ ) (see Figure B-9 on the next page).

Pipe arch culverts are available by manufacturers in over 200 shapes and sizes (see Appendix A.8), making it impractical to produce a sequent depth chart for each one individually (Normann et al. 1985). In previous hydraulic analyses, for simplification the pipe arch shape has been generalized either by assuming a single span-to-rise ratio for all culverts or by using a superimposed ellipse of 2:1 eccentricity (Hager 1999). Both of these assumptions introduce an unknown amount of error (Normann et al. 1985) that is eliminated by the more precise approach presented here. Again, it would still be impractical to generate a sequent depth chart for each unique shape individually, so an example set of parameters, listed in Table B-1 on the next page, is used to demonstrate how the methods presented in this section may be applied. As shown in this table, each of the parameters (except for  $D$ ) may instead be expressed as a fraction of the culvert rise, denoted in this study by the 'prime' symbol, thereby facilitating the continued use of dimensionless parameters.

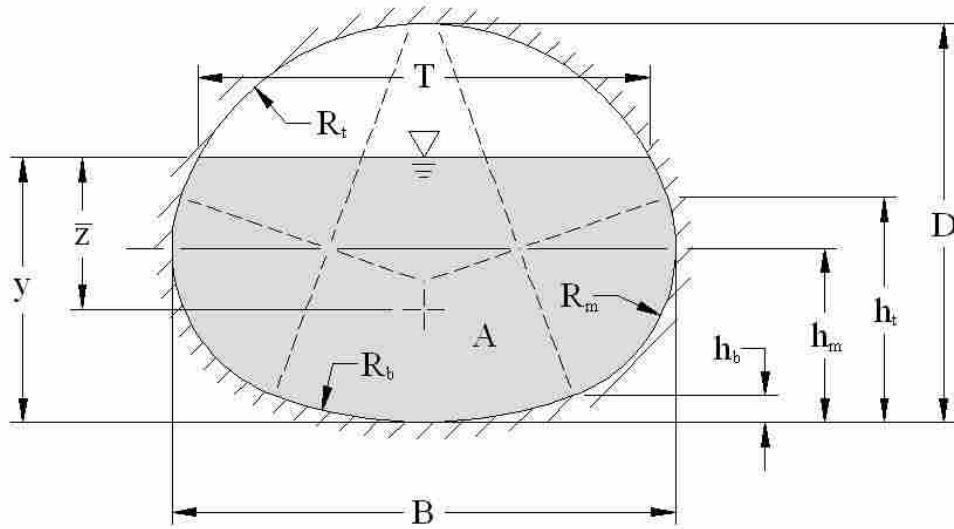


Figure B-9 Cross section for pipe arch culverts

Table B-1 Example Pipe Arch Parameters

Shape Parameter	Symbol	Value (in)	Dimensionless Ratio	Symbol	Value
Span*	B	157.0	B/D	B'	1.570
Rise*	D	100.0	-	-	-
Bottom Radius*	R <sub>b</sub>	300.8	R <sub>b</sub> /D	R' <sub>b</sub>	3.008
Middle Radius*	R <sub>m</sub>	31.75	R <sub>m</sub> /D	R' <sub>m</sub>	0.318
Top Radius**	R <sub>t</sub>	81.67	R <sub>t</sub> /D	R' <sub>t</sub>	0.817
Bottom Transition**	h <sub>b</sub>	4.576	h <sub>b</sub> /D	h' <sub>b</sub>	0.046
Neutral Axis Height**	h <sub>m</sub>	35.84	h <sub>m</sub> /D	h' <sub>m</sub>	0.358
Top Transition**	h <sub>t</sub>	46.98	h <sub>t</sub> /D	h' <sub>t</sub>	0.470

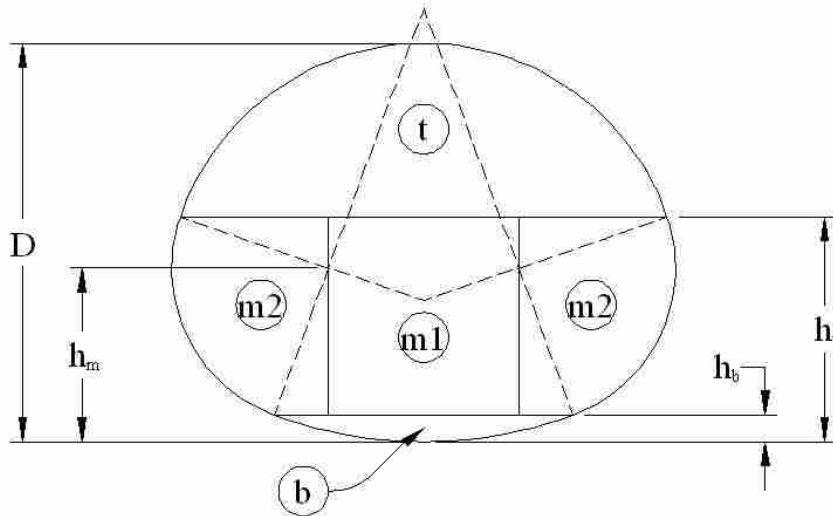
\* Source: (CONTECH 2007)

\*\* Derived from other parameters for continuity (see Appendix A.8)



### B.5.1.2 Dimensions

Because of the complex geometry of pipe arch culverts, the top width ( $\Gamma$ ), area ( $\Omega$ ), and centroid-area ( $\Psi$ ) functions must be derived in a piecewise fashion (delimited by the location of  $y$  relative to  $h_b$ ,  $h_m$ , and  $h_t$ ), using the functions defined for rectangular and circular conduits. Figure B-10 below shows that pipe arch culverts may be divided into four sections, hereafter referred to as the 'Bottom Section', 'Middle Section 1,' 'Middle Section 2,' and 'Top Section'. The labels 'b', 'm1', 'm2', and 't' refer to the subscripts used to differentiate the functions and parameters for each section, respectively.



**Figure B-10 Bottom, middle and top pipe arch sections**

The top width, area, and centroid-area functions for pipe arch culverts may therefore be defined as follows:

$$\Gamma(\text{p arch}, y') = T = \sum T_i$$

$$= \begin{cases} \Gamma_b|^{y'} & \text{for } 0 < y' \leq h'_b \\ \Gamma_{m1}|^{y'} + \Gamma_{m2}|^{y'} & \text{for } h'_b < y' \leq h'_t \\ \Gamma_t|^{y'} & \text{for } h'_t < y' \leq 1 \end{cases} \quad (\text{B-37a})$$

$$\Omega(\text{p arch}, y') = A' = \sum A'_i =$$

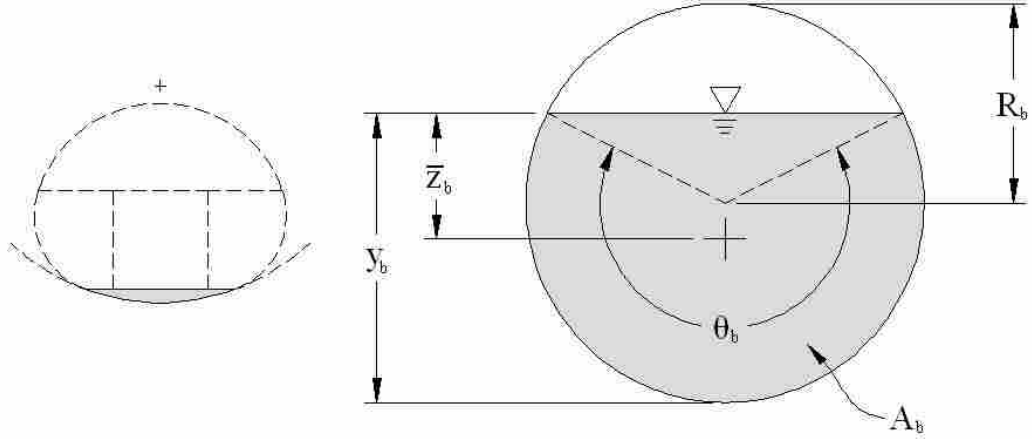
$$= \begin{cases} \Omega_b|^{y'} & \text{for } 0 < y' \leq h'_b \\ \Omega_b|^{h'_b} + \Omega_{m1}|_{h'_b}^{y'} + \Omega_{m2}|_{h'_b}^{y'} & \text{for } h'_b < y' \leq h'_t \\ \Omega_b|^{h'_b} + \Omega_{m1}|_{h'_b}^{h'_t} + \Omega_{m2}|_{h'_b}^{h'_t} + \Omega_t|_{h'_t}^{y'} & \text{for } h'_t < y' \leq 1 \end{cases} \quad (\text{B-37b})$$

$$\Psi(\text{p arch}, y') = (\bar{z}A)' = \sum (\bar{z}A)'_i$$

$$= \begin{cases} \Psi_b|^{y'} & \text{for } 0 < y' \leq h'_b \\ \Psi_b|^{h'_b} + (y' - h'_b)\Omega_b|^{h'_b} \\ + \Psi_{m1}|^{y'}_{h'_b} - (y' - h'_b)\Omega_{m1}|^{y'}_{h'_b} \\ + \Psi_{m2}|^{y'}_{h'_b} - (y' - h'_b)\Omega_{m2}|^{y'}_{h'_b} & \text{for } h'_b < y' \leq h'_t \\ \Psi_b|^{h'_b} + (y' - h'_b)\Omega_b|^{h'_b} + \Psi_{m1}|^{h'_t}_{h'_b} \\ + (y' - h'_t)\Omega_{m1}|^{h'_t} - (y' - h'_b)\Omega_{m1}|^{h'_b} \\ + \Psi_{m2}|^{h'_t}_{h'_b} + (y' - h'_t)\Omega_{m2}|^{h'_t} & \text{for } h'_t < y' \leq 1 \\ -(y' - h'_b)\Omega_{m2}|^{h'_b} + \Psi_t|^{y'}_{h'_t} \\ -(y' - h'_t)\Omega_t|^{h'_t} \end{cases} \quad (\text{B-37c})$$

### B.5.1.3 Bottom Section ( $0 < y' \leq h'_b$ )

The bottom section of a pipe arch culvert could be treated as a simple circular conduit, with the exception that the diameter of the bottom arc does not equal the rise of the culvert. Because of this difference, both parameters must be considered. Figure B-11 on the next page gives a visual representation of the parameters to be used for this section. Note that the subscript 'b' signifies that these parameters and the equations that follow are unique to the bottom section of the culvert only. The functions  $\Gamma_b$ ,  $\Omega_b$ , and  $\Psi_b$  are all dependant upon  $y'_b \equiv y_b/D = y/D$ , and as with circular culverts, the internal flow angle  $\theta_b$  may be used as an intermediate variable. The top width ( $\Gamma_b$ ), area ( $\Omega_b$ ), and centroid-area ( $\Psi_b$ ) functions for the bottom section may then be derived in terms of  $\theta_b$ , as shown in the equations following Figure B-11.



**Figure B-11 Parameters used for the bottom section of a pipe arch**

$$\Gamma_b(y') = T'_b \equiv \frac{T_b}{B} = \frac{2R_b \sin(\theta_b/2)}{B} \left( \frac{D}{D} \right) = 2 \left( \frac{R'_b}{B'} \right) \sin(\theta_b/2) \quad (\text{B-38a})$$

$$\begin{aligned} \Omega_b(y') = A'_b &\equiv \frac{A_b}{BD} = \frac{1}{BD} \left( \frac{(2R_b)^2}{8} (\theta_b - \sin\theta_b) \right) \left( \frac{D}{D} \right) \\ &= \frac{R'_b{}^2}{2B'} (\theta_b - \sin\theta_b) \end{aligned} \quad (\text{B-38b})$$

$$\begin{aligned} \Psi_b(y') = (\bar{z}A)'_b &\equiv \frac{(\bar{z}A)_b}{BD^2} \\ &= \frac{1}{BD^2} \left\{ \frac{(2R_b)^3}{24} \left[ 3 \sin\left(\frac{\theta_b}{2}\right) - \sin^3\left(\frac{\theta_b}{2}\right) - 3\left(\frac{\theta_b}{2}\right) \cos\left(\frac{\theta_b}{2}\right) \right] \right\} \left( \frac{D}{D} \right) \\ &= \frac{R'_b{}^3}{3B'} \left[ 3 \sin(\theta_b/2) - \sin^3(\theta_b/2) - 3(\theta_b/2) \cos(\theta_b/2) \right] \end{aligned} \quad (\text{B-38c})$$



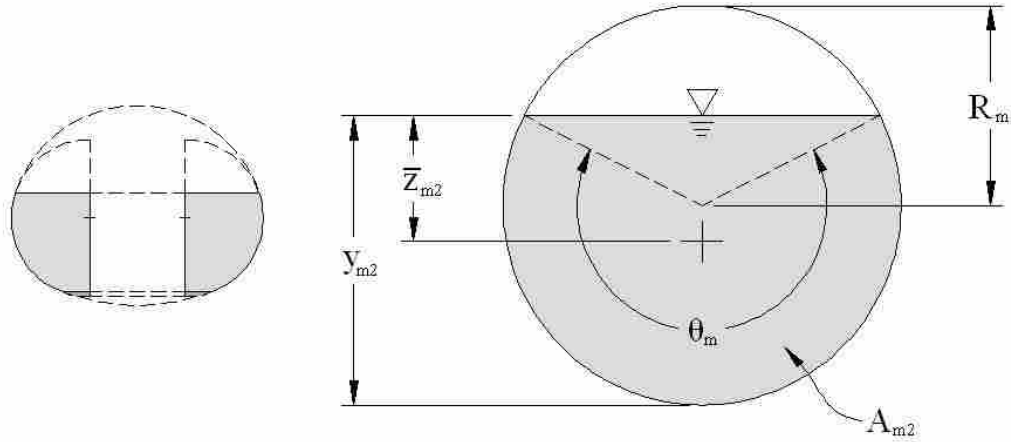
$$\Gamma_{m1}(y') = T_{m1} \equiv \frac{T_{m1}}{B} = \frac{B - 2R_m}{B} \left( \frac{D}{D} \right) = \frac{1}{B'} (B' - 2R'_m) \quad (\text{B-39a})$$

$$\begin{aligned} \Omega_{m1}(y') = A'_{m1} &\equiv \frac{A_{m1}}{BD} = \frac{B_{m1}y_{m1}}{BD} = \frac{(B - 2R_m)(y - h_m + R_m)}{BD} \left( \frac{D}{D} \right) \\ &= \frac{1}{B'} (B' - 2R'_m)(y' - h'_m + R'_m) \end{aligned} \quad (\text{B-39b})$$

$$\begin{aligned} \Psi_{m1}(y') = (\bar{z}A)'_{m1} &\equiv \frac{(\bar{z}A)_{m1}}{BD^2} = \frac{B_{m1}y_{m1}^2}{2BD^2} = \frac{(B - 2R_m)(y - h_m + R_m)^2}{2BD^2} \left( \frac{D}{D} \right) \\ &= \frac{1}{2B'} (B' - 2R'_m)(y' - h'_m + R'_m)^2 \end{aligned} \quad (\text{B-39c})$$

#### B.5.1.5 Middle Section 2 ( $h'_b < y' \leq h'_t$ )

The second middle section of a pipe arch culvert may be treated as two halves of a circular conduit. Figure B-13 on the next page gives a visual representation of the parameters to be used for this section. The functions  $\Gamma_{m2}$ ,  $\Omega_{m2}$ , and  $\Psi_{m2}$  are all dependant upon  $y'_{m2} \equiv y_{m2}/D = (y - h_m + R_m)/D$ , and as with the bottom section, the internal flow angle  $\theta_m$  may be used as an intermediate variable. The top width ( $\Gamma_{m2}$ ), area ( $\Omega_{m2}$ ), and centroid-area ( $\Psi_{m2}$ ) functions for the second middle section may then be derived in terms of  $\theta_m$ , as shown in the equations following Figure B-13.



**Figure B-13 Parameters used for the second middle section of a pipe arch culvert**

$$\Gamma_{m2}(y') = T_{m2} \equiv \frac{T_{m2}}{B} = \frac{2R_m \sin(\theta_m/2)}{B} \left(\frac{D}{D}\right) = 2 \left(\frac{R'_m}{B'}\right) \sin(\theta_m/2) \quad (\text{B-40a})$$

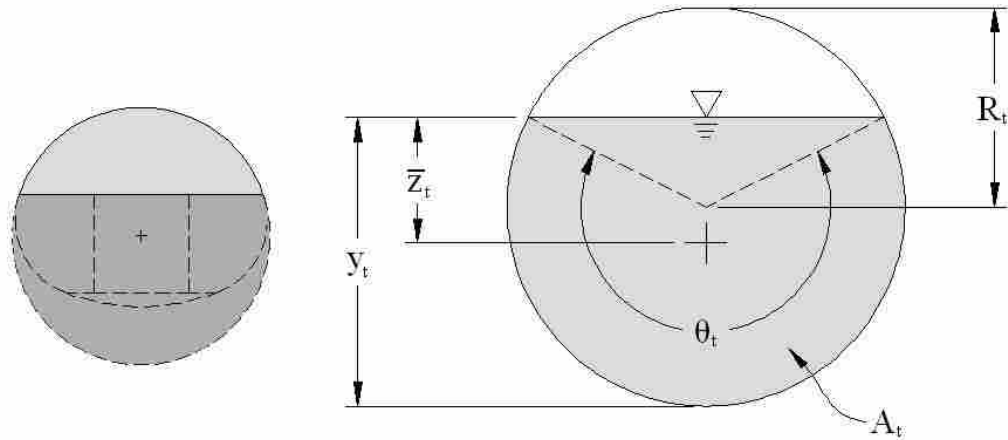
$$\begin{aligned} \Omega_{m2}(y') = A'_{m2} &\equiv \frac{A_{m2}}{BD} = \frac{1}{BD} \left( \frac{(2R_m)^2}{8} (\theta_m - \sin\theta_m) \right) \left(\frac{D}{D}\right) \\ &= \frac{R'_m{}^2}{2B'} (\theta_m - \sin\theta_m) \end{aligned} \quad (\text{B-40b})$$

$$\begin{aligned} \Psi_{m2}(y') = (\bar{z}A)'_{m2} &\equiv \frac{(\bar{z}A)_{m2}}{BD^2} \\ &= \frac{1}{BD^2} \left\{ \frac{(2R_m)^3}{24} \left[ 3 \sin\left(\frac{\theta_m}{2}\right) - \sin^3\left(\frac{\theta_m}{2}\right) - 3\left(\frac{\theta_m}{2}\right) \cos\left(\frac{\theta_m}{2}\right) \right] \right\} \left(\frac{D}{D}\right) \\ &= \frac{R'_m{}^3}{3B'} \left[ 3 \sin(\theta_m/2) - \sin^3(\theta_m/2) - 3(\theta_m/2) \cos(\theta_m/2) \right] \end{aligned} \quad (\text{B-40c})$$

$$\begin{aligned}\theta_m &= 2\cos^{-1}\left[1 - 2\left(\frac{y_b}{2R_m}\right)\right] = 2\cos^{-1}\left(1 - \frac{1}{R_m}(y - h_m + R_m)\left(\frac{D}{D}\right)\right) \\ &= 2\cos^{-1}\left(1 - \frac{1}{R'_m}(y' - h'_m + R'_m)\right)\end{aligned}\quad (\text{B-40d})$$

### B.5.1.6 Top Section ( $h'_t < y' \leq 1$ )

Like the bottom and second middle sections, the top section of a pipe arch culvert may be treated as a circular conduit. Figure B-14 below gives a visual representation of the parameters to be used for this section.



**Figure B-14 Parameters used for the top section of a pipe arch culvert**

The functions  $\Gamma_t$ ,  $\Omega_t$ , and  $\Psi_t$  are all dependant upon  $y'_t \equiv y_t/D = (y + 2R_t - D)/D$ , and as with the bottom section, the internal flow angle  $\theta_t$  may be used as an intermediate variable. The top width ( $\Gamma_t$ ), area ( $\Omega_t$ ), and centroid-area ( $\Psi_t$ ) functions for the top section may then be derived in terms of  $\theta_t$ , as follows:



$$\Gamma_t(y') = T_t \equiv \frac{T_t}{B} = \frac{2R_t \sin(\theta_t/2)}{B} \left( \frac{D}{D} \right) = 2 \left( \frac{R'_t}{B'} \right) \sin(\theta_t/2) \quad (\text{B-41a})$$

$$\begin{aligned} \Omega_t(y') = A'_t &\equiv \frac{A_t}{BD} = \frac{1}{BD} \left( \frac{(2R_t)^2}{8} (\theta_t - \sin\theta_t) \right) \left( \frac{D}{D} \right) \\ &= \frac{R'_t{}^2}{2B'} (\theta_t - \sin\theta_t) \end{aligned} \quad (\text{B-41b})$$

$$\begin{aligned} \Psi_t(y') = (\bar{z}A)'_t &\equiv \frac{(\bar{z}A)_t}{BD^2} \\ &= \frac{1}{BD^2} \left\{ \frac{(2R_t)^3}{24} \left[ 3\sin\left(\frac{\theta_t}{2}\right) - \sin^3\left(\frac{\theta_t}{2}\right) - 3\left(\frac{\theta_t}{2}\right)\cos\left(\frac{\theta_t}{2}\right) \right] \right\} \left( \frac{D}{D} \right) \\ &= \frac{R'_t{}^3}{3B'} \left[ 3\sin(\theta_t/2) - \sin^3(\theta_t/2) - 3(\theta_t/2)\cos(\theta_t/2) \right] \end{aligned} \quad (\text{B-41c})$$

$$\begin{aligned} \theta_t &= 2\cos^{-1} \left[ 1 - 2 \left( \frac{y_t}{2R_t} \right) \right] = 2\cos^{-1} \left( 1 - \frac{1}{R_t} (y + 2R_t - D) \left( \frac{D}{D} \right) \right) \\ &= 2\cos^{-1} \left( 1 - \frac{1}{R'_t} (y' + 2R'_t - 1) \right) = 2\cos^{-1} \left( \frac{1 - y'}{R'_t} - 1 \right) \end{aligned} \quad (\text{B-41d})$$

### B.5.2 Solution

The sequent depth equation for complete jumps in pipe arch culverts may be derived from Equation B-20. In this case  $y'_2$  cannot be obtained explicitly in terms of  $y'_1$  and  $Fr_1^2$ , so the sequent depth must be obtained iteratively. Likewise, the sequent depth equation for incomplete jumps may be derived from Equation B-24, and the transitional

Froude number may be derived from Equation B-25. In each of these cases, Equations B-37a through B-41d are used to evaluate Equations B-16 through B-18.

### **B.5.3 Sequent Depth Chart**

A visual representation of this solution is shown in Figure B-15 on the next page. This is modeled after the format used by Montes (1998), and provides a simple and effective shortcut for finding the sequent depth for any upstream depth and Froude number in pipe arch conduits. Note that this chart only applies to the pipe arch culvert as defined in Table B-1. It is merely an illustration that such a chart may be created for any pipe arch shape.

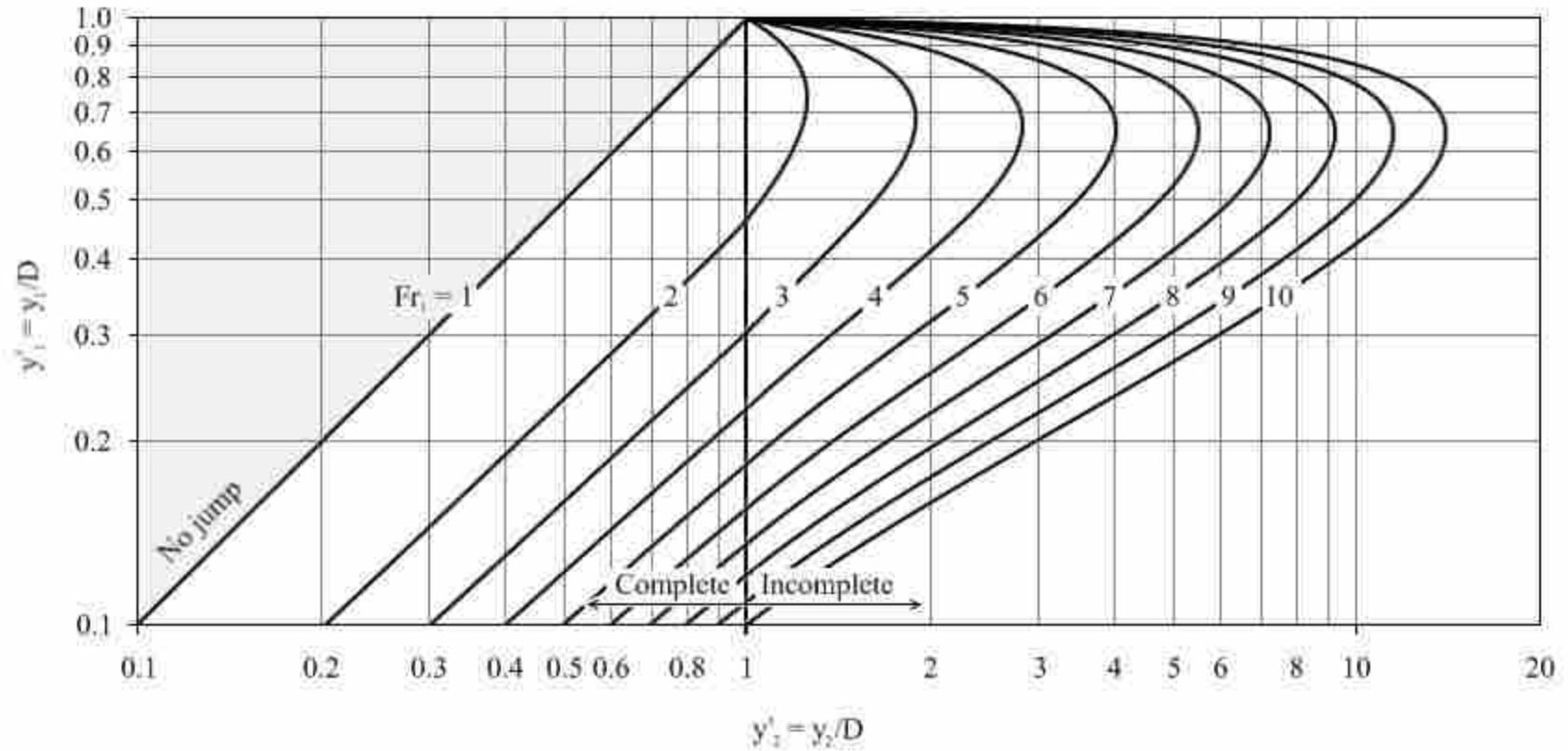


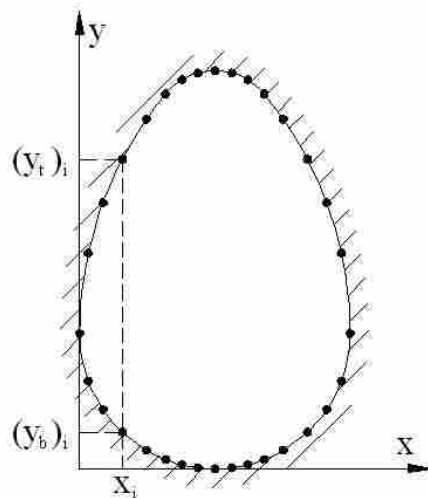
Figure B-15 Sequent depth ratio chart for the pipe arch culvert associated with the parameters listed Table B-1

## B.6 User-Defined Conduits

### B.6.1 Definitions

#### B.6.1.1 Coordinates

In general, for any conduit shape (including the four defined above), the top width, area, and centroid-area may be defined numerically rather than geometrically. This is accomplished by defining a sufficient number of coordinates along the inner walls of the barrel to accurately represent the conduit shape. These coordinates should be defined such that for every horizontal distance,  $x_i$ , away from the left-most point, perpendicular to the conduit axis, two vertical ordinates exist relative to the lowest point in the conduit representing the location of the bottom and top inner edges of the barrel at that point, denoted by  $(y_b)_i$  and  $(y_t)_i$ , respectively. Figure B-16 below depicts an example of how these coordinates might be defined for an “inverted egg-shaped” culvert. The coordinates for this figure are listed in Table B-2 on the next page.



**Figure B-16 Example cross section for user-defined coordinates in Table B-2**

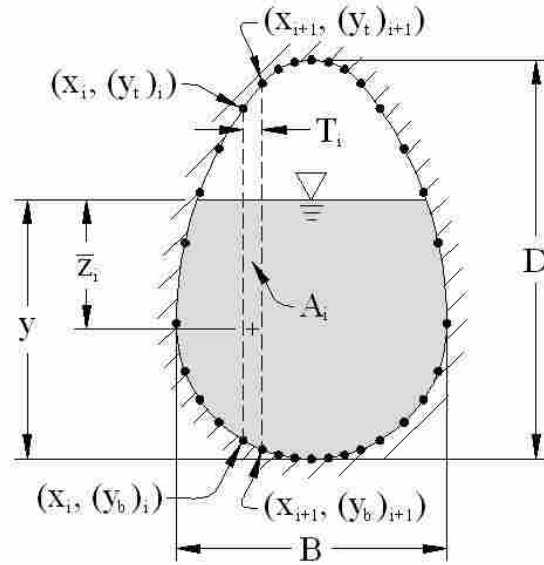
**Table B-2 Example User-Defined Coordinates**

<b>i</b>	<b>x (m)</b>	<b>y<sub>t</sub> (m)</b>	<b>y<sub>b</sub> (m)</b>
1	0.00	0.51	0.51
2	0.03	0.81	0.33
3	0.09	1.00	0.22
4	0.16	1.17	0.14
5	0.25	1.32	0.07
6	0.32	1.41	0.03
7	0.38	1.47	0.02
8	0.45	1.49	0.00
9	0.51	1.50	0.00
10	0.57	1.49	0.00
11	0.63	1.47	0.02
12	0.69	1.41	0.03
13	0.77	1.32	0.07
14	0.86	1.17	0.14
15	0.93	1.00	0.22
16	0.99	0.81	0.33
17	1.02	0.51	0.51

### **B.6.1.2 Dimensions**

Defining the coordinates in this manner rather than listing two x values for every y value provides two major advantages for this analysis. First, it significantly simplifies the calculation of the centroid-area, and second, it allows for the addition of multiple top widths and areas, which may occur when sediment deposits or embedment split the flow

into two or more streams. The conduit is therefore divided into multiple vertical sections, each with a thickness  $\Delta x = x_{i+1} - x_i$ , as shown in Figure B-17 below.



**Figure B-17 Example cross section for a user-defined conduit**

From this figure it is evident that the top width ( $\Gamma$ ), area ( $\Omega$ ), and centroid-area ( $\Psi$ ) functions for user-defined conduits may be expressed by the following equations:

$$\Gamma(\text{u.d.}, y') = T = \sum_{i=1}^{n-1} T_i \quad (\text{B-42a})$$

$$\Omega(\text{u.d.}, y') = A' = \sum_{i=1}^{n-1} A'_i \quad (\text{B-42b})$$

$$\Psi(\text{u.d.}, y') = (\bar{z}A)' = \sum_{i=1}^{n-1} (\bar{z}A)'_i \quad (\text{B-42c})$$

where the subscript 'i' denotes an incremental value, and 'n' is the total number of x-coordinates used.

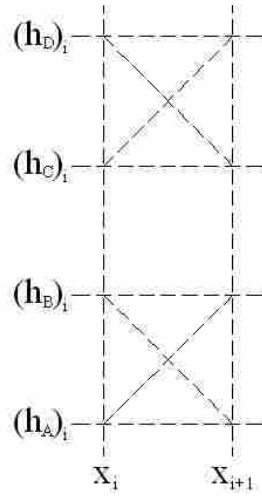
The span (B) and rise (D) of the conduit may be found by taking the difference between the horizontal and vertical upper and lower limits of the coordinates used. If the subscripts 'max' and 'min' are used to denote maximum and minimum values, respectively, then:

$$B = (x_i)_{\max} - x_{i=n} \quad (\text{B-43})$$

$$D = ((y_t)_i)_{\max} \quad (\text{B-44})$$

### **B.6.1.3 Dimensionless Coordinates**

In order to find the incremental top width, area, and centroid-area, the location of the flow depth with respect to the top and bottom coordinates of the conduit becomes important. This relationship must be evaluated for each of the four y-coordinates defining the shape of the incremental vertical section being analyzed:  $(y_b)_i$ ,  $(y_t)_i$ ,  $(y_b)_{i+1}$ , and  $(y_t)_{i+1}$ . It is worth mentioning that none of these coordinates are dependant upon another. That is,  $(y_b)_i$  may be less than, equal to, or greater than  $(y_b)_{i+1}$ , and  $(y_t)_i$  may be less than, equal to, or greater than  $(y_t)_{i+1}$ . The only restriction is that  $(y_b)_i$  must be less than or equal to  $(y_t)_i$ . Because of this variability, when finding the relative location of y it is useful first to order the four conduit coordinates from smallest to greatest, using the terms  $h_A$ ,  $h_B$ ,  $h_C$ , and  $h_D$ , as shown in Figure B-18 on the next page.



**Figure B-18 Definition of terms used for incremental vertical sections**

The four incremental dimensionless relative vertical coordinates are therefore defined as follows, again using the terms ‘min’ and ‘max’ to denote the minimum and maximum value, respectively:

$$(h'_A)_i \equiv \frac{(h_A)_i}{D} = \frac{1}{D} \min((y_b)_i, (y_b)_{i+1}) \quad (\text{B-45a})$$

$$(h'_B)_i \equiv \frac{(h_B)_i}{D} = \frac{1}{D} \max((y_b)_i, (y_b)_{i+1}) \quad (\text{B-45b})$$

$$(h'_C)_i \equiv \frac{(h_C)_i}{D} = \frac{1}{D} \min((y_t)_i, (y_t)_{i+1}) \quad (\text{B-45c})$$



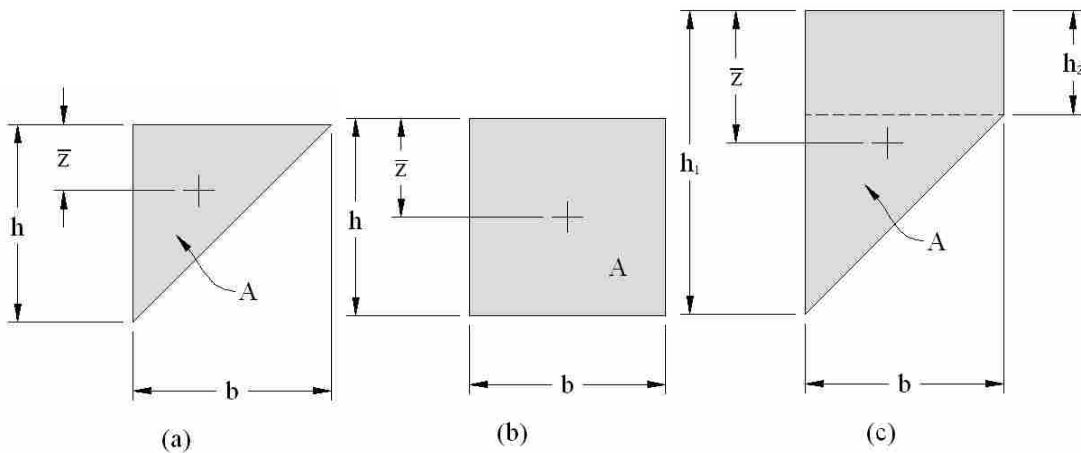
$$(h'_D)_i \equiv \frac{(h_D)_i}{D} = \frac{1}{D} \max((y_t)_i, (y_t)_{i+1}) \quad (\text{B-45d})$$

For convenience and consistency, the incremental horizontal coordinates may also be expressed in a dimensionless form, by dividing them by the conduit span:

$$x'_i \equiv \frac{x_i}{B} \quad (\text{B-46})$$

#### B.6.1.4 Basic Shape Characteristics

Before continuing with the analysis of the user-defined conduit, it is necessary to study the characteristics of some of the basic shapes that are used hereafter to find the incremental top width, area, and centroid area for each vertical section. These basic shapes are shown in Figure B-19 below.



**Figure B-19 Parameters for (a) triangular, (b) rectangular, and (c) trapezoidal cross sections**

The top width, area, and centroid-area for the triangle may be found as follows:

$$T_{\text{tri}} = b \quad (\text{B-47a})$$

$$A_{\text{tri}} = \frac{1}{2}bh \quad (\text{B-47b})$$

$$\bar{z}_{\text{tri}} = \frac{1}{3}h \quad (\text{B-47c})$$

$$(\bar{z}A)_{\text{tri}} = \left(\frac{1}{3}h\right)\left(\frac{1}{2}bh\right) = \frac{1}{6}bh^2 \quad (\text{B-47d})$$

Likewise, the top width, area, and centroid-area for the rectangle may be found by:

$$T_{\text{rect}} = b \quad (\text{B-48a})$$

$$A_{\text{rect}} = bh \quad (\text{B-48b})$$

$$\bar{z}_{\text{rect}} = \frac{1}{2}h \quad (\text{B-48c})$$

$$(\bar{z}A)_{\text{rect}} = \left(\frac{1}{2}h\right)(bh) = \frac{1}{2}bh^2 \quad (\text{B-48d})$$

By combining the triangle and rectangle together, the top width, area, and centroid-area for the trapezoid may be found:

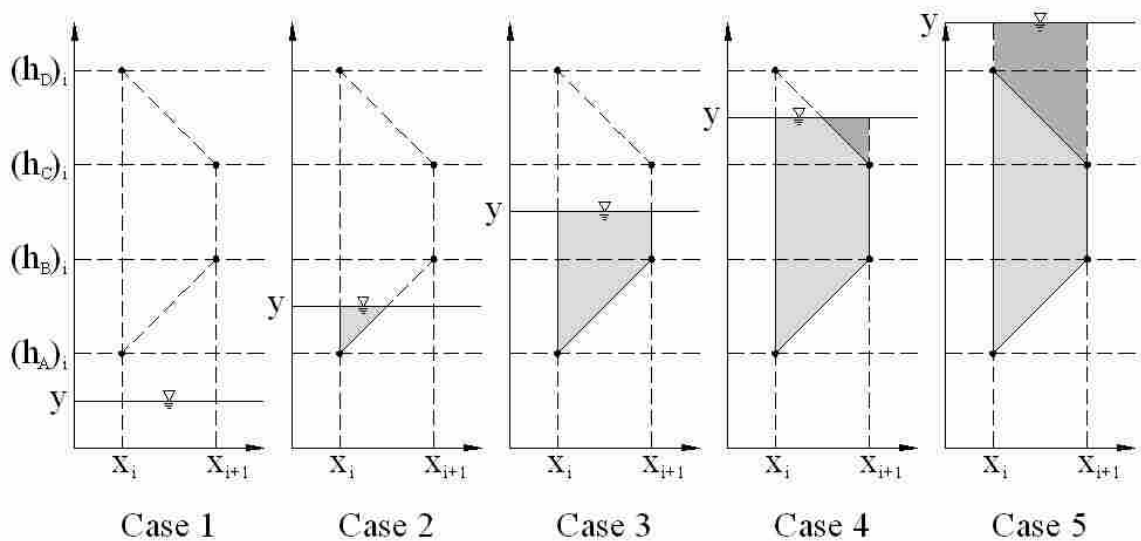
$$T_{\text{trap}} = b \quad (\text{B-49a})$$

$$A_{\text{trap}} = A_{\text{rect}} + A_{\text{tri}} = bh_2 + \frac{1}{2}b(h_1 - h_2) = \frac{1}{2}b(h_1 + h_2) \quad (\text{B-49b})$$

$$\begin{aligned} (\bar{z}A)_{\text{trap}} &= (\bar{z}A)_{\text{rect}} + (\bar{z}A)_{\text{tri}} + h_2A_{\text{tri}} \\ &= \frac{1}{2}bh_2^2 + \frac{1}{6}b(h_1 - h_2)^2 + \frac{1}{2}bh_2(h_1 - h_2) \\ &= \frac{3}{6}bh_2^2 + \frac{1}{6}bh_1^2 - \frac{2}{6}bh_1h_2 + \frac{1}{6}bh_2^2 + \frac{3}{6}bh_1h_2 - \frac{3}{6}bh_2^2 \\ &= \frac{1}{6}b(h_1^2 + h_1h_2 + h_2^2) \end{aligned} \quad (\text{B-49c})$$

### B.6.1.5 Incremental Shape Characteristics

Again, depending on the relative position of  $y$  with respect to the conduit coordinates, the shape of the incremental vertical section will be different, and therefore the top width, area, and centroid-area must be calculated differently. Figure B-20 on the next page shows that for each incremental section considered, one of five cases may occur and must be considered:



**Figure B-20 Cases to consider for the analysis of each incremental vertical section of a user-defined conduit**

In each of these cases, the incremental shape characteristics may be derived from the basic formulas for triangular and trapezoidal cross sections, given by Equations B-47a through B-47d and B-49a through B-49c, respectively. These derivations are shown by case as follows.

**B.6.1.6 Case 1 ( $0 < y \leq h_A$ )**

In Case 1, the flow depth falls below  $h_A$ , which means that the section being analyzed does not contribute at all to the overall top width, area, or centroid-area of the conduit (see Figure B-20). Therefore,

$$T_i = 0 \tag{B-50a}$$

$$A'_i = 0 \quad (\text{B-50b})$$

$$(\bar{z}A)'_i = 0 \quad (\text{B-50c})$$

### B.6.1.7 Case 2 ( $h_A < y \leq h_B$ )

In Case 2, the flow depth falls between  $h_A$  and  $h_B$ , creating a triangular cross-section of flow (see Figure B-20), which may be analyzed according to Equations B-47a through B-47d as follows:

$$\begin{aligned} T'_i &\equiv \frac{T_i}{B} = \frac{(T_{\text{tri}})_i}{B} = \frac{(x_{i+1} - x_i)}{B} \left( \frac{y - (h_A)_i}{(h_B)_i - (h_A)_i} \right) \left( \frac{D}{D} \right) \\ &= (x'_{i+1} - x'_i) \left( \frac{y' - (h'_A)_i}{(h'_B)_i - (h'_A)_i} \right) \end{aligned} \quad (\text{B-51a})$$

$$A'_i \equiv \frac{A_i}{BD} = \frac{(A_{\text{tri}})_i}{BD} = A_{\text{tri}} = \frac{T_i}{2BD} (y - (h_A)_i) = \frac{1}{2} T'_i (y' - (h'_A)_i) \quad (\text{B-51b})$$

$$(\bar{z}A)'_i \equiv \frac{(\bar{z}A)_i}{BD^2} = \frac{((\bar{z}A)_{\text{tri}})_i}{BD^2} = \frac{T_i}{6BD^2} (y - (h_A)_i)^2 = \frac{1}{6} T'_i (y' - (h'_A)_i)^2 \quad (\text{B-51c})$$

### B.6.1.8 Case 3 ( $h_B < y \leq h_C$ )

In Case 3, the flow depth falls between  $h_B$  and  $h_C$ , creating a trapezoidal cross-section of flow (see Figure B-20), and may be analyzed according to Equations B-49a through B-49c as follows:

$$T_i \equiv \frac{T_i}{B} = \frac{(T_{\text{trap}})_i}{B} = \frac{(x_{i+1} - x_i)}{B} = x'_{i+1} - x'_i \quad (\text{B-52a})$$

$$\begin{aligned} A'_i &\equiv \frac{A_i}{BD} = \frac{(A_{\text{trap}})_i}{BD} = \frac{T_i}{2BD} [(y - (h_A)_i) + (y - (h_B)_i)] \\ &= \frac{1}{2} T_i [(y' - (h'_A)_i) + (y' - (h'_B)_i)] \end{aligned} \quad (\text{B-52b})$$

$$\begin{aligned} (\bar{z}A)'_i &\equiv \frac{(\bar{z}A)_i}{BD^2} = \frac{((\bar{z}A)_{\text{trap}})_i}{BD^2} \\ &= \frac{T_i}{6BD^2} [(y - (h_A)_i)^2 + (y - (h_A)_i)(y - (h_B)_i) + (y - (h_B)_i)^2] \\ &= \frac{1}{6} T_i [(y' - (h'_A)_i)^2 + (y' - (h'_A)_i)(y' - (h'_B)_i) + (y' - (h'_B)_i)^2] \end{aligned} \quad (\text{B-52c})$$

#### B.6.1.9 Case 4 ( $h_C < y \leq h_D$ )

In Case 4, the flow depth falls between  $h_C$  and  $h_D$ , creating a complex shape which may be treated as a triangular section subtracted from a trapezoidal section (see Figure B-20), and may be analyzed according to Equations B-47a through B-47d and B-49a through B-49c as follows:

$$\begin{aligned} T_i &\equiv \frac{T_i}{B} = \frac{(T_{\text{trap}} - T_{\text{tri}})_i}{B} = \frac{(x_{i+1} - x_i)}{B} \left( \frac{(h_D)_i - y}{(h_D)_i - (h_C)_i} \right) \left( \frac{D}{D} \right) \\ &= (x'_{i+1} - x'_i) \left( \frac{(h'_D)_i - y'}{(h'_D)_i - (h'_C)_i} \right) \end{aligned} \quad (\text{B-53a})$$

$$\begin{aligned}
A'_i &\equiv \frac{A_i}{BD} = \frac{(A_{\text{trap}} - A_{\text{tri}})_i}{BD} = \frac{1}{2BD} \left\{ (x_{i+1} - x_i) \left[ (y - (h_A)_i) + (y - (h_B)_i) \right] \right. \\
&\quad \left. - (x_{i+1} - x_i - T_i) (y - (h_C)_i) \right\} \\
&= \frac{1}{2} \left\{ (x'_{i+1} - x'_i) \left[ (y' - (h'_A)_i) + (y' - (h'_B)_i) \right] \right. \\
&\quad \left. - (x'_{i+1} - x'_i - T'_i) (y' - (h'_C)_i) \right\} \tag{B-53b}
\end{aligned}$$

$$\begin{aligned}
(\bar{z}A)'_i &\equiv \frac{(\bar{z}A)_i}{BD^2} = \frac{((\bar{z}A)_{\text{trap}} - (\bar{z}A)_{\text{tri}})_i}{BD^2} = \\
&= \frac{1}{6BD^2} \left\{ (x_{i+1} - x_i) \left[ (y - (h_A)_i)^2 + (y - (h_A)_i)(y - (h_B)_i) + (y - (h_B)_i)^2 \right] \right. \\
&\quad \left. - (x_{i+1} - x_i - T_i) (y - (h_C)_i)^2 \right\} \\
&= \frac{1}{6} \left\{ (x'_{i+1} - x'_i) \left[ (y' - (h'_A)_i)^2 + (y' - (h'_A)_i)(y' - (h'_B)_i) + (y' - (h'_B)_i)^2 \right] \right. \\
&\quad \left. - (x'_{i+1} - x'_i - T'_i) (y' - (h'_C)_i)^2 \right\} \tag{B-53c}
\end{aligned}$$

#### B.6.1.10 Case 5 ( $h_D < y$ )

In Case 5, the flow depth falls above  $h_D$ , creating a complex shape which may be treated as a trapezoidal section subtracted from another trapezoidal section (see Figure B-20), and may be analyzed according to Equations B-49a through B-49c as follows:

$$T'_i \equiv \frac{T_i}{B} = \frac{(T_{\text{trap1}} - T_{\text{trap2}})_i}{B} = 0 \tag{B-54a}$$

$$\begin{aligned}
A'_i &\equiv \frac{A_i}{BD} = \frac{(A_{\text{trap1}} - A_{\text{trap2}})_i}{BD} \\
&= \frac{1}{2BD} (x_{i+1} - x_i) \left[ (y - (h_A)_i) + (y - (h_B)_i) - (y - (h_C)_i) - (y - (h_D)_i) \right] \\
&= \frac{1}{2} (x'_{i+1} - x'_i) \left[ (h'_D)_i + (h'_C)_i - (h'_B)_i - (h'_A)_i \right] \tag{B-54b}
\end{aligned}$$

$$\begin{aligned}
(\bar{z}A)'_i &\equiv \frac{(\bar{z}A)_i}{BD^2} = \frac{((\bar{z}A)_{\text{trap1}} - (\bar{z}A)_{\text{trap2}})_i}{BD^2} \\
&= \frac{1}{6BD^2} (x_{i+1} - x_i) \left[ \begin{aligned} &(y - (h_A)_i)^2 + (y - (h_A)_i)(y - (h_B)_i) + (y - (h_B)_i)^2 \\ &- (y - (h_C)_i)^2 - (y - (h_C)_i)(y - (h_D)_i) - (y - (h_D)_i)^2 \end{aligned} \right] \\
&= \frac{1}{6} (x'_{i+1} - x'_i) \left[ \begin{aligned} &3y'((h'_D)_i + (h'_C)_i - (h'_B)_i - (h'_A)_i) \\ &+ ((h'_A)_i)^2 + (h'_A)_i(h'_B)_i + (h'_B)_i^2 \\ &- ((h'_C)_i)^2 + (h'_C)_i(h'_D)_i + (h'_D)_i^2 \end{aligned} \right] \tag{B-54c}
\end{aligned}$$

### B.6.1.11 Summary

In summary, the top width ( $\Gamma$ ), area ( $\Omega$ ), and centroid-area ( $\Psi$ ) functions for user-defined conduits may be expressed by Equations B-42a through B-42c, where depending on the flow depth relative to the conduit walls, Equations B-50a through B-54c are used to evaluate  $T_i$ ,  $A_i$ , and  $(\bar{z}A)_i$  at each incremental vertical section.

### B.6.2 Solution

The sequent depth equation for complete jumps in user-defined conduits may be derived from Equation B-20. In this case  $y'_2$  cannot be obtained explicitly in terms of  $y'_1$  and  $Fr_1^2$ , so the sequent depth must be obtained iteratively. Likewise, the sequent depth equation for incomplete jumps may be derived from Equation B-24, and the transitional Froude number may be derived from Equation B-25. In each of these cases, Equations B-42a through B-42c and B-50a through B-54c are used to evaluate Equations B-16 through B-18.



### **B.6.3 Sequent Depth Chart**

A visual representation of this solution is shown in Figure B-21 on the next page. This is modeled after the format used by Montes (1998), and provides a simple and effective shortcut for finding the sequent depth for any upstream depth and Froude number in a user-defined conduit. Note that this chart only applies to the user-defined culvert corresponding to the coordinates listed in Table B-2. It is merely an illustration that such a chart may be created for any set of coordinates as defined in this section.

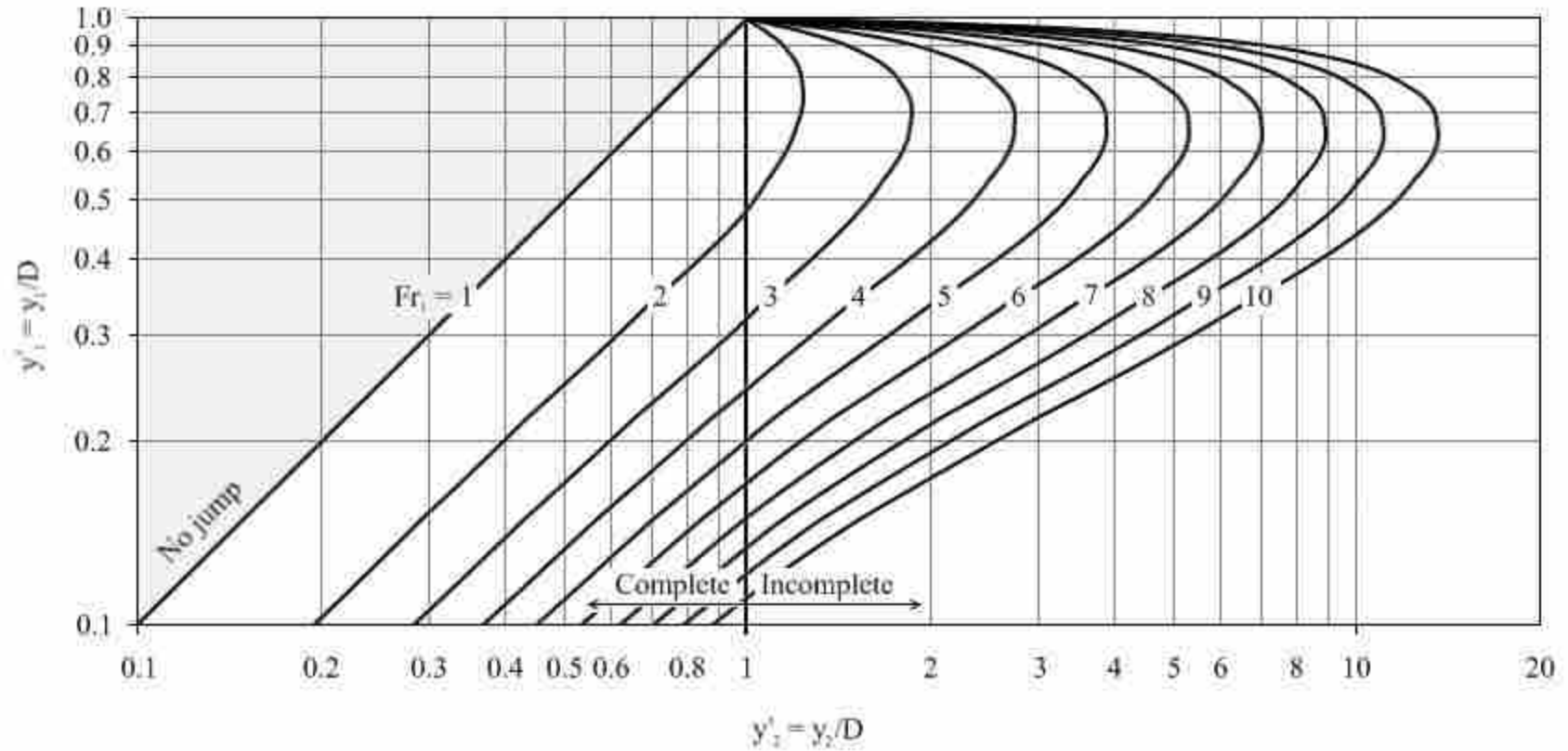


Figure B-21 Sequent depth ratio chart for the user-defined culvert associated with the coordinates listed Table B-2



## Appendix C. Example Problems

### C.1 Example 1: Box Culvert

Determine the subcritical sequent depth of a hydraulic jump in a box culvert with a 6-ft span and a 4-ft rise, passing a flow of 300 cfs at an upstream depth of 2 ft.

GIVEN:  $B = 6$  ft,  $D = 4$  ft,  $Q = 300$  cfs,  $y_1 = 2$  ft

FIND:  $y_2$

SOLUTION: (From Figure 8)

*Step 1: Calculate dimensionless parameters*

$$y'_1 = \frac{y_1}{D} = \frac{(2 \text{ ft})}{(4 \text{ ft})} = 0.5$$

*Step 2: Calculate upstream Froude number*

$$Fr_1 = \frac{Q}{\sqrt{gB^2 y_1^3}} = \frac{(300 \text{ ft}^3/\text{s})}{\sqrt{(32.2 \text{ ft}/\text{s}^2)(6 \text{ ft})^2 (2 \text{ ft})^3}} = 3.12$$

Since  $Fr_1 > 1$ , the flow is supercritical and a hydraulic jump can occur.

*Step 3: Calculate transitional upstream Froude number*

$$(Fr_1)_t = \sqrt{\frac{(1 + y'_1)}{2(y'_1)^2}} = \sqrt{\frac{(1 + 0.5)}{2(0.5)^2}} = 1.73$$

Since  $Fr_1 > (Fr_1)_t$ , the jump will be incomplete.

*Step 4: Calculate downstream depth*

$$y'_2 = \frac{1}{2} + \left( Fr_1^2 + \frac{1}{2} \right) y_1'^2 - Fr_1^2 y_1'^3 = \frac{1}{2} + \left( (3.12)^2 + \frac{1}{2} \right) (0.5)^2 - (3.12)^2 (0.5)^3 = 1.84$$

$$y_2 = y'_2 * D = (1.84)(4 \text{ ft}) = \mathbf{7.35 \text{ ft}}$$

Alternatively,  $y'_2$  may be found graphically using the values for  $y'_1$  and  $Fr_1$  calculated in Steps 1 and 2, respectively, as shown below in Figure C-1 on the next page.

## **C.2 Example 2: Circular Culvert**

Determine the subcritical sequent depth of a hydraulic jump in a circular culvert with a 1.0-m diameter, passing a flow of 0.7 cms at an upstream depth of 0.3 m.

GIVEN:  $D = 1.0 \text{ m}$ ,  $Q = 0.7 \text{ cms}$ ,  $y_1 = 0.3 \text{ m}$

FIND:  $y_2$

SOLUTION: (From Figure 9)

*Step 1: Calculate dimensionless parameters*

$$y'_1 = \frac{y_1}{D} = \frac{(0.3 \text{ m})}{(1.0 \text{ m})} = 0.3$$

$$\theta_1 = 2\cos^{-1}(1 - 2y'_1) = 2\cos^{-1}(1 - 2(0.3)) = 2.32 \text{ radians}$$

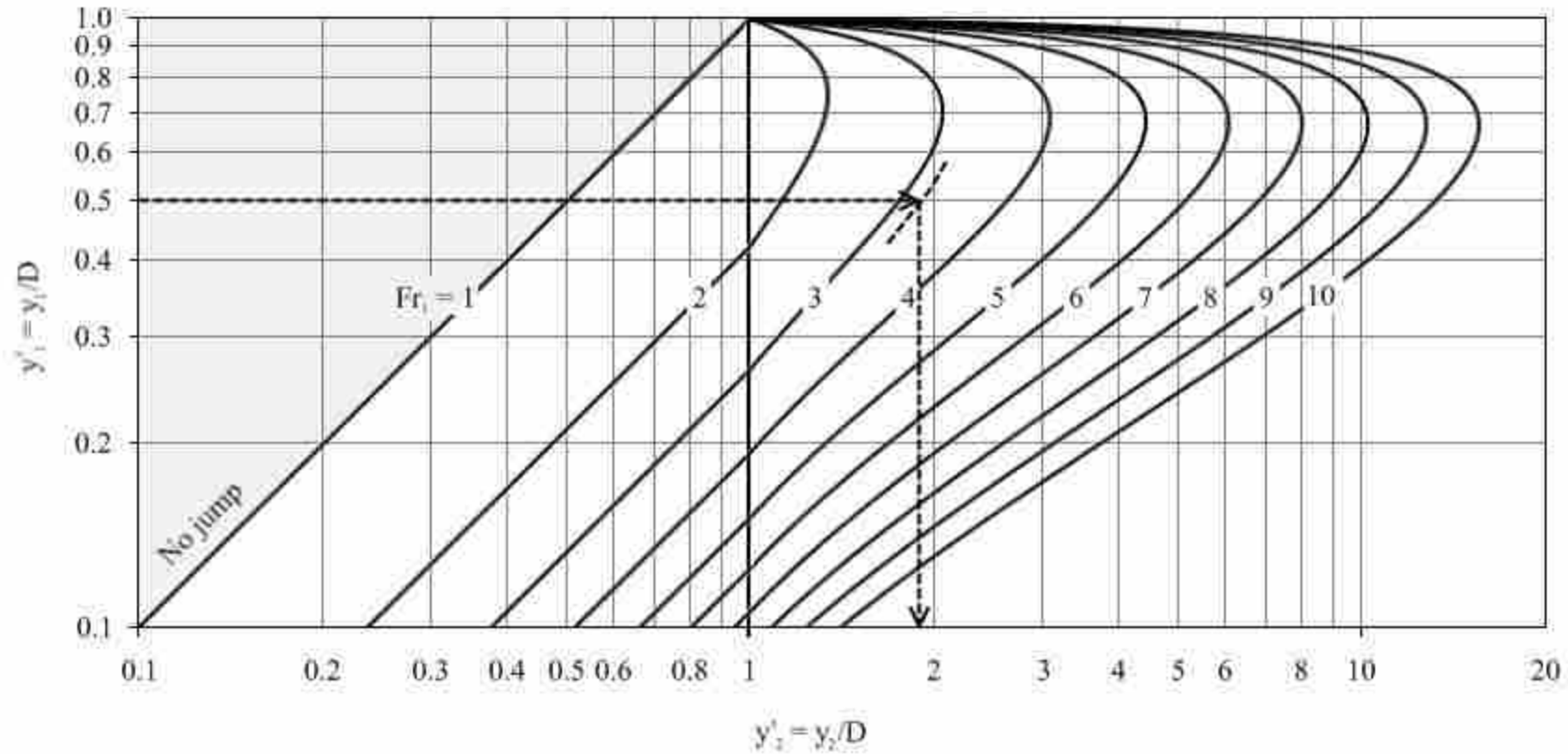


Figure C-1 Graphical solution to Example 1

$$T_1 = \sin(\theta_1/2) = \sin(2.32/2) = 0.917$$

$$A'_1 = \frac{1}{8}(\theta_1 - \sin\theta_1) = \frac{1}{8}((2.32) - \sin(2.32)) = 0.198$$

$$\begin{aligned} (\bar{z}A)'_1 &= \frac{1}{24} [3\sin(\theta_1/2) - \sin^3(\theta_1/2) - 3(\theta_1/2)\cos(\theta_1/2)] \\ &= \frac{1}{24} [3\sin(2.32/2) - \sin^3(2.32/2) - 3(2.32/2)\cos(2.32/2)] = 0.0245 \end{aligned}$$

$$\theta_f = 2\cos^{-1}(1 - 2y'_f) = 2\cos^{-1}(1 - 2(1)) = 2\pi \text{ radians}$$

$$A'_f = \frac{1}{8}(\theta_f - \sin\theta_f) = \frac{1}{8}((2\pi) - \sin(2\pi)) = 0.785$$

$$\begin{aligned} (\bar{z}A)'_f &= \frac{1}{24} [3\sin(\theta_f/2) - \sin^3(\theta_f/2) - 3(\theta_f/2)\cos(\theta_f/2)] \\ &= \frac{1}{24} [3\sin(2\pi/2) - \sin^3(2\pi/2) - 3(2\pi/2)\cos(2\pi/2)] = 0.393 \end{aligned}$$

*Step 2: Calculate upstream Froude number*

$$Fr_1 = \frac{Q}{\sqrt{g B^2 D^3 A_1'^3 / T_1}} = \frac{(0.7 \text{ m}^3/\text{s})}{\sqrt{(9.81 \text{ m/s}^2)(1 \text{ m})^5 (0.198)^3 / (0.917)}} = 2.43$$

Since  $Fr_1 > 1$ , the flow is supercritical and a hydraulic jump can occur.

*Step 3: Calculate transitional upstream Froude number*

$$(Fr_1)_t = \sqrt{\frac{T_1 A'_f [(\bar{z}A)'_f - (\bar{z}A)'_1]}{A_1'^2 (A'_f - A'_1)}} = \sqrt{\frac{(0.917)(0.785)[(0.393) - (0.0245)]}{(0.198)^2 (0.785 - 0.198)}} = 3.39$$

Since  $Fr_1 < (Fr_1)_t$ , the jump will be complete.

*Step 4: Calculate downstream depth*

$$\theta_2 = 2\cos^{-1}(1 - 2y'_2)$$

$$A'_2 = \frac{1}{8}(\theta_2 - \sin\theta_2)$$

$$(\bar{z}A)'_2 = \frac{1}{24} [3\sin(\theta_2/2) - \sin^3(\theta_2/2) - 3(\theta_2/2)\cos(\theta_2/2)]$$

$$Fr_1^2 = \frac{T_1 A'_2 [(\bar{z}A)'_2 - (\bar{z}A)'_1]}{A_1'^2 (A'_2 - A'_1)} \Rightarrow (2.43)^2 = \frac{(0.917)A'_2 [(\bar{z}A)'_2 - (0.0245)]}{(0.198)^2 (A'_2 - (0.198))}$$

Solving these equations iteratively yields  $y'_2 = 0.721$

$$y_2 = y'_2 * D = (0.72)(1 \text{ m}) = \mathbf{0.721 \text{ m}}$$

Alternatively,  $y'_2$  may be found graphically using the values for  $y'_1$  and  $Fr_1$  calculated in Steps 1 and 2, respectively, as shown below in Figure C-2 on the next page.

### **C.3 Example 3: Elliptical Culvert**

Determine the subcritical sequent depth of a hydraulic jump in an elliptical culvert with an 11-ft span, an 8-ft rise, 82-in top radius, and 38-in side radius (CONTECH 2007), passing a flow of 500 cfs at an upstream depth of 4 ft.

GIVEN:  $B = 11 \text{ ft}$ ,  $D = 8 \text{ ft}$ ,  $Q = 500 \text{ cfs}$ ,  $y_1 = 4 \text{ ft}$

FIND:  $y_2$

SOLUTION: (From Figure 10)

*Step 1: Calculate dimensionless parameters*

$$y'_1 = \frac{y_1}{D} = \frac{(4 \text{ ft})}{(8 \text{ ft})} = 0.5$$



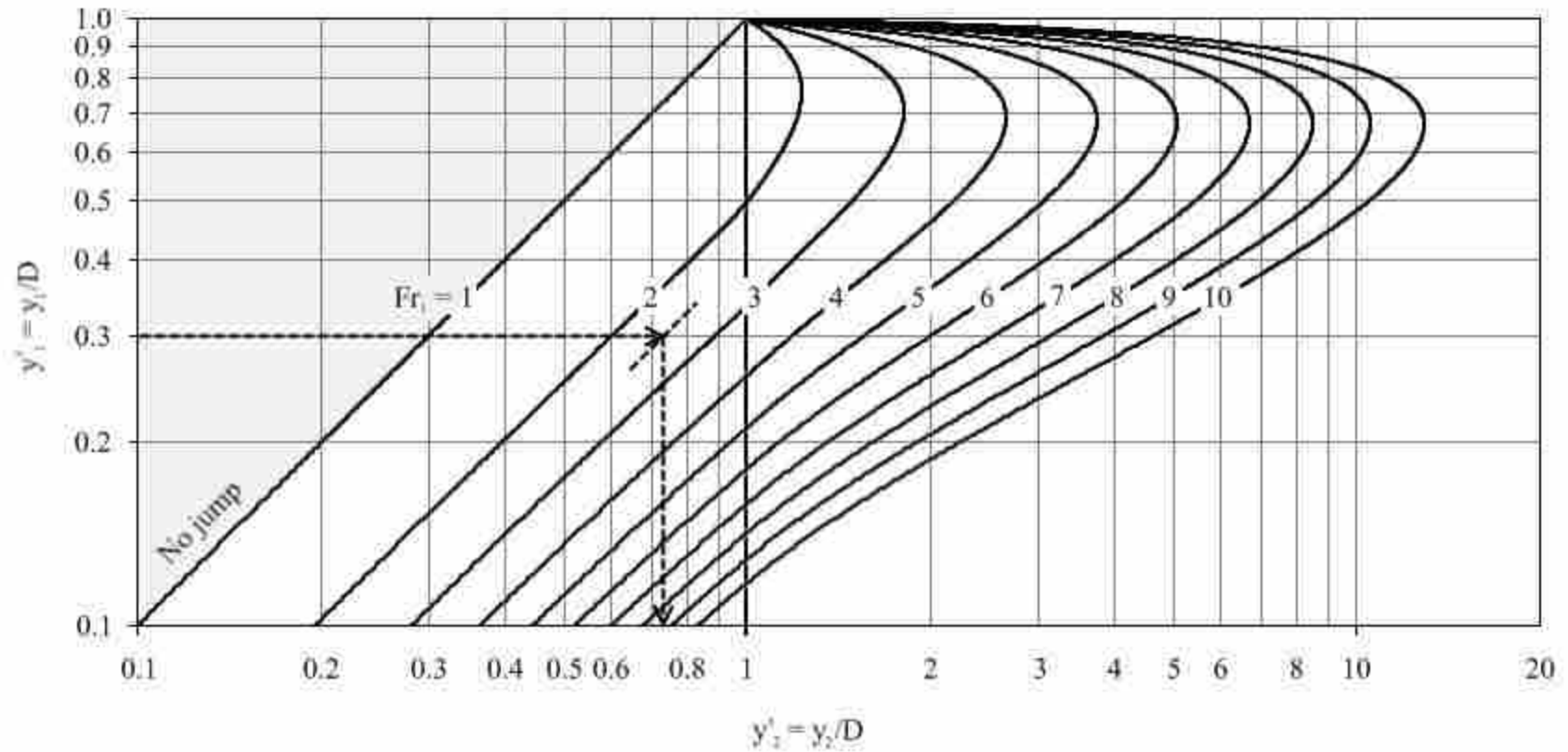


Figure C-2 Graphical solution to Example 2

$$T_1 = 2\sqrt{y'_1 - y_1'^2} = 2\sqrt{(0.5) - (0.5)^2} = 1$$

$$A'_1 = \frac{1}{4} [\cos^{-1}(1 - 2y'_1) - T_1(1 - 2y'_1)] = \frac{1}{4} [\cos^{-1}(1 - 2(0.5)) - (1)(1 - 2(0.5))] = 0.393$$

$$(\bar{z}A)'_1 = \frac{1}{12} [T_1^3 - 6A'_1(1 - 2y'_1)] = \frac{1}{12} [(1)^3 - 6(0.393)(1 - 2(0.5))] = 0.0833$$

$$T_f = 2\sqrt{y'_f - y_f'^2} = 2\sqrt{(1) - (1)^2} = 0$$

$$A'_f = \frac{1}{4} [\cos^{-1}(1 - 2y'_f) - T_f(1 - 2y'_f)] = \frac{1}{4} [\cos^{-1}(1 - 2(1)) - (0)(1 - 2(1))] = 0.785$$

$$(\bar{z}A)'_f = \frac{1}{12} [T_f^3 - 6A'_f(1 - 2y'_f)] = \frac{1}{12} [(0)^3 - 6(0.785)(1 - 2(1))] = 0.393$$

*Step 2: Calculate upstream Froude number*

$$Fr_1 = \frac{Q}{\sqrt{gB^2D^3A_1'^3/T_1}} = \frac{(500 \text{ ft}^3/\text{s})}{\sqrt{(32.2 \text{ ft}/\text{s}^2)(11 \text{ ft})^2(8 \text{ ft})^3(0.393)^3/(1)}} = 1.44$$

Since  $Fr_1 > 1$ , the flow is supercritical and a hydraulic jump can occur.

*Step 3: Calculate transitional upstream Froude number*

$$(Fr_1)_t = \sqrt{\frac{T_1 A'_f [(\bar{z}A)'_f - (\bar{z}A)'_1]}{A_1'^2 (A'_f - A'_1)}} = \sqrt{\frac{(1)(0.785)[(0.393) - (0.0833)]}{(0.393)^2(0.785 - 0.393)}} = 2.00$$

Since  $Fr_1 < (Fr_1)_t$ , the jump will be complete.

*Step 4: Calculate downstream depth*

$$T_2 = 2\sqrt{y'_2 - y_2'^2}$$

$$A'_2 = \frac{1}{4} [\cos^{-1}(1 - 2y'_2) - T_2(1 - 2y'_2)]$$

$$(\bar{z}A)'_2 = \frac{1}{12} [T_2^3 - 6A'_2(1 - 2y'_2)]$$

$$Fr_1^2 = \frac{T_1 A'_2 [(\bar{z}A)'_2 - (\bar{z}A)'_1]}{A_1'^2 (A'_2 - A'_1)} \Rightarrow (1.44)^2 = \frac{(1)A'_2 [(\bar{z}A)'_2 - (0.0833)]}{(0.393)^2 (A'_2 - (0.393))}$$

Solving these equations iteratively yields  $y'_2 = 0.726$

$$y_2 = y'_2 * D = (0.726)(8 \text{ ft}) = \mathbf{5.81 \text{ ft}}$$

Alternatively,  $y'_2$  may be found graphically using the values for  $y'_1$  and  $Fr_1$  calculated in Steps 1 and 2, respectively, as shown below in Figure C-3 on the next page.

#### C.4 Example 4: Pipe Arch Culvert

Determine the subcritical sequent depth of a hydraulic jump in a pipe arch culvert with a 13-ft 1-in span, an 8-ft 4-in rise, 31.75-in “haunch” radius, 81.7-in “crown” radius, and 300.8-in “Invert” radius (CONTECH 2007), passing a flow of 4000 cfs at an upstream depth of 6.0 ft.

GIVEN:  $B = 157 \text{ in}$ ,  $D = 100 \text{ in}$ ,  $R_b = 300.8 \text{ in}$ ,  $R_m = 31.75 \text{ in}$ ,  $R_t = 81.7 \text{ in}$ ,  $Q = 4000 \text{ cfs}$ ,

$y_1 = 6.0 \text{ ft}$

FIND:  $y_2$

SOLUTION: (From Figure 11)

First, calculate the remaining shape parameters, as follows:

$$\begin{aligned} h_m &= R_b - \sqrt{(R_b - R_m)^2 - (B/2 - R_m)^2} \\ &= (300.8 \text{ in}) - \sqrt{(300.8 \text{ in} - 31.75 \text{ in})^2 - ((157 \text{ in})/2 - 31.75 \text{ in})^2} = 35.8 \text{ in} \end{aligned}$$

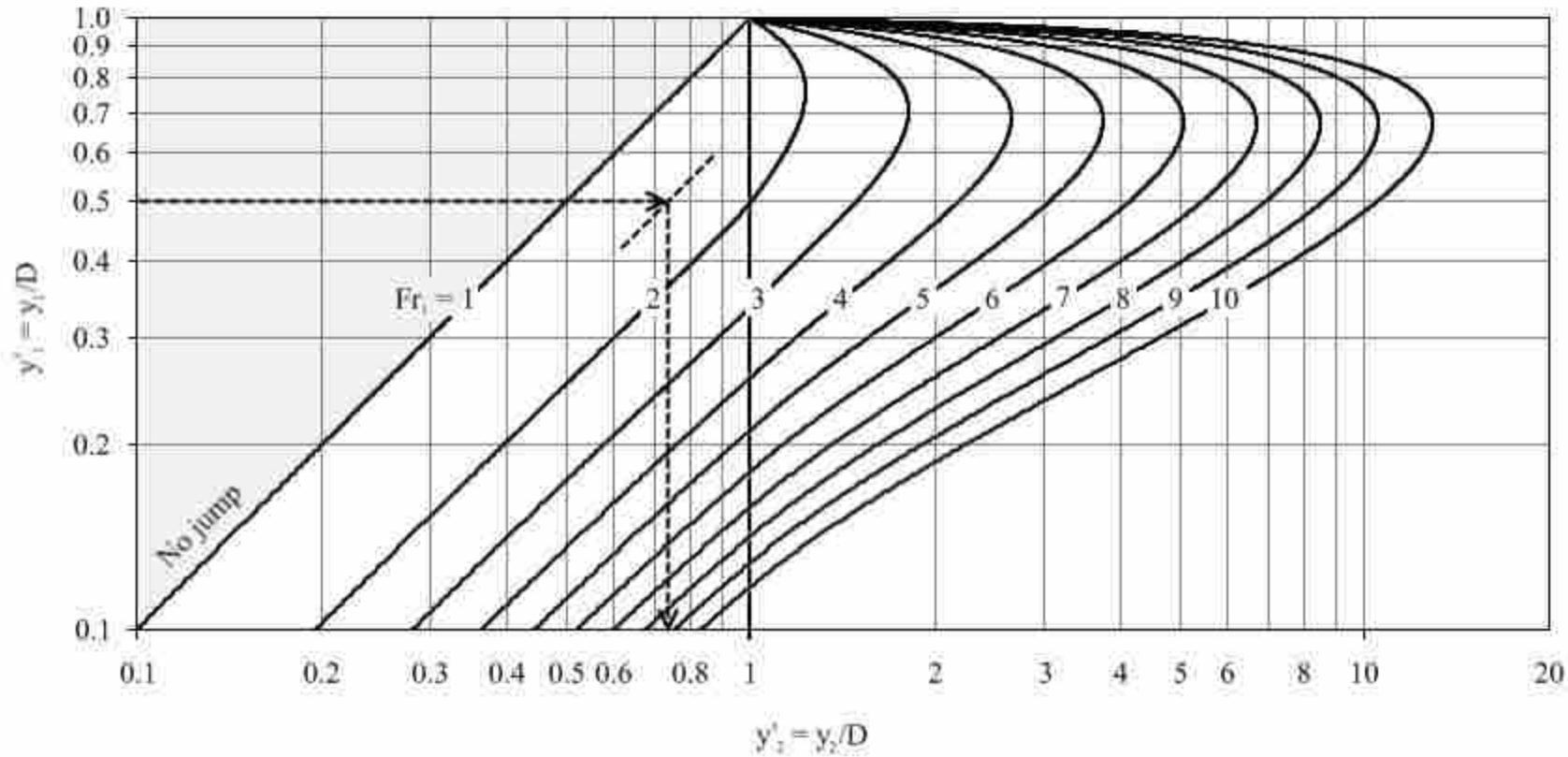


Figure C-3 Graphical solution to Example 3

$$R_t = \frac{B(4R_m - B) - 4(D - h_m)^2}{8(R_m - D + h_m)}$$

$$= \frac{(157 \text{ in})(4(31.75 \text{ in}) - (157 \text{ in})) - 4((100 \text{ in}) - (35.8 \text{ in}))^2}{8((31.75 \text{ in}) - (100 \text{ in}) + (35.8 \text{ in}))} = 81.7 \text{ in}$$

$$h_b = R_b \left( \frac{h_m - R_m}{R_b - R_m} \right) = (300.8 \text{ in}) \left( \frac{35.8 \text{ in} - 31.75 \text{ in}}{300.8 \text{ in} - 31.75 \text{ in}} \right) = 4.58 \text{ in}$$

$$h_t = D - R_t \left[ 1 - \frac{\sqrt{(R_t - R_m)^2 - (B/2 - R_m)^2}}{(R_t - R_m)} \right]$$

$$= (100 \text{ in}) - (81.7 \text{ in}) \left[ 1 - \frac{\sqrt{(81.7 \text{ in} - 31.75 \text{ in})^2 - ((157 \text{ in})/2 - 31.75 \text{ in})^2}}{(81.7 \text{ in} - 31.75 \text{ in})} \right]$$

$$= 47.0 \text{ in}$$

*Step 1: Calculate dimensionless parameters*

Dividing each shape parameter (except for D) by D, the dimensionless shape parameters are then calculated as follows:

$$B' \equiv \frac{B}{D} = \frac{(157 \text{ in})}{(100 \text{ in})} = 1.57$$

$$R'_b \equiv \frac{R_b}{D} = \frac{(300.8 \text{ in})}{(100 \text{ in})} = 3.008$$

$$R'_m \equiv \frac{R_m}{D} = \frac{(31.75 \text{ in})}{(100 \text{ in})} = 0.3175$$

$$R'_t \equiv \frac{R_t}{D} = \frac{(81.7 \text{ in})}{(100 \text{ in})} = 0.817$$

$$h'_b \equiv \frac{h_b}{D} = \frac{(4.58 \text{ in})}{(100 \text{ in})} = 0.0458$$

$$h'_m \equiv \frac{h_m}{D} = \frac{(35.8 \text{ in})}{(100 \text{ in})} = 0.358$$

$$h'_t \equiv \frac{h_t}{D} = \frac{(47.0 \text{ in})}{(100 \text{ in})} = 0.470$$

Next, determine the upstream depth ratio:

$$y'_1 = \frac{y_1}{D} = \frac{(72 \text{ in})}{(100 \text{ in})} = 0.72$$

Since  $h'_t < y'_1 \leq 1$ ,  $T'_1$ ,  $A'^1_1$ , and  $(\bar{z}A)'_1$  are calculated as follows:

$$\theta_b|^{h'_b} = 2\cos^{-1}\left(1 - \frac{h'_b}{R'_b}\right) = 2\cos^{-1}\left(1 - \frac{0.0458}{3.008}\right)$$

$$= 0.349 \text{ radians}$$

$$\theta_m|^{h'_b} = 2\cos^{-1}\left(1 - \frac{1}{R'_m}(h'_b - h'_m + R'_m)\right)$$

$$= 2\cos^{-1}\left(1 - \frac{1}{(0.3175)}(0.0458 - 0.358 + 0.3175)\right) = 0.349 \text{ radians}$$

$$\theta_m|^{h'_t} = 2\cos^{-1}\left(1 - \frac{1}{R'_m}(h'_t - h'_m + R'_m)\right)$$

$$= 2\cos^{-1}\left(1 - \frac{1}{(0.3175)}(0.470 - 0.358 + 0.3175)\right) = 3.86 \text{ radians}$$

$$\theta_t|^{h'_t} = 2\cos^{-1}\left(\frac{1 - h'_t}{R'_t} - 1\right) = 2\cos^{-1}\left(\frac{1 - 0.470}{(0.817)} - 1\right) = 3.86 \text{ radians}$$

$$\theta_t|^{y'_1} = 2\cos^{-1}\left(\frac{1 - y'_1}{R'_t} - 1\right) = 2\cos^{-1}\left(\frac{1 - 0.72}{(0.817)} - 1\right) = 4.58 \text{ radians}$$

$$\Gamma_1 = \Gamma_t|^{y_i} = 2 \left( \frac{R'_t}{B'} \right) \sin(\theta_t|^{y_i} / 2) = 2 \left( \frac{0.817}{3.008} \right) \sin(4.58/2) = 0.784$$

$$\Omega_b|^{h_b} = \frac{R'_b{}^2}{2B'} \left( \theta_b|^{h_b} - \sin(\theta_b|^{h_b}) \right) = \frac{(3.008)^2}{2(1.57)} (0.349 - \sin(0.349)) = 0.0203$$

$$\begin{aligned} \Omega_{m1}|^{h_b} &= \frac{1}{B'} (B' - 2R'_m) (h'_b - h'_m + R'_m) \\ &= \frac{1}{(1.57)} (1.57 - 2(0.3175)) (0.0458 - 0.358 + 0.3175) = 0.00288 \end{aligned}$$

$$\Omega_{m2}|^{h_b} = \frac{R'_m{}^2}{2B'} \left( \theta_m|^{h_b} - \sin(\theta_m|^{h_b}) \right) = \frac{(0.3175)^2}{2(1.57)} (0.349 - \sin(0.349)) = 0.000227$$

$$\begin{aligned} \Omega_{m1}|^{h_i} &= \frac{1}{B'} (B' - 2R'_m) (h'_t - h'_m + R'_m) \\ &= \frac{1}{(1.57)} (1.57 - 2(0.3175)) (0.470 - 0.358 + 0.3175) = 0.255 \end{aligned}$$

$$\Omega_{m2}|^{h_i} = \frac{R'_m{}^2}{2B'} \left( \theta_m|^{h_i} - \sin(\theta_m|^{h_i}) \right) = \frac{(0.3175)^2}{2(1.57)} (3.86 - \sin(3.86)) = 0.145$$

$$\Omega_t|^{h_i} = \frac{R'_t{}^2}{2B'} \left( \theta_t|^{h_i} - \sin(\theta_t|^{h_i}) \right) = \frac{(0.817)^2}{2(1.57)} (3.86 - \sin(3.86)) = 0.959$$

$$\Omega_t|^{y_i} = \frac{R'_t{}^2}{2B'} \left( \theta_t|^{y_i} - \sin(\theta_t|^{y_i}) \right) = \frac{(0.817)^2}{2(1.57)} (4.58 - \sin(4.58)) = 1.18$$

$$\begin{aligned} A'_1 &= \Omega_b|^{h_b} + \Omega_{m1}|^{h_b} + \Omega_{m2}|^{h_b} + \Omega_t|^{y_i} \\ &= (0.0203) + (0.255 - 0.00288) + (0.145 - 0.000227) + (1.18 - 0.959) \\ &= 0.641 \end{aligned}$$

$$\begin{aligned}\Psi_b|^{h_b} &= \frac{R'_b{}^3}{3B'} \left[ 3\sin(\theta_b|^{h_b}/2) - \sin^3(\theta_b|^{h_b}/2) - 3(\theta_b|^{h_b}/2)\cos(\theta_b|^{h_b}/2) \right] \\ &= \frac{(3.008)^3}{3(1.57)} \left[ 3\sin(0.349/2) - \sin^3(0.349/2) - 3(0.349/2)\cos(0.349/2) \right] \\ &= 0.000373\end{aligned}$$

$$\begin{aligned}\Psi_{m1}|^{h_b} &= \frac{1}{2B'} (B' - 2R'_m)(h'_b - h'_m + R'_m)^2 \\ &= \frac{1}{2(1.57)} (1.57 - 2(0.3175))(0.0458 - 0.358 + 0.3175)^2 = 6.95 \times 10^{-6}\end{aligned}$$

$$\begin{aligned}\Psi_{m2}|^{h_b} &= \frac{R'_m{}^3}{3B'} \left[ 3\sin(\theta_m|^{h_b}/2) - \sin^3(\theta_m|^{h_b}/2) - 3(\theta_m|^{h_b}/2)\cos(\theta_m|^{h_b}/2) \right] \\ &= \frac{(0.3175)^3}{3(1.57)} \left[ 3\sin(0.349/2) - \sin^3(0.349/2) - 3(0.349/2)\cos(0.349/2) \right] \\ &= 4.38 \times 10^{-7}\end{aligned}$$

$$\begin{aligned}\Psi_{m1}|^{h_t} &= \frac{1}{2B'} (B' - 2R'_m)(h'_t - h'_m + R'_m)^2 \\ &= \frac{1}{2(1.57)} (1.57 - 2(0.3175))(0.470 - 0.358 + 0.3175)^2 = 0.0548\end{aligned}$$

$$\begin{aligned}\Psi_{m2}|^{h_t} &= \frac{R'_m{}^3}{3B'} \left[ 3\sin(\theta_m|^{h_t}/2) - \sin^3(\theta_m|^{h_t}/2) - 3(\theta_m|^{h_t}/2)\cos(\theta_m|^{h_t}/2) \right] \\ &= \frac{(0.3175)^3}{3(1.57)} \left[ 3\sin(3.86/2) - \sin^3(3.86/2) - 3(3.86/2)\cos(3.86/2) \right] = 0.0273\end{aligned}$$

$$\begin{aligned}\Psi_t|^{h_t} &= \frac{R'_t{}^3}{3B'} \left[ 3\sin(\theta_t|^{h_t}/2) - \sin^3(\theta_t|^{h_t}/2) - 3(\theta_t|^{h_t}/2)\cos(\theta_t|^{h_t}/2) \right] \\ &= \frac{(0.817)^3}{3(1.57)} \left[ 3\sin(3.86/2) - \sin^3(3.86/2) - 3(3.86/2)\cos(3.86/2) \right] = 0.465\end{aligned}$$



$$\Psi_t|^{y_i} = \frac{R_t^3}{3B'} \left[ 3\sin(\theta_t|^{y_i}/2) - \sin^3(\theta_t|^{y_i}/2) - 3(\theta_t|^{y_i}/2)\cos(\theta_t|^{y_i}/2) \right]$$

$$= \frac{(0.817)^3}{3(1.57)} \left[ 3\sin(4.58/2) - \sin^3(4.58/2) - 3(4.58/2)\cos(4.58/2) \right] = 0.734$$

$$(\bar{z}A)_1 = \Psi_b|^{h_b} + (y_1 - h'_b)\Omega_b|^{h_b} + \Psi_{m1}|_{h_b}^{h_t} + (y_1 - h'_t)\Omega_{m1}|^{h_t}$$

$$- (y_1 - h'_b)\Omega_{m1}|^{h_b} + \Psi_{m2}|_{h_b}^{h_t} + (y_1 - h'_t)\Omega_{m2}|^{h_t} - (y_1 - h'_b)\Omega_{m2}|^{h_b}$$

$$+ \Psi_t|_{h_t}^{y_i} - (y_1 - h'_t)\Omega_t|^{h_t}$$

$$= (0.000373) + (0.72 - 0.0458)(0.0203) + (0.0548 - 6.95 \times 10^{-6})$$

$$+ (0.72 - 0.470)(0.255) - (0.72 - 0.0458)(0.00288)$$

$$+ (0.0273 - 4.38 \times 10^{-7}) + (0.72 - 0.470)(0.145)$$

$$- (0.72 - 0.0458)(0.000227) + (0.734 - 0.465)$$

$$- (0.72 - 0.470)(0.959) = 0.223$$

Since  $y'_f = 1$ ,  $A'_f$  and  $(\bar{z}A)'_f$  are calculated as follows:

$$\theta_t|^{y'_f} = 2\cos^{-1}\left(1 - \frac{1}{R'_t}(y'_f + 2R'_t - 1)\right) = 2\cos^{-1}\left(1 - \frac{1}{(0.817)}(1 + 2(0.817) - 1)\right)$$

$$= 2\pi \text{ radians}$$

$$\Omega_t|^{y'_f} = \frac{R_t^2}{2B'} \left( \theta_t|^{y'_f} - \sin(\theta_t|^{y'_f}) \right) = \frac{(0.817)^2}{2(1.57)} (2\pi - \sin(2\pi)) = 1.335$$

$$A'_f = \Omega_b|^{h_b} + \Omega_{m1}|_{h_b}^{h_t} + \Omega_{m2}|_{h_b}^{h_t} + \Omega_t|_{h_t}^{y'_f}$$

$$= (0.0203) + (0.255 - 0.00288) + (0.145 - 0.000227) + (1.335 - 0.959)$$

$$= 0.793$$

$$\Psi_t|^{y'_f} = \frac{R_t^3}{3B'} \left[ 3\sin(\theta_t|^{y'_f}/2) - \sin^3(\theta_t|^{y'_f}/2) - 3(\theta_t|^{y'_f}/2)\cos(\theta_t|^{y'_f}/2) \right]$$

$$= \frac{(0.817)^3}{3(1.57)} \left[ 3\sin(2\pi/2) - \sin^3(2\pi/2) - 3(2\pi/2)\cos(2\pi/2) \right] = 1.09$$

$$(\bar{z}A)'_f = \Psi_b|^{h'_b} + (y'_f - h'_b)\Omega_b|^{h'_b} + \Psi_{m1}|^{h'_t} + (y'_f - h'_t)\Omega_{m1}|^{h'_t}$$

$$- (y'_f - h'_b)\Omega_{m1}|^{h'_b} + \Psi_{m2}|^{h'_t} + (y'_f - h'_t)\Omega_{m2}|^{h'_t} - (y'_f - h'_b)\Omega_{m2}|^{h'_b}$$

$$+ \Psi_t|^{y'_f} - (y'_f - h'_t)\Omega_t|^{h'_t}$$

$$= (0.000373) + (1 - 0.0458)(0.0203) + (0.0548 - 6.95 \times 10^{-6})$$

$$+ (1 - 0.470)(0.255) - (1 - 0.0458)(0.00288)$$

$$+ (0.0273 - 4.38 \times 10^{-7}) + (1 - 0.470)(0.145)$$

$$- (1 - 0.0458)(0.000227) + (1.09 - 0.465)$$

$$- (1 - 0.470)(0.959) = 0.428$$

Step 2: Calculate upstream Froude number

$$Fr_1 = \frac{Q}{\sqrt{gB^2D^3A_1^3/T_1}}$$

$$= \frac{(4000 \text{ ft}^3/\text{s})}{\sqrt{(32.2 \text{ ft}/\text{s}^2)(157 \text{ in})^2(100 \text{ in})^3(1 \text{ ft}/12 \text{ in})^5(0.641)^3/(0.784)}} = 3.87$$

Since  $Fr_1 > 1$ , the flow is supercritical and a hydraulic jump can occur.

Step 3: Calculate transitional upstream Froude number

$$(Fr_1)_t = \sqrt{\frac{T_1 A'_f [(\bar{z}A)'_f - (\bar{z}A)'_1]}{A_1'^2 (A'_f - A'_1)}} = \sqrt{\frac{(0.784)(0.793)[(0.428) - (0.223)]}{(0.641)^2 (0.793 - 0.641)}} = 1.43$$

Since  $Fr_1 > (Fr_1)_t$ , the jump will be incomplete.

Step 4: Calculate downstream depth

$$y'_2 = 1 + \frac{1}{T_1 A_1'^2} \left\{ Fr_1^2 A_1'^2 (A'_f - A'_1) - T_1 A'_f [(\bar{z}A)'_f - (\bar{z}A)'_1] \right\}$$

$$= 1 + \frac{1}{(0.784)(0.793)^2} \left\{ (3.87)^2 (0.641)^2 (0.793 - 0.641) - (0.784)(0.793)[(0.428) - (0.223)] \right\} = 2.637$$

$$y_2 = y'_2 * D = (2.637)(100 \text{ in})(1 \text{ ft}/12 \text{ in}) = \mathbf{22.0 \text{ ft}}$$

Alternatively,  $y'_2$  may be found from Figure B-15, which was developed for this culvert shape, using the values for  $y'_1$  and  $Fr_1$  calculated in Steps 1 and 2, respectively, as shown below in Figure C-4 on the next page.

### C.5 Example 5: User-Defined Culvert

Determine the subcritical sequent depth of a hydraulic jump in a culvert defined by the coordinates in Table B-2, passing a flow of 3.5 cms at an upstream depth of 0.9 m.

GIVEN:  $Q = 3.5 \text{ cms}$ ,  $y_1 = 0.9 \text{ m}$

FIND:  $y_2$

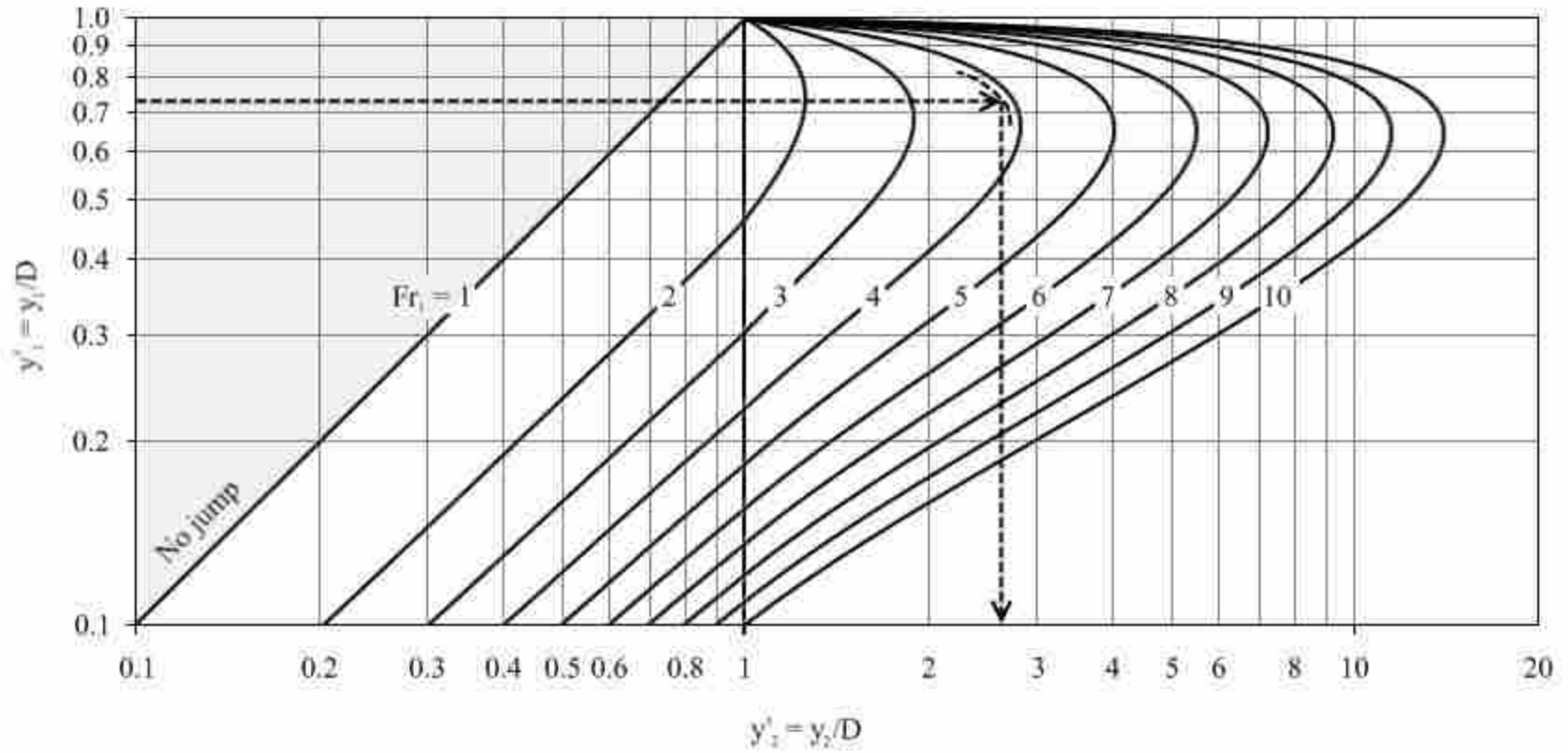


Figure C-4 Graphical solution to Example 4

SOLUTION: (from Figure 12)

*Step 1: Calculate dimensionless parameters*

$$B = x_{i=n} = 1.02 \text{ m}$$

$$D = ((y_t)_i)_{\max} = 1.50 \text{ m}$$

For  $i = 1$ , find dimensionless coordinates of cross section as follows:

$$x'_{i=1} = \frac{x_{i=1}}{B} = \frac{(0.00 \text{ m})}{(1.02 \text{ m})} = 0$$

$$(h'_A)_{i=1} = \frac{1}{D} \min((y_b)_{i=1}, (y_b)_{i=2}) = \frac{\min(0.51 \text{ m}, 0.33 \text{ m})}{(1.50 \text{ m})} = 0.220$$

$$(h'_B)_{i=1} = \frac{1}{D} \max((y_b)_{i=1}, (y_b)_{i=2}) = \frac{\max(0.51 \text{ m}, 0.33 \text{ m})}{(1.50 \text{ m})} = 0.340$$

$$(h'_C)_{i=1} = \frac{1}{D} \min((y_t)_{i=1}, (y_t)_{i=2}) = \frac{\min(0.51 \text{ m}, 0.81 \text{ m})}{(1.50 \text{ m})} = 0.340$$

$$(h'_D)_{i=1} = \frac{1}{D} \max((y_t)_{i=1}, (y_t)_{i=2}) = \frac{\max(0.51 \text{ m}, 0.81 \text{ m})}{(1.50 \text{ m})} = 0.540$$

The dimensionless horizontal coordinates for  $i = 1$  to 17 and dimensionless relative vertical coordinates for  $i = 1$  to 16 are listed in Table C-1 on the next page.

**Table C-1 Dimensionless Coordinates for Example 5**

i	Coordinates			Dimensionless Coordinates				
	x (m)	y <sub>t</sub> (m)	y <sub>b</sub> (m)	x'	h' <sub>A</sub>	h' <sub>B</sub>	h' <sub>C</sub>	h' <sub>D</sub>
1	0.00	0.51	0.51	0.000	0.220	0.340	0.340	0.540
2	0.03	0.81	0.33	0.029	0.147	0.220	0.540	0.667
3	0.09	1.00	0.22	0.088	0.093	0.147	0.667	0.780
4	0.16	1.17	0.14	0.157	0.047	0.093	0.780	0.880
5	0.25	1.32	0.07	0.245	0.020	0.047	0.880	0.940
6	0.32	1.41	0.03	0.314	0.013	0.020	0.940	0.980
7	0.38	1.47	0.02	0.373	0.000	0.013	0.980	0.993
8	0.45	1.49	0.00	0.441	0.000	0.000	0.993	1.000
9	0.51	1.50	0.00	0.500	0.000	0.000	0.993	1.000
10	0.57	1.49	0.00	0.559	0.000	0.013	0.980	0.993
11	0.63	1.47	0.02	0.618	0.013	0.020	0.940	0.980
12	0.69	1.41	0.03	0.676	0.020	0.047	0.880	0.940
13	0.77	1.32	0.07	0.755	0.047	0.093	0.780	0.880
14	0.86	1.17	0.14	0.843	0.093	0.147	0.667	0.780
15	0.93	1.00	0.22	0.912	0.147	0.220	0.540	0.667
16	0.99	0.81	0.33	0.971	0.220	0.340	0.340	0.540
17	1.02	0.51	0.51	1.000	-	-	-	-

The upstream depth ratio is calculated as follows:

$$y'_1 = \frac{y_1}{D} = \frac{(0.9 \text{ m})}{(1.50 \text{ m})} = 0.6$$

For  $i = 1$ , since  $y'_1 > (h'_D)_{i=1}$ , the incremental dimensionless top widths, areas, and centroid-areas at section 1 are calculated as follows:

$$(T'_1)_{i=1} = 0$$

$$\begin{aligned} (A'_1)_{i=1} &= \frac{1}{2}(x'_{i=2} - x'_{i=1})[(h'_D)_{i=1} + (h'_C)_{i=1} - (h'_B)_{i=1} - (h'_A)_{i=1}] \\ &= \frac{1}{2}(0.029 - 0.000)(0.540 + 0.340 - 0.340 - 0.220) = 0.005 \end{aligned}$$

$$\begin{aligned} ((\bar{z}A)')_{i=1} &= \frac{1}{6}(x'_{i=2} - x'_{i=1}) \left[ \begin{array}{l} 3y'_1 ((h'_D)_{i=1} + (h'_C)_{i=1} - (h'_B)_{i=1} - (h'_A)_{i=1}) \\ + ((h'_A)_{i=1})^2 + (h'_A)_{i=1}(h'_B)_{i=1} + (h'_B)_{i=1}^2 \\ - ((h'_C)_{i=1})^2 + (h'_C)_{i=1}(h'_D)_{i=1} + (h'_D)_{i=1}^2 \end{array} \right] \\ &= \frac{1}{6}(0.029 - 0.000) \left[ \begin{array}{l} 3(0.6)(0.540 + 0.340 - 0.340 - 0.220) \\ + ((0.220)^2 + (0.220)(0.340) + (0.340)^2) \\ - ((0.340)^2 + (0.340)(0.540) + (0.540)^2) \end{array} \right] = 0.001 \end{aligned}$$

The incremental dimensionless upstream top widths, areas, and centroid-areas for  $i = 1$  to 16 are listed in Table C-2 on the next page. By summation,  $T'_1$ ,  $A'_1$ , and  $(\bar{z}A)'_1$  are found to be 0.885, 0.514, and 0.140, respectively.

For  $i = 1$ , since  $1 > (h'_D)_{i=1}$ , the incremental dimensionless top widths, areas, and centroid-areas at full conditions are calculated as follows:

$$\begin{aligned} (A'_f)_{i=1} &= \frac{1}{2}(x'_{i+1} - x'_i)[(h'_D)_i + (h'_C)_i - (h'_B)_i - (h'_A)_i] \\ &= \frac{1}{2}(0.029 - 0.000)(0.540 + 0.340 - 0.340 - 0.220) = 0.005 \end{aligned}$$

**Table C-2 Upstream Condition Calculations for Example 5**

i	Dimensionless Relative Coordinates					Upstream Conditions			
	x'	h' <sub>A</sub>	h' <sub>B</sub>	h' <sub>C</sub>	h' <sub>D</sub>	Case	T' <sub>1</sub>	A' <sub>1</sub>	(zA') <sub>1</sub>
1	0.000	0.220	0.340	0.340	0.540	5	0.000	0.005	0.001
2	0.029	0.147	0.220	0.540	0.667	4	0.031	0.024	0.005
3	0.088	0.093	0.147	0.667	0.780	3	0.069	0.033	0.008
4	0.157	0.047	0.093	0.780	0.880	3	0.088	0.047	0.012
5	0.245	0.020	0.047	0.880	0.940	3	0.069	0.039	0.011
6	0.314	0.013	0.020	0.940	0.980	3	0.059	0.034	0.010
7	0.373	0.000	0.013	0.980	0.993	3	0.069	0.041	0.012
8	0.441	0.000	0.000	0.993	1.000	3	0.059	0.035	0.011
9	0.500	0.000	0.000	0.993	1.000	3	0.059	0.035	0.011
10	0.559	0.000	0.013	0.980	0.993	3	0.059	0.035	0.010
11	0.618	0.013	0.020	0.940	0.980	3	0.059	0.034	0.010
12	0.676	0.020	0.047	0.880	0.940	3	0.078	0.044	0.013
13	0.755	0.047	0.093	0.780	0.880	3	0.088	0.047	0.012
14	0.843	0.093	0.147	0.667	0.780	3	0.069	0.033	0.008
15	0.912	0.147	0.220	0.540	0.667	4	0.031	0.024	0.005
16	0.971	0.220	0.340	0.340	0.540	5	0.000	0.005	0.001
17	1.000	-	-	-	-	-	-	-	-
<b>TOTAL</b>						-	<b>0.885</b>	<b>0.514</b>	<b>0.140</b>

$$\begin{aligned}
 ((\bar{z}A)')_{i=1} &= \frac{1}{6}(x'_{i=2} - x'_{i=1}) \left[ \begin{aligned} &3y'_f ((h'_D)_{i=1} + (h'_C)_{i=1} - (h'_B)_{i=1} - (h'_A)_{i=1}) \\ &+ ((h'_A)_{i=1})^2 + (h'_A)_{i=1}(h'_B)_{i=1} + (h'_B)_{i=1}^2 \\ &- ((h'_C)_{i=1})^2 + (h'_C)_{i=1}(h'_D)_{i=1} + (h'_D)_{i=1}^2 \end{aligned} \right] \\
 &= \frac{1}{6}(0.029 - 0.000) \left[ \begin{aligned} &3(1)(0.540 + 0.340 - 0.340 - 0.220) \\ &+ ((0.220)^2 + (0.220)(0.340) + (0.340)^2) \\ &- ((0.340)^2 + (0.340)(0.540) + (0.540)^2) \end{aligned} \right] = 0.003
 \end{aligned}$$



The incremental dimensionless upstream centroid-areas and incremental areas and centroid-areas at full conditions for  $i = 1$  to 16 are listed in Table C-3 below. By summation,  $A'_f$  and  $(\bar{z}A')_f$  are found to be 0.758 and 0.404, respectively.

**Table C-3 Full Condition Calculations for Example 5**

i	Dimensionless Relative Coordinates					Full Conditions		
	x'	h' <sub>A</sub>	h' <sub>B</sub>	h' <sub>C</sub>	h' <sub>D</sub>	Case	A' <sub>f</sub>	(zA') <sub>f</sub>
1	0.000	0.220	0.340	0.340	0.540	5	0.005	0.003
2	0.029	0.147	0.220	0.540	0.667	4	0.025	0.015
3	0.088	0.093	0.147	0.667	0.780	3	0.041	0.024
4	0.157	0.047	0.093	0.780	0.880	3	0.067	0.037
5	0.245	0.020	0.047	0.880	0.940	3	0.060	0.032
6	0.314	0.013	0.020	0.940	0.980	3	0.055	0.028
7	0.373	0.000	0.013	0.980	0.993	3	0.067	0.034
8	0.441	0.000	0.000	0.993	1.000	3	0.059	0.029
9	0.500	0.000	0.000	0.993	1.000	3	0.059	0.029
10	0.559	0.000	0.013	0.980	0.993	3	0.058	0.029
11	0.618	0.013	0.020	0.940	0.980	3	0.055	0.028
12	0.676	0.020	0.047	0.880	0.940	3	0.069	0.036
13	0.755	0.047	0.093	0.780	0.880	3	0.067	0.037
14	0.843	0.093	0.147	0.667	0.780	3	0.041	0.024
15	0.912	0.147	0.220	0.540	0.667	4	0.025	0.015
16	0.971	0.220	0.340	0.340	0.540	5	0.005	0.003
17	1.000	-	-	-	-	-	-	-
<b>TOTAL</b>						-	<b>0.758</b>	<b>0.404</b>

Step 2: Calculate upstream Froude number

$$Fr_1 = \frac{Q}{\sqrt{g B^2 D^3 A'_1{}^3 / T_1}} = \frac{(3.5 \text{ m}^3/\text{s})}{\sqrt{(9.81 \text{ m/s}^2)(1.02 \text{ m})^2 (1.50 \text{ m})^3 (0.514)^3 / (0.885)}} = 1.52$$

Since  $Fr_1 > 1$ , the flow is supercritical and a hydraulic jump can occur.

Step 3: Calculate transitional upstream Froude number

$$(Fr_1)_t = \sqrt{\frac{T_1 A'_f [(\bar{z}A)'_f - (\bar{z}A)'_1]}{A'_1{}^2 (A'_f - A'_1)}} = \sqrt{\frac{(0.885)(0.758)[(0.404) - (0.140)]}{(0.514)^2 (0.758 - 0.514)}} = 1.66$$

Since  $Fr_1 < (Fr_1)_t$ , the jump will be complete.

Step 4: Calculate downstream depth

$$A'_2 = \sum_{i=1}^{n-1} (A'_2)_i$$

$$(\bar{z}A)'_2 = \sum_{i=1}^{n-1} ((\bar{z}A)'_2)_i$$

$$(T_2)_i = \begin{cases} 0 & \text{for } (0 < y'_2 \leq (h'_A)_i) \\ (x'_{i+1} - x'_i) \left( \frac{y'_2 - (h'_A)_i}{(h'_B)_i - (h'_A)_i} \right) & \text{for } ((h'_A)_i < y'_2 \leq (h'_B)_i) \\ x'_{i+1} - x'_i & \text{for } ((h'_B)_i < y'_2 \leq (h'_C)_i) \\ (x'_{i+1} - x'_i) \left( \frac{(h'_D)_i - y'_2}{(h'_D)_i - (h'_C)_i} \right) & \text{for } ((h'_C)_i < y'_2 \leq (h'_D)_i) \\ 0 & \text{for } ((h'_D)_i < y'_2) \end{cases}$$

$$(A'_2)_i = \begin{cases} 0 & \text{for } (0 < y'_2 \leq (h'_A)_i) \\ \frac{1}{2}(T_2)_i(y'_2 - (h'_A)_i) & \text{for } ((h'_A)_i < y'_2 \leq (h'_B)_i) \\ \frac{1}{2}(T_2)_i[(y'_2 - (h'_A)_i) + (y'_2 - (h'_B)_i)] & \text{for } ((h'_B)_i < y'_2 \leq (h'_C)_i) \\ \frac{1}{2} \left\{ (x'_{i+1} - x'_i) [(y'_2 - (h'_A)_i) + (y'_2 - (h'_B)_i)] \right. \\ \left. - (x'_{i+1} - x'_i - (T_2)_i)(y'_2 - (h'_C)_i) \right\} & \text{for } ((h'_C)_i < y'_2 \leq (h'_D)_i) \\ \frac{1}{2}(x'_{i+1} - x'_i) \begin{bmatrix} (h'_D)_i + (h'_C)_i \\ -(h'_B)_i - (h'_A)_i \end{bmatrix} & \text{for } ((h'_D)_i < y'_2) \end{cases}$$

$$((\bar{z}A)'_2)_i = \begin{cases} 0 & \text{for } (0 < y'_2 \leq (h'_A)_i) \\ \frac{1}{6}(T_2)_i(y'_2 - (h'_A)_i)^2 & \text{for } ((h'_A)_i < y'_2 \leq (h'_B)_i) \\ \frac{1}{6}(T_2)_i \begin{bmatrix} (y'_2 - (h'_A)_i)^2 \\ + (y'_2 - (h'_A)_i)(y'_2 - (h'_B)_i) \\ + (y'_2 - (h'_B)_i)^2 \end{bmatrix} & \text{for } ((h'_B)_i < y'_2 \leq (h'_C)_i) \\ \frac{1}{6} \left\{ (x'_{i+1} - x'_i) \begin{bmatrix} (y'_2 - (h'_A)_i)^2 \\ + (y'_2 - (h'_A)_i) \\ \times (y'_2 - (h'_B)_i) \\ + (y'_2 - (h'_B)_i)^2 \end{bmatrix} \right. \\ \left. - (x'_{i+1} - x'_i - (T_2)_i)(y'_2 - (h'_C)_i)^2 \right\} & \text{for } ((h'_C)_i < y'_2 \leq (h'_D)_i) \\ \frac{1}{6}(x'_{i+1} - x'_i) + \begin{bmatrix} 3y'_2 \begin{pmatrix} (h'_D)_i + (h'_C)_i \\ -(h'_B)_i - (h'_A)_i \end{pmatrix} \\ \begin{pmatrix} (h'_A)_i^2 \\ + (h'_A)_i(h'_B)_i \\ + (h'_B)_i^2 \end{pmatrix} \\ - \begin{pmatrix} (h'_C)_i^2 \\ + (h'_C)_i(h'_D)_i \\ + (h'_D)_i^2 \end{pmatrix} \end{bmatrix} & \text{for } ((h'_D)_i < y'_2) \end{cases}$$

$$Fr_1^2 = \frac{T_1 A'_2 [(\bar{z}A)'_2 - (\bar{z}A)'_1]}{A_1'^2 (A'_2 - A'_1)} \Rightarrow (1.53)^2 = \frac{(0.885)A'_2 [(\bar{z}A)'_2 - (0.140)]}{(0.514)^2 (A'_2 - (0.514))}$$

Solving these equations iteratively yields  $y'_2 = 0.928$

$$y_2 = y'_2 * D = (0.928)(1.50 \text{ m}) = \mathbf{1.39 \text{ m}}$$

Alternatively,  $y'_2$  may be found from Figure B-21, which was developed for this user-defined shape, using the values for  $y'_1$  and  $Fr_1$  calculated in Steps 1 and 2, respectively, as shown below in Figure C-5 on the next page.

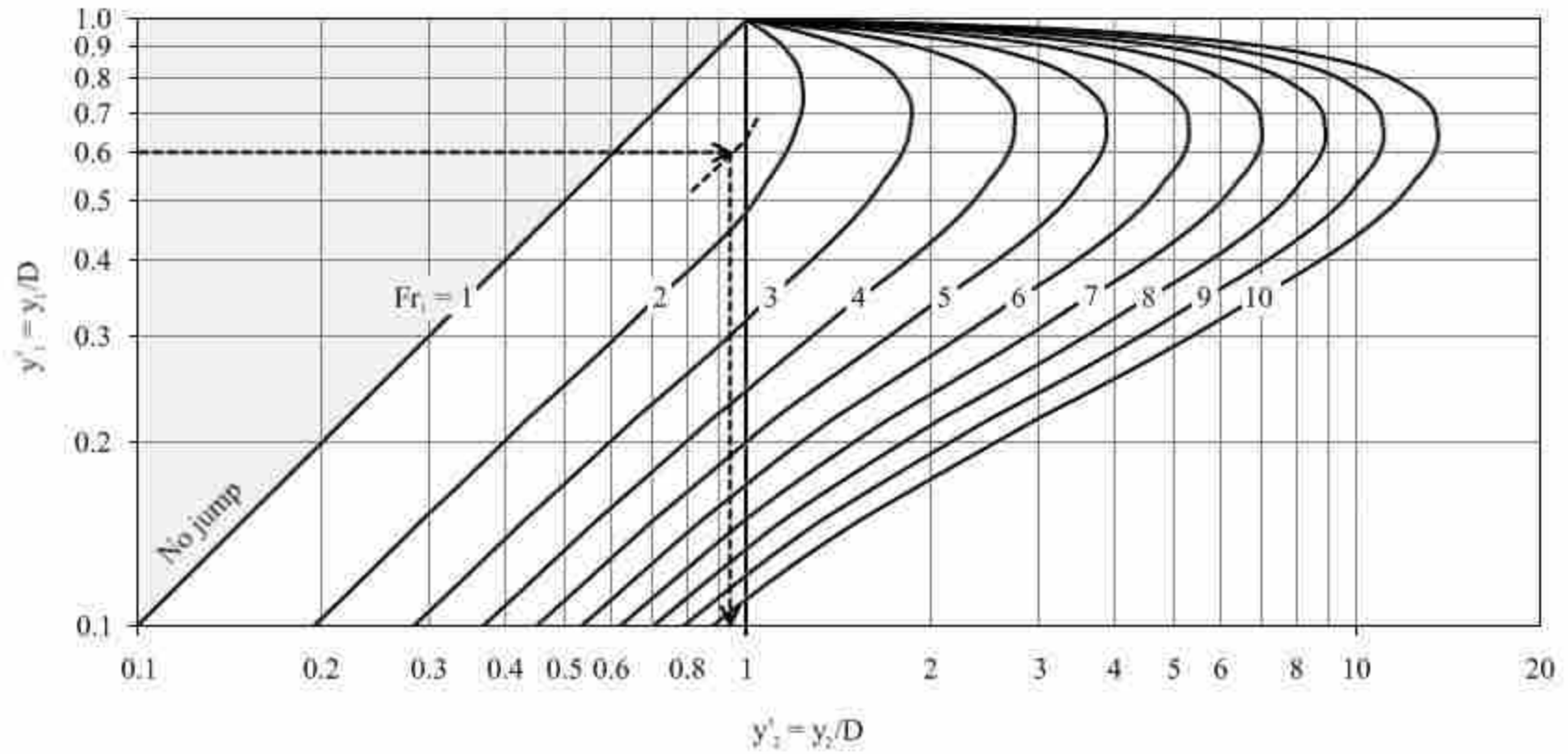


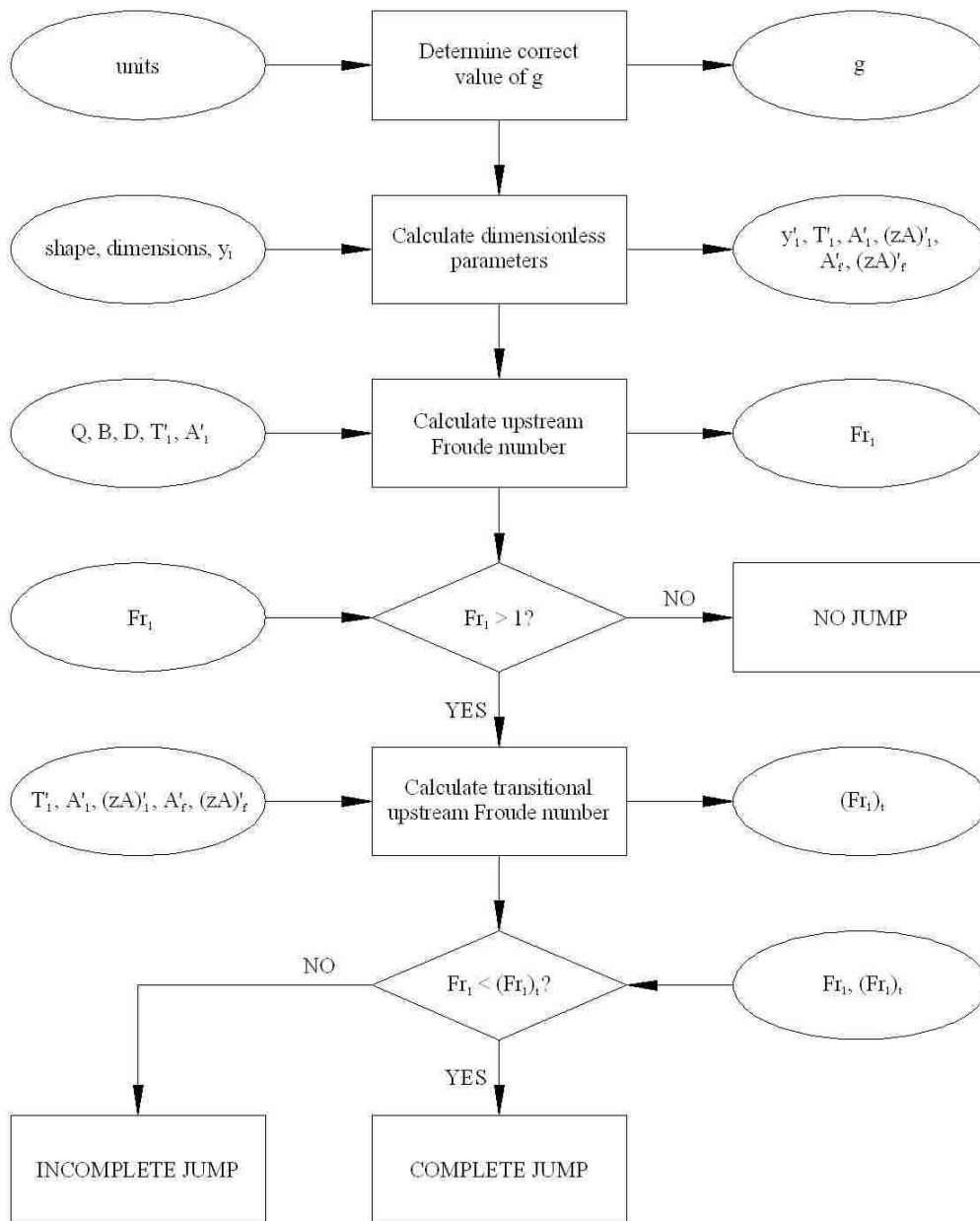
Figure C-5 Graphical solution to Example 5

## **Appendix D. Computer Implementation**

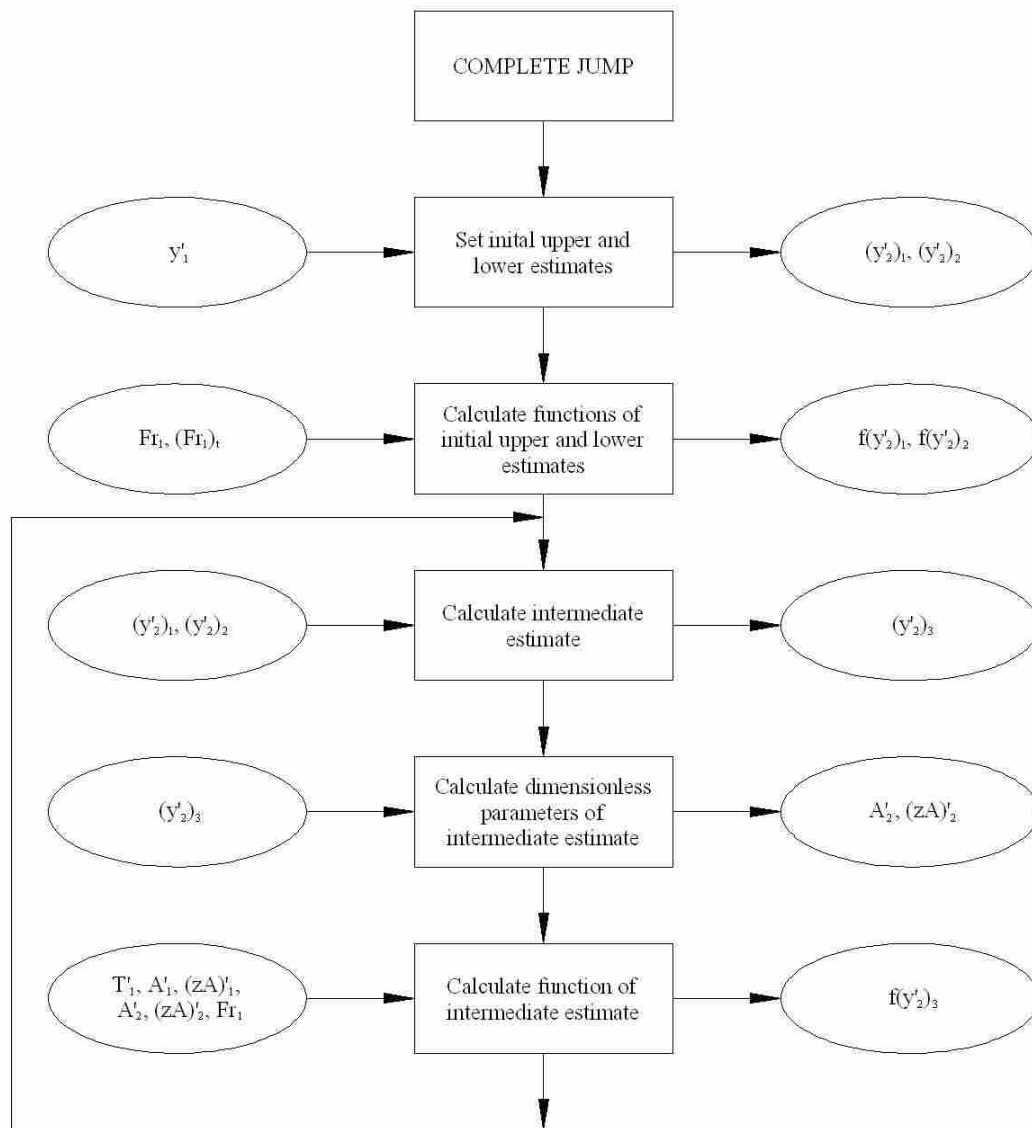
The solutions presented in this study may be solved by hand calculations, but as these tend to be tedious and prone to error, automation is preferable. This appendix therefore presents the logic and Visual Basic code that may be used within Microsoft Excel to compute the solutions for each shape.

### **D.1 General Logic**

The general logic for computing the subcritical sequent depth is displayed in Figures D-1 through D-4 below. This logic follows the solution steps given in Chapter 4, and may be adapted to any of the conduit shapes of this study, with the exception of rectangular conduits which are treated somewhat differently due to their simple, explicit solutions. As shown in Figure D-2, the interval halving method is used for complete jumps to iteratively compute the subcritical sequent depth.

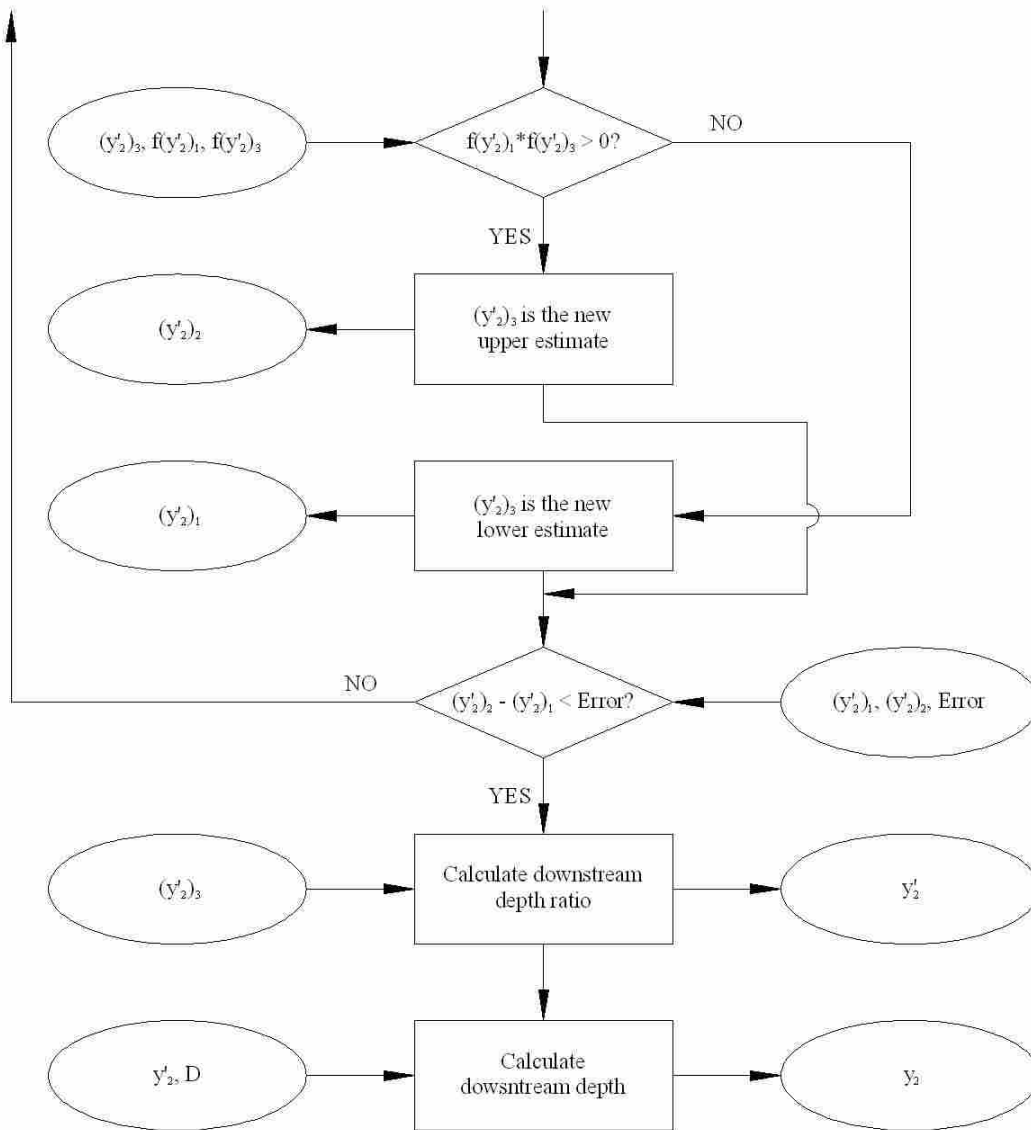


**Figure D-1 General logic for sequent depth calculation**

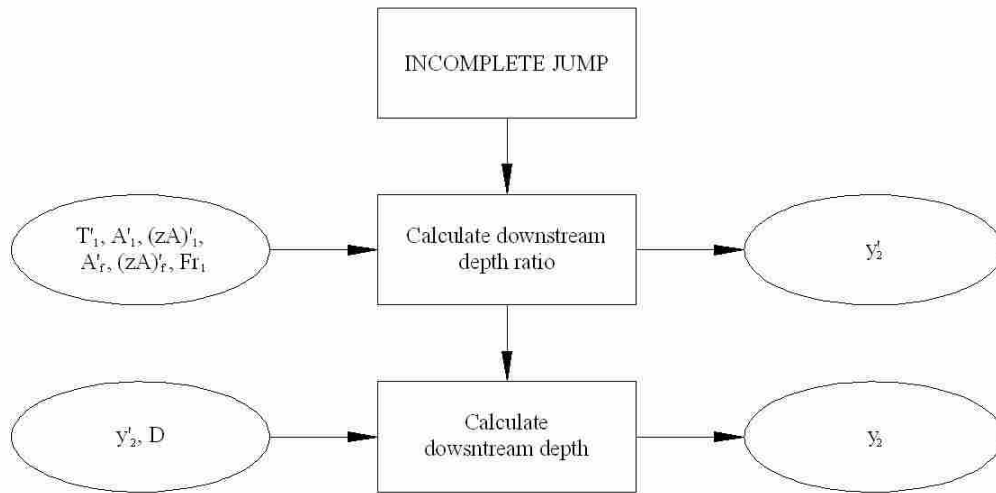


**Figure D-2 General logic for complete jumps**

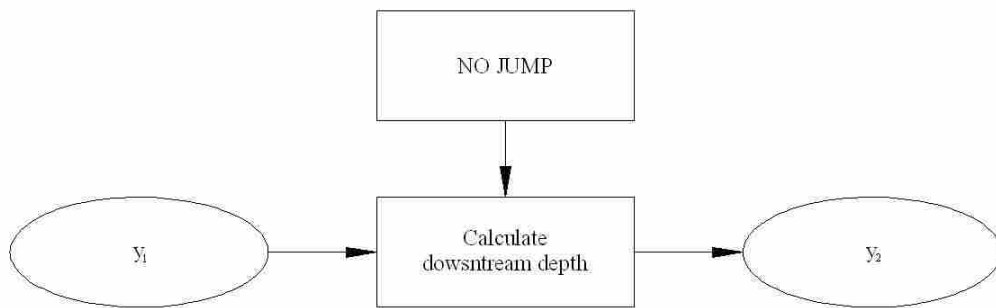




**Figure D-2 (cont.) General logic for complete jumps**



**Figure D-3 General logic for incomplete jumps**



**Figure D-4 General logic for no jump**

## D.2 Rectangular Conduits

'Returns y2 value for given rectangular dimensions, Q, and y1  
Public Function Rectangular\_y2(B As Double, D As Double, Q As Double, \_  
y1 As Double, units As String)

```
    '**Absolute Variables**
    Dim g As Double 'Acceleration due to gravity

    Dim y1_prime As Double 'Upstream depth ratio
    Dim T1_prime As Double 'Upstream dimensionless top width
    Dim A1_prime As Double 'Upstream dimensionless area

    Dim Fr1 As Double 'Upstream Froude number
    Dim Fr1_t As Double 'Transitional upstream Froude number

    Dim y2_prime As Double 'Downstream depth ratio

    'Determine correct value of g
    If units = "BG" Then 'English units
        g = 32.21
    ElseIf units = "SI" Then 'International units
        g = 9.81
    End If

    'Step 1: Calculate dimensionless parameters
    y1_prime = y1 / D
    T1_prime = Rectangular_T_prime(y1_prime)
    A1_prime = Rectangular_A_prime(y1_prime)

    'Step 2: Calculate upstream Froude number
    Fr1 = Q / Sqr(g * B ^ 2 * D ^ 3 * A1_prime ^ 3 / T1_prime)

    If Fr1 <= 1 Then 'No Jump
        Rectangular_y2 = y1
    Else 'Jump may occur

        'Step 3: Calculate transitional upstream Froude number
        Fr1_t = Sqr((1 + y1_prime) / (2 * y1_prime ^ 2))

        'Step 4: Calculate downstream depth
        If Fr1 < Fr1_t Then 'Complete jump
            y2_prime = 0.5 * y1_prime * (Sqr(1 + 8 * Fr1 ^ 2) - 1)
        Else 'Incomplete jump
            y2_prime = 0.5 + (Fr1 ^ 2 + 0.5) * y1_prime ^ 2 _
                - Fr1 ^ 2 * y1_prime ^ 3

        End If

        Rectangular_y2 = y2_prime * D
    End If

End Function

'Returns T' = T/B value for given y' value
Public Function Rectangular_T_prime(y_prime As Double) As Double

    Rectangular_T_prime = 1
```

```

End Function

'Returns A' = A/BD value for given y' value
Public Function Rectangular_A_prime(y_prime As Double) As Double

    Rectangular_A_prime = y_prime

End Function

'Returns (zA)' = zA/BD^2 value for given y' value
Public Function Rectangular_zA_prime(y_prime As Double) As Double

    Rectangular_zA_prime = 1 / 2 * y_prime ^ 2

End Function

```

### D.3 Circular Conduits

```

'Returns y2 value for given circular dimensions, Q, and y1
Public Function Circular_y2(D As Double, Q As Double, y1 As Double, _
units As String)

    '**Absolute Variables**
    Dim g As Double 'Acceleration due to gravity

    Dim y1_prime As Double 'Upstream depth ratio
    Dim T1_prime As Double 'Upstream dimensionless top width
    Dim A1_prime As Double 'Upstream dimensionless area
    Dim zA1_prime As Double 'Upstream dimensionless centroid-area

    Dim Af_prime As Double 'Full conditions dimensionless area
    Dim zAf_prime As Double 'Full conditions dimensionless
        'centroid-area

    Dim y2_prime As Double 'Downstream depth ratio
    Dim A2_prime As Double 'Downstream dimensionless area
    Dim zA2_prime As Double 'Downstream dimensionless centroid-area

    Dim Fr1 As Double 'Upstream Froude number
    Dim Fr1_t As Double 'Transitional upstream Froude number

    '**Iterative variables** (interval halving method)
    Dim y2_prime1 As Double 'Lower estimate
    Dim f1 As Double 'Function at lower estimate

    Dim y2_prime2 As Double 'Upper estimate
    Dim f2 As Double 'Function at upper estimate

    Dim y2_prime3 As Double 'Intermediate estimate
    Dim f3 As Double 'Function at intermediate estimate

    Dim Error As Double 'Allowable error in y'2
    Error = 0.00001

    'Determine correct value of g
    If units = "BG" Then 'English units
        g = 32.21
    ElseIf units = "SI" Then 'International units
        g = 9.81
    End If

```

```

'Step 1: Calculate dimensionless parameters
y1_prime = y1 / D
T1_prime = Circular_T_prime(y1_prime)
A1_prime = Circular_A_prime(y1_prime)
zA1_prime = Circular_zA_prime(y1_prime)

Af_prime = Circular_A_prime(1)
zAf_prime = Circular_zA_prime(1)

'Step 2: Calculate upstream Froude number
Fr1 = Q / Sqr(g * D ^ 5 * A1_prime ^ 3 / T1_prime)

If Fr1 <= 1 Then 'No Jump
    Circular_y2 = y1
Else 'Jump may occur

'Step 3: Calculate transitional upstream Froude number
Fr1_t = Sqr((T1_prime * Af_prime / A1_prime ^ 2)
    * (zAf_prime - zA1_prime) / (Af_prime - A1_prime))

'Step 4: Calculate downstream depth
If Fr1 < Fr1_t Then 'Complete jump

    y2_prime1 = y1_prime 'Lower Limit
    f1 = 1 - Fr1 ^ 2

    y2_prime2 = 1 'Upper Limit
    f2 = Fr1_t ^ 2 - Fr1 ^ 2

    Do

        y2_prime3 = (y2_prime1 + y2_prime2) / 2
        A2_prime = Circular_A_prime(y2_prime3)
        zA2_prime = Circular_zA_prime(y2_prime3)
        f3 = (T1_prime * A2_prime / A1_prime ^ 2)
            * (zA1_prime - zA2_prime) / (A1_prime - A2_prime) -
            Fr1 ^ 2

        If f1 * f3 > 0 Then 'y2_prime3 is new upper estimate
            y2_prime1 = y2_prime3
            f1 = f3
        Else 'y2_prime3 is new lower estimate
            y2_prime2 = y2_prime3
            f2 = f3
        End If

    Loop Until y2_prime2 - y2_prime1 < Error

    y2_prime = y2_prime3

Else 'Incomplete jump

    y2_prime = (Fr1 ^ 2 * A1_prime ^ 2 -
        * (Af_prime - A1_prime) -
        - T1_prime * Af_prime -
        * (zAf_prime - zA1_prime))
        / (T1_prime * Af_prime ^ 2) + 1

End If

Circular_y2 = y2_prime * D

```

```

End If

End Function

'Returns T' = T/B value for given y' value
Public Function Circular_T_prime(y_prime As Double) As Double

    Dim theta As Double 'Internal flow angle
    theta = 2 * Application.Acos(1 - 2 * y_prime)

    Circular_T_prime = Sin(theta / 2)

End Function

'Returns A' = A/BD value for given y' value
Public Function Circular_A_prime(y_prime As Double) As Double

    Dim theta As Double 'Internal flow angle
    theta = 2 * Application.Acos(1 - 2 * y_prime)

    Circular_A_prime = 1 / 8 * (theta - Sin(theta))

End Function

'Returns (zA)' = zA/BD^2 value for given y' value
Public Function Circular_zA_prime(y_prime As Double) As Double

    Dim theta As Double 'Internal flow angle
    theta = 2 * Application.Acos(1 - 2 * y_prime)

    Circular_zA_prime = (3 * Sin(theta / 2) - Sin(theta / 2) ^ 3 -
        - 3 * (theta / 2) * Cos(theta / 2)) / 24

End Function

```

#### **D.4 Elliptical Conduits (Simple)**

```

'Returns y2 value for given Elliptical dimensions, Q, and y1
Public Function Elliptical_y2_simple(B As Double, D As Double, Q
    Q As Double, y1 As Double, units As String)

    '**Absolute Variables**
    Dim g As Double 'Acceleration due to gravity

    Dim y1_prime As Double 'Upstream depth ratio
    Dim T1_prime As Double 'Upstream dimensionless top width
    Dim A1_prime As Double 'Upstream dimensionless area
    Dim zA1_prime As Double 'Upstream dimensionless centroid-area

    Dim yf_prime As Double 'Full conditions depth ratio
    Dim Af_prime As Double 'Full conditions dimensionless area
    Dim zAf_prime As Double 'Full conditions dimensionless
        'centroid-area

    Dim y2_prime As Double 'Downstream depth ratio
    Dim A2_prime As Double 'Downstream dimensionless area
    Dim zA2_prime As Double 'Downstream dimensionless centroid-area

    Dim Fr1 As Double 'Upstream Froude number
    Dim Fr1_t As Double 'Transitional upstream Froude number

```

```


***Iterative variables*** (interval halving method)
Dim y2_prime1 As Double 'Lower estimate
Dim f1 As Double 'Function at lower estimate

Dim y2_prime2 As Double 'Upper estimate
Dim f2 As Double 'Function at upper estimate

Dim y2_prime3 As Double 'Intermediate estimate
Dim f3 As Double 'Function at intermediate estimate

Dim Error As Double 'Allowable error in y'2
Error = 0.00001

'Determine correct value of g
If units = "BG" Then 'English units
    g = 32.21
ElseIf units = "SI" Then 'International units
    g = 9.81
End If

'Step 1: Calculate dimensionless parameters
y1_prime = y1 / D
T1_prime = Elliptical_T_prime_simple(y1_prime)
A1_prime = Elliptical_A_prime_simple(y1_prime)
zA1_prime = Elliptical_zA_prime_simple(y1_prime)

Af_prime = Elliptical_A_prime_simple(1)
zAf_prime = Elliptical_zA_prime_simple(1)

'Step 2: Calculate upstream Froude number
Fr1 = Q / Sqr(g * B ^ 2 * D ^ 3 * A1_prime ^ 3 / T1_prime)

If Fr1 <= 1 Then 'No Jump
    Elliptical_y2_simple = y1
Else 'Jump may occur

'Step 3: Calculate transitional upstream Froude number
Fr1_t = Sqr((T1_prime * Af_prime / A1_prime ^ 2) _
    * (zAf_prime - zA1_prime) / (Af_prime - A1_prime))

'Step 4: Calculate downstream depth
If Fr1 < Fr1_t Then 'Complete jump

    y2_prime1 = y1_prime 'Lower Limit
    f1 = 1 - Fr1 ^ 2

    y2_prime2 = 1 'Upper Limit
    f2 = Fr1_t ^ 2 - Fr1 ^ 2

    Do

        y2_prime3 = (y2_prime1 + y2_prime2) / 2
        A2_prime = Elliptical_A_prime_simple(y2_prime3)
        zA2_prime = Elliptical_zA_prime_simple(y2_prime3)
        f3 = (T1_prime * A2_prime / A1_prime ^ 2) _
            * (zA1_prime - zA2_prime) / (A1_prime - A2_prime) _
            - Fr1 ^ 2

        If f1 * f3 > 0 Then 'y2_prime3 is new upper estimate
            y2_prime1 = y2_prime3
            f1 = f3


```

```

        Else 'y2_prime3 is new lower estimate
            y2_prime2 = y2_prime3
            f2 = f3
        End If

        Loop Until y2_prime2 - y2_prime1 < Error

        y2_prime = y2_prime3

    Else 'Incomplete jump

        y2_prime = (Fr1 ^ 2 * A1_prime ^ 2 _
            * (Af_prime - A1_prime) _
            - T1_prime * Af_prime _
            * (zAf_prime - zA1_prime))
            / (T1_prime * Af_prime ^ 2) + 1

        End If

        Elliptical_y2_simple = y2_prime * D

    End If

End Function

'Returns T' = T/B value for given y' value
Public Function Elliptical_T_prime_simple(y_prime As Double) As Double

    Elliptical_T_prime_simple = 2 * Sqr(y_prime - y_prime ^ 2)

End Function

'Returns A' = A/BD value for given y' value
Public Function Elliptical_A_prime_simple(y_prime As Double) As Double

    Dim T_prime As Double 'Dimensionless top width (T/B)
    T_prime = Elliptical_T_prime_simple(y_prime)

    Elliptical_A_prime_simple = (Application.Acos(1 - 2 * y_prime) _
        - T_prime * (1 - 2 * y_prime)) / 4

End Function

'Returns (zA)' = zA/BD^2 value for given y' value
Public Function Elliptical_zA_prime_simple(y_prime As Double) As Double

    Dim T_prime As Double
    Dim A_prime As Double
    T_prime = Elliptical_T_prime_simple(y_prime)
    A_prime = Elliptical_A_prime_simple(y_prime)

    Elliptical_zA_prime_simple = 1 / 12 * (T_prime ^ 3 _
        - 6 * (1 - 2 * y_prime) * A_prime)

End Function

```



## D.5 Elliptical Conduits (Complex)

'Returns y2 value for given Elliptical dimensions, Q, and y1  
Public Function Elliptical\_y2\_complex(B As Double, D As Double, Rb As Double, Rm As Double, Q As Double, y1 As Double, units As String)

```
    '**Absolute Variables**
    Dim g As Double 'Acceleration due to gravity

    Dim Rt As Double
    Dim hb As Double 'Bottom transition height
    Dim hm As Double 'Neutral axis height
    Dim ht As Double 'Top transition height

    Dim B_prime As Double 'Dimensionless span
    Dim Rb_prime As Double 'Dimensionless bottom radius
    Dim Rm_prime As Double 'Dimensionless middle radius
    Dim Rt_prime As Double 'Dimensionless top radius
    Dim hb_prime As Double 'Dimensionless bottom transition height
    Dim hm_prime As Double 'Dimensionless neutral axis height
    Dim ht_prime As Double 'Dimensionless top transition height

    Dim y1_prime As Double 'Upstream depth ratio
    Dim T1_prime As Double 'Upstream dimensionless top width
    Dim A1_prime As Double 'Upstream dimensionless area
    Dim zA1_prime As Double 'Upstream dimensionless centroid-area

    Dim yf_prime As Double 'Full conditions depth ratio
    Dim Af_prime As Double 'Full conditions dimensionless area
    Dim zAf_prime As Double 'Full conditions dimensionless
        'centroid-area

    Dim y2_prime As Double 'Downstream depth ratio
    Dim A2_prime As Double 'Downstream dimensionless area
    Dim zA2_prime As Double 'Downstream dimensionless centroid-area

    Dim Fr1 As Double 'Upstream Froude number
    Dim Fr1_t As Double 'Transitional upstream Froude number

    '**Iterative variables** (interval halving method)
    Dim y2_prime1 As Double 'Lower estimate
    Dim f1 As Double 'Function at lower estimate

    Dim y2_prime2 As Double 'Upper estimate
    Dim f2 As Double 'Function at upper estimate

    Dim y2_prime3 As Double 'Intermediate estimate
    Dim f3 As Double 'Function at intermediate estimate

    Dim Error As Double 'Allowable error in y'2
    Error = 0.00001

    'Determine correct value of g
    If units = "BG" Then 'English units
        g = 32.21
    ElseIf units = "SI" Then 'International units
        g = 9.81
    End If

    'Calculate remaining shape parameters
    Rt = Rb
    hm = D / 2
    Rm = 1 / 2 * (Rb + B / 2 - (Rb - D / 2) ^ 2 / (Rb - B / 2))
    hb = Rb * (hm - Rm) / (Rb - Rm)
```

```

ht = D - hb

'Step 1: Calculate dimensionless parameters
B_prime = B / D
Rb_prime = Rb / D
Rm_prime = Rm / D
Rt_prime = Rt / D
hb_prime = hb / D
hm_prime = hm / D
ht_prime = ht / D

y1_prime = y1 / D
T1_prime = Elliptical_T_prime_complex(B_prime, Rb_prime, _
    Rm_prime, Rt_prime, hb_prime, hm_prime, ht_prime, _
    y1_prime)
A1_prime = Elliptical_A_prime_complex(B_prime, Rb_prime, _
    Rm_prime, Rt_prime, hb_prime, hm_prime, ht_prime, _
    y1_prime)
zA1_prime = Elliptical_zA_prime_complex(B_prime, Rb_prime, _
    Rm_prime, Rt_prime, hb_prime, hm_prime, ht_prime, _
    y1_prime)

Af_prime = Elliptical_A_prime_complex(B_prime, Rb_prime, _
    Rm_prime, Rt_prime, hb_prime, hm_prime, ht_prime, 1)
zAf_prime = Elliptical_zA_prime_complex(B_prime, Rb_prime, _
    Rm_prime, Rt_prime, hb_prime, hm_prime, ht_prime, 1)

'Step 2: Calculate upstream Froude number
Fr1 = Q / Sqr(g * B ^ 2 * D ^ 3 * A1_prime ^ 3 / T1_prime)

If Fr1 <= 1 Then 'No Jump
    Elliptical_y2_complex = y1
Else 'Jump may occur

'Step 3: Calculate transitional upstream Froude number
Fr1_t = Sqr((T1_prime * Af_prime / A1_prime ^ 2) _
    * (zAf_prime - zA1_prime) / (Af_prime - A1_prime))

'Step 4: Calculate downstream depth
If Fr1 < Fr1_t Then 'Complete jump

    y2_prime1 = y1_prime 'Lower Limit
    f1 = 1 - Fr1 ^ 2

    y2_prime2 = 1 'Upper Limit
    f2 = Fr1_t ^ 2 - Fr1 ^ 2

Do

    y2_prime3 = (y2_prime1 + y2_prime2) / 2
    A2_prime = Elliptical_A_prime_complex(B_prime, _
        Rb_prime, Rm_prime, Rt_prime, hb_prime, _
        hm_prime, ht_prime, y2_prime3)
    zA2_prime = Elliptical_zA_prime_complex(B_prime, _
        Rb_prime, Rm_prime, Rt_prime, hb_prime, _
        hm_prime, ht_prime, y2_prime3)
    f3 = (T1_prime * A2_prime / A1_prime ^ 2) _
        * (zA1_prime - zA2_prime) _
        / (A1_prime - A2_prime) - Fr1 ^ 2

    If f1 * f3 > 0 Then 'y2_prime3 is new upper estimate
        y2_prime1 = y2_prime3

```

```

        f1 = f3
    Else 'y2_prime3 is new lower estimate
        y2_prime2 = y2_prime3
        f2 = f3
    End If

    Loop Until y2_prime2 - y2_prime1 < Error

    y2_prime = y2_prime3

Else 'Incomplete jump

    y2_prime = (Fr1 ^ 2 * A1_prime ^ 2 _
        * (Af_prime - A1_prime) _
        - T1_prime * Af_prime _
        * (zAf_prime - zA1_prime)) _
        / (T1_prime * Af_prime ^ 2) + 1

End If

    Elliptical_y2_complex = y2_prime * D

End If

End Function

'Returns T' = T/B value for given pipe arch parameters and y' value
Public Function Elliptical_T_prime_complex(B_prime As Double, _
Rb_prime As Double, Rm_prime As Double, Rt_prime As Double, _
hb_prime As Double, hm_prime As Double, ht_prime As Double, _
y_prime As Double) As Double

    Dim Tb_prime As Double
    Dim Tm1_prime As Double
    Dim Tm2_prime As Double
    Dim Tt_prime As Double

    If y_prime <= hb_prime Then

        Tb_prime = Elliptical_Tb_prime(B_prime, Rb_prime, y_prime)

    ElseIf y_prime <= ht_prime Then

        Tm1_prime = Elliptical_Tm1_prime(B_prime, Rm_prime, hm_prime, _
            y_prime)
        Tm2_prime = Elliptical_Tm2_prime(B_prime, Rm_prime, hm_prime, _
            y_prime)

    ElseIf y_prime <= 1 Then

        Tt_prime = Elliptical_Tt_prime(B_prime, Rt_prime, y_prime)

    End If

    Elliptical_T_prime_complex = Tb_prime + Tm1_prime + Tm2_prime _
        + Tt_prime

End Function

'Returns A' = A/BD value for given pipe arch parameters and y' value
Public Function Elliptical_A_prime_complex(B_prime As Double, _
Rb_prime As Double, Rm_prime As Double, Rt_prime As Double, _
hb_prime As Double, hm_prime As Double, ht_prime As Double, _
y_prime As Double) As Double

```

```

Dim Ab_prime As Double
Dim Am1_prime As Double
Dim Am2_prime As Double
Dim At_prime As Double

If y_prime <= hb_prime Then

    Ab_prime = Elliptical_Ab_prime(B_prime, Rb_prime, y_prime)

ElseIf y_prime <= ht_prime Then

    Ab_prime = Elliptical_Ab_prime(B_prime, Rb_prime, hb_prime)
    Am1_prime = Elliptical_Am1_prime(B_prime, Rm_prime, hm_prime, _
        y_prime)
        - Elliptical_Am1_prime(B_prime, Rm_prime, hm_prime, _
        hb_prime)
    Am2_prime = Elliptical_Am2_prime(B_prime, Rm_prime, hm_prime, _
        y_prime)
        - Elliptical_Am2_prime(B_prime, Rm_prime, hm_prime, _
        hb_prime)

ElseIf y_prime <= 1 Then

    Ab_prime = Elliptical_Ab_prime(B_prime, Rb_prime, hb_prime)
    Am1_prime = Elliptical_Am1_prime(B_prime, Rm_prime, hm_prime, _
        ht_prime)
        - Elliptical_Am1_prime(B_prime, Rm_prime, hm_prime, _
        hb_prime)
    Am2_prime = Elliptical_Am2_prime(B_prime, Rm_prime, hm_prime, _
        ht_prime)
        - Elliptical_Am2_prime(B_prime, Rm_prime, hm_prime, _
        hb_prime)
    At_prime = Elliptical_At_prime(B_prime, Rt_prime, y_prime) _
        - Elliptical_At_prime(B_prime, Rt_prime, ht_prime)

End If

Elliptical_A_prime_complex = Ab_prime + Am1_prime + Am2_prime _
    + At_prime

End Function

'Returns (zA)' = zA/BD^2 value for given pipe arch parameters and y'
Public Function Elliptical_zA_prime_complex(B_prime As Double, _
    Rb_prime As Double, Rm_prime As Double, Rt_prime As Double, _
    hb_prime As Double, hm_prime As Double, ht_prime As Double, _
    y_prime As Double) As Double

```

```

    Dim zAb_prime As Double
    Dim zAm1_prime As Double
    Dim zAm2_prime As Double
    Dim zAt_prime As Double

    If y_prime <= hb_prime Then

        zAb_prime = Elliptical_zAb_prime(B_prime, Rb_prime, y_prime)

    ElseIf y_prime <= ht_prime Then

        zAb_prime = Elliptical_zAb_prime(B_prime, Rb_prime, hb_prime) _
            + (y_prime - hb_prime) _
            * Elliptical_Ab_prime(B_prime, Rb_prime, hb_prime)
        zAm1_prime = Elliptical_zAm1_prime(B_prime, Rm_prime, _

```

```

        hm_prime, y_prime) _
    - Elliptical_zAm1_prime(B_prime, Rm_prime, _
      hm_prime, hb_prime) _
    - (y_prime - hb_prime) _
    * Elliptical_Am1_prime(B_prime, Rm_prime, _
      hm_prime, hb_prime) _
zAm2_prime = Elliptical_zAm2_prime(B_prime, Rm_prime, _
      hm_prime, y_prime) _
    - Elliptical_zAm2_prime(B_prime, Rm_prime, _
      hm_prime, hb_prime) _
    - (y_prime - hb_prime) _
    * Elliptical_Am2_prime(B_prime, Rm_prime, _
      hm_prime, hb_prime) _

ElseIf y_prime <= 1 Then

    zAb_prime = Elliptical_zAb_prime(B_prime, Rb_prime, hb_prime) _
      + (y_prime - hb_prime) _
    * Elliptical_Ab_prime(B_prime, Rb_prime, hb_prime) _
zAm1_prime = Elliptical_zAm1_prime(B_prime, Rm_prime, _
      hm_prime, ht_prime) _
    - Elliptical_zAm1_prime(B_prime, Rm_prime, _
      hm_prime, hb_prime) _
    + (y_prime - ht_prime) _
    * Elliptical_Am1_prime(B_prime, Rm_prime, _
      hm_prime, ht_prime) _
    - (y_prime - hb_prime) _
    * Elliptical_Am1_prime(B_prime, Rm_prime, _
      hm_prime, hb_prime) _
zAm2_prime = Elliptical_zAm2_prime(B_prime, Rm_prime, _
      hm_prime, ht_prime) _
    - Elliptical_zAm2_prime(B_prime, Rm_prime, _
      hm_prime, hb_prime) _
    + (y_prime - ht_prime) _
    * Elliptical_Am2_prime(B_prime, Rm_prime, _
      hm_prime, ht_prime) _
    - (y_prime - hb_prime) _
    * Elliptical_Am2_prime(B_prime, Rm_prime, _
      hm_prime, hb_prime) _
zAt_prime = Elliptical_zAt_prime(B_prime, Rt_prime, y_prime) _
    - Elliptical_zAt_prime(B_prime, Rt_prime, ht_prime) _
    - (y_prime - ht_prime) _
    * Elliptical_At_prime(B_prime, Rt_prime, ht_prime) _

End If

Elliptical_zA_prime_complex = zAb_prime + zAm1_prime _
      + zAm2_prime + zAt_prime _

End Function

'Bottom section functions
Function Elliptical_Tb_prime(B_prime As Double, Rb_prime As Double, _
  y_prime As Double) As Double

    Dim theta_b As Double
    theta_b = 2 * Application.Acos(1 - y_prime / Rb_prime)

    Elliptical_Tb_prime = 2 * Rb_prime / B_prime * Sin(theta_b / 2)

End Function

Function Elliptical_Ab_prime(B_prime As Double, Rb_prime As Double, _
  y_prime As Double) As Double

```

```

Dim theta_b As Double
theta_b = 2 * Application.Acos(1 - y_prime / Rb_prime)

Elliptical_Ab_prime = Rb_prime ^ 2 / (2 * B_prime) _
                    * (theta_b - Sin(theta_b))

End Function

Function Elliptical_zAb_prime(B_prime As Double, Rb_prime As Double, _
y_prime As Double) As Double

Dim theta_b As Double
theta_b = 2 * Application.Acos(1 - y_prime / Rb_prime)

Elliptical_zAb_prime = Rb_prime ^ 3 / (3 * B_prime) _
                    * (3 * Sin(theta_b / 2) - Sin(theta_b / 2) ^ 3 _
                    - 3 * (theta_b / 2) * Cos(theta_b / 2))

End Function

'Middle section 1 functions
Function Elliptical_Tm1_prime(B_prime As Double, Rm_prime As Double, _
hm_prime As Double, y_prime As Double) As Double

Elliptical_Tm1_prime = 1 / B_prime * (B_prime - 2 * Rm_prime)

End Function

Function Elliptical_Am1_prime(B_prime As Double, Rm_prime As Double, _
hm_prime As Double, y_prime As Double) As Double

Elliptical_Am1_prime = 1 / B_prime * (B_prime - 2 * Rm_prime) _
                    * (y_prime - hm_prime + Rm_prime)

End Function

Function Elliptical_zAm1_prime(B_prime As Double, Rm_prime As Double, _
hm_prime As Double, y_prime As Double) As Double

Elliptical_zAm1_prime = 1 / (2 * B_prime) * (B_prime - 2 * Rm_prime)
-
                    * (y_prime - hm_prime + Rm_prime) ^ 2

End Function

'Middle section 2 functions
Function Elliptical_Tm2_prime(B_prime As Double, Rm_prime As Double, _
hm_prime As Double, y_prime As Double) As Double

Dim theta_m As Double
theta_m = 2 * Application.Acos(1 - 1 / Rm_prime _
                    * (y_prime - hm_prime + Rm_prime))

Elliptical_Tm2_prime = 2 * Rm_prime / B_prime * Sin(theta_m / 2)

End Function

Function Elliptical_Am2_prime(B_prime As Double, Rm_prime As Double, _
hm_prime As Double, y_prime As Double) As Double

Dim theta_m As Double
theta_m = 2 * Application.Acos(1 - 1 / Rm_prime _
                    * (y_prime - hm_prime + Rm_prime))

```

```

    Elliptical_Am2_prime = Rm_prime ^ 2 / (2 * B_prime) _
                        * (theta_m - Sin(theta_m))
End Function

Function Elliptical_zAm2_prime(B_prime As Double, Rm_prime As Double, _
hm_prime As Double, y_prime As Double) As Double

    Dim theta_m As Double
    theta_m = 2 * Application.Acos(1 - 1 / Rm_prime _
    * (y_prime - hm_prime + Rm_prime))

    Elliptical_zAm2_prime = Rm_prime ^ 3 / (3 * B_prime) _
    * (3 * Sin(theta_m / 2) ^ 3 _
    - Sin(theta_m / 2) ^ 3 _
    - 3 * (theta_m / 2) * Cos(theta_m / 2))

End Function

'Top section functions
Function Elliptical_Tt_prime(B_prime As Double, Rt_prime As Double, _
y_prime As Double) As Double

    Dim theta_t As Double
    theta_t = 2 * Application.Acos((1 - y_prime) / Rt_prime - 1)

    Elliptical_Tt_prime = 2 * Rt_prime / B_prime * Sin(theta_t / 2)

End Function

Function Elliptical_At_prime(B_prime As Double, Rt_prime As Double, _
y_prime As Double) As Double

    Dim theta_t As Double
    theta_t = 2 * Application.Acos((1 - y_prime) / Rt_prime - 1)

    Elliptical_At_prime = Rt_prime ^ 2 / (2 * B_prime) _
    * (theta_t - Sin(theta_t))

End Function

Function Elliptical_zAt_prime(B_prime As Double, Rt_prime As Double, _
y_prime As Double) As Double

    Dim theta_t As Double
    theta_t = 2 * Application.Acos((1 - y_prime) / Rt_prime - 1)

    Elliptical_zAt_prime = Rt_prime ^ 3 / (3 * B_prime) _
    * (3 * Sin(theta_t / 2) - Sin(theta_t / 2) ^ 3 _
    - 3 * (theta_t / 2) * Cos(theta_t / 2))

End Function

```

## D.6 Pipe Arch Conduits

'Returns y2 value for given Pipe Arch dimensions, Q, and y1  
Public Function PipeArch\_y2(B As Double, D As Double, Rb As Double, Rm As Double, Rt As Double, Q As Double, y1 As Double, units As String)

```
    '**Absolute Variables**
    Dim g As Double 'Acceleration due to gravity

    Dim hb As Double 'Bottom transition height
    Dim hm As Double 'Neutral axis height
    Dim ht As Double 'Top transition height

    Dim B_prime As Double 'Dimensionless span
    Dim Rb_prime As Double 'Dimensionless bottom radius
    Dim Rm_prime As Double 'Dimensionless middle radius
    Dim Rt_prime As Double 'Dimensionless top radius
    Dim hb_prime As Double 'Dimensionless bottom transition height
    Dim hm_prime As Double 'Dimensionless neutral axis height
    Dim ht_prime As Double 'Dimensionless top transition height

    Dim y1_prime As Double 'Upstream depth ratio
    Dim T1_prime As Double 'Upstream dimensionless top width
    Dim A1_prime As Double 'Upstream dimensionless area
    Dim zA1_prime As Double 'Upstream dimensionless centroid-area

    Dim yf_prime As Double 'Full conditions depth ratio
    Dim Af_prime As Double 'Full conditions dimensionless area
    Dim zAf_prime As Double 'Full conditions dimensionless
        'centroid-area

    Dim y2_prime As Double 'Downstream depth ratio
    Dim A2_prime As Double 'Downstream dimensionless area
    Dim zA2_prime As Double 'Downstream dimensionless centroid-area

    Dim Fr1 As Double 'Upstream Froude number
    Dim Fr1_t As Double 'Transitional upstream Froude number

    '**Iterative variables** (interval halving method)
    Dim y2_prime1 As Double 'Lower estimate
    Dim f1 As Double 'Function at lower estimate

    Dim y2_prime2 As Double 'Upper estimate
    Dim f2 As Double 'Function at upper estimate

    Dim y2_prime3 As Double 'Intermediate estimate
    Dim f3 As Double 'Function at intermediate estimate

    Dim Error As Double 'Allowable error in y'2
    Error = 0.00001

    'Determine correct value of g
    If units = "BG" Then 'English units
        g = 32.21
    ElseIf units = "SI" Then 'International units
        g = 9.81
    End If

    'Calculate remaining shape parameters
    hm = Rb - Sqr((Rb - Rm) ^ 2 - (B / 2 - Rm) ^ 2)
    Rt = (B * (4 * Rm - B) - 4 * (D - hm) ^ 2) / 8 / (Rm - D + hm)
    hb = Rb * (hm - Rm) / (Rb - Rm)
    ht = D - Rt * (1 - Sqr((Rt - Rm) ^ 2 - (B / 2 - Rm) ^ 2)) /
        / (Rt - Rm)
```



```

'Step 1: Calculate dimensionless parameters
B_prime = B / D
Rb_prime = Rb / D
Rm_prime = Rm / D
Rt_prime = Rt / D
hb_prime = hb / D
hm_prime = hm / D
ht_prime = ht / D

y1_prime = y1 / D
T1_prime = PipeArch_T_prime(B_prime, Rb_prime, Rm_prime,
    Rt_prime, hb_prime, hm_prime, ht_prime, y1_prime)
A1_prime = PipeArch_A_prime(B_prime, Rb_prime, Rm_prime,
    Rt_prime, hb_prime, hm_prime, ht_prime, y1_prime)
zA1_prime = PipeArch_zA_prime(B_prime, Rb_prime, Rm_prime,
    Rt_prime, hb_prime, hm_prime, ht_prime, y1_prime)

Af_prime = PipeArch_A_prime(B_prime, Rb_prime, Rm_prime,
    Rt_prime, hb_prime, hm_prime, ht_prime, 1)
zAf_prime = PipeArch_zA_prime(B_prime, Rb_prime, Rm_prime,
    Rt_prime, hb_prime, hm_prime, ht_prime, 1)

'Step 2: Calculate upstream Froude number
Fr1 = Q / Sqr(g * B ^ 2 * D ^ 3 * A1_prime ^ 3 / T1_prime)

If Fr1 <= 1 Then 'No Jump

    PipeArch_y2 = y1

Else 'Jump may occur

    'Step 3: Calculate transitional upstream Froude number
    Fr1_t = Sqr((T1_prime * Af_prime / A1_prime ^ 2)
        * (zAf_prime - zA1_prime) / (Af_prime - A1_prime))

    'Step 4: Calculate downstream depth
    If Fr1 < Fr1_t Then 'Complete jump

        y2_prime1 = y1_prime 'Lower Limit
        f1 = 1 - Fr1 ^ 2

        y2_prime2 = 1 'Upper Limit
        f2 = Fr1_t ^ 2 - Fr1 ^ 2

    Do

        y2_prime3 = (y2_prime1 + y2_prime2) / 2
        A2_prime = PipeArch_A_prime(B_prime, Rb_prime,
            Rm_prime, Rt_prime, hb_prime, hm_prime,
            ht_prime, y2_prime3)
        zA2_prime = PipeArch_zA_prime(B_prime, Rb_prime,
            Rm_prime, Rt_prime, hb_prime, hm_prime,
            ht_prime, y2_prime3)
        f3 = (T1_prime * A2_prime / A1_prime ^ 2)
            * (zA1_prime - zA2_prime)
            / (A1_prime - A2_prime) - Fr1 ^ 2

        If f1 * f3 > 0 Then 'y2_prime3 is new upper estimate
            y2_prime1 = y2_prime3
            f1 = f3
        Else 'y2_prime3 is new lower estimate
            y2_prime2 = y2_prime3
            f2 = f3

```

```

        End If

        Loop Until y2_prime2 - y2_prime1 < Error
        y2_prime = y2_prime3
    Else 'Incomplete jump
        y2_prime = (Fr1 ^ 2 * A1_prime ^ 2 -
            * (Af_prime - A1_prime) -
            - T1_prime * Af_prime -
            * (zAf_prime - zA1_prime))
            / (T1_prime * Af_prime ^ 2) + 1

    End If

    PipeArch_y2 = y2_prime * D

End If

End Function

'Returns T' = T/B value for given pipe arch parameters and y' value
Public Function PipeArch_T_prime(B_prime As Double,
Rb_prime As Double, Rm_prime As Double, Rt_prime As Double,
hb_prime As Double, hm_prime As Double, ht_prime As Double,
y_prime As Double) As Double

    Dim Tb_prime As Double
    Dim Tm1_prime As Double
    Dim Tm2_prime As Double
    Dim Tt_prime As Double

    If y_prime <= hb_prime Then
        Tb_prime = PipeArch_Tb_prime(B_prime, Rb_prime, y_prime)
    ElseIf y_prime <= ht_prime Then
        Tm1_prime = PipeArch_Tm1_prime(B_prime, Rm_prime, hm_prime,
            y_prime)
        Tm2_prime = PipeArch_Tm2_prime(B_prime, Rm_prime, hm_prime,
            y_prime)
    ElseIf y_prime <= 1 Then
        Tt_prime = PipeArch_Tt_prime(B_prime, Rt_prime, y_prime)
    End If

    PipeArch_T_prime = Tb_prime + Tm1_prime + Tm2_prime + Tt_prime

End Function

'Returns A' = A/BD value for given pipe arch parameters and y' value
Public Function PipeArch_A_prime(B_prime As Double,
Rb_prime As Double, Rm_prime As Double, Rt_prime As Double,
hb_prime As Double, hm_prime As Double, ht_prime As Double,
y_prime As Double) As Double

    Dim Ab_prime As Double
    Dim Am1_prime As Double
    Dim Am2_prime As Double
    Dim At_prime As Double

```

```

If y_prime <= hb_prime Then
    Ab_prime = PipeArch_Ab_prime(B_prime, Rb_prime, y_prime)
ElseIf y_prime <= ht_prime Then
    Ab_prime = PipeArch_Ab_prime(B_prime, Rb_prime, hb_prime)
    Am1_prime = PipeArch_Am1_prime(B_prime, Rm_prime, hm_prime, _
        y_prime)
        - PipeArch_Am1_prime(B_prime, Rm_prime, hm_prime, _
        hb_prime)
    Am2_prime = PipeArch_Am2_prime(B_prime, Rm_prime, hm_prime, _
        y_prime)
        - PipeArch_Am2_prime(B_prime, Rm_prime, hm_prime, _
        hb_prime)
ElseIf y_prime <= 1 Then
    Ab_prime = PipeArch_Ab_prime(B_prime, Rb_prime, hb_prime)
    Am1_prime = PipeArch_Am1_prime(B_prime, Rm_prime, hm_prime, _
        ht_prime)
        - PipeArch_Am1_prime(B_prime, Rm_prime, hm_prime, _
        hb_prime)
    Am2_prime = PipeArch_Am2_prime(B_prime, Rm_prime, hm_prime, _
        ht_prime)
        - PipeArch_Am2_prime(B_prime, Rm_prime, hm_prime, _
        hb_prime)
    At_prime = PipeArch_At_prime(B_prime, Rt_prime, y_prime)
        - PipeArch_At_prime(B_prime, Rt_prime, ht_prime)
End If

PipeArch_A_prime = Ab_prime + Am1_prime + Am2_prime + At_prime

End Function

'Returns (zA)' = zA/BD^2 value for given pipe arch parameters and y'
Public Function PipeArch_zA_prime(B_prime As Double, _
    Rb_prime As Double, Rm_prime As Double, Rt_prime As Double, _
    hb_prime As Double, hm_prime As Double, ht_prime As Double, _
    y_prime As Double) As Double

    Dim zAb_prime As Double
    Dim zAm1_prime As Double
    Dim zAm2_prime As Double
    Dim zAt_prime As Double

    If y_prime <= hb_prime Then
        zAb_prime = PipeArch_zAb_prime(B_prime, Rb_prime, y_prime)
    ElseIf y_prime <= ht_prime Then
        zAb_prime = PipeArch_zAb_prime(B_prime, Rb_prime, hb_prime)
            + (y_prime - hb_prime)
            * PipeArch_Ab_prime(B_prime, Rb_prime, hb_prime)
        zAm1_prime = PipeArch_zAm1_prime(B_prime, Rm_prime, hm_prime, _
            y_prime)
            - PipeArch_zAm1_prime(B_prime, Rm_prime, hm_prime, _
            hb_prime)
            - (y_prime - hb_prime)
            * PipeArch_Am1_prime(B_prime, Rm_prime, hm_prime, _
            hb_prime)
    End If
End Function

```

```

zAm2_prime = PipeArch_zAm2_prime(B_prime, Rm_prime, hm_prime, _
    y_prime)
- PipeArch_zAm2_prime(B_prime, Rm_prime, hm_prime, _
    hb_prime)
- (y_prime - hb_prime)
* PipeArch_Am2_prime(B_prime, Rm_prime, hm_prime, _
    hb_prime)

ElseIf y_prime <= 1 Then

zAb_prime = PipeArch_zAb_prime(B_prime, Rb_prime, hb_prime) _
+ (y_prime - hb_prime)
* PipeArch_Ab_prime(B_prime, Rb_prime, hb_prime)
zAm1_prime = PipeArch_zAm1_prime(B_prime, Rm_prime, hm_prime, _
    ht_prime)
- PipeArch_zAm1_prime(B_prime, Rm_prime, hm_prime, _
    hb_prime)
+ (y_prime - ht_prime)
* PipeArch_Am1_prime(B_prime, Rm_prime, hm_prime, _
    ht_prime)
- (y_prime - hb_prime)
* PipeArch_Am1_prime(B_prime, Rm_prime, hm_prime, _
    hb_prime)
zAm2_prime = PipeArch_zAm2_prime(B_prime, Rm_prime, hm_prime, _
    ht_prime)
- PipeArch_zAm2_prime(B_prime, Rm_prime, hm_prime, _
    hb_prime)
+ (y_prime - ht_prime)
* PipeArch_Am2_prime(B_prime, Rm_prime, hm_prime, _
    ht_prime)
- (y_prime - hb_prime)
* PipeArch_Am2_prime(B_prime, Rm_prime, hm_prime, _
    hb_prime)
zAt_prime = PipeArch_zAt_prime(B_prime, Rt_prime, y_prime) _
- PipeArch_zAt_prime(B_prime, Rt_prime, ht_prime) _
- (y_prime - ht_prime)
* PipeArch_At_prime(B_prime, Rt_prime, ht_prime)

End If

PipeArch_zA_prime = zAb_prime + zAm1_prime + zAm2_prime + zAt_prime

End Function

'Bottom section functions
Function PipeArch_Tb_prime(B_prime As Double, Rb_prime As Double, _
    y_prime As Double) As Double

    Dim theta_b As Double
    theta_b = 2 * Application.Acos(1 - y_prime / Rb_prime)

    PipeArch_Tb_prime = 2 * Rb_prime / B_prime * Sin(theta_b / 2)

End Function

Function PipeArch_Ab_prime(B_prime As Double, Rb_prime As Double, _
    y_prime As Double) As Double

    Dim theta_b As Double
    theta_b = 2 * Application.Acos(1 - y_prime / Rb_prime)

    PipeArch_Ab_prime = Rb_prime ^ 2 / (2 * B_prime) _
        * (theta_b - Sin(theta_b))

```

```

End Function

Function PipeArch_zAb_prime(B_prime As Double, Rb_prime As Double, _
y_prime As Double) As Double

    Dim theta_b As Double
    theta_b = 2 * Application.Acos(1 - y_prime / Rb_prime)

    PipeArch_zAb_prime = Rb_prime ^ 3 / (3 * B_prime)
        * (3 * Sin(theta_b / 2) - Sin(theta_b / 2) ^ 3 -
        - 3 * (theta_b / 2) * Cos(theta_b / 2))

End Function

'Middle section 1 functions
Function PipeArch_Tm1_prime(B_prime As Double, Rm_prime As Double, _
hm_prime As Double, y_prime As Double) As Double

    PipeArch_Tm1_prime = 1 / B_prime * (B_prime - 2 * Rm_prime)

End Function

Function PipeArch_Am1_prime(B_prime As Double, Rm_prime As Double, _
hm_prime As Double, y_prime As Double) As Double

    PipeArch_Am1_prime = 1 / B_prime * (B_prime - 2 * Rm_prime) _
        * (y_prime - hm_prime + Rm_prime)

End Function

Function PipeArch_zAm1_prime(B_prime As Double, Rm_prime As Double, _
hm_prime As Double, y_prime As Double) As Double

    PipeArch_zAm1_prime = 1 / (2 * B_prime) _
        * (B_prime - 2 * Rm_prime) _
        * (y_prime - hm_prime + Rm_prime) ^ 2

End Function

'Middle section 2 functions
Function PipeArch_Tm2_prime(B_prime As Double, Rm_prime As Double, _
hm_prime As Double, y_prime As Double) As Double

    Dim theta_m As Double
    theta_m = 2 * Application.Acos(1 - 1 / Rm_prime _
        * (y_prime - hm_prime + Rm_prime))

    PipeArch_Tm2_prime = 2 * Rm_prime / B_prime * Sin(theta_m / 2)

End Function

Function PipeArch_Am2_prime(B_prime As Double, Rm_prime As Double, _
hm_prime As Double, y_prime As Double) As Double

    Dim theta_m As Double
    theta_m = 2 * Application.Acos(1 - 1 / Rm_prime _
        * (y_prime - hm_prime + Rm_prime))

    PipeArch_Am2_prime = Rm_prime ^ 2 / (2 * B_prime) _
        * (theta_m - Sin(theta_m))

End Function

Function PipeArch_zAm2_prime(B_prime As Double, Rm_prime As Double, _

```

```

hm_prime As Double, y_prime As Double) As Double

    Dim theta_m As Double
    theta_m = 2 * Application.Acos(1 - 1 / Rm_prime _
        * (y_prime - hm_prime + Rm_prime))

    PipeArch_zAm2_prime = Rm_prime ^ 3 / (3 * B_prime) _
        * (3 * Sin(theta_m / 2) - Sin(theta_m / 2) ^ 3 _
        - 3 * (theta_m / 2) * Cos(theta_m / 2))

End Function

'Top section functions
Function PipeArch_Tt_prime(B_prime As Double, Rt_prime As Double, _
y_prime As Double) As Double

    Dim theta_t As Double
    theta_t = 2 * Application.Acos((1 - y_prime) / Rt_prime - 1)

    PipeArch_Tt_prime = 2 * Rt_prime / B_prime * Sin(theta_t / 2)

End Function

Function PipeArch_At_prime(B_prime As Double, Rt_prime As Double, _
y_prime As Double) As Double

    Dim theta_t As Double
    theta_t = 2 * Application.Acos((1 - y_prime) / Rt_prime - 1)

    PipeArch_At_prime = Rt_prime ^ 2 / (2 * B_prime) _
        * (theta_t - Sin(theta_t))

End Function

Function PipeArch_zAt_prime(B_prime As Double, Rt_prime As Double, _
y_prime As Double) As Double

    Dim theta_t As Double
    theta_t = 2 * Application.Acos((1 - y_prime) / Rt_prime - 1)

    PipeArch_zAt_prime = Rt_prime ^ 3 / (3 * B_prime) _
        * (3 * Sin(theta_t / 2) - Sin(theta_t / 2) ^ 3 _
        - 3 * (theta_t / 2) * Cos(theta_t / 2))

End Function

```

## D.7 User-Defined Conduits

```

'Returns y2 value for given user defined dimensions, Q, and y1
Public Function UserDefined_y2(x_Range As Range, ybot_Range As Range, _
ytop_Range As Range, Q As Double, y1 As Double, units As String)

    '**Absolute Variables**
    Dim g As Double 'Acceleration due to gravity

    Dim i As Integer 'Incremental coordinate
    Dim n As Integer 'Number of coordinates
    n = x_Range.Rows.Count
    Dim B As Double 'Conduit span
    Dim D As Double 'Conduit rise
    ReDim x_prime(1 To n) As Double 'Array of x' coordinates

```

```

ReDim hA_prime(1 To n - 1) As Double 'Array of h'(A) values
ReDim hb_prime(1 To n - 1) As Double 'Array of h'(B) values
ReDim hC_prime(1 To n - 1) As Double 'Array of h'(C) values
ReDim hD_prime(1 To n - 1) As Double 'Array of h'(D) values

Dim y1_prime As Double 'Upstream depth ratio
Dim T1_prime As Double 'Upstream dimensionless top width
Dim A1_prime As Double 'Upstream dimensionless area
Dim zA1_prime As Double 'Upstream dimensionless centroid-area

Dim yf_prime As Double 'Full conditions depth ratio
Dim Af_prime As Double 'Full conditions dimensionless area
Dim zAf_prime As Double 'Full conditions dimensionless
    'centroid-area

Dim y2_prime As Double 'Downstream depth ratio
Dim A2_prime As Double 'Downstream dimensionless area
Dim zA2_prime As Double 'Downstream dimensionless centroid-area

Dim Fr1 As Double 'Upstream Froude number
Dim Fr1_t As Double 'Transitional upstream Froude number

'***Iterative variables** (interval halving method)
Dim y2_prime1 As Double 'Lower estimate
Dim f1 As Double 'Function at lower estimate

Dim y2_prime2 As Double 'Upper estimate
Dim f2 As Double 'Function at upper estimate

Dim y2_prime3 As Double 'Intermediate estimate
Dim f3 As Double 'Function at intermediate estimate

Dim Error As Double 'Allowable error in y'2
Error = 0.00001

'Determine correct value of g
If units = "BG" Then 'English units
    g = 32.21
ElseIf units = "SI" Then 'International units
    g = 9.81
End If

'Step 1: Calculate dimensionless parameters
B = x_Range.Rows(n)
For i = 1 To n
    If ytop_Range.Rows(i) > D Then
        D = ytop_Range.Rows(i)
    End If
Next

For i = 1 To n

    x_prime(i) = x_Range.Rows(i) / B

    If i <> n Then

        If ybot_Range.Rows(i) <= ybot_Range.Rows(i + 1) Then
            hA_prime(i) = ybot_Range.Rows(i) / D
            hb_prime(i) = ybot_Range.Rows(i + 1) / D
        Else
            hA_prime(i) = ybot_Range.Rows(i + 1) / D
            hb_prime(i) = ybot_Range.Rows(i) / D
        End If
    End If

```

```

    If ytop_Range.Rows(i) <= ytop_Range.Rows(i + 1) Then
        hC_prime(i) = ytop_Range.Rows(i) / D
        hD_prime(i) = ytop_Range.Rows(i + 1) / D
    Else
        hC_prime(i) = ytop_Range.Rows(i + 1) / D
        hD_prime(i) = ytop_Range.Rows(i) / D
    End If

End If

Next

y1_prime = y1 / D
T1_prime = UserDefined_T_prime(x_prime, hA_prime, hb_prime, _
    hC_prime, hD_prime, n, y1_prime)
A1_prime = UserDefined_A_prime(x_prime, hA_prime, hb_prime, _
    hC_prime, hD_prime, n, y1_prime)
zA1_prime = UserDefined_zA_prime(x_prime, hA_prime, hb_prime, _
    hC_prime, hD_prime, n, y1_prime)

Af_prime = UserDefined_A_prime(x_prime, hA_prime, hb_prime, _
    hC_prime, hD_prime, n, 1)
zAf_prime = UserDefined_zA_prime(x_prime, hA_prime, hb_prime, _
    hC_prime, hD_prime, n, 1)

'Step 2: Calculate upstream Froude number
Fr1 = Q / Sqr(g * B ^ 2 * D ^ 3 * A1_prime ^ 3 / T1_prime)

If Fr1 <= 1 Then 'No Jump

    UserDefined_y2 = y1

Else 'Jump may occur

    'Step 3: Calculate transitional upstream Froude number
    Fr1_t = Sqr((T1_prime * Af_prime / A1_prime ^ 2)
        * (zAf_prime - zA1_prime) / (Af_prime - A1_prime))

    'Step 4: Calculate downstream depth
    If Fr1 < Fr1_t Then 'Complete jump

        y2_prime1 = y1_prime 'Lower Limit
        f1 = 1 - Fr1 ^ 2

        y2_prime2 = 1 'Upper Limit
        f2 = Fr1_t ^ 2 - Fr1 ^ 2

    Do

        y2_prime3 = (y2_prime1 + y2_prime2) / 2
        A2_prime = UserDefined_A_prime(x_prime, hA_prime,
            hb_prime, hC_prime, hD_prime, n, y2_prime3)
        zA2_prime = UserDefined_zA_prime(x_prime, hA_prime,
            hb_prime, hC_prime, hD_prime, n, y2_prime3)
        f3 = (T1_prime * A2_prime / A1_prime ^ 2)
            * (zA1_prime - zA2_prime) / (A1_prime - A2_prime)
            - Fr1 ^ 2

        If f1 * f3 > 0 Then 'y2_prime3 is new upper estimate
            y2_prime1 = y2_prime3
            f1 = f3
        Else 'y2_prime3 is the new lower estimate
            y2_prime2 = y2_prime3
            f2 = f3
    End Do

```



```

        End If

        Loop Until y2_prime2 - y2_prime1 < Error
        y2_prime = y2_prime3
    Else 'Incomplete jump
        y2_prime = (Fr1 ^ 2 * A1_prime ^ 2 -
            * (Af_prime - A1_prime) -
            - T1_prime * Af_prime -
            * (zAf_prime - zA1_prime))
            / (T1_prime * Af_prime ^ 2) + 1

    End If

    UserDefined_y2 = y2_prime * D

End If

End Function

'Returns T' = T/B value for given y' value
Public Function UserDefined_T_prime(x_prime As Variant,
hA_prime As Variant, hb_prime As Variant, hC_prime As Variant,
hD_prime As Variant, n As Integer, y_prime As Double) As Double

    Dim i As Integer
    Dim T_prime_i As Double
    Dim T_prime As Double

    For i = 1 To n - 1

        If y_prime <= hA_prime(i) Then 'Case 1
            T_prime_i = 0

        ElseIf y_prime <= hb_prime(i) Then 'Case 2
            T_prime_i = (x_prime(i + 1) - x_prime(i)) -
                * (y_prime - hA_prime(i)) -
                / (hb_prime(i) - hA_prime(i))

        ElseIf y_prime <= hC_prime(i) Then 'Case 3
            T_prime_i = x_prime(i + 1) - x_prime(i)

        ElseIf y_prime <= hD_prime(i) Then 'Case 4
            T_prime_i = (x_prime(i + 1) - x_prime(i)) -
                * (hD_prime(i) - y_prime) -
                / (hD_prime(i) - hC_prime(i))

        Else 'Case 5
            T_prime_i = 0

        End If

        T_prime = T_prime + T_prime_i

    Next

    UserDefined_T_prime = T_prime

```

End Function

'Returns A' = A/BD value for given y' value  
Public Function UserDefined\_A\_prime(x\_prime As Variant, \_  
hA\_prime As Variant, hb\_prime As Variant, hC\_prime As Variant, \_  
hD\_prime As Variant, n As Integer, y\_prime As Double) As Double

Dim i As Integer  
Dim T\_prime\_i As Double  
Dim A\_prime\_i As Double  
Dim A\_prime As Double

For i = 1 To n - 1

If y\_prime <= hA\_prime(i) Then 'Case 1

A\_prime\_i = 0

ElseIf y\_prime <= hb\_prime(i) Then 'Case 2

T\_prime\_i = (x\_prime(i + 1) - x\_prime(i)) \_  
\* (y\_prime - hA\_prime(i)) \_  
/ (hb\_prime(i) - hA\_prime(i))  
A\_prime\_i = 1 / 2 \* T\_prime\_i \* (y\_prime - hA\_prime(i))

ElseIf y\_prime <= hC\_prime(i) Then 'Case 3

T\_prime\_i = x\_prime(i + 1) - x\_prime(i)  
A\_prime\_i = 1 / 2 \* T\_prime\_i \* ((y\_prime - hA\_prime(i)) \_  
+ (y\_prime - hb\_prime(i)))

ElseIf y\_prime <= hD\_prime(i) Then 'Case 4

T\_prime\_i = (x\_prime(i + 1) - x\_prime(i)) \_  
\* (hD\_prime(i) - y\_prime)  
/ (hD\_prime(i) - hC\_prime(i))  
A\_prime\_i = 1 / 2 \* ((x\_prime(i + 1) - x\_prime(i)) \_  
\* ((y\_prime - hA\_prime(i)) \_  
+ (y\_prime - hb\_prime(i))) \_  
- (x\_prime(i + 1) - x\_prime(i) - T\_prime\_i) \_  
\* (y\_prime - hC\_prime(i)))

Else 'Case 5

A\_prime\_i = 1 / 2 \* (x\_prime(i + 1) - x\_prime(i)) \_  
\* (hD\_prime(i) + hC\_prime(i) \_  
- hb\_prime(i) - hA\_prime(i))

End If

A\_prime = A\_prime + A\_prime\_i

Next

UserDefined\_A\_prime = A\_prime

End Function

'Returns (zA)' = zA/BD^2 value for given y' value  
Public Function UserDefined\_zA\_prime(x\_prime As Variant, \_  
hA\_prime As Variant, hb\_prime As Variant, hC\_prime As Variant, \_  
hD\_prime As Variant, n As Integer, y\_prime As Double) As Double

```

Dim i As Integer
Dim T_prime_i As Double
Dim zA_prime_i As Double
Dim zA_prime As Double

For i = 1 To n - 1

    If y_prime <= hA_prime(i) Then 'Case 1
        zA_prime_i = 0

    ElseIf y_prime <= hb_prime(i) Then 'Case 2
        T_prime_i = (x_prime(i + 1) - x_prime(i)) _
            * (y_prime - hA_prime(i)) _
            / (hb_prime(i) - hA_prime(i))
        zA_prime_i = 1 / 6 * T_prime_i _
            * (y_prime - hA_prime(i)) ^ 2

    ElseIf y_prime <= hC_prime(i) Then 'Case 3
        T_prime_i = x_prime(i + 1) - x_prime(i)
        zA_prime_i = 1 / 6 * T_prime_i _
            * ((y_prime - hA_prime(i)) ^ 2 _
            + (y_prime - hA_prime(i)) _
            * (y_prime - hb_prime(i)) _
            + (y_prime - hb_prime(i)) ^ 2)

    ElseIf y_prime <= hD_prime(i) Then 'Case 4
        T_prime_i = (x_prime(i + 1) - x_prime(i)) _
            * (hD_prime(i) - y_prime) _
            / (hD_prime(i) - hC_prime(i))
        zA_prime_i = 1 / 6 * ((x_prime(i + 1) - x_prime(i)) _
            * ((y_prime - hA_prime(i)) ^ 2 _
            + (y_prime - hA_prime(i)) _
            * (y_prime - hb_prime(i)) _
            + (y_prime - hb_prime(i)) ^ 2) _
            - (x_prime(i + 1) - x_prime(i)) * T_prime_i) _
            * (y_prime - hC_prime(i)) ^ 2

    Else 'Case 5
        zA_prime_i = 1 / 6 * (x_prime(i + 1) - x_prime(i)) _
            * (3 * y_prime _
            * (hD_prime(i) + hC_prime(i) _
            - hb_prime(i) - hA_prime(i)) _
            + (hA_prime(i) ^ 2 _
            + hA_prime(i) * hb_prime(i) _
            + hb_prime(i) ^ 2) _
            - (hC_prime(i) ^ 2 _
            + hC_prime(i) * hD_prime(i) _
            + hD_prime(i) ^ 2))

    End If

    zA_prime = zA_prime + zA_prime_i

Next

UserDefined_zA_prime = zA_prime

End Function

```